DOCTOR OF PHILOSOPHY

Synthesis and characterisation of some new complexes of molybdenum(II) and tungsten(II) containing anionic and neutral sulphur donor ligands

Clark, Alec Ian

Award date:
1997

Awarding institution:
University of Wales, Bangor

SYNTHESIS AND CHARACTERISATION OF SOME NEW COMPLEXES OF MOLYBDENUM(II) AND TUNGSTEN(II) CONTAINING ANIONIC AND NEUTRAL SULPHUR DONOR LIGANDS

A thesis submitted to the
University of Wales
by

Alec Ian Clark

In candidature for the degree of
Philosophiae Doctor

University of Wales
Bangor
1997

Acknowledgements

I would like to thank my supervisor, Dr. Paul Baker for his help and guidance throughout the course of this Ph.D. Thanks also to Dr. Ray Richards and Dr. David Evans for their time and help during my visits to the NFL at both Sussex and Norwich. I am also very grateful to Dr. M. C. Durrant, Mrs. E. Barclay and Dr. S. Fairhurst for their invaluable help during both visits. I would also like to thank Dr. M. G. B. Drew at the University of Reading for solving the crystal structures contained within this thesis.

I would also like to thank all the technical staff at the Department of Chemistry, University of Wales, Bangor for all their help and assistance and all my friends and colleagues who have made my time at Bangor so enjoyable.

Finally thanks to the BBSRC for their financial support.

Abstract

The reaction of $[WI_2(CO)_3(NCMe)_2]$ with two equivalents of PEt_3 gives the new seven-coordinate complex $[WI_2(CO)_3(PEt_3)_2]$. Reaction of the complexes $[MI_2(CO)_3(PEt_3)_2]$ (M= Mo, W) with one equivalent of the dithiolate ligands $Na_2[S(CH_2)_nS]$ (n = 2 and 3) and two equivalents of Na[SPh], gave the new six-coordinate complexes $[W\{S(CH_2)_nS\}(CO)_2(PEt_3)_2]$ (n = 2 and 3) and $[W(SPh)_2(CO)_2(PEt_3)_2]$. Similarly, reaction of $[MoI_2(CO)_3(PEt_3)_2]$ with one equivalent of $Na_2[S(CH_2)_2S]$ gave $[Mo\{S(CH_2)_2S\}(CO)_2(PEt_3)_2]$. All four thiolate complexes were crystallographically characterised. The reactions of the complexes $[MI_2(CO)_3(PEt_3)_2]$ (M = Mo or W) with one equivalent of Na[acac] gave the seven-coordinate complexes $[MI(acac)(CO)_2(PEt_3)_2]$ again both complexes were characterised by X-ray crystallography.

The reactions of the di-bromo complexes $[MBr_2(CO)_3(NCMe)_2]$ (M = Mo or W) with a slight excess of $RS(CH_2)_2SR$ (R = Ph or 4-FC_6H_4) afforded the seven-coordinate complexes $[MBr_2(CO)_3\{RS(CH_2)_2SR\}]$. The seven-coordinate tungsten complex $[WBr_2(CO)_3\{PhS(CH_2)_2SPh\}]$ was crystallographically characterised. Similarly, reactions of $[WBr_2(CO)_3(NCMe)_2]$ with two equivalents of $RS(CH_2)_2SR$ (R = Ph or 4-FC_6H_4) gave the complexes $[WBr(CO)_3\{RS(CH_2)_2SR\text{-}S\}\{RS(CH_2)_2SR\text{-}S,S'\}]Br$. Similarly, the reactions of the complex $[WBr_2(CO)_3(NCMe)_2]$ with one and two equivalents of $Ph_2P(S)CH_2(S)PPh_2$ are reported. The reactions of $[MBr_2(CO)_3(NCMe)_2]$ (M = Mo or W) with one equivalent of the trithioether $MeS(CH_2)_2S(CH_2)_2SMe$ (TTN) gave $[MoBr_2(CO)_2\{MeS(CH_2)_2S(CH_2)_2SMe\text{-}S,S',S''\}]$ and $[WBr_2(CO)_3\{MeS(CH_2)_2S(CH_2)_2SMe\text{-}S,S'\}]$. Also described is the synthesis of the complex $[MoBr_2(CO)_2\{ttob\text{-}S,S',S''\}]$ (ttob = 2,5,8-trithia[9]-o-benzenophane).

The reaction of the complex $[WI_2(CO)(NCMe)(\eta^2\text{-}PhC_2Ph)_2]$ with one equivalent of $MeS(CH_2)_2S(CH_2)_2SMe$ (TTN) gave the structurally characterised complex $[WI_2(CO)(TTN\text{-}S,S')(\eta^2\text{-}PhC_2Ph)]$. The complex $[WI_2(CO)(TTN\text{-}S,S')(\eta^2\text{-}PhC_2Ph)]$ reacts with one equivalent of $[FeI(CO)_2Cp]$ to give the bimetallic complex $[Cp(CO)_2Fe(TTN\text{-}S,S',S'')WI_2(CO)(\eta^2\text{-}PhC_2Ph)]I$. The mono(alkyne) complexes $[MI(CO)(L\text{-}S,S',S'')(\eta^2\text{-}RC_2R)]I$, $[MoI(CO)([9]aneS_3\text{-}S,S',S'')(\eta^2\text{-}RC_2R)]I$ and $[WBr(CO)(L\text{-}S,S',S'')(\eta^2\text{-}PhC_2Ph)]Br$ (M = Mo, W; L = ttob, TTN; R = Me, Ph) were successfully prepared and characterised. The complexes $[MoI(CO)([9]aneS_3\text{-}S,S',S'')(\eta^2\text{-}PhC_2Ph)]I$ $[WI(ttob\text{-}S,S',S'')(\eta^2\text{-}PhC_2Ph)_2]I_3$ were also characterised by X-ray crystallography.

The new seven-coordinate cluster complexes $[MI_2(CO)_3(Fe_4Cp_4S_6\text{-}S,S')]$ were prepared by the reaction of $[MI_2(CO)_3(NCMe)_2]$ (M = Mo or W) with one equivalent of $[Fe_4Cp_4S_6]$. Further reactions with one and two equivalents of Na[SAr] (Ar = Ph or $C_6H_2Me_3$-2,4,6{tmt}) gave the new cluster complexes $[MI(SAr)(CO)_3(Fe_4Cp_4S_6\text{-}S,S')]$ and $[M(SAr)_2(CO)_3(Fe_4Cp_4S_6\text{-}S,S')]$. Also described are the complexes $[M(CO)_3(L\text{^}L\text{-}P,P')Fe_4Cp_4S_6\text{-}S,S')]2I$ (L^L = dppe or dppr) and the bis(alkyne) cluster complexes $[WI(CO)(Fe_4Cp_4S_6\text{-}S,S')(\eta^2\text{-}RC_2R)_2]I$ (R = Me or Ph).

All new complexes described have been characterised by elemental analysis (C, H, N and S), infra red and ^1H NMR spectroscopy, and in selected cases, ^{13}C NMR and Mössbauer spectroscopy.

Abbreviations

acac	acetylacetonato
ADP	adenosine diphosphate
ATP	adenosine triphosphate
CON	capped octahedron
CTP	capped trigonal prism
Cp	cyclopentadienyl (C_5H_5)
dmf	dimethylformamide
dmso	dimethylsulphoxide
dppm	bis(diphenylphosphino)methane
dpppr	bis(diphenylphosphino)propane
$dppmS_2$	bis(diphenylphosphinothioyl)methane
Et	ethyl
His	histidene
IR	infra red
i.s.	isomer shift
Me	methyl
NFL	Nitrogen Fixation Laboratory, Norwich
NMR	Nuclear Magnetic Resonance
Pr	propyl
q.s.	quadrupole split
thf	tetrahydrofuran
TTN	2,5,8-trithianonane
ttob	2,5,8-trithia[9]-o-benzenophane
$[9]aneS_3$	1,4,7-trithiacyclononane

Units

Å	Angstroms
°C	Degrees centigrade
cm	Centimetres
g	Grammes
hrs	Hours
Hz	Hertz
K	Degrees Kelvin
min	Minutes
mol	Moles
mmol	Millimoles
ppm	Parts per million
S	Siemens (Ω^{-1})

Contents

CHAPTER 1:
INTRODUCTION

CHAPTER 1: INTRODUCTION

1.1 THE METALS MOLYBDENUM AND TUNGSTEN

Both molybdenum and tungsten are d-block transition metals and are members of group VIB of the periodic table. Both metals have a varied chemistry with complexes of both exhibiting several oxidation states from -2 to +6 and a wide range of co-ordination numbers. The metals themselves are very similar in many ways. Some of their important features are shown below in **Table 1.1**.

Table 1.1 Some physical properties of molybdenum and tungsten

Property	Mo	W
Atomic Number	42	74
Atomic Mass	95.94	183.85
Electron Configuration	[Kr] $4d^5\ 5s^1$	[Xe] $5d^4\ 6s^2$
Atomic Radius (Å)	1.40	1.41
ΔH Ionisation 1^{st} (KJ mol^{-1})	685	770

Both molybdenum and tungsten are found in similar quantities within the earth's crust (~10^{-4} %). Molybdenum occurs mainly as molybdenite, while tungsten is found in the form of the tungstates, Wolframite and Scheelite. Tungsten is used industrially in tungsten alloys, and is also found in a small number of bacterial enzymes[1]. Molybdenum, in contrast, is a very biologically active metal being found in several metalloenzymes.

1.2 MOLYBDENOENZYMES

Studies have shown molybdenum to be a highly biologically active transition metal[2,3]. It is found to be present in over thirty enzymes. Molybdenum enzymes can generally be classified as one of two groups. The first group of enzymes containing molybdoproteins[4] consisting of a single molybdenum atom and a pterin-ene-dithiolate organic ligand making up a molybdenum cofactor, Moco. The second class of molybdenum enzyme contain an iron-molybdenum cofactor, FeMoco. This second group consists of a single enzyme called molybdenum nitrogenase.

Nitrogenases are the enzymes responsible for the natural fixation of atmospheric dinitrogen. Three types of nitrogenase enzymes are known of which only one contains molybdenum. The other types contain either the metals vanadium and iron or iron alone.

1.3 THE NITROGEN CYCLE

Nitrogen is the fourth most abundant element in the biosphere and in the form of gaseous dinitrogen constitutes four fifths of the earth's atmosphere. The continuous fixation of dinitrogen, and it's reduction to ammonia forms the essential step of the nitrogen cycle, which is essential to all life (**Figure 1.1**).

In the nitrogen cycle solid ammonium salts are converted to nitrate by nitrifying bacteria. The resulting nitrates are then converted by plants to simple organic molecules. The simple organic molecules are used by animals and are converted to more complex organic molecules. Animals then return organic nitrogen to the soil in the form of their waste products and also upon their death and subsequent decay. This organic nitrogen is subsequently used by plants or converted to ammonia.

Figure 1.1 The nitrogen cycle

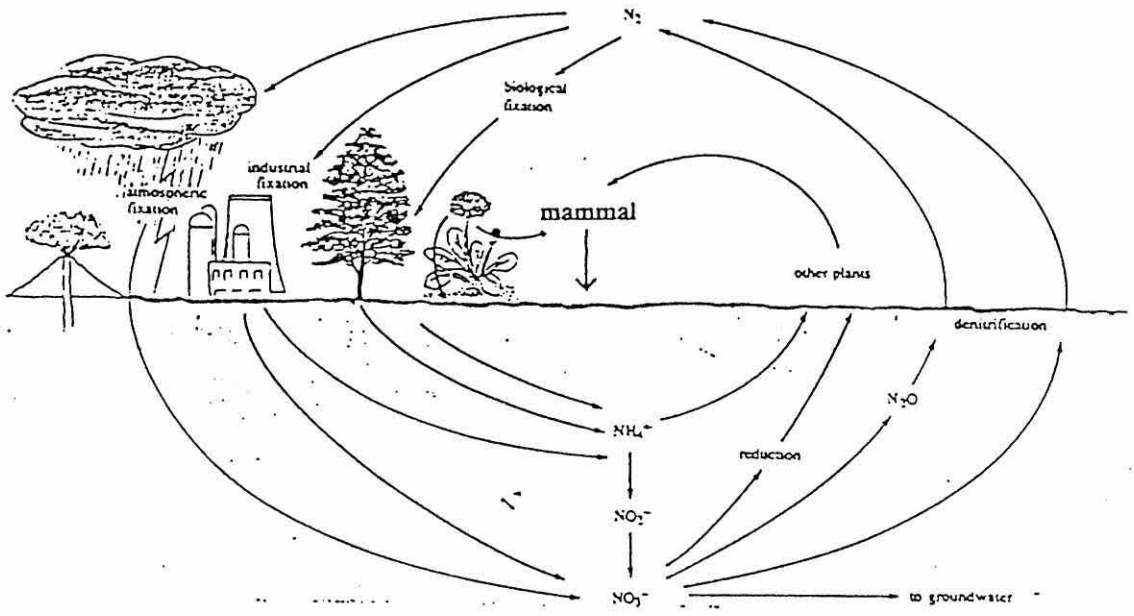

1.4 NITROGEN FIXATION

Global fixation of dinitrogen occurs *via* two main processes:

1) Industrially *via* the Haber-Bosch process.

2) Naturally *via* the action of nitrogen fixing bacteria.

Both processes convert atmospheric dinitrogen to ammonia, but by markedly different means and under greatly differing physical conditions.

1.4.1 Industrial Nitrogen Fixation

Industrial nitrogen fixation is carried out mainly by the Haber-Bosch process, involving the catalytic reduction of atmospheric dinitrogen to ammonia. However,

dinitrogen is extremely inert and a large amount of energy is required for it's reduction. The Haber-Bosch process therefore requires a catalyst coupled with greatly elevated temperatures and pressures[5] (**Equation 1.1**).

Equation 1.1

$$N_2 + 3H_2 \xrightarrow[\text{Iron Catalyst}]{\text{250 atm, 500°C}} 2NH_3$$

As is the case with all industrial plants there is a large initial capital outlay and continuous running and maintenance costs to consider. The energy intensive Haber-Bosch process is no different, with expensive plants and high running costs, making it unavailable to the developing and third world nations.

One of the main purposes of industrial nitrogen fixation is the production of nitrogen based fertilisers. However, due to the high manufacturing costs commercially available fertilisers are expensive and are inaccessible to the world's less wealthy nations.

1.4.2 Biological Nitrogen Fixation

In contrast with industrial methods, biological nitrogen fixation is carried out at ambient temperatures and pressures by nitrogen fixing bacteria. Nitrogen fixing bacteria are responsible for the cycling of 10^8 tonnes of nitrogen per year and all contain the enzyme nitrogenase. The bacteria may be free living or symbiotic with some plants.

However, the action of nitrogenase is both complicated and relatively slow (**Equation 1.2**).

Equation 1.2

$$N_2 + 16MgATP + 8e^- + 8H^+ \longrightarrow 2NH_3 + 16MgADP + 16PO_4^{3-} + H_2$$

These reasons combined with the sensitivity of nitrogenase to oxygen rule out it's direct industrial use. It is therefore of great interest to develop a greater understanding of the mechanisms and the molecules involved in the biological fixation process in order to attempt to mimic the action of nitrogenase.

1.5 MOLYBDENUM NITROGENASE

The enzyme molybdenum nitrogenase is a binary enzyme consisting of two separate proteins[6], an iron molybdenum protein (MoFe) and a smaller iron protein (Fe). The larger MoFe protein contains two iron molybdenum cofactor[7] (FeMoco) units and four Fe_4S_4 p-clusters[8]. The action of nitrogenase, however, requires both the Fe and FeMo proteins together in the presence of a reducing agent and ATP (Adenosine triphosphate) to make the reduction of N_2 possible.

1.5.1 The MoFe protein

The MoFe- protein has been shown to have a molecular mass of approximately 240 KD. The protein is made up of two identical pairs of subunits and can be described as an $\alpha_2\beta_2$ tetromer, α and β subunits being respectively, 65 and 50 KD in mass. Analysis has shown the overall MoFe has been shown to contain 2 molybdenum atoms, 28-33 iron atoms and approximately 30 labile sulphur atoms[9-11].

The MoFe protein contains two distinct redox centres, the P-clusters and the FeMo-cofactor. The first low resolution crystallographic data[12] for the MoFe protein

showed the two FeMoco centres to be approximately 70Å apart while each P-cluster and FeMoco centre were separated by 19Å. This study was carried out on protein isolated from the bacteria *Clostridium pasteurianium* (Cp1). The relatively large distance between each FeMo-cofactor ruled out dinitrogen bridging the two active sites during it's reduction. A later refined crystal structure at 2.7Å resolution[13] of the MoFe protein from *azobacter vinelandi* (Av1), confirmed the separation of the two FeMoco sites and their relative separations from the P-clusters.

1.5.2 The FeMoco site

The FeMoco site is almost certainly the active site of nitrogen reduction within nitrogenase. In 1992 Rees and co-workers[13] solved the crystal structure of the of the MoFe protein of Av1 to 2.7Å resolution showing each FeMoco centre to consist of Fe_3S_4 and $MoFe_3S_3$ clusters bridged by three non-protein ligands. Two of the three bridging ligands were assigned as sulphides while the third bridge consisted of a ligand of relatively light electron density.

However, in 1993 Rees and co-workers further refined the structure of the MoFe protein of Av1 and Cp1 to 2.2Å resolution[14] (**Figure1.2**). The 2.2Å structure thus confirmed their previous structure for FeMoco, but showed all three bridging ligands to be sulphides.

Figure 1.2 Schematic representation of FeMoco structure of Av1[15] (2.2Å resolution)

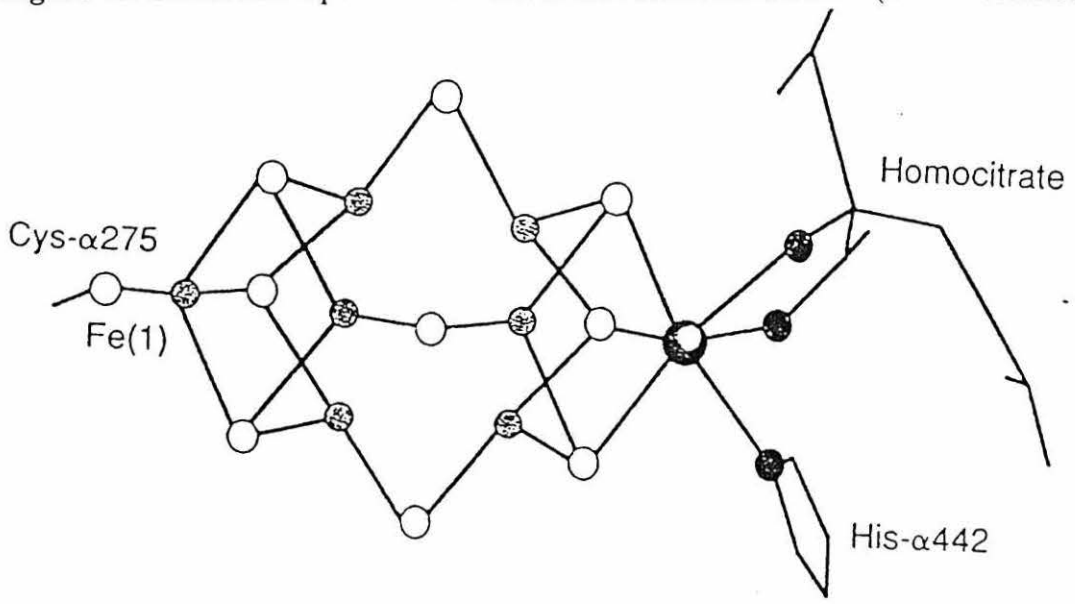

The molybdenum atom, situated at one end of the cluster, is coordinated to a homocitrate molecule *via* carboxylate and hydroxide oxygens, and to the imidazole nitrogen atom of α-His-442. At the other end of FeMoco, the terminal iron atom is bound to the thiolate sulphur of α-Cys-275. The structure of FeMoco poses a number of questions, one of which is the position and mode of binding of N_2 to the cluster.

Several modes of binding have been suggested other than nitrogen binding directly to the molybdenum atom of FeMoco. For example, it has been suggested that nitrogen may be bound within the cavity at the centre of the cluster. However, the cluster cavity in this configuration is too small to accommodate dinitrogen. Nitrogenase is also capable of reducing other larger substrates such as C_2H_2 and CNMe, which would almost certainly be too large for this "caged" mode of binding. It is therefore more likely that nitrogen is bound to either the molybdenum atom or one or more iron atoms of the cluster alone or some combination of these modes.

1.5.3 The P-Clusters

The second type of cluster contained within the MoFe protein are the P-clusters[16]. Based on crystal data the P-clusters are believed to consist of two Fe_4S_4 clusters bridged by two cysteine thiolate ligands[13,14]. These structures are best described as bridged double cubanes.

The P-clusters are buried some 12 Å below the protein surface and are situated between the α and β subunits. The clusters are bridged by cysteines α88 and β95 and are further attached to the protein by 5 amino acid linkages to the remaining iron sites (**Figure 1.3**). In total each cluster is attached to three α cysteine residues, three βcysteines and one serine β188. The purpose of the P-clusters is most probably that of electron transfer between the iron protein and the FeMoco site.

1.5.4 The Fe protein

The Fe protein is smaller than the MoFe protein with a molecular mass of approximately 60 KD and is extremely sensitive to dioxygen. It can be described as a dimer, that is it consists of two identical subunits but those subunits are different from those contained in the MoFe protein. The Fe protein has been shown to contain a metal content of 4S atoms and 4Fe atoms suggesting the presence of a cubane type structure.

Figure 1.3 Schematic representation of a P-cluster of Av1[15]

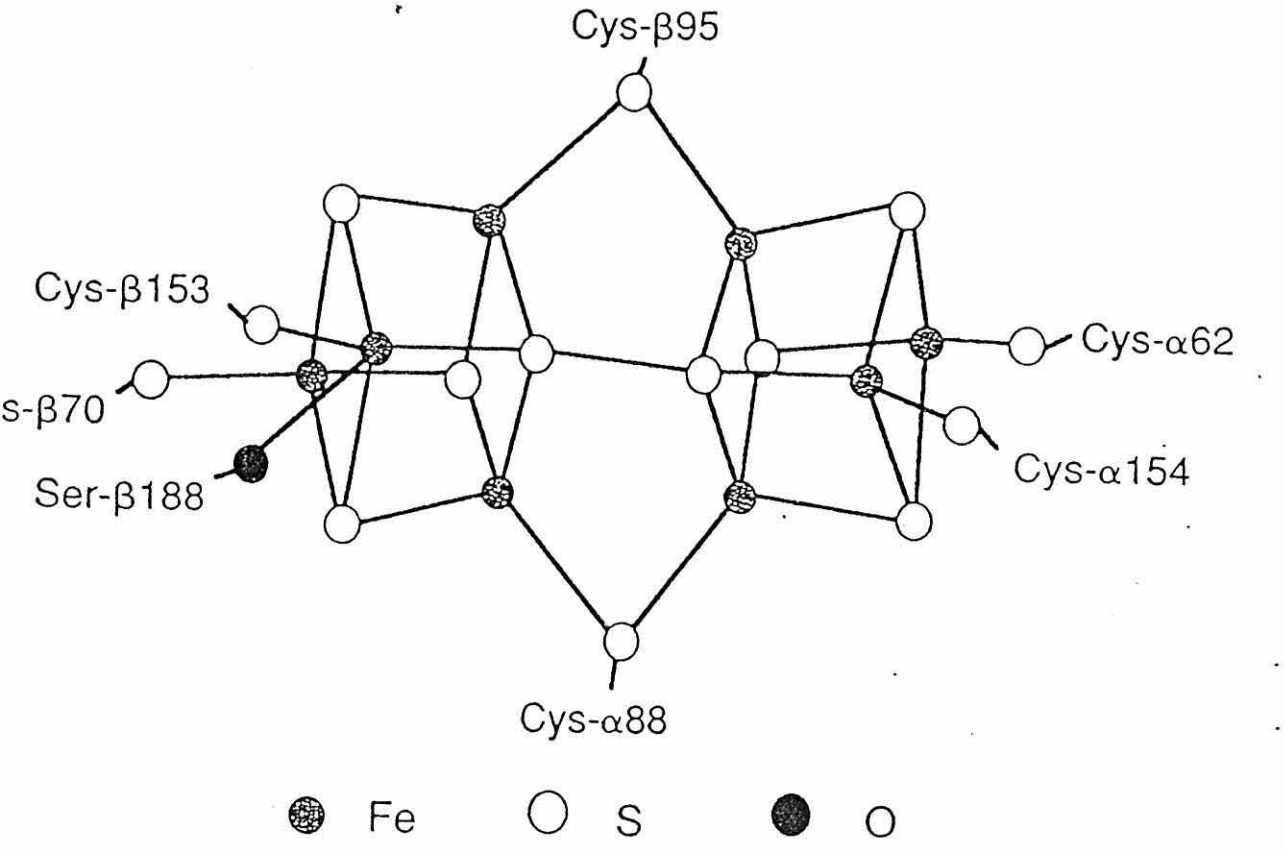

The crystal structure of the Fe protein of Av1 at 2.9 Å resolution[17] shows a single Fe_4S_4 cluster attached symmetrically to the two g subunits through cysteine residues 97 and 132[18,19]. The Fe protein transports electrons to the MoFe protein by acting as a one electron donor. This is carried out by the cluster converting between the +1 and +2 oxidation states. The protein also contains two binding sites for MgATP or MgADP. Both sites are at the interface of the two protein subunits. Upon binding the structure of the Fe protein is changed and hence the clusters redox potential, this may be an important part of the system of electron transfer to the MoFe protein. As well as its role in electron transfer the iron protein also plays an important part in the biosynthesis of the MoFe protein, being closely involved at several stages of its production.

1.5.5 Nitrogenase action.

The reduction of N_2 by nitrogenase involves the interaction of both Fe and MoFe proteins. Electrons are transferred from the Fe-protein to the MoFe-protein. This close interaction is made possible by two residues of the Fe-protein which are able to interact with the P-clusters of the MoFe-protein. Electrons from a reduced ferrodoxin or flavodoxin are transferred to the Fe-protein. Overall, reduction of nitrogen requires 8 electrons. The overall process of electron transfer is powered by the hydrolysis of MgATP to MgADP at the two nucleotide binding sites of the Fe-protein. Two molecules of ATP are hydrolysed for each electron transferred, therefore 16 molecules of MgATP are required (**Scheme 1.1**).

Scheme 1.1 Simple scheme of nitrogenase action

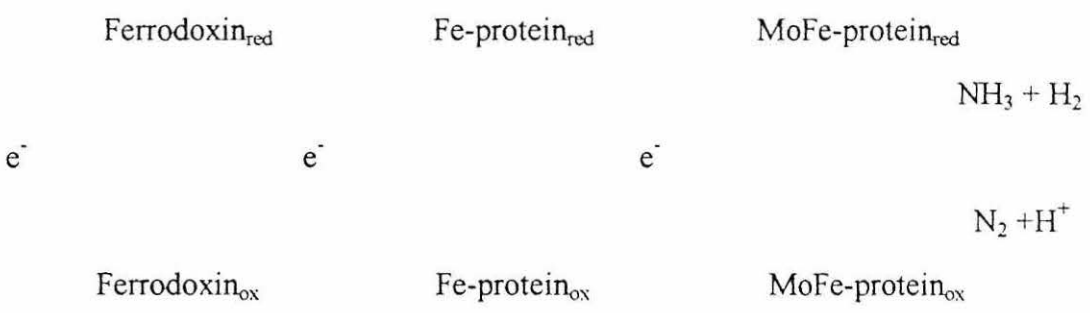

Extensive kinetic studies of the stages of electron transfer have been carried out by Lowe and Thorneley[20-22], resulting in the development of the Lowe-Thorneley scheme for nitrogenase function[23] (**Scheme 1.2**).

Scheme 1.2 Lowe-Thorneley scheme of nitrogenase function

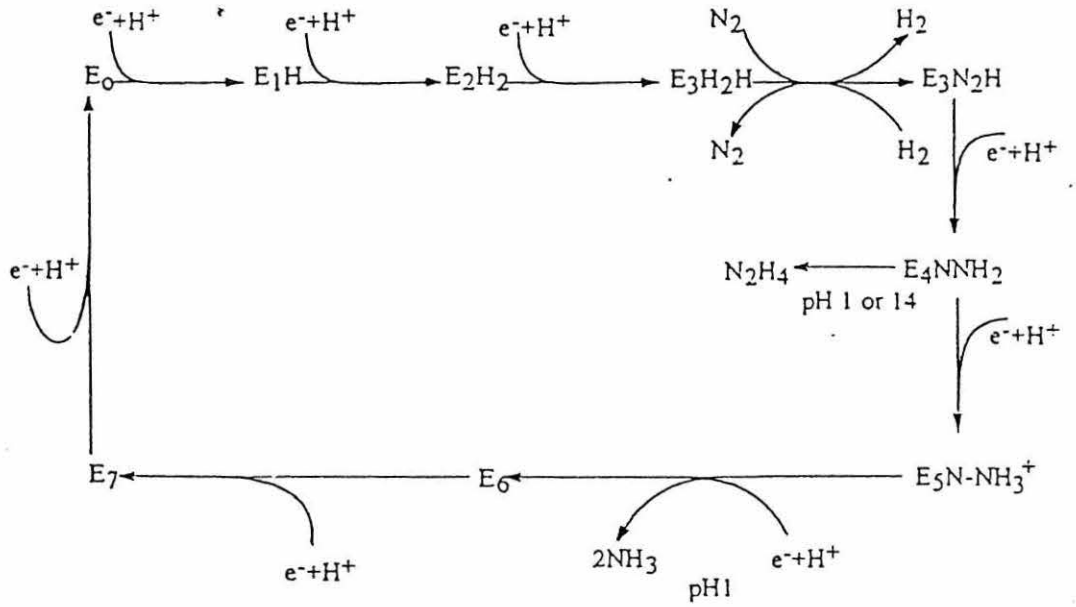

1.6 SEVEN-COORDINATE COMPLEXES OF MOLYBDENUM (II) AND TUNGSTEN (II)

1.6.1 Introduction

In the early 1960's there was much interest in the seven-coordinate halocarbonyls of molybdenum(II) and tungsten(II). The first seven-coordinate molybdenum(II) halocarbonyl complexes, $[MoX_2(CO)_3(diars)]$ (X = Br or I), were described in 1960 by Nyholm and co-workers[24]. The synthesis of $[MoX_2(CO)_3(diars)]$ involved the controlled oxidation of the previously substituted metal carbonyl $[Mo(CO)_4(diars)]$ with iodine or bromine.

A similar controlled oxidation of the analogous tungsten complex, $[W(CO)_4(diars)]$ gives two seven-coordinate products depending on the oxidising agent used. The reaction with bromine gave the seven coordinate tungsten(III) complex $[WBr_2(CO)_3(diars)]Br$, whilst the similar oxidation with iodine produces the tungsten (II) complex $[WI(CO)_4(diars)]I_3$.

It is also important to mention the pioneering work of Colton *et al*[25,26] on the dimeric complexes[{M(μ-X)X(CO)$_4$}$_2$] (M= Mo,W; X=Cl, Br, I), the metal in each of these complexes being seven-coordinate. The first complex of this type, [{Mo(μ-Cl)Cl(CO)$_4$}$_2$] was prepared in 1966[27] by the reaction of [Mo(CO)$_6$] with liquid chlorine at -78 °C. In the same year[28] the analogous bromo-bridged dimers, [{M(μ-Cl)Cl(CO)$_4$}$_2$] (M = Mo, W) were prepared by similar methodology.

The tungsten dihalide-bridged dimers [{W(μ-X)X(CO)$_4$}$_2$] (X=Cl, Br)[29] were prepared in a similar fashion to their molybdenum analogues. The X-ray crystal structure of [{W(μ-Br)Br(CO)$_4$}$_2$] has been determined[30] and shows each tungsten atom to be a *fac*-[WBr$_3$(CO)$_3$] octahedron with a capping carbonyl on the tricarbonyl face (**Figure 1.4**).

Figure 1.4 Crystal structure of [{W(μ-Br)Br(CO)$_4$}$_2$]

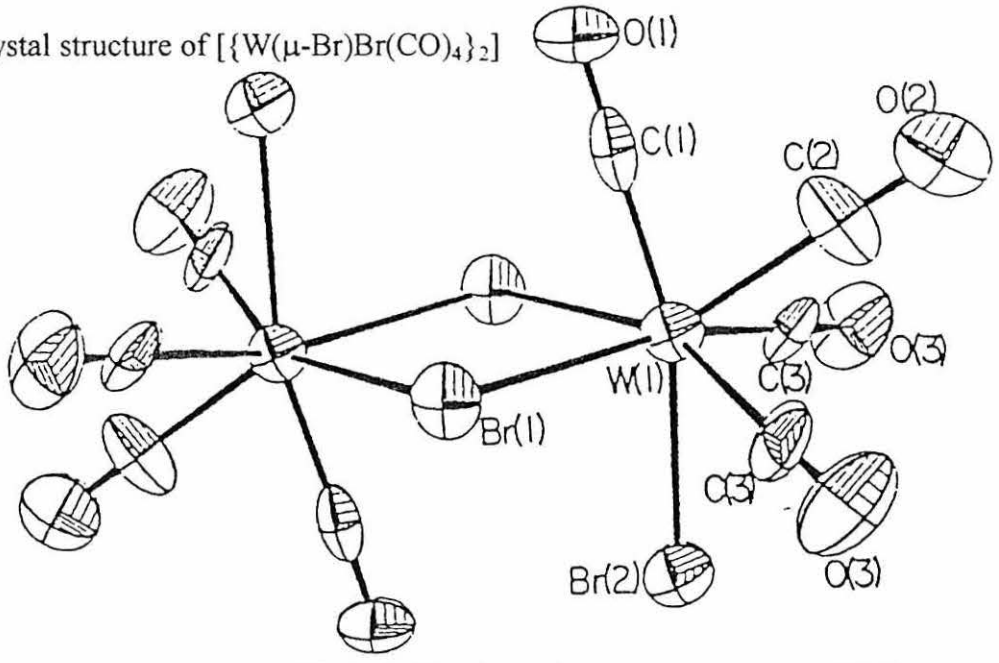

However, the analogous diiodo-bridged carbonyl complexes, [{M(μ-I)I(CO)$_4$}$_2$] (M= Mo,W) were prepared by the photochemical reaction of I_2 with [W(CO)$_6$] at ambient temperatures. Some examples of the wide range of reactions of these dihalide-bridged complexes[31-46] are shown in **Scheme 1.3**.

Scheme 1.3 Reactions of the complexes $[\{M(\mu\text{-}X)X(CO)_4\}_2]$ (M= Mo or W)

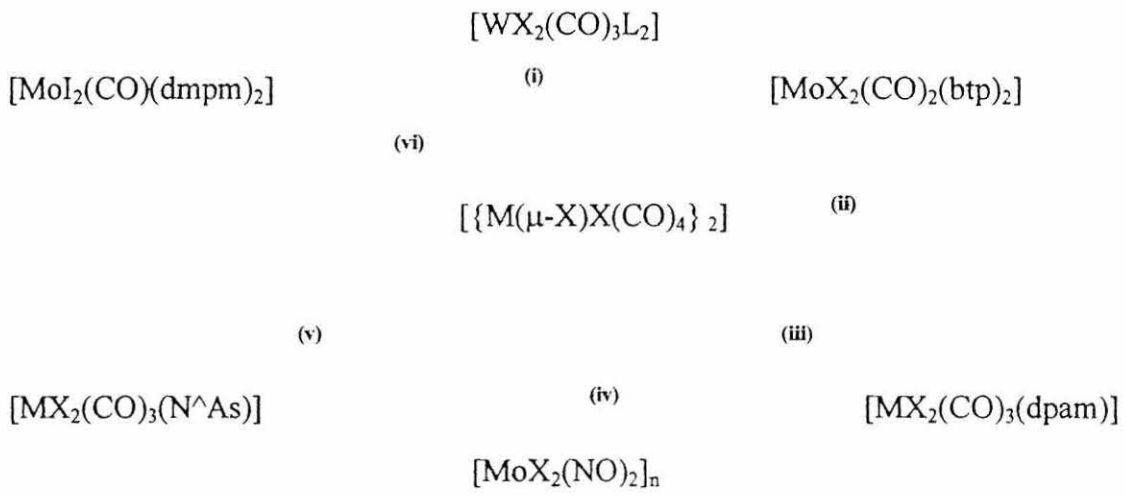

(I) X = Cl, Br; L = PPh_3, $AsPh_3$, $SbPh_3$.

(ii) X = Cl, Br; btp = N-n-butylthiopicolinamide.

(iii) X = Cl, Br; dpam.

(iv) X = Cl, Br; NO.

(v) X = Cl, Br; N^As = 8-dimethylarsinoquinoline.

(vi) dmpm (dmpm = bis(dimethylphosphino)methane.

1.6.2 Stuctures of seven-coordinate complexes

There are three main geometries for seven-coordinate complexes[47,48] :-

i) Pentagonal Bipyramid,

ii) Capped Octahedron,

iii) Capped Trigonal Prism.

All the above geometries involve the placing of seven ligands around the metal centre.

i) Pentagonal Bipyramid (PB)

A pentagonal bipyramid consists of five equatorial ligands and two axial ligands (**Figure 1.5**). The five equatorial ligands create a very crowded girdle around the metal and are not suited to bulky substituents. The equatorial positions are suited to tri, tetra and pentadentate ligands that are able to remain planar while occupying the equatorial girdle.

ii) Capped Octahedron (COct)

The capped octahedron consists of a distorted octahedron made up of six ligands with the seventh ligand "capping" one of the trigonal faces of the octahedron (**Figure 1.6**). A capped octahedral geometry is exhibited by many seven-coordinate halide complexes of Mo(II) and W(II).

Figure 1.5 Pentagonal Bipyramid (PB)

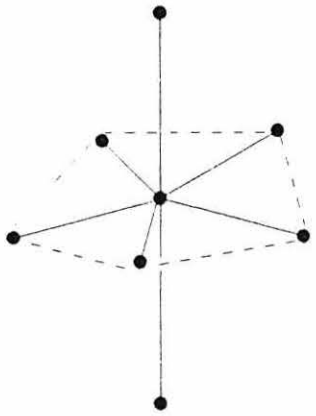

Figure 1.6 Capped Octahedron (COct)

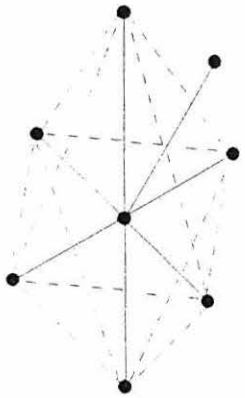

iii) Capped Trigonal Prism (CTP)

The capped trigonal prismatic geometry is the structure least frequently observed by seven-coordinate halocarbonyl complexes. It consists of a trigonal prism with six ligands at each vertice and a seventh ligand "capping" one of the rectangular faces of the prism (**Figure1.7**). As is the case with the COct geometry, the CTP is rarely found with bidentate donor ligands.

Figure 1.7 Capped Trigonal Prism (CTP)

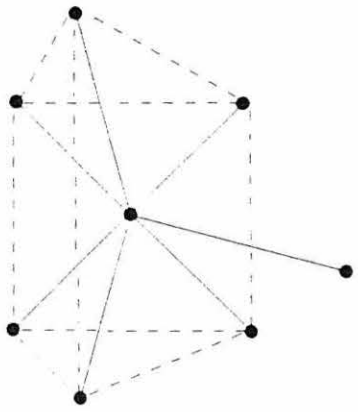

1.6.3 The synthesis of the seven-coordinate complexes $[MI_2(CO)_3(NCMe)_2]$ (M = Mo or W)

In 1962, Tate, Knipple and Augl[49], produced the zero-valent yellow complexes *fac*-$[M(CO)_3(NCMe)_3]$ (M = Mo or W) by refluxing the appropriate metal hexacarbonyl in an excess of acetonitrile. Further reaction of *fac*-$[W(CO)_3(NCMe)_3]$ with I_2 in methanol, produced a non-carbonyl containing product.

In 1986, Baker *et al*[50] refluxed the metal hexacarbonyls $[M(CO)_6]$ (M= Mo or W) in acetonitrile. The resulting yellow complexes *fac*-$[M(CO)_3(NCMe)_3]$ were

treated *in situ* with I_2 at 0°C, giving the brown seven-coordinate complexes $[MI_2(CO)_3(NCMe)_2]$ in quantitative yields .

The tungsten (II) complex $[WI_2(CO)_3(NCMe)_2]$ has been characterised by X-ray crystallography[51] and exhibits a capped octahedral geometry with a carbonyl group in the capping position. The remaining two carbonyls are *cis* to one another and with one iodide make up the capped face of the octahedron. The uncapped face, trans to the capping carbonyl is made up of the remaining iodide and both acetonitrile groups. The iodide groups are positioned *trans* to one another (**Figure 1. 5**).

The seven-coordinate complexes $[MI_2(CO)_3(NCMe)_2]$ (M= Mo or W) have been used as starting materials in the synthesis of over eighteen hundred new organometallic complexes[52]. Their versatility is mainly due to the presence of the two labile acetonitrile ligands which may be replaced with a wide range of monodentate and bidentate donor ligands (**Scheme 1. 4**).

Figure 1.5 Molecular structure of $[WI_2(CO)_3(NCMe)_2]$.

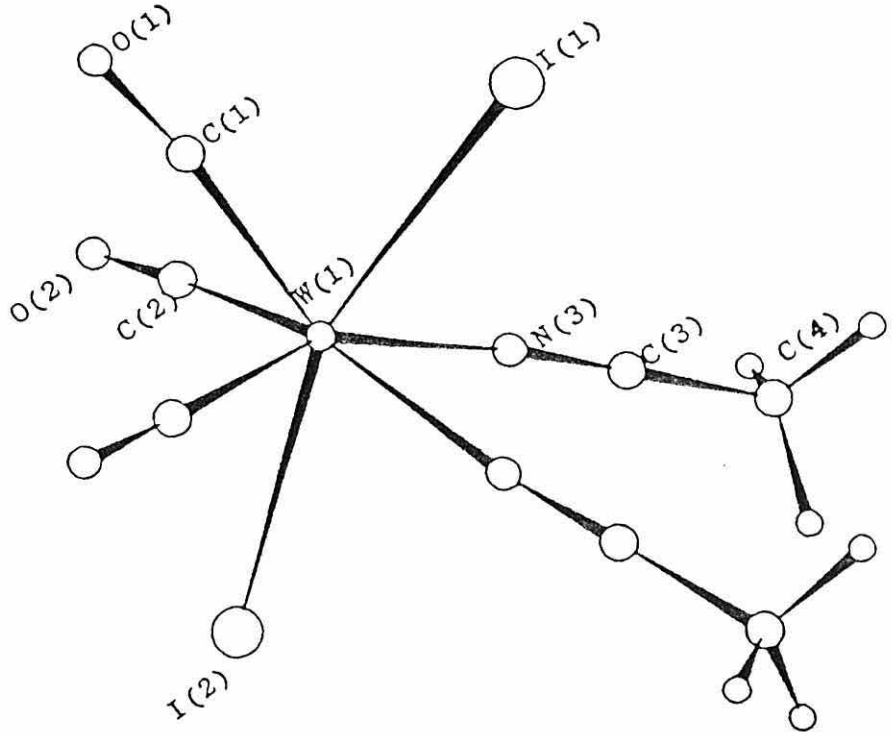

Scheme 1.4 Some reactions of the complexes $[MI_2(CO)_3(NCMe)_2]$ (M = Mo,W)

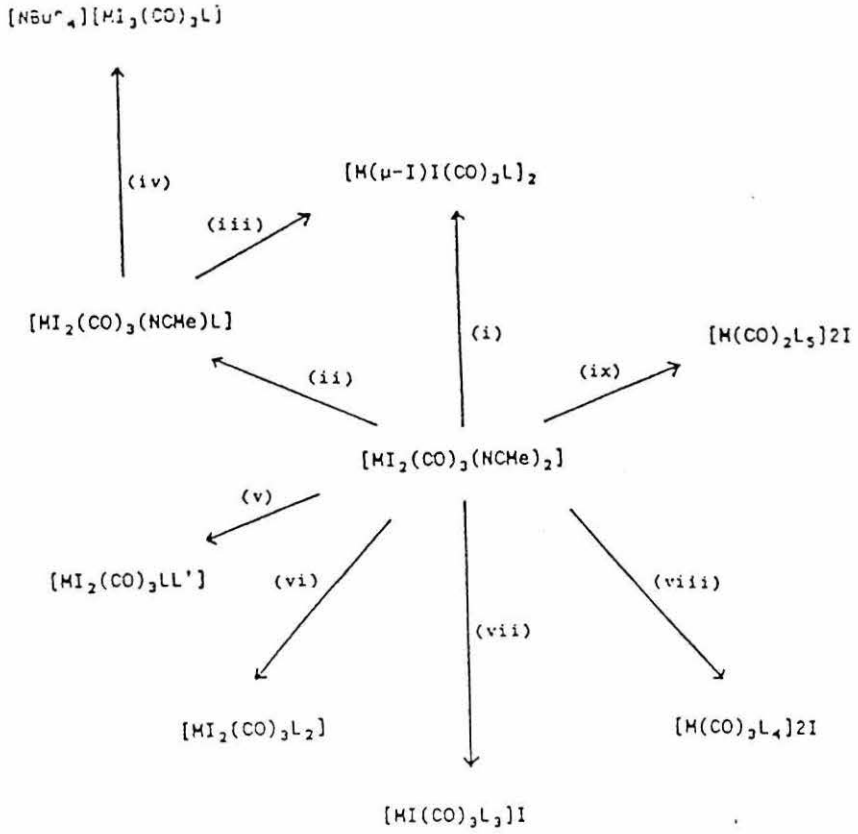

All reactions carried out in CH_2Cl_2 at room temperature. For (i) → (vii) and (ix), M = Mo or W. Reagents: (i) L = $OPPh_3$ for 30 s. (ii) L = $SPPh_3$ for 30 s. (iii) Stirring in CH_2Cl_2 for 24 h. (iv) L = $SPPh_3$; $[NBu_4^n]I$ for 45 min. (v) L' = PPh_3 (1 min), $AsPh_3$ (3 min) or $SbPh_3$ (5 min) followed by an *in situ* reaction with L = $OPPh_3$ or $SPPh_3$ for 18 h. (vi) 2L = $OPPh_3$ or $SPPh_3$ for 18 h. (vii) 2L = $OPPh_3$ or $SPPh_3$ for 2 h, followed by one further equivalent of L added *in situ* for 18 h. (viii) M = Mo, 2L = $SPPh_3$ for 2 h followed by two further equivalents of L added *in situ* for 18 h. M = W, 2L = $OPPh_3$ or $SPPh_3$ for 2 h followed by two further equivalents of L added *in situ* for 18 h. (ix) 2L = $OPPh_3$ for 2 h followed by three further equivalents of L added *in situ* for 18 h.

1.7 REACTIONS OF $[MI_2(CO)_3(NCMe)_2]$ (M = MO,W) WITH NEUTRAL SULPHUR DONOR LIGANDS

The following section describes some of the varied reactions of the seven coordinate complexes with both mono and polydentate sulphur donor ligands.

1.7.1 Reactions of $[MI_2(CO)_3(NCMe)_2]$ (where M=Mo or W) with monodentate neutral sulphur donor ligands

In 1990, Baker *et al* reported numerous triphenylphosphinesulphide seven-coordinate complexes of molybdenum and tungsten[53,54]. Over twenty complexes of this kind were made and some are shown in **Scheme 1.5**.

Other neutral sulphur ligands have been shown to bind to the seven-coordinate complexes $[MI_2(CO)_3(NCMe)_2]$ (where M= Mo or W) in a monodentate fashion. For example the tricyclohexylphosphinecarbondisulphide ligand can coordinate in either a monodentate or bidentate fashion to the metal centre (**Figure 1.6**).

Figure 1.6 Bidentate (a) and monodentate (b) coordination of the S_2CPCy_3 ligand

Scheme 1.5 Reactions of the complexes $[MI_2(CO)_3(NCMe)_2]$ with $SPPh_3$

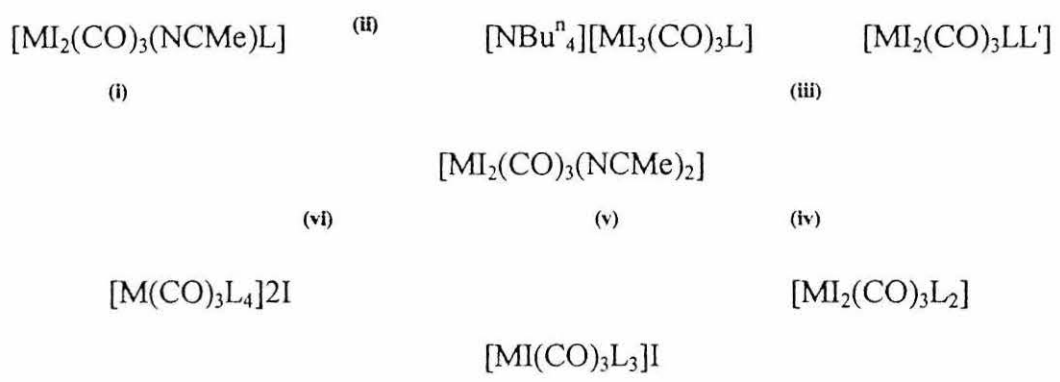

All reactions carried out in CH_2Cl_2 at room temp. For (i)-(v) , M= Mo or W. (i) L = $SPPh_3$, 30s. (ii) L = $SPPh_3$; $[NBu^n_4]I$, 45min. (iii) L = PPh_3, $AsPh_3$, $SbPh_3$; L' = $SPPh_3$, 18h. (iv) 2L = $SPPh_3$, 18hrs. (v) 2L = $SPPh_3$, 2h.,followed by L = $SPPh_3$, 18h. (vi) M= Mo, 2L = $SPPh_3$, 2h.,followed by 2L = $SPPh_3$, 18h.

The reaction of $[WI_2(CO)_3(NCMe)_2]$ with one equivalent of S_2CPCy_3 affords the complex $[WI_2(CO)_3(S_2CPCy_3)]$, however, the reaction of $[WI_2(CO)_3(NCMe)_2]$ with two equivalents of S_2CPCy_3 followed by one further equivalent of S_2CPCy_3 afforded the purple complex $[W(CO)_3(S_2CPCy_3)_3]2I$[55]. This complex has two S_2CPCy_3 ligands bound in a bidentate fashion and one monodentately to the metal centre. Eighteen related complexes have been made in a similar fashion.

Also the ligands thiourea (tu) or *N,N,N',N'*-tetramethylthiourea (tmtu) have been shown to react in a monodentate fashion with $[MI_2(CO)_3(NCMe)_2]$. The reaction of two equivalents of tu or tmtu with $[WI_2(CO)_3(NCMe)_2]$ afforded the complexes $[WI_2(CO)_3\{SC(NH_2)_2\}_2]$ and $[WI_2(CO)_3\{SC(NMe_2)_2\}_2]$ respectively[56]. However, similar reactions of tu or tmtu with $[MoI_2(CO)_3(NCMe)_2]$ afforded the dimeric iodide-bridged complexes $[Mo(\mu\text{-}I)I(CO)_2L_2]_2$ (L = tu or tmtu) involving the loss of a carbonyl ligand. The addition of one equivalent of tu or tmtu to

$[MI_2(CO)_3(NCMe)_2]$ afforded the iodide-bridged complexes $[\{M(\mu\text{-}I)I(CO)_3L\}_2]$ (L = tu or tmtu).

1.7.2 Reactions of $[MI_2(CO)_3(NCMe)_2]$ (where M= Mo or W) with polydentate neutral sulphur donor ligands

The following reactions of $[MI_2(CO)_3(NCMe)_2]$ with polydentate neutral sulphur donor ligands have been reported.

(I) Reactions of $[MI_2(CO)_3(NCMe)_2]$ with $RS(CH_2)_2SR$ (R= Ph, 4-MeC_6H_4 or 4-FC_6H_4)

The seven-coordinate complexes $[MI_2(CO)_3(NCMe)_2]$ (M= Mo or W) have been reported to react with a slight excess $RS(CH_2)_2SR$ of in dichloromethane at room temperature to give the seven-coordinate complexes $[MI_2(CO)_3\{RS(CH_2)_2SR\}]$[57]. The tungsten(II) complex $[WI_2(CO)_3\{4\text{-}MeC_6H_4S(CH_2)_2SC_6H_4Me\text{-}4\}]$ has been characterised by X-ray crystallography and exhibits a distorted capped octahedral geometry with a carbonyl ligand in the capping position (**Figure1.7**).

The reaction of $[WI_2(CO)_3(NCMe)_2]$ with two equivalents of $PhS(CH_2)_2SPh$ in dichloromethane at room temperature has been reported to give the light brown cationic complex $[WI(CO)_3\{PhS(CH_2)_2SPh\text{-}S\}\{PhS(CH_2)_2SPh\text{-}S,S'\}]I$. This may be reduced by $Li[Bu^n]$ in thf to give the zero valent complex *cis*- $[W(CO)_2\{PhS(CH_2)_2SPh\text{-}S,S'\}_2]$ in low yield.

Figure 1.7 Molecular structure of $[WI_2(CO)_3\{4\text{-}MeC_6H_4S(CH_2)_2SC_6H_4Me\text{-}4\}]$

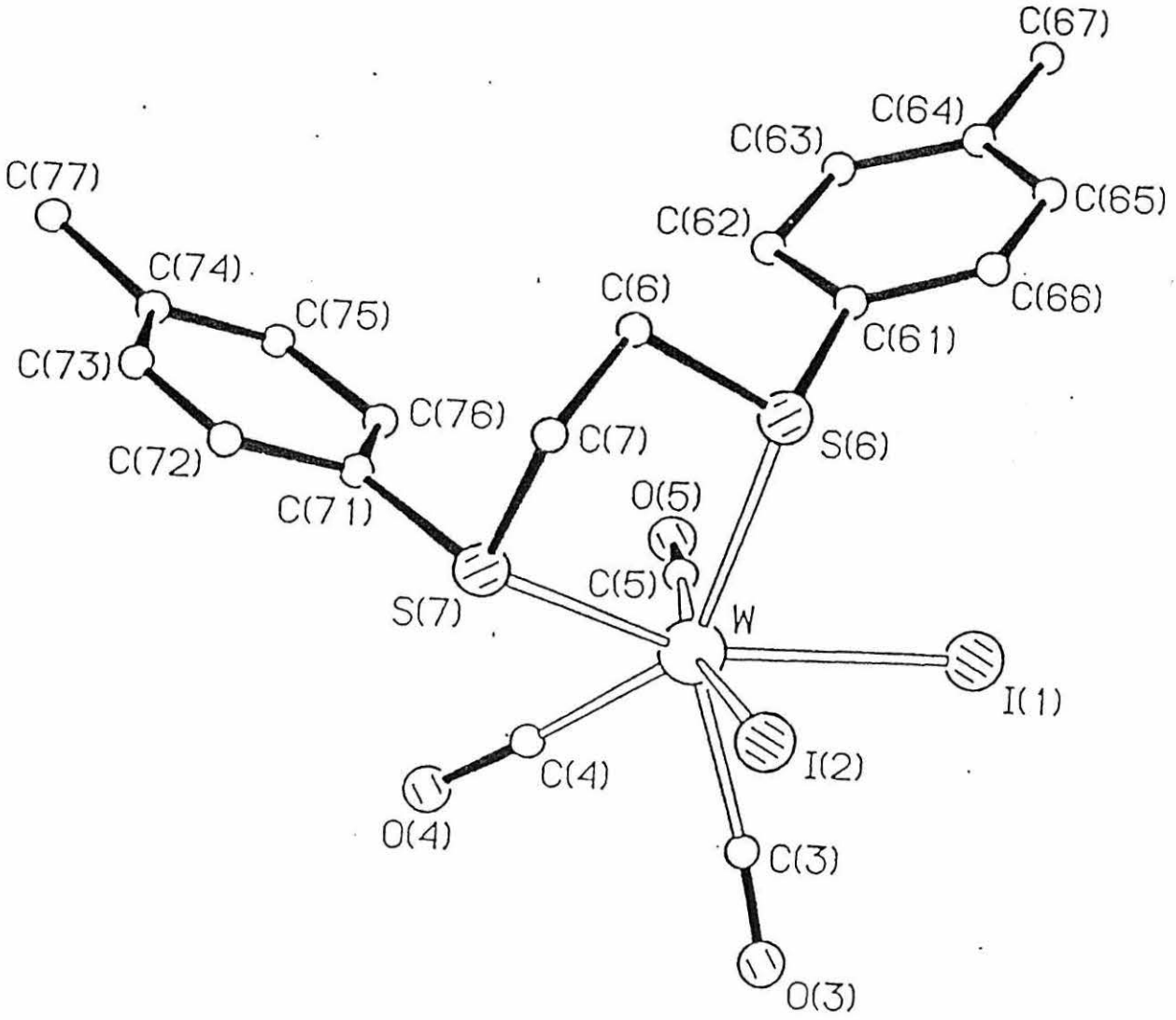

(ii) Reactions of $[MI_2(CO)_3(NCMe)_2]$ with $Ph_2P(S)CH_2P(S)Ph_2$

It has been reported that the complexes $[MI_2(CO)_3(NCMe)_2]$ (M= Mo or W) react with one equivalent of $Ph_2P(S)CH_2P(S)Ph_2$[58] in CH_2Cl_2 at room temperature giving the acetonitrile displaced products $[MI_2(CO)_3\{Ph_2P(S)CH_2P(S)Ph_2\}]$[59].

(iii) Reactions of $[MI_2(CO)_3(NCMe)_2]$ with $MeS(CH_2)_2S(CH_2)_2SMe$

The trithioether ligand, $MeS(CH_2)_2S(CH_2)_2SMe$, has been reported to react with the molybdenum(II) complex $[MoI_2(CO)_3(NCMe)_2]$ in a tridentate fashion, thus displacing both acetonitrile groups and a carbonyl, to give the complex $[MoI_2(CO)_2\{MeS(CH_2)_2S(CH_2)SMe\text{-}S,S',S''\}]$. The tungsten complex $[WI_2(CO)_3(NCMe)_2]$ reacts in a similar fashion to give the dicarbonyl complex $[WI_2(CO)_2\{MeS(CH_2)_2S(CH_2)_2SMe\text{-}S,S',S''\}]$[57]. However a tricarbonyl intermediate $[WI_2(CO)_3\{MeS(CH_2)_2S(CH_2)SMe\text{-}S,S'\}]$ has been isolated with the thioether behaving as a bidentate ligand with one sulphur hanging free. The molecular structure of $[WI_2(CO)_2\{MeS(CH_2)_2S(CH_2)_2SMe\text{-}S,S',S''\}]$ is shown in **Figure 1.8**.

(iv) Reactions of $[MI_2(CO)_3(NCMe)_2]$ with the trithiamacrocycles 1,4,7-Trithiacyclononane([9]aneS_3) and 2,5,8-Trithia-[9]-*o*-benzenophane (ttob)

The reactions of the seven-coordinate complexes $[MI_2(CO)_3(NCMe)_2]$ (M= Mo or W) with [9]aneS_3 in dichloromethane at room temperature have been reported to give the cationic complexes $[MI(CO)_3([9]aneS_3\text{-}S,S',S'')]I$. Reaction of $[WI(CO)_3([9]aneS_3\text{-}S,S',S'')]I$ with $Na[BPh_4]$ gave the crystallographically determined complex $[WI(CO)_3([9]aneS_3)][BPh_4]$ shown in **Figure 1.9.** Similar reactions with the ligand ttob gave the dicarbonyl molybdenum complex $[MoI_2(CO)_2(ttob\text{-}S,S',S'')]$ or the cationic tungsten complex $[WI(CO)_3(ttob\text{-}S,S',S'')][WI_3(CO)_4]$ respectively[60].

Figure 1.8 Molecular structure of $[WI_2(CO)_2\{MeS(CH_2)_2S(CH_2)_2SMe\text{-}S,S',S''\}]$

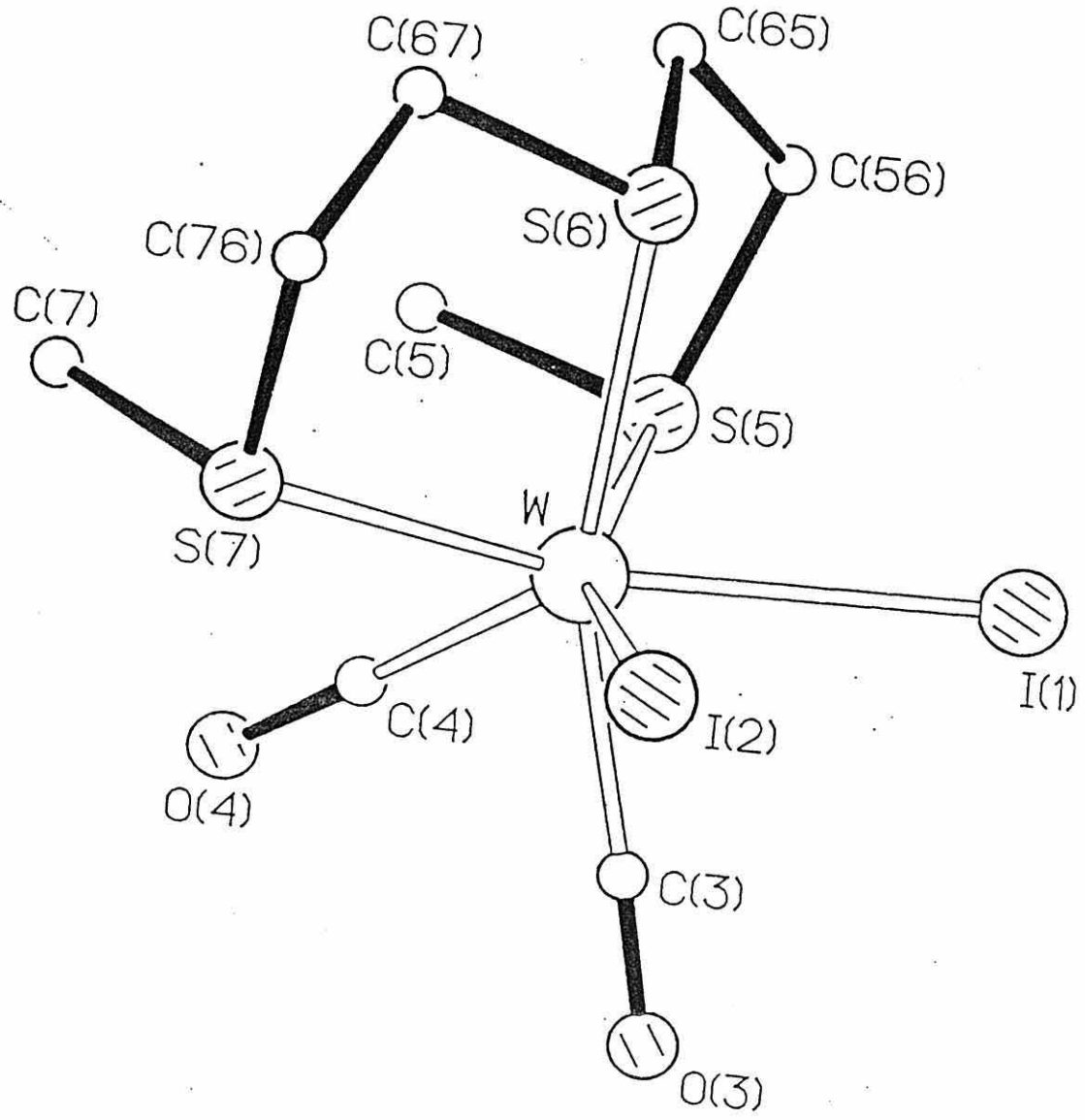

Figure 1.9 Molecular structure of [[WI(CO)$_3$([9]aneS$_3$-*S*,*S*',*S*'')][BPh$_4$]

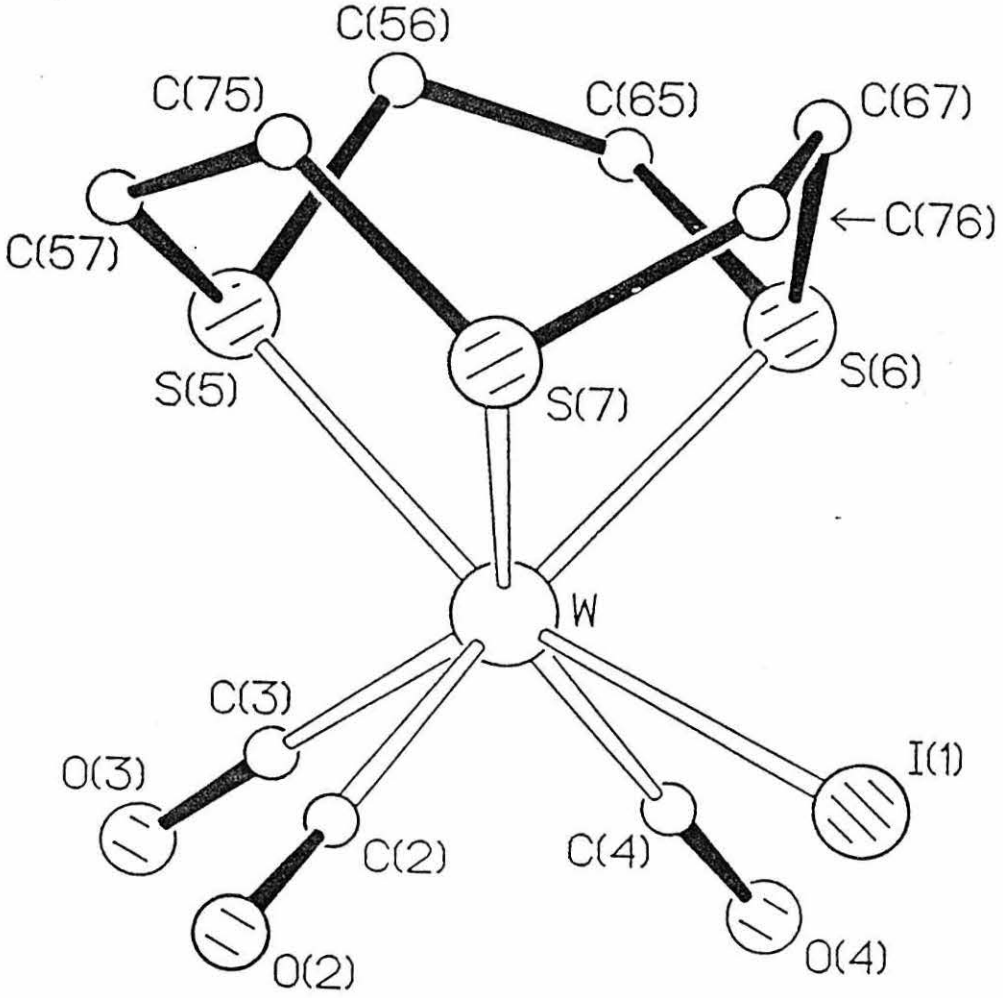

(v) Reactions of $[MI_2(CO)_3(NCMe)_2]$ with the tetrathiamacrocycles [12]aneS_4, [14]aneS_4, [16]aneS_4 and Me_8[16]aneS_4

Macrocyclic tetrathioethers (**Figure 1.10**) are able to react in several different ways with $[MI_2(CO)_3(NCMe)_2]$ (M = Mo or W), binding in either a bidentate, tridentate or tetradentate fashion[63].

Figure 1.10 Schematic representation of tetrathioether ligands and systematic nomenclature.

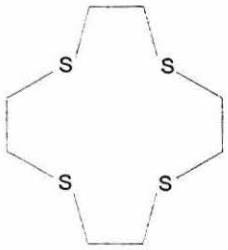

(a) [12]aneS_4

1,4,7,10-tetrathiacyclododecane

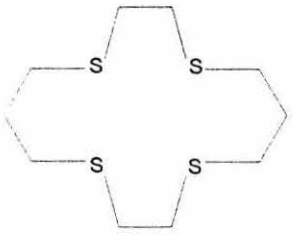

(b) [14]aneS_4

1,4,8,11-tetrathiacyclotetradecane

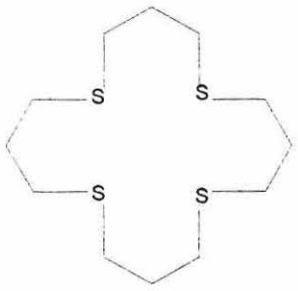

(c) [16]aneS_4

1,5,9,13-tetrathiacyclohexadecane

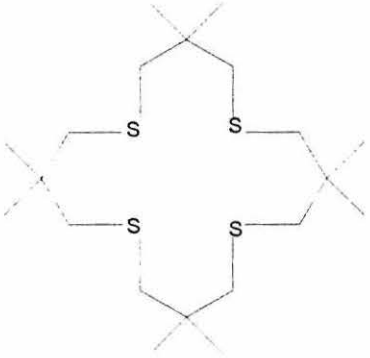

(d) Me_8[16]aneS_4

3,3,7,7,11,11,15,15-octamethyl-1,5,9,13-tetrathia-cyclohexadecane

For example, the reaction of two equivalents of $[WI_2(CO)_3(NCMe)_2]$ with one equivalent of Me_8[16]aneS_4 affords two seven-coordinate cation/anion complexes

$[WI(CO)_3\{Me_8[16]aneS_4\text{-}S,S',S'']][WI_3(CO)_4]$ and $[WI(CO)_2\{(Me_8[16]aneS_4\text{-}S,S',S'',S'''\}][WI_3(CO)_4]$. Both complexes exhibit a "piano-stool" geometry for the cation while the anions $[WI_3(CO)_4]^-$ exhibit a more usual capped octahedral geometry [61,62]. In both complexes we see $Me_8[16]aneS_4$ behaving as both a tridentate and a tetradentate ligand. The structure of $[WI(CO)_3\{Me_8[16]aneS_4\text{-}S,S',S'']][WI_3(CO)_4]$ is the first crystallographically characterised example whereby an S_4 thioether is bound in a tridentate fashion. The molecular structures of $[WI(CO)_3\{Me_8[16]aneS_4\text{-}S,S',S'']][WI_3(CO)_4]$ and $[WI(CO)_2\{(Me_8[16]aneS_4\text{-}S,S',S'',S'''\}][WI_3(CO)_4]$ are shown in **Figures 1.11 and 1.12** respectively. The analogous molybdenum reaction of two equivalents of $[MoI_2(CO)_3(NCMe)_2]$ with one equivalent of $Me_8[16]aneS_4$ affords the complex $[MoI(CO)_2\{Me_8[16]aneS_4\text{-}S,S',S'',S'''\}][MoI_3(CO)_4]$ however, no molybdenum tricarbonyl product is observed.

Figure 1.11 The molecular structure of $[WI(CO)_3\{Me_8[16]aneS_4\text{-}S,S',S'']][WI_3(CO)_4]$

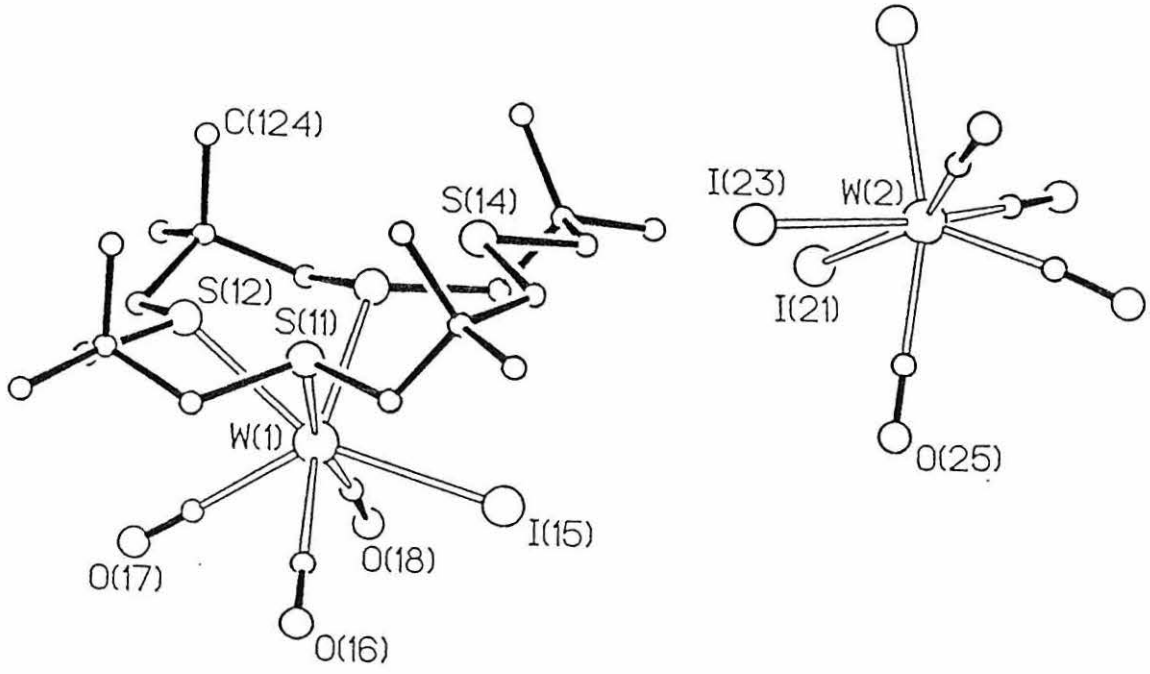

Figure 1.12 The molecular structure of $[WI(CO)_2\{(Me_8[16]aneS_4\text{-}S,S',S'',S'''\}]$ $[WI_3(CO)_4]$

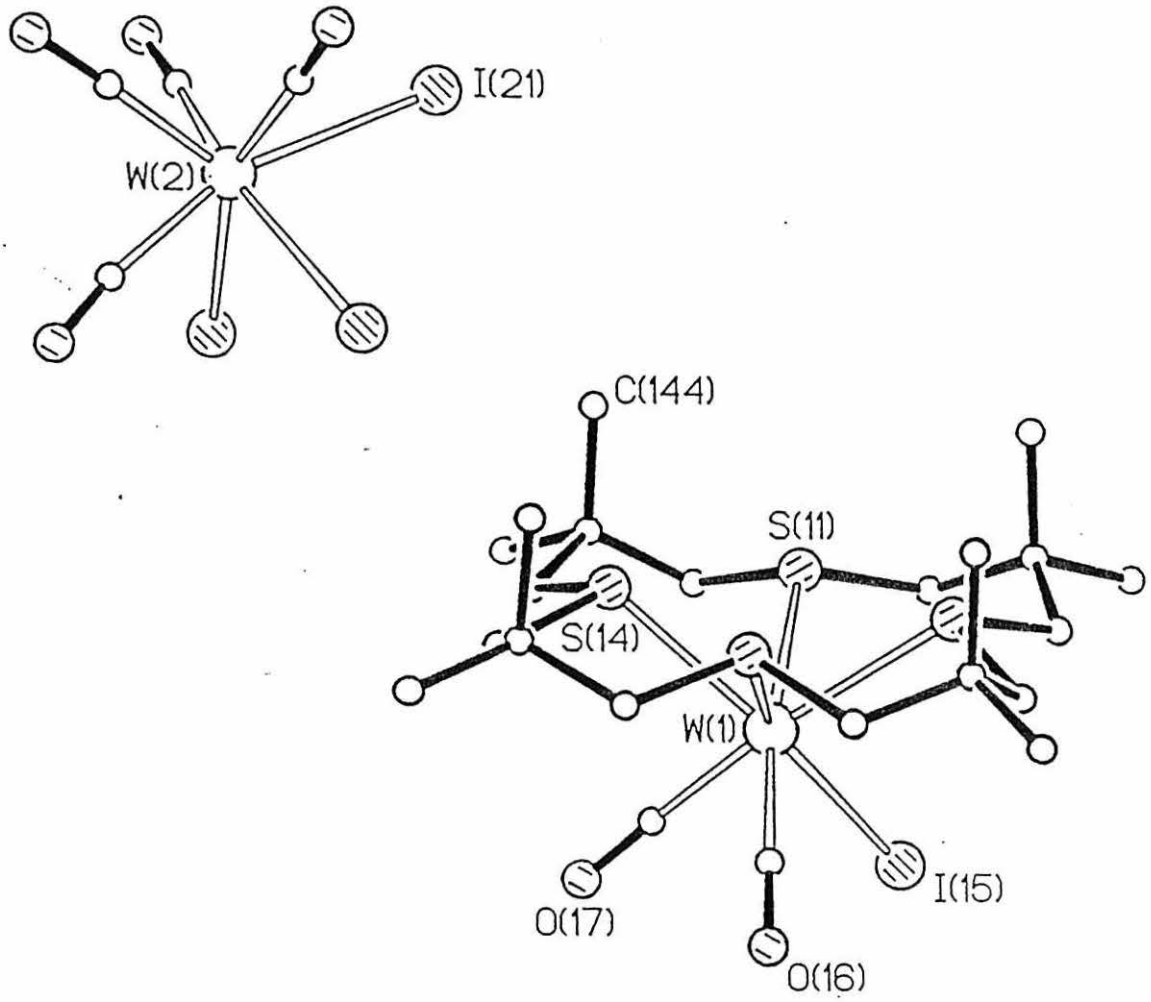

However, the reaction of equimolar amounts of $[MoI_2(CO)_3(NCMe)_2]$ and $[n]aneS_4$ (n = 16, 14 or 12) afford complexes of the type $[Mo_2I_4(CO)_6([n]aneS_4\text{-}S,S,'S'',S''')]$. The reaction of $[WI_2(CO)_3(NCMe)_2]$ with $[14]aneS_4$ affords the analogous tungsten complex $[W_2I_4(CO)_6[14]aneS_4\text{-}S,S,'S'',S''')]$. Here the ligand binds in a bidentate fashion to two metal centres creating bimetallic complexes *via* two bridging sulphur atoms[63].

1.8 REACTIONS OF $[MI_2(CO)_3(NCMe)_2]$ WITH ANIONIC SULPHUR DONOR LIGANDS

1.8.1 Reactions of $[MI_2(CO)_3(NCMe)_2]$ (M = Mo or W) with dithiocarbamate ligands

Numerous dithiocarbamate complexes have been prepared *via* the reactions of $[MI_2(CO)_3(NCMe)_2]$ and $[MI_2(CO)_3(NCMe)L]$ (L = PPh_3, $AsPh_3$, $SbPh_3$) and several different dithiocarbamate and related ligands[64-67]. For example, the complexes $[MI_2(CO)_3(NCMe)_2]$ react with one equivalent of $Na[S_2CN(CH_2Ph)_2]$ affords the iodo-bridged dimers $[\{M(\mu\text{-}I)(CO)_3[S_2CN(CH_2Ph)_2]\}_2]$. In these dimeric complexes the dithiocarbamate acts as a bidentate ligand attached to the metal *via* two metal-sulphur bonds. However, the reaction $[MI_2(CO)_3(NCMe)_2]$ with one equivalent of L (L = PPh_3, $AsPh_3$, $SbPh_3$) followed by one equivalent of $Na[S_2CNR_2]$ (R = Me, Et, or CH_2Ph) gave complexes of the type $[MI(CO)_3L(S_2CNR_2)]$, the dithiocarbamate again acting as a bidentate ligand. Further reaction of $[WI(CO)_3(PPh_3)(S_2CNR_2)]$ (R = Me, Et, or CH_2Ph) with one equivalent of $Na[S_2CNR'_2]$ gave the mixed-ligand complexes $[W(CO)_2(PPh_3)(S_2CNR_2)(S_2CNR'_2)]$ (R = Me, R' = Et; R = Me, R' = CH_2Ph; R = Et, R' = CH_2Ph) or the complex $[W(CO)_2(PPh_3)(S_2CNEt_2)_2]$. In both types of complex the dithiocarbamate is bound in a bidentate manner to the metal (**Figure 1.13**).

1.8.2 Reactions of $[MI_2(CO)_3(NCMe)_2]$ (M = Mo or W) with pyridine-2-thionate [pyS] and pyrimidine-2-thionate [pymS] ligands

Thionate ligands are able to adopt a number of binding modes to transition metal centres. For example, pyridine-2-thionate has been shown to bind in four main

ways [68-72], (i) monodentate *via* S, (ii) chelating *via* S,N, (iii) bridging via S,N, (iv) monodentate-S with weak M····N interaction.

Figure 1.13 Proposed structure of $[W(CO)_2(PPh_3)(S_2CNEt_2)_2]$

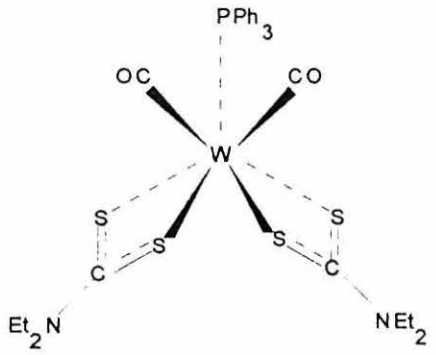

The reaction $[WI_2(CO)_3(NCMe)_2]$ with two equivalents of K[pymS] affords the bis(pymS) complex $[W(CO)_3(\eta^2\text{-pymS})_2]$ analogous to the $[W(CO)_3(\eta^2\text{-pyS})_2]$ complex previously reported by Deeming *et al*[73]. The structure of $[W(CO)_3(\eta^2\text{-pymS})_2]$ has been solved crystallographically, and is best described as a distorted monocapped trigonal prism with a carbonyl ligand in the capping position.. In this complex both thionate ligands are bidentate and are bound to the metal in a chelating-S,N type mode (**Figure 1.14**).

Other related complexes are prepared *via* the reaction of $[MI_2(CO)_3(NCMe)_2]$ with L (L = PPh_3, dppe) followed by one equivalent of K[pymS] *in situ* giving the complexes $[MI(CO)_3(PPh_3)(\eta^2\text{-pymS})]$ and $[MI(CO)_2(dppe)(\eta^2\text{-pymS})]$ (M = Mo or W) containing only one thionate ligand again bound to the metal centre in a bidentate fashion [74].

Figure 1.14 X-ray crystal structure of $[W(CO)_3(\eta^2\text{-pymS})_2]$

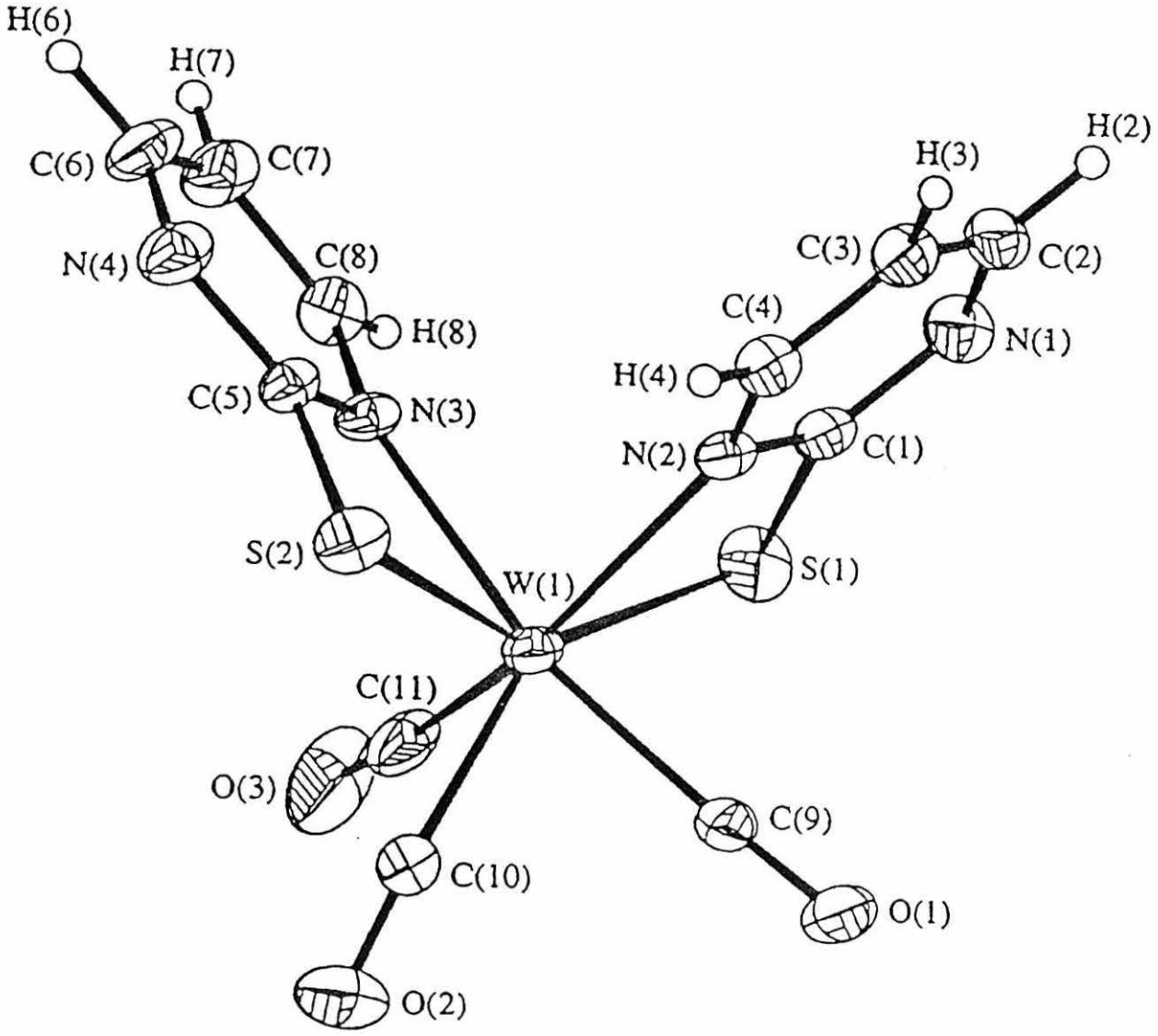

This thesis greatly extends the previous work described in **sections 1.7** and **1.8** of this introduction. Chapter two describes the reactions of $[MI_2(CO)_3(NCMe)_2]$ (M = Mo,W) with thiolate and acetylacetonato ligands. Chapter three describes the reactions of the seven-coordinate dibromo complexes $[MBr_2(CO)_3(NCMe)_2]$ (M = Mo,W) with thioether and disulphide ligands. Chapter four describes the reactions of the alkyne complexes $[MX_2(CO)(NCMe)(\eta^2\text{-}RC_2R)_2]$ (M = Mo, W; X= I, Br; R =Me, Ph) with both acyclic and cyclic thioether ligands. Chapter five describes the reactions of both $[MI_2(CO)_3(NCMe)_2]$ (M = Mo,W) and $[MI_2(CO)(NCMe)(\eta^2\text{-}RC_2R)_2]$ (M = Mo, W; R =Me, Ph) with the cubane-type cluster $[Fe_4Cp_4S_6]$. Finally, chapter six describes all the experimental procedures for chapters two to five.

CHAPTER 2:
Synthesis and characterisation of molybdenum(II) and tungsten(II) thiolate and acetylacetonato complexes.

CHAPTER 2: THE SYNTHESIS AND CHARACTERISATION OF MOLYBDENUM(II) AND TUNGSTEN(II) THIOLATE AND ACETYLACETONATO COMPLEXES

2.1 INTRODUCTION

Although a large number of six- and seven-coordinate complexes of molybdenum(II) and tungsten(II) have been described in the literature[33,37,65,67] very few complexes containing thiolate and dithiolate ligands have been reported. Although a the syntheses of a large number of complexes containing dithiocarbamates and related ligands have been reported[75-80]. Two examples of thiolate complexes of molybdenum(II) and tungsten(II) are, the anionic complex, $[Mo(CO)_2(tipt)_3]^-$ (tipt = triisopropylthiophenolate)[81] and the norbornadiene containing complex $[WBr(SC_6H_5)(CO)_2(\eta^4\text{-nbd})]$[82].

Hitherto, very few complexes containing anionic oxygen donor ligands have been reported. In 1986 the preparation and characterisation of $[MoBr(XOCR)(CO)_2(PPh_3)_2]$ (X = O, R = H, Me, Ph; X = S, R= Me, Ph)[83] Similarly the reactions of $[MCl_2(CO)_3L_2]$ with Na[acac] (acac = acetylacetonato) to give the seven-coordinate complexes $[MCl(CO)_2L'_2(LL)]$ (M = Mo or W; L' = PEt_3 or PPh_3; LL = acac) have been described by Templeton *et al*[84] . In more recent years Archer *et al*[85,86] have described the synthesis of the seven-coordinate complexes $[WCl(CO)_3(PPh_3)(dcq)]$, $[W(CO)_2(PPh_3)(dcq)_2]$ and $[WCl(CO)_2(PPh_3)_2(dcq)]$ (dcq = 5,7-dichloro-8-quinolato). In 1991, Baker *et al*[87] synthesised a similar series of seven-coordinate complexes of the type $[MI(CO)_3(PPh_3)(L\hat{}L)]$ and $[MI(CO)(PPh_3)_2(L\hat{}L)]$ (M = Mo or W; L^L = acac, hfacac and bzacac).

2.2 RESULTS AND DISCUSSION

2.2.1 Synthesis of the mono- and dithiolate ligands NaSPh and $Na_2[S(CH_2)_nS]$ (n = 2 or 3)

The symmetrical dithiolate ligands $Na_2[S(CH_2)_nS]$ (n = 2 or 3) were prepared by the reaction of sodium metal with the appropriate dithiol in THF. Tetrahydrofuran was used instead of more conventional solvents such as ethanol or methanol in order to stop the formation of alkoxide impurities. However, the dithiolates were formed much more slowly in THF than in ethanol. Removal of the solvent by vacuum distillation gave white crystalline solids which were suitably analytically pure and were used without further purification. However, the monothiolate ligand NaSPh was prepared by a similar reaction in ethanol. Similarly removal of the solvent by vacuum distillation gave an analytically pure white crystalline solid which was again used without further purification.

All of the thiolate ligands prepared were insoluble in chlorinated solvents, such as dichloromethane, and in diethyl ether and hexane. Due to their relative insolubility in suitable solvents the NMR data for the corresponding free thiols was used in further comparisons. The infra red spectra of the free thiolate ligands were of little significance due to the relatively weak intensity of the C-S stretching bands.

2.2.2 Reaction of the complexes $[WI_2(CO)_3(NCMe)_2]$ with two equivalents of PEt_3.

The reaction of the tungsten complex $[WI_2(CO)_3(NCMe)_2]$ with two equivalents of PEt_3 at room temperature gave the new seven-coordinate complex $[WI_2(CO)_3(PEt_3)_2]$ (**1**) in high yield. The complex was characterised by elemental analysis C, H, N, S (**Table 2.1**), IR spectroscopy ^1H and ^{13}C NMR (**Table 2.2-2.3**). The complex is orange-yellow in colour and is very soluble in chlorinated solvents such as dichloromethane and acetone. Unusually the complex is also soluble, to a lesser extent, in diethyl ether. The complex is fairly air-stable in the solid-state

being easily handled in air over a period of several minutes. It can be stored under nitrogen for several weeks without significant decomposition, but is more sensitive in solution.

The IR spectrum of $[WI_2(CO)_3(PEt_3)_2]$ (**1**) was also investigated. The clarity of the carbonyl resonances makes them very useful in providing information as to the bonding and structure of carbonyl complexes. The IR spectrum of complex (**1**) shows the expected distinctive three strong carbonyl stretches in CH_2Cl_2 which suggests a single isomer in solution. The spectra was also recorded as a KBr disk (**Table 2.2**) and again showed three carbonyl stretches in the solid state suggesting a similar structure to that in solution.

Crystals of suitable quality were grown by E.Parker[88] and complex (**1**) has been structurally characterised by X-ray crystallography. The molecular structure is shown in **Figure 2.1** together with the atomic numbering scheme. The solid state structure shows the complex to be capped octahedral with a carbonyl ligand in the capping position. The remaining two carbonyl ligands and one of the phosphines make up the capped face of the octahedron. The two phosphines are *trans*-to one another and the iodides are *trans*-to the two carbonyls in approximately the same plane.

2.2.3 Reactions of the complex $[WI_2(CO)_3(PEt_3)_2]$ with the dithiolate ligands $Na_2[S(CH_2)_nS]$ (n = 2 and 3).

The reaction of $[WI_2(CO)_3(PEt_3)_2]$ with one equivalent of the dithiolate ligands $Na_2[S(CH_2)_nS]$ (n = 2 and 3) in diethyl ether at room temperature gave the six-coordinate dicarbonyl complexes $[W\{S(CH_2)_2S\}(CO)_2(PEt_3)_2]$ (**2**) and $[W\{S(CH_2)_3S\}(CO)_2(PEt_3)_2]$ (**3**) in high yield. Both complexes have been characterised by elemental analysis C, H, N, S (**Table 2.1**), IR spectroscopy, ^1H and ^{13}C NMR (**Table 2.2-2.3**). Both complexes are red in colour and are very soluble in diethyl ether and chlorinated solvents. Conductivity measurements in acetone showed

the complexes to be non-electrolytes (result = 20 and 18 S cm^2 mol^{-1} respectively) (**Equation 2.1**).

Figure 2.1 Molecular Structure of $[WI_2(CO)_3(PEt_3)_2]$ (**1**)[88]

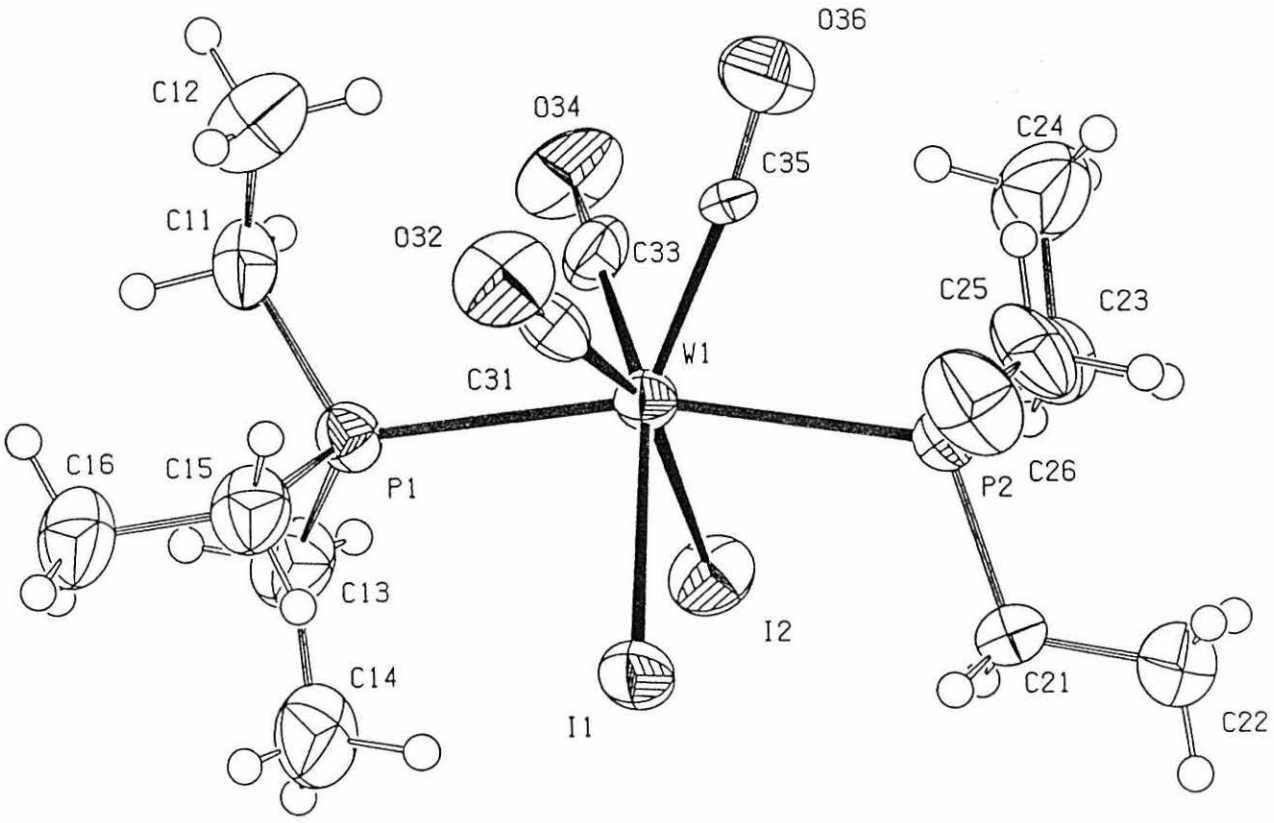

Equation 2.1 Equation used to calculate molar conductance (Λm)

$$\Lambda m = \frac{\text{cell constant x conductance x } 10^{-6} \text{ x molecular weight x Volume}}{\text{mass x } 10^{-3}}$$

Units
volume = cm3
mass = mg
Λ_m = S cm^2 mol^{-1}

conductance = S (Ω^{-1})

Some reference conductivity values (S cm^2 mol^{-1})in common solvents

Solvent:	1:1 electrolyte	2:1 electrolyte
CH_3NO_2	75 - 95	150 - 180
$PhNO_2$	20 - 30	50 - 60
acetone	100 - 140	160 - 200
acetonitrile	120 - 160	220 - 300
dmf	65 - 90	130 - 170

The IR spectra of the complexes (**2**) and (**3**) both show two strong carbonyl bands in CH_2Cl_2 which suggests a single isomer in solution. The spectra were also recorded as a KBr disks (**Table 2.2**), and again showed two carbonyl stretches corresponding to two *cis*-carbonyl groups attached to the tungsten centres, suggesting a similar structure to that in solution. The capping carbonyl band observed for complex (**1**) at 2012cm^{-1} is no longer present. This is supported by the crystal structures (Figures **2.2** and **2.3**) which show the presence of two *cis*-carbonyls in the solid state. The stretching frequencies of the remaining two carbonyl ligands in both complexes are lower than the corresponding carbonyls of complex (**1**). This is most likely due to the loss of the third carbonyl ligand resulting in greater electron density at the tungsten centre and more π-bonding between the metal and the remaining two carbonyl ligands.

Both complexes (**2**) and (**3**) have been structurally characterised by X-ray crystallography and the structures are shown in Figures **2.2** and **2.3** with the atomic numbering schemes. The tungsten centres of both complexes have very similar distorted octahedral geometries with *cis*-carbonyl ligands and *trans*-phosphines. Atomic coordinates and selected bond lengths can be found in **Tables A1.1** and **A1.2** in **Appendix 1**.

The structures of both complexes (**2**) and (**3**) compared with the structure of the seven coordinate complex (**1**) show the sulphur atoms of the dithiolate ligands have replaced the *cis*-iodides and the capping carbonyl has been lost. Also the *trans*-phosphine ligands now incline towards the remaining two carbonyl ligands rather than away from them as in complex (**1**). Both structures (**2**) and (**3**) are isomorphous, exhibiting a trigonal prismatic structure with twist angles of 13.7 and 13.2° respectively between the two triangular faces of the prism. This is in comparison to a twist angle of 60° for the octahedral geometry and 0° for the ideal trigonal prism[89,90].

The ^{1}H NMR spectra of complexes (**2**) and (**3**) are consistent with the structures shown in Figures **2.2** and **2.3**. The ^{1}H NMR spectra of complex (**2**) shows a singlet at δ = 2.6 ppm which corresponds to the two CH_2 groups of the bound ethanedithiolate which have equivalent protons. However, the spectra of complex (**3**) shows a triplet at δ = 2.6 ppm which corresponds to the two CH_2 groups closest to the sulphur atoms of the bound propanedithiolate which are coupled to the single central CH_2 group of the ligand. The resonance for the central CH_2 group is hidden under the ethyl resonance of the phosphine at ca. δ = 2.3 ppm. The $^{13}C\{^{1}H\}$ NMR (CD_2Cl_2, 25 °C) of complexes (**2**) and (**3**) are very similar suggesting very closely related structures in solution. Both complexes show a carbonyl resonance at δ = 236 ppm which corresponds to the cis-carbonyl ligands. The resonance is observed as a triplet which is due to coupling to the two phosphorus atoms of the triethylphosphine ligands. This suggests the two carbonyl ligands are equivalent at ambient temperatures.

Figure 2.2 X-ray crystal structure of the complex $[W\{S(CH_2)_2S\}(CO)_2(PEt_3)_2]$(**2**) Thermal ellipsoids shown at 30% probability.

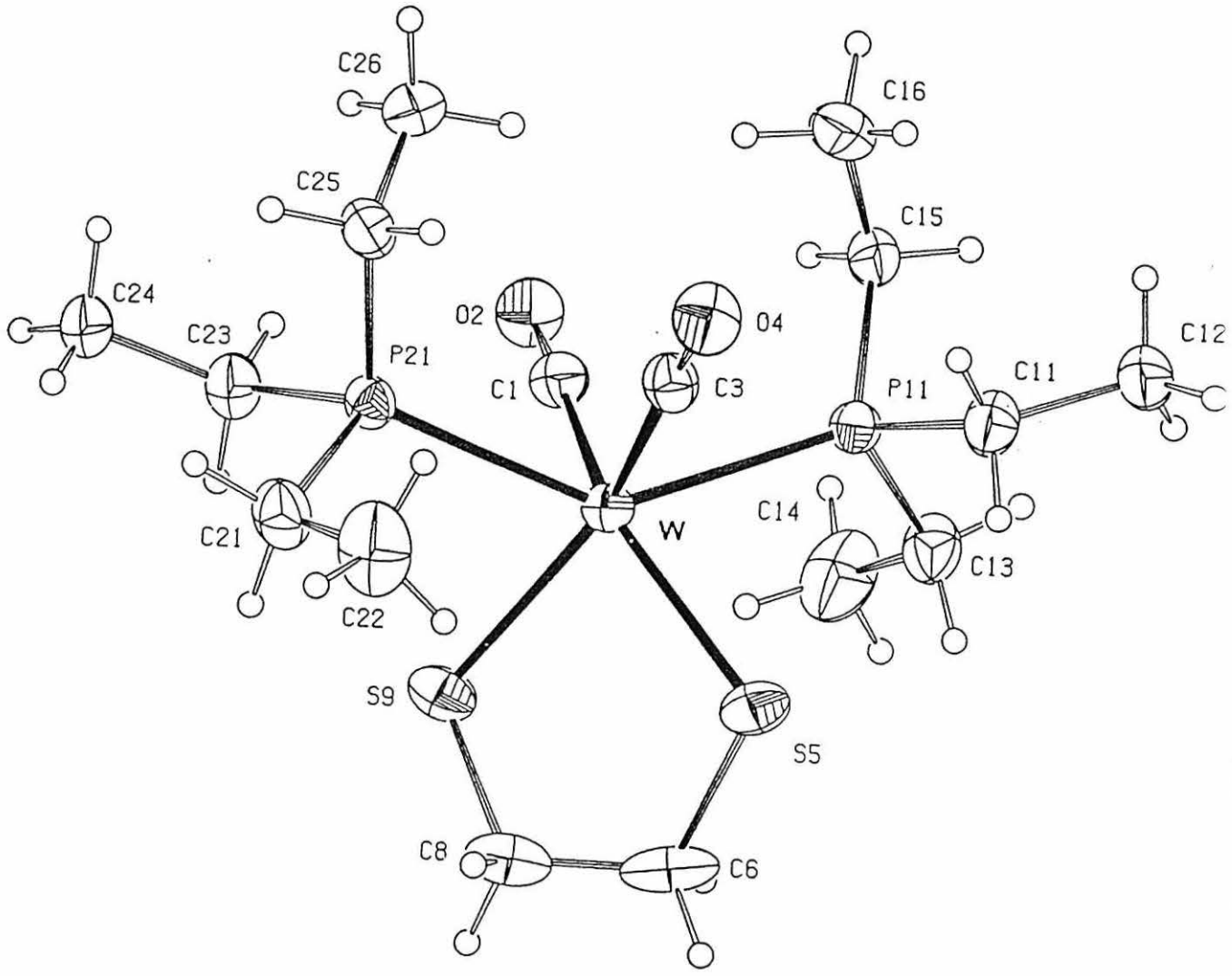

Figure 2.3 X-ray crystal structure of the complex $[W\{S(CH_2)_3S\}(CO)_2(PEt_3)_2]$(**3**) Thermal ellipsoids shown at 30% probability.

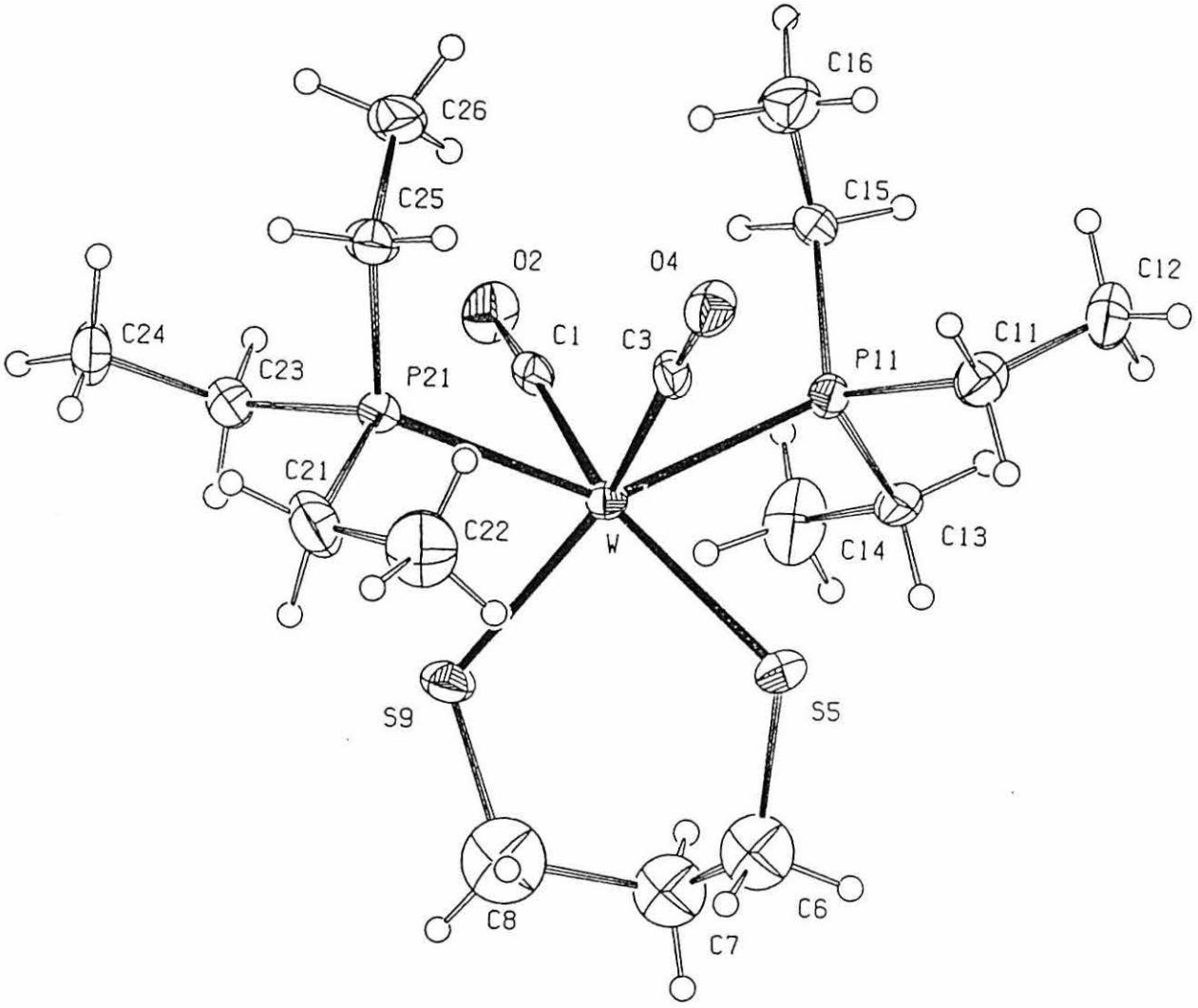

Finally, attempts to introduce a third carbonyl ligand by saturation of solutions of complexes (**2**) and (**3**) in dichloromethane with carbon monoxide were unsuccessful.

2.2.4 Reaction of the complex $[WI_2(CO)_3(PEt_3)_2]$ with two equivalents of NaSPh

The reaction of $[WI_2(CO)_3(PEt_3)_2]$ with two equivalents of NaSPh in diethyl ether at room temperature gave the six-coordinate dicarbonyl complex $[W(SPh)_2(CO)_2(PEt_3)_2]$ (**4**) in reasonable yield. The complex has been characterised by elemental analysis C, H, N, S (**Table 2.1**), IR spectroscopy, ^1H and ^{13}C NMR (**Table 2.2-2.3**). The complex (**4**) is green in colour and is very soluble in diethyl ether and chlorinated solvents. Conductivity measurements in acetone showed the complex to be a non-electrolyte (result = 23 S cm^2 mol^{-1} respectively) (**Equation 2.1**).

The IR spectrum of the complex (**4**) showed only one strong carbonyl stretch in CH_2Cl_2 which suggests a single isomer in solution. The spectrum was also recorded as a KBr disk (**Table 2.2**), and again showed one carbonyl stretch suggesting a similar structure to that in solution and corresponding to two *trans*-carbonyl groups attached to the tungsten centre. The capping carbonyl band observed for complex (**1**) is again no longer present. This is supported by the crystal structure (Figure **2.4**) which shows the presence of two *trans*-carbonyls in the solid state.

Complex (**4**) has been structurally characterised by X-ray crystallography and it's structure is shown in **Figure 2.4** with the atomic numbering scheme. The tungsten centre has an octahedral geometry which is much less distorted than those of complexes (**2**) and (**3**) shown previously. Complex (**4**) exhibits a crystallographic centre of symmetry, complex (**4**) has *trans*-carbonyl ligands but retains the *trans*-phosphines. Atomic dimensions are; to the carbonyl groups 2.04(3)Å, to the triethylphosphines 2.563(6)Å and to the phenylsulphides 2.402(5)Å. The *cis*-angles of the structure are all within 5.2° of 90°.Atomic coordinates and selected bond lengths can be found in **Table A1.3** in **Appendix 1**.

The ^1H NMR spectrum of complex (**4**) is consistent with the structure shown in Figures **2.4**. The $^{13}C\{^1H\}$ NMR (CD_2Cl_2, 25 °C) shows a carbonyl resonance at δ =

228 ppm which corresponds to the *cis*-carbonyl ligands. This suggests the two carbonyl ligands are equivalent at ambient temperatures.

2.2.5 Reaction of the complex $[MoI_2(CO)_3(PEt_3)_2]$ with the dithiolate ligand $Na_2[S(CH_2)_2S]$

The reaction of $[MoI_2(CO)_3(PEt_3)_2]$ with one equivalent of the dithiolate ligand $Na_2[S(CH_2)_2S]$ in diethyl ether at room temperature gave the six-coordinate dicarbonyl complexes $[Mo\{S(CH_2)_2S\}(CO)(PEt_3)_2]$ (**5**) in high yield. The complex has been characterised by elemental analysis C, H, N, S (**Table 2.1**), IR spectroscopy and ^1H NMR (**Tables 2.2-2.3**). The complex is red in colour, and is very soluble in diethyl ether and chlorinated solvents. As previously with the analogous tungsten complex (**2**), complex (**5**) is a non electrolyte in acetone (**Equation 2.1**).

The IR spectrum of the complex (**5**) was recorded as a KBr disk and showed four strong carbonyl stretches (**Figure 2.5**) suggesting two isomeric products in the solid state. The capping carbonyl band observed for complex (**1**) is again no longer present.

Complex (**5**) has been structurally characterised by X-ray crystallography and it's structure is shown in **Figure 2.6** with the atomic numbering scheme. The molybdenum centre has a trigonal prismatic structure isomorphous to those of the previously described tungsten complexes (**1**) and (**2**). Atomic coordinates and selected bond lengths can be found in **Table A1.4** in **Appendix 1**.

Figure 2.4 X-ray crystal structure of the complex $[W(SPh)_2(CO)_2(PEt_3)_2]$ (**4**)
Thermal ellipsoids shown at 30% probability.

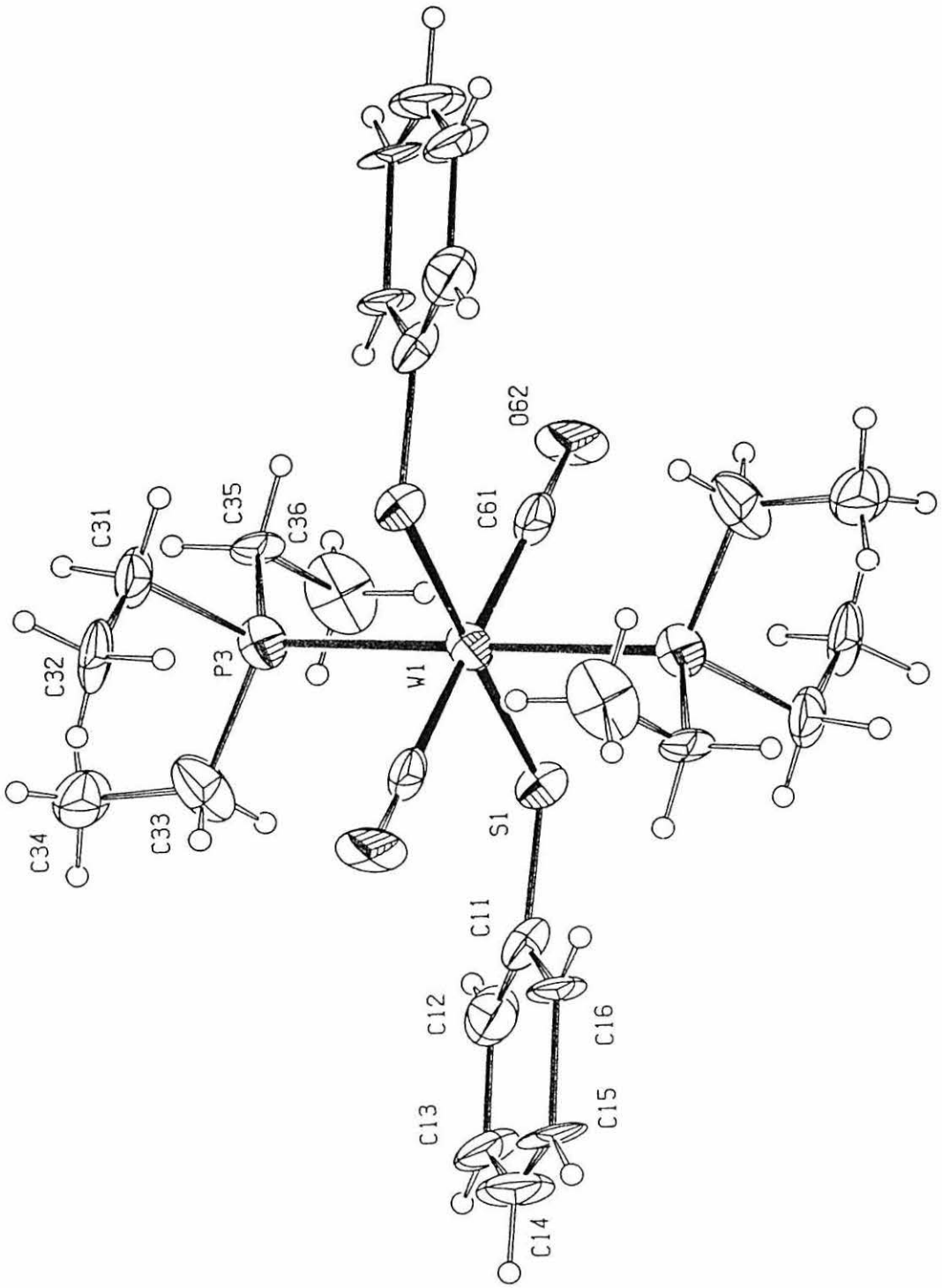

Figure 2.5 IR spectrum of $[Mo\{S(CH_2)_2S\}(CO)_2(PEt_3)_2]$ (**5**) in the carbonyl region

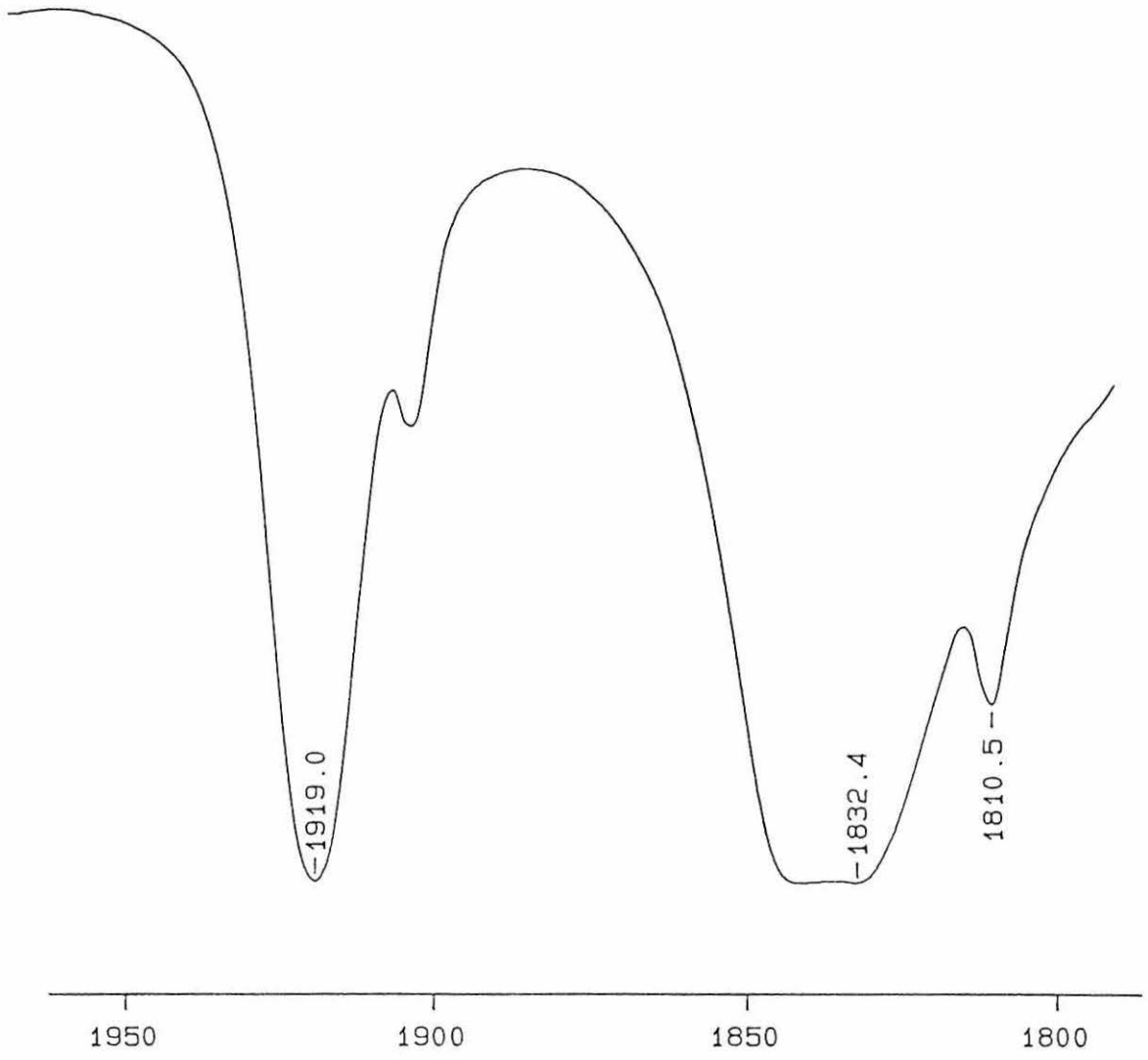

Figure 2.6 X-ray crystal structure of the complex $[Mo\{S(CH_2)_2S\}(CO)_2(PEt_3)_2]$(**5**)
Thermal ellipsoids shown at 30% probability.

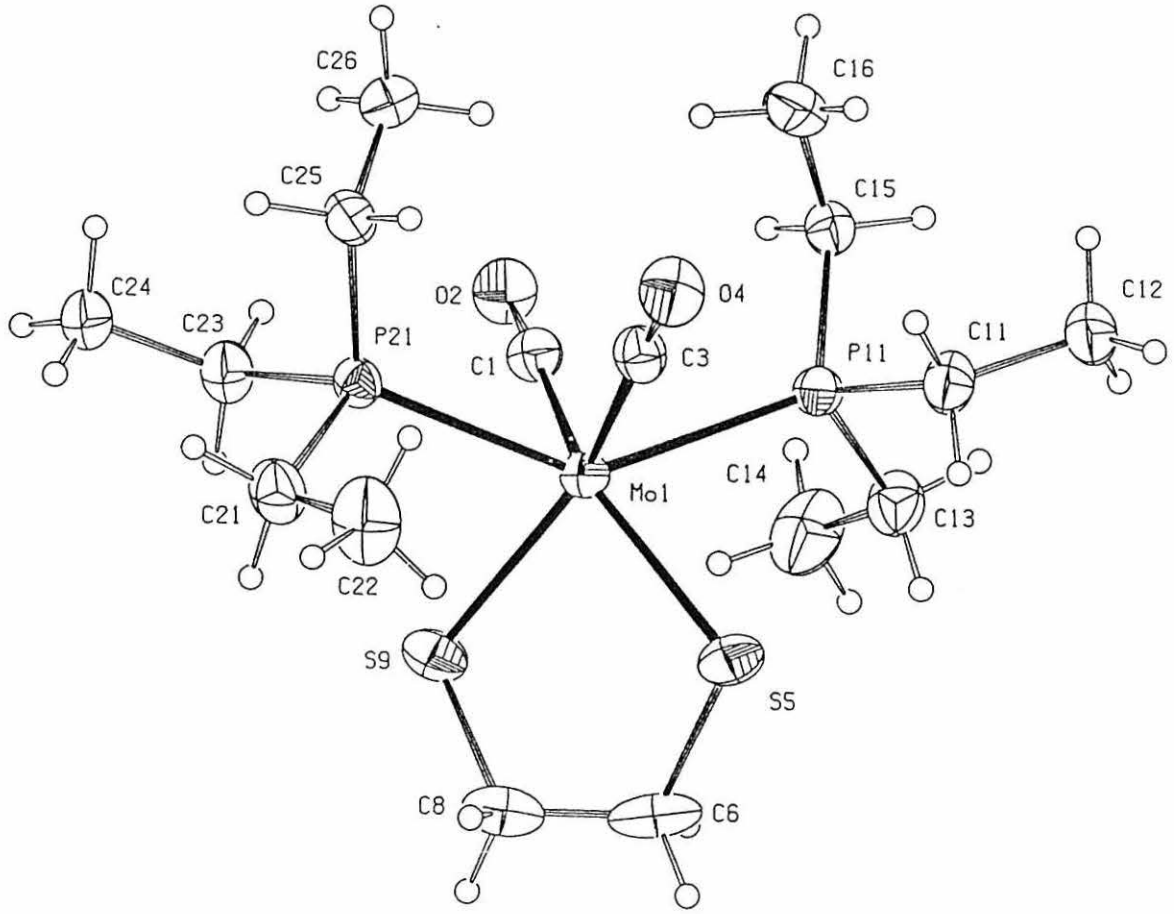

2.3 THE SYNTHESIS OF SEVEN-COORDINATE ACETYLACETONATO COMPLEXES OF MOLYBDENUM(II) AND TUNGSTEN(II)

2.3.1 Reactions of the complexes $[MI_2(CO)_3(PEt_3)_2]$ (M = Mo or W) Na[acac]

The reaction of $[MI_2(CO)_3(PEt_3)_2]$ (Mo or W) with one equivalent of Na[acac] in a mixture of diethyl ether/ dichloromethane/ ethanol at room temperature gave the seven-coordinate dicarbonyl complexes $[WI(acac)(CO)_2(PEt_3)_2]$ (**6**) and $[MoI(acac)(CO)_2(PEt_3)_2]$ (**7**) in high yield. The complexes have been characterised by elemental analysis C, H, N, S (**Table 2.1**), IR spectroscopy and ^1H NMR (**Table 2.2-2.3**). Both complexes are red-orange in colour and are very soluble in chlorinated solvents such as dichloromethane. The complexes are both relatively air stable in the solid state and can be handled in air for several minutes without any discernible decomposition.

The IR spectrum of the complexes (**6**) and (**7**) show two strong carbonyl stretches in CH_2Cl_2 which suggests a single isomer in solution. The spectra were also recorded as a KBr disks (**Table 2.2**), and again showed two carbonyl stretches suggesting *cis*-dicarbonyl products. This is supported by the crystal structures (**Figures 2.7 and 2.8**) which. The stretching frequencies of the remaining two carbonyl ligands in both complexes are lower than the corresponding carbonyls of complex (**1**). This is most likely due to the loss of the third carbonyl ligand resulting in greater electron density at the tungsten centre and more π-bonding between the metal and the carbonyl ligand. Carbonyl stretches are also observed at lower wave numbers ca. $1550cm^{-1}$, for the bound acetylacetonato ligand.

Both complexes (**6**) and (**7**) have been structurally characterised by X-ray crystallography (**Figures 2.7 and 2.8**). The structures of complexes (**6**) and (**7**) are very similar , though not isomorphous, the only significant difference being the position of the ethyl groups. The geometry of both structures is a highly distorted one, best described as a pentagonal bipyramid with approximate mirror symmetry passing

through the metal, the axial atoms C(100) and I(2) and the equatorial atom C(200) of the carbonyl ligand.

It is most likely the major cause of the distortion is the chelate angle of the acetylacetonato ligand which is 80.7 (3) in (**7**) and 81.7 in (**6**) compared to the ideal angle of 72° in the equatorial plane. Atomic coordinates and selected bond lengths can be found in **Tables A1.5** and **A1.6** in **Appendix 1**.

The ^{1}H NMR spectra of complexes (**6**) and (**7**) are consistent with the structures shown in Figures **2.7** and **2.8**. The $^{13}C\{^{1}H\}$ NMR (CD_2Cl_2, 25 °C) of complexes (**6**) and (**7**) are very similar suggesting very closely related structures in solution. Complex (**6**) shows a carbonyl resonance at δ = 237 ppm which corresponds to the *cis*-carbonyl ligands.

Figure 2.7 X-ray crystal structure of the complex $[WI(acac)(CO)_2(PEt_3)_2]$ (**6**)
Thermal ellipsoids shown at 30% probability.

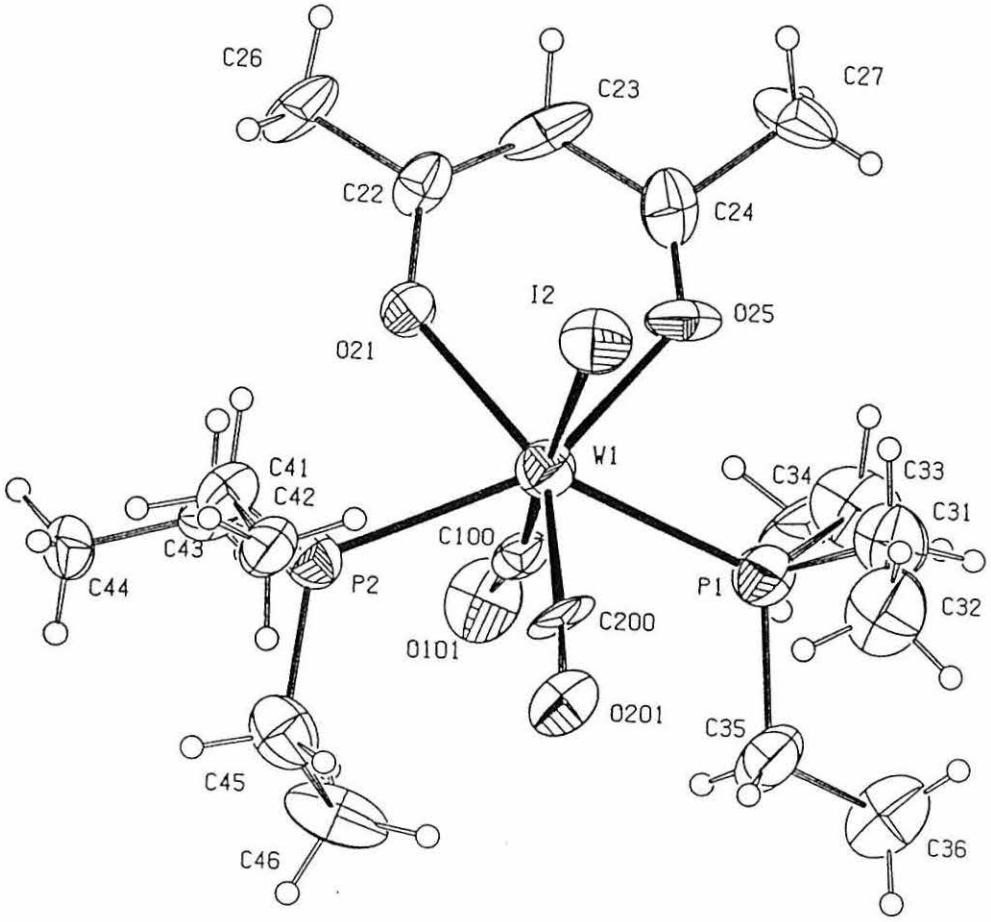

Figure 2.8 X-ray crystal structure of the complex $[MoI(acac)(CO)_2(PEt_3)_2]$ (**7**) Thermal ellipsoids shown at 30% probability.

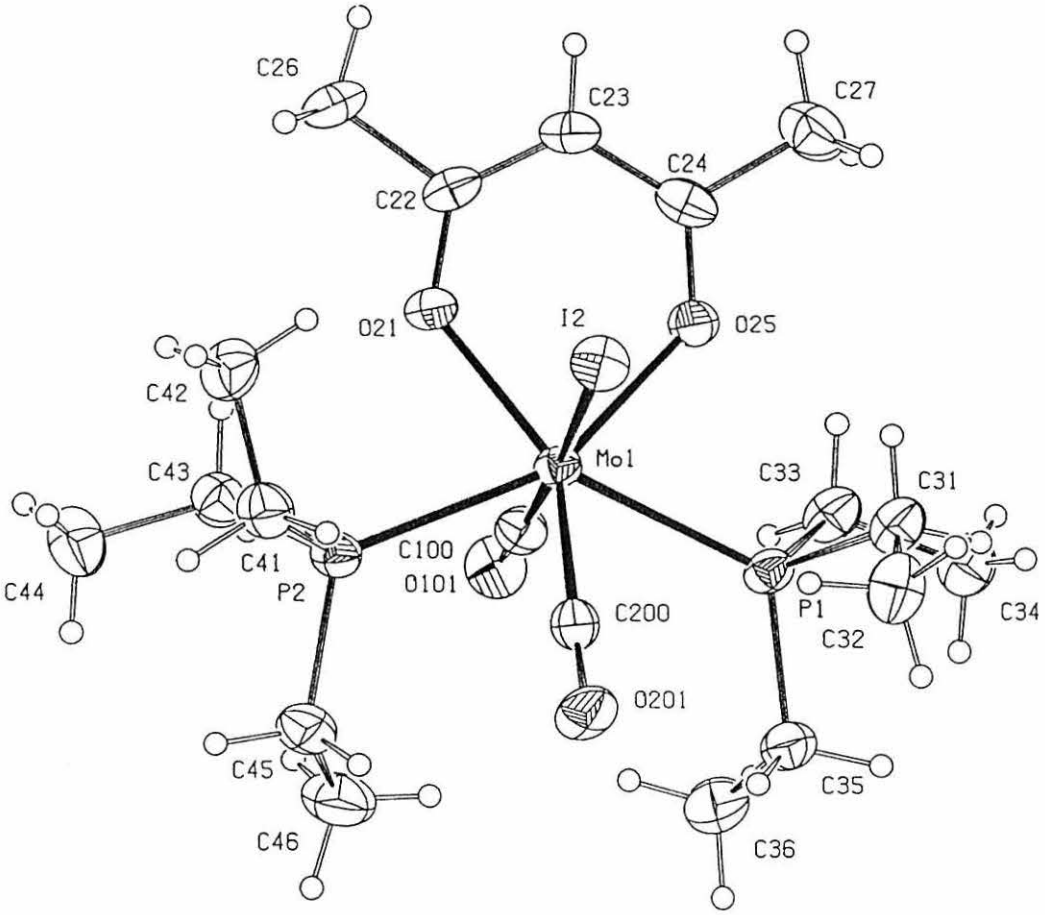

Table 2.1: Physical and analytical data[a] for six-coordinate dithiolate and seven-coordinate acetylacetonato complexes of molybdenum and tungsten.

Compound	Yield (%)	Colour	%C	%H	%S
$[WI_2(CO)_3(PEt_3)_2]$ (1)	78	Orange-yellow	37.6 (37.8)	2.3 (2.6)	-
$[W\{S(CH_2)_2S\}(CO)_2(PEt_3)_2]$ (2)	85	Dark Red	33.4 (33.8)	5.5 (5.6)	12.0 (11.3)
$[W\{S(CH_2)_3S\}(CO)_2(PEt_3)_2]$ (3)	80	Dark Red	35.1 (35.0)	5.7 (6.2)	10.3 (11.0)
$[W(SPh)_2(CO)_2(PEt_3)_2]$ (4)	60	Dark Green	45.1 (44.9)	5.9 (5.8)	9.0 (9.2)
$[Mo\{S(CH_2)_2S\}(CO)_2(PEt_3)_2]$ (5)	90	Dark Red	40.2 (40.0)	7.7 (7.1)	14.7 (13.4)
$[WI(acac)(CO)_2(PEt_3)_2]$ (6)	76	Red-Orange	32.8 (32.5)	5.3 (5.3)	-
$[MoI(acac)(CO)_2(PEt_3)_2]$ (7)	82	Red-Orange	37.1 (37.2)	6.7 (6.1)	-

[a] Calculated values in parentheses

Table 2.2 Infra-red data for complexes (1) - (7)*

Complex	C =O cm^{-1}
(1)	2010 (s), 1930 (s), 1894 (s).
(2)	1910 (s), 1832 (br).
(3)	1908 (s), 1831 (br).
(4)	1839 (br).
(5)	1906 (s), 1810 (br) 1919 (s), 1832 (br).
(6)	1913 (s), 1811 (s).
(7)	1919 (s), 1810 (s).

* all spectra recorded as KBr Disks.
s = Strong, br = Broad.

Table 2.3 1H- NMR data for complexes (1) to (7)[a] at 25°C referenced to $SiMe_4$.

Complex	^1H δ (ppm)[a]
(**2**)	2.7 (s, 4H, CH_2-S); 2.15 (m, 12H, CH_2-P); 1.1 (m, 18H,CH_3).
(**3**)	2.9 (t, 4H, CH_2-S); 2.3 (m, 2H, CH_2); 2.25 (m, 12H, CH_2-P); 1.1 (m, 18H,CH_3).
(**4**)	7.4 (brm, 10H, Ph-S); 2.5 (m, 12H, CH_2-P); 0.9 (m, 18H,CH_3).
(**5**)	2.8 (s, 4H, CH_2-S); 2.15 (m, 12H, CH_2-P); 1.0 (m, 18H,CH_3).
(**6**)	5.5 (s, 1H, CH); 2.2 (m, 12H, CH_2-P); 2.0 (s, 6H, OC-CH_3); 1.2 (m, 18H,CH_3).
(**7**)	5.5 (s, 1H, CH); 2.3 (m, 12H, CH_2-P); 2.0 (s, 6H, OC-CH_3); 1.2 (m, 18H,CH_3).

[a] s = singlet, t = triplet, m = multiplet and br = broad.

All spectra recorded in $CDCl_3$.

CHAPTER 3:

Synthesis of seven-coordinate di-bromo thioether and disulphide complexes of molybdenum(II) and tungsten(II).

CHAPTER 3: THE SYNTHESIS OF SEVEN-COORDINATE DI-BROMO THIOETHER AND DISULPHIDE COMPLEXES OF MOLYBDENUM(II) AND TUNGSTEN(II)

3.1 INTRODUCTION

The following chapter describes the reactions of the seven coordinate di-bromo complexes $[MBr_2(CO)_3(NCMe)_2]$ (M = Mo or W) with both di- and trithioether ligands. The dithioether ligands used were $RS(CH_2)_2SR$ (R = Ph, 4-FC_6H_4). The trithioether ligands used were the acyclic $MeS(CH_2)_2S(CH_2)_2SMe$ (2,5,8-trithianonane, TTN) and the cyclic crown-trithioether 2,5,8-trithia[9]-σ-benzenophane (ttob). The phosphine disulphide ligand, $Ph_2P(S)CH_2(S)PPh_2$ ($dppmS_2$) was also used.

3.2 THIOETHERS AS LIGANDS

Thioethers may be grouped as mono- (RSR'), di- (RSSR') or polythioethers. These may also be acyclic or so called crown-thioethers (thiamacrocycles). Thioethers constitute a large class of ligands and have been shown to coordinate with a wide range of metals. In all types of thioethers the sulphur atoms can be described as sp^3 hybridised with two lone pairs of electrons occupying two of the sp^3 orbitals. Each sulphur atom therefore exhibits a bent geometry.

Bonding to a metal centre can occur *via* one or both of the two sp^3 orbitals containing lone pairs of electrons. As well as σ- donation of electrons to the metal centre from the sulphur sp^3 orbitals, π- back donation of electrons to unoccupied sulphur d-orbitals, of suitable symmetry, also occurs. Although, thioethers are not as strong - donors or π- acceptors as phosphines they are stronger than similar nitrogen donor ligands. Upon coordination the sulphur atoms of the thioether tend to adopt a pyramidal geometry.

3.2.1 Reactions of dithioethers with complexes of molybdenum and tungsten

Dithioethers may react in either a monodentate or a bidentate manner to a metal centre such as molybdenum or tungsten. For example, molybdenum and tungsten pentacarbonyl complexes of the type $[M(CO)_5\{MeS(CH_2)_{3-n}(SMe)_n\}]$ have been prepared[91] where the dithioether is bound in a monodentate fashion to the single metal centre. Another similar example is the tungsten complex $[W(CO)_5\{S(CH_2)_3SCHMe\}]$ where a five membered ring containing two sulphur atoms is bound *via* one of the sulphur atoms to the tungsten centre.

However, bidentate dithioether complexes of molybdenum and tungsten are more common. For example, a whole range of zero-valent molybdenum and tungsten tetracarbonyl dithioether complexes of the type $[M(CO)_4\{RS(CH_2)_nSR\}]$ (n = 1-5) have been synthesised[92-97]. The most common complexes of this type are the dithioethane-derivative complexes $[M(CO)_4\{RS(CH_2)_2SR\}]$ (R = Me, Et, Bu^t, Pr^i) where the sulphur atoms of the dithioether are separated by two methylene groups. Complexes of this type contain bidentate dithioethers bound to the metal *via* two sulphur atoms. Bidentate thioether complexes are more stable and numerous than monodentate thioether complexes. The increase in stability is mainly due to the chelate effect caused by the binding of the second sulphur atom to the metal.

3.2.2 Reactions of crown-thioethers with molybdenum and tungsten complexes

Crown thioether ligands have been used recently as ligands with a wide range of transition-metals. This discussion will look only at S_3-thioethers in particular the 1,4,7-trithiacyclononane ([9]aneS_3) and 2,5,8-trithia[9]-σ-benzenophane (ttob) as shown in **Figure 3.1**.

The coordination chemistry of [9]aneS_3 is particularly well studied with numerous transition-metal complexes containing [9]aneS_3 being known[98,99]. The molybdenum tricarbonyl complex $[Mo(CO)_3([9]aneS_3)]$ has been prepared[100] as well as the analogous tungsten complex $[W(CO)_3([9]aneS_3)]$[101]. The structures of both complexes have been crystallographically determined, showing the [9]aneS_3 ligand to be coordinated facially to the molybdenum or tungsten metal centre (**Figure 3.2**).

Figure 3.1 Diagrams showing the ligands (a) [9]aneS$_3$ and (b) ttob

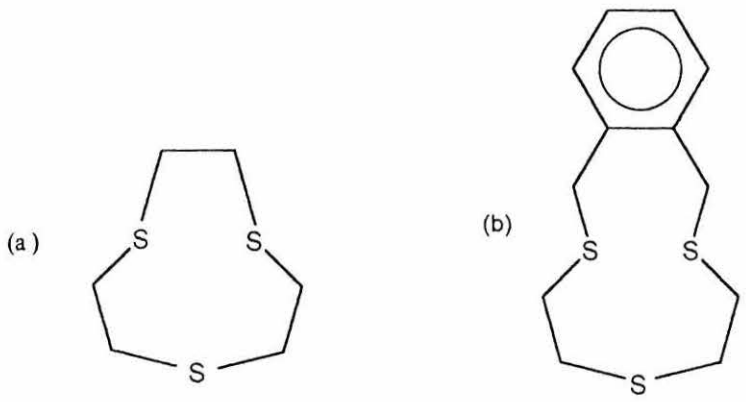

Figure 3.2 Structure of the complex [W(CO)$_3$([9]aneS$_3$)]

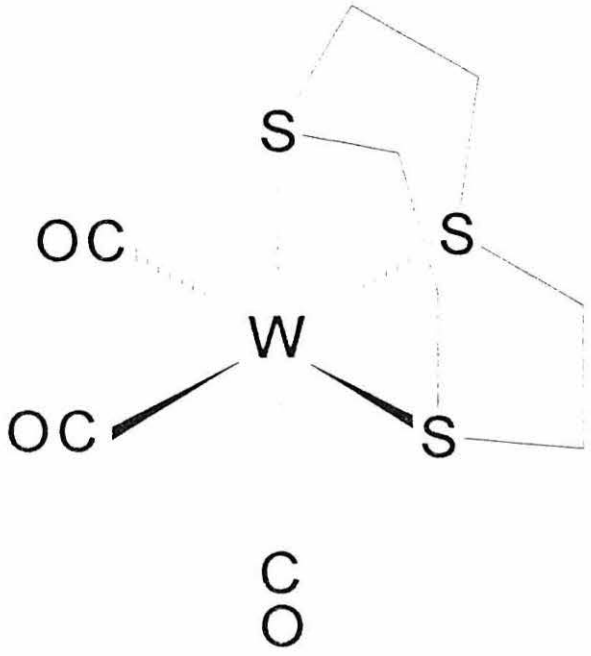

Complexes containing [9]aneS$_3$ tend to be very stable due to the ligand having an endodentate conformation[102], that is all three sulphur atoms point inwards within the ring. This conformation means there is little structural change needed upon

coordination to the metal. Unlike [9]aneS$_3$, the ligand ttob has an exodentate conformation. However, upon binding to a metal centre the ligand is able to undergo a conformational change to a endodentate conformation as seen in the complex [Mo(CO)$_3$(ttob)][103].

So far this introduction has only discussed thioether complexes of zero-valent molybdenum or tungsten. However, there are wide variety of complexes of molybdenum(II) and tungsten(II) containing both acyclic and cyclic thioethers. Some of the complexes prepared by Baker *et al* have been briefly described previously in **section 1.7** [57-62]. All of the complexes described therein are based upon the reactions of the seven-coordinate di-iodo starting materials [MI$_2$(CO)$_3$(NCMe)$_2$] (M= Mo, W) with both polydentate acyclic and crown-thioether ligands. In the following section similar reactions of the analogous dibromo-complexes [MBr$_2$(CO)$_3$(NCMe)$_2$] (M= Mo, W) are described.

3.3 RESULTS AND DISCUSSION

The starting materials [MBr$_2$(CO)$_3$(NCMe)$_2$] (M= Mo, W) were prepared by the literature method involving the reaction of *fac*-[M(CO)$_3$(NCMe)$_3$] with an equimolar amount of Br$_2$ at -78°C[104]. The dithioether ligands RS(CH$_2$)$_2$SR (R = Ph, 4-FC$_6$H$_4$) were prepared in a similar fashion to the literature method[105,106] involving the condensation of the appropriate dithiol. All of the dithiolate ligands prepared were white crystalline solids. The trithioether MeS(CH$_2$)$_2$S(CH$_2$)$_2$SMe (TTN) was prepared by a different method[106] to that described in the literature[107]. The ligand is a colourless oil at room temperature which solidifies when it is cooled. The cyclic trithioether ttob was prepared *via* a one-step synthesis as described in the literature[108](**Scheme 2.1**).

Scheme 3.1 Literature synthesis of the ligand ttob[105,106]

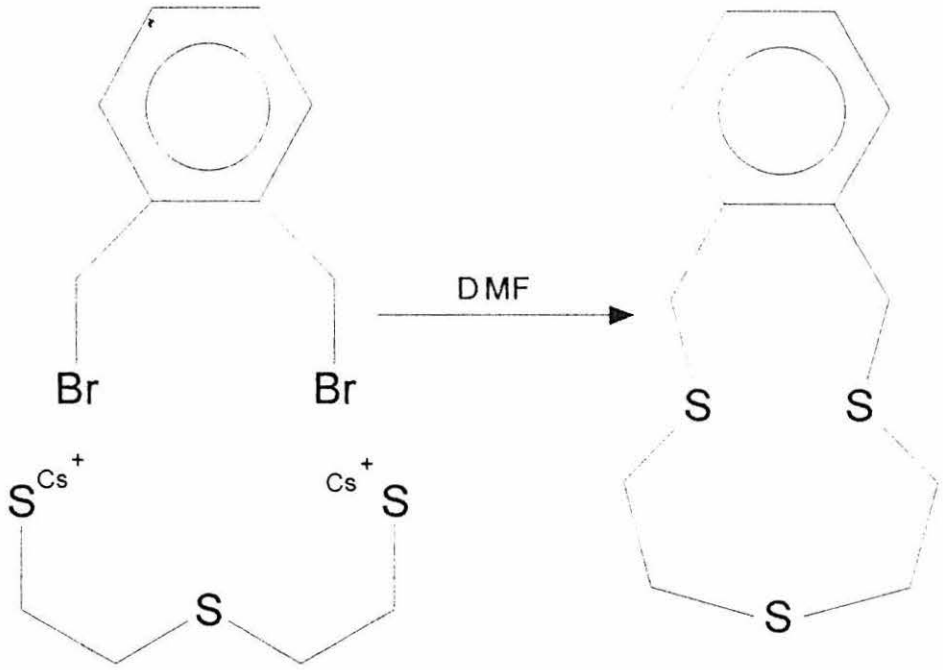

For analytical and spectroscopic data for the ligands $RS(CH_2)_2SR$ (R = Ph, 4-FC_6H_4), $MeS(CH_2)_2S(CH_2)_2SMe$ (TTN) and ttob refer to **Tables 3.1 and 3.2**.

3.3.1 Reactions of the complexes $[MBr_2(CO)_3(NCMe)_2]$ with a slight excess of $RS(CH_2)_2SR$ (R = Ph, 4-FC_6H_4)

The reaction of $[MBr_2(CO)_3(NCMe)_2]$ (M = Mo, W) with a slight excess of either $PhS(CH_2)_2SPh$ or 4-$FC_6H_4S(CH_2)_2SC_6H_4$-F gave the seven-coordinate complexes $[MBr_2(CO)_3\{PhS(CH_2)_2SPh\text{-}S,S'\}]$ (**8** and **9**) and $[MBr_2(CO)_3\{4\text{-}FC_6H_4S(CH_2)_2SC_6H_4\text{-}F\text{-}S,S'\}]$ (**10** and **11**) respectively in reasonable yields. All complexes were characterised by elemental analysis C, H, and S (**Table 3.3**), infra red (**Table 3.4**) and ^1H NMR spectroscopy (**Table 3.5**). All four complexes are soluble in dichloromethane and dmso, but are totally insoluble in diethyl ether; the molybdenum complexes being more soluble than their tungsten analogues. Complexes (**8-11**) are all very air-sensitive in solution and only slightly less so in the solid state. Hence, the complexes were handled in air only for very short periods of time and decomposed after short periods of storage. Conductivity measurements in

acetone showed complexes (**8-11**) to be non-electrolytes as was expected (**Equation 2.1**).

The infra red spectra of complexes (**8-11**) were recorded as KBr disks. No solution infra red spectra were obtained due to the extremely air-sensitive nature of the complexes. Three carbonyl stretching bands were observed for the four complexes (**Table 3.4**). This is consistent with the complexes being seven-coordinate and having one configuration in the solid-state. The ^{1}H NMR spectra (**Table 3.5**) showed the coordinated thioether resonances to be shifted slightly down field compared to those of the free thioethers.

The solid-state structure of the tungsten complex (**8**) has been solved by X-ray crystallography and is shown in **Figure 3.3**. The complex is very similar to the analogous di-iodo complex[57] $[WI_2(CO)_3\{4\text{-}MeC_6H_4S(CH_2)_2SC_6H_4\text{-}Me\text{-}S,S'\}]$ already described in **Section 1.7.2** of this thesis. The complex has a distorted capped octahedral geometry with two carbonyl ligands and one sulphur S(2) in the capped face and the two bromides and the other sulphur atom S(1) making up the uncapped face. The two W-S distances are equivalent within experimental error and Br(1) being *trans*-to carbonyl C(300) while the other bromine Br(2) is *trans*-to the S(2) atom of the dithiolate ligand. See **Table A1.7** in **Appendix 1** for further bond angles and lengths. It is likely that the three other complexes (**9-11**) will have the same geometry in the solid state.

Figure 3.3 X-ray crystal structure of $[WBr_2(CO)_3\{PhS(CH_2)_2SPh\text{-}S,S'\}]$ (**8**)

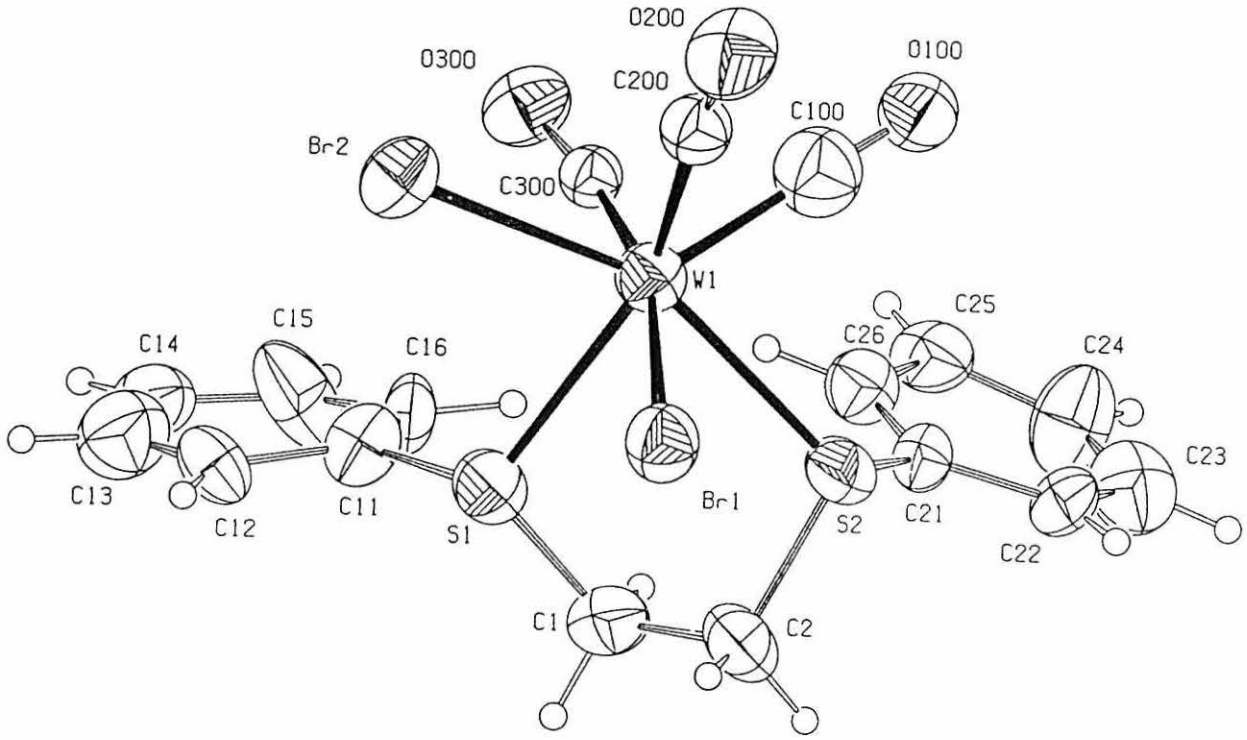

3.3.2 Reactions of the complex $[WBr_2(CO)_3(NCMe)_2]$ with two equivalents of $RS(CH_2)_2SR$ (R = Ph, 4-FC_6H_4)

The reaction of $[WBr_2(CO)_3(NCMe)_2]$ with two equivalents of either $PhS(CH_2)_2SPh$ or $4\text{-}FC_6H_4S(CH_2)_2SC_6H_4\text{-}F$ gave the seven-coordinate complexes $[WBr(CO)_3\{RS(CH_2)_2SR\text{-}S\}\{RS(CH_2)_2SR\text{-}S,S'\}]$ Br (R = Ph, 4-FC_6H_4) (**12** and **13**) respectively in good yield. Both complexes were characterised by elemental analysis C, H, and S (**Table 3.3**), infra red (**Table 3.4**) and ^1H NMR spectroscopy (**Table 3.5**). Both complexes are soluble in dichloromethane and dmso but are totally insoluble in diethyl ether, both are very air-sensitive in solution and only slightly less so in the solid state. Hence, the complexes were handled in air only for very short periods and were used very quickly in order to avoid decomposition. Conductivity measurements in acetone showed both complexes to be typical 1:1 electrolytes (Λm =123 and 126 S cm^2 mol^{-1}) (**Equation 2.1**). This data suggests that one of the sulphur atoms from the second thioether ligand has displaced one of the bromides from the starting material.

The infra red spectra of both complexes were recorded as KBr disks. Three carbonyl stretches were observed for both complexes (**Table 3.4**). This is consistent with the complexes being seven-coordinate and having one conformation in the solid-state. The ^1H NMR spectra (**Table 3.5**) again showed the coordinated thioether resonances to be shifted down field compared to those of the free thioethers. In these cases, however, resonances are also observed for the uncoordinated end of the monodentately bound thioether ligand. It is likely given the similarities in spectroscopic data between complexes (**12**) and the crystallographically characterised product (**8**) that they may have similar solid-state structures both exhibiting a capped octahedral type structure (**Figure 3.4**).

Figure 3.4 Proposed structure of $[WBr(CO)_3\{PhS(CH_2)_2SPh\text{-}S\}\{PhS(CH_2)_2SPh\text{-}S,S'\}]Br$ (**12**)

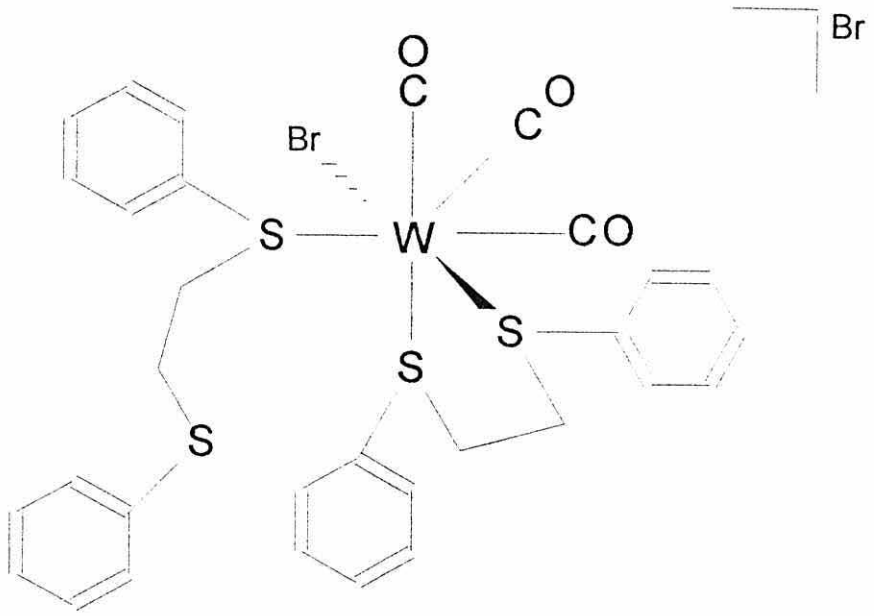

Further reactions were attempted with the molybdenum complex $[MoBr_2(CO)_3(NCMe)_2]$, however, no products were isolated, probably due to their greater instability.

3.3.3 The reactions of $[WBr_2(CO)_3(NCMe)_2]$ with one and two equivalents of $Ph_2P(S)CH_2P(S)Ph_2$

The reactions of $[WBr_2(CO)_3(NCMe)_2]$ with one or two equivalents of $Ph_2P(S)CH_2P(S)Ph_2$ gave the green seven-coordinate complexes $[WBr(CO)_3\{Ph_2P(S)CH_2P(S)Ph_2\text{-}S,S'\}]$ (**14**) and $[WBr(CO)_3\{Ph_2P(S)CH_2P(S)Ph_2\text{-}S\}\{Ph_2P(S)CH_2P(S)Ph_2\text{-}S,S'\}]Br$ (**15**) respectively in good yield. Both complexes were characterised by elemental analysis C, H, and S (**Table 3.3**), infra red (**Table 3.4**) and ^1H NMR spectroscopy (**Table 3.5**). Both complexes are soluble in dichloromethane and dmso but are totally insoluble in diethyl ether. Both complexes are very air-sensitive in solution and only slightly less so in the solid state. Hence, the complexes were handled in air only for very short periods and were used very quickly in order to avoid decomposition. Conductivity measurements of complex (**14**) showed

the complex to be a non-electrolyte in acetone however similar measurement showed complex (**15**) to be a typical 1:1 electrolyte (Λm = 128 S cm^2 mol^{-1}) (**Equation 2.1**) . The conductivity data suggests that in complex (**15**) one of the sulphur atoms from the second thioether ligand has displaced one of the bromides from the starting material.

The infra red spectra of both complexes were recorded as KBr disks. Three carbonyl stretches were observed for both complexes (**Table 3.4**). This is consistent with the complexes being seven-coordinate and having one conformation in the solid-state. The ^1H NMR spectra (**Table 3.5**) again showed the coordinated diphosphine disulphide resonances to be shifted down field compared to those of the free ligand. In the case of complex (**14**), however, resonances were also observed for the uncoordinated end of the monodentately bound ligand. Further reactions were attempted with the molybdenum complex $[MoBr_2(CO)_3(NCMe)_2]$, however, no products were isolated probably due to their greater instability compared to their diiodo analogues.

3.3.4 Reactions of the complexes $[MBr_2(CO)_3(NCMe)_2]$ with one equivalent of $MeS(CH_2)_2S(CH_2)_2SMe$

The reaction of $[MoBr_2(CO)_3(NCMe)_2]$ with an equimolar amount of $MeS(CH_2)_2S(CH_2)_2SMe$ gave the seven-coordinate dicarbonyl complex $[MoBr_2(CO)_2\{MeS(CH_2)_2S(CH_2)_2SMe\text{-}S,S',S''\}]$(**16**) in high yield. Similar treatment of $[WBr_2(CO)_3(NCMe)_2]$ with one equivalent of $MeS(CH_2)_2S(CH_2)_2SMe$ gave the tricarbonyl complex $[WBr_2(CO)_3\{MeS(CH_2)_2S(CH_2)_2SMe\text{-}S,S'\}]$(**17**) again in high yield. Complex (**16**) was red-brown in colour while complex (**17**) was green in colour. Both complexes were characterised by elemental analysis C, H, and S (**Table 3.4**), infra red (**Table 3.4**) and ^1H NMR spectroscopy (**Table 3.5**). Both complexes are soluble in dichloromethane and dmso but are totally insoluble in diethyl ether, the molybdenum complex this time being less soluble than it's tungsten analogue. Both complexes are highly air-sensitive in solution and only slightly less so in the solid state. Hence, both complexes were handled in air only for very short periods of time and used over as short a time as possible. Conductivity measurements in acetone

showed both complexes to be non-electrolytes (**Equation 2.1**). The infra red spectra of both complexes were recorded as KBr disks (**Table 3.4**). Complex (**16**) showed two carbonyl stretching bands suggesting a dicarbonyl complex while three carbonyl stretches were observed for complex (**17**) (**Figure 3.5**).

In the case of both complexes the ^{1}H NMR spectra (**Table 3.5**) showed the coordinated thioether resonances to be shifted down field compared to those of the free thioethers. However, in the case of complex (**17**), a resonance can be assigned to the methyl group of the uncoordinated sulphur atom. It is possible to suggest a capped octahedral structure (**Figure 3.6**) for the dicarbonyl molybdenum complex $[MoBr_2(CO)_2\{MeS(CH_2)_2S(CH_2)_2SMe\text{-}S,S',S''\}]$ (**16**) this is supported by the previously confirmed crystallographic structure of the diiodo-complex $[WI_2(CO)_2\{MeS(CH_2)_2S(CH_2)_2SMe\text{-}S,S',S''\}]$[57].

Figure 3.5 IR carbonyl stretching regions for (a) Complex (**16**) and (b) Complex (**17**)

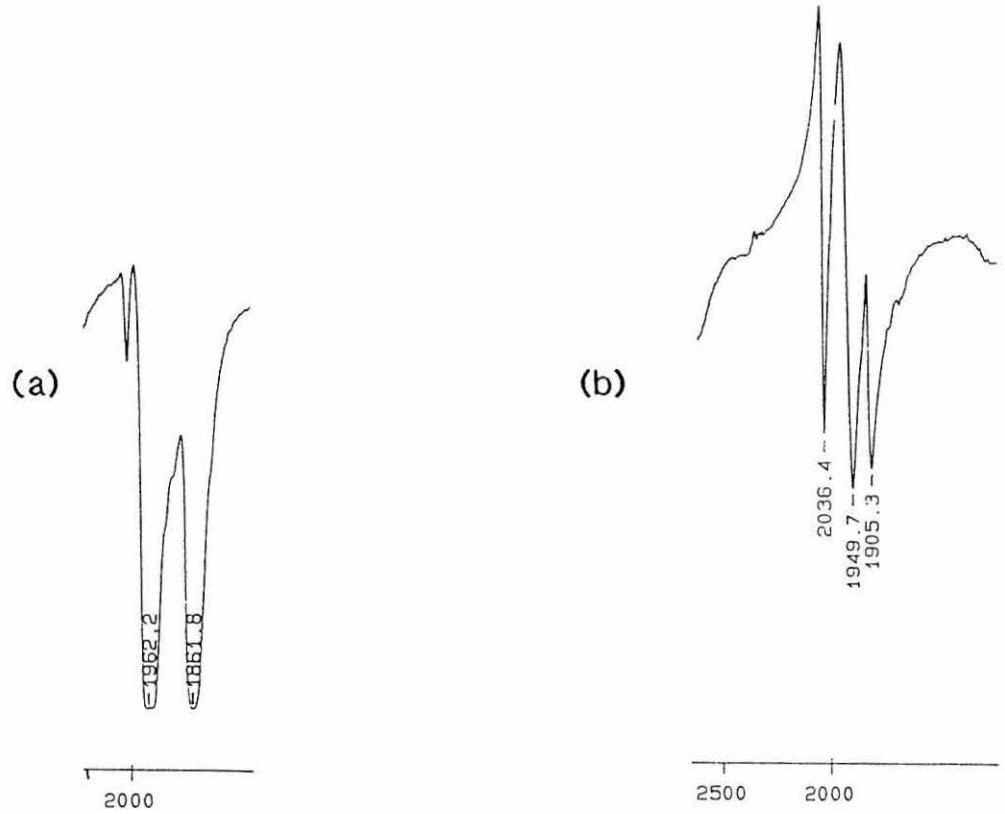

Figure 3.6 Proposed structure of $[MoBr_2(CO)_2\{MeS(CH_2)_2S(CH_2)_2SMe\text{-}S,S',S''\}]$ **(16)**

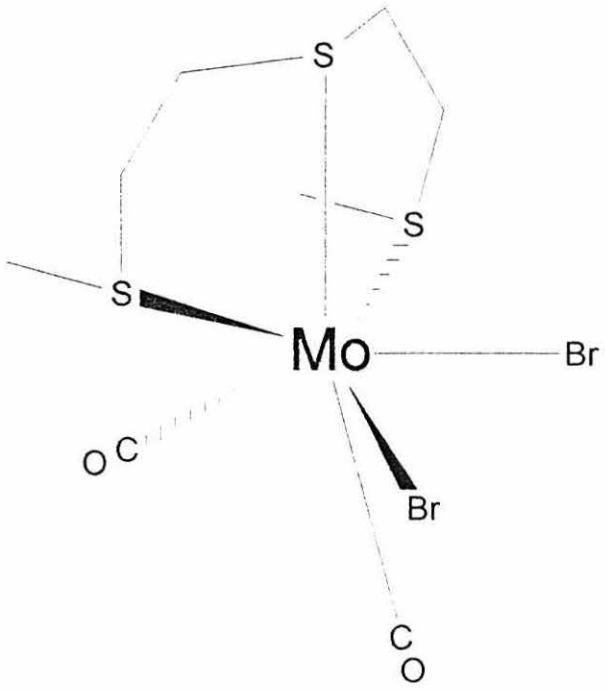

Attempts to produce a dicarbonyl tungsten complex over longer reaction periods were unsuccessful probably due to the stronger W-C bond strengths, as is generally observed for tungsten carbonyl complexes compared to their molybdenum analogues.

3.3.5 Reaction of the complex $[MoBr_2(CO)_3(NCMe)_2]$ with one equivalent of 2,5,8-trithia[9]-*F*-benzenophane (ttob)

The reaction of $[MoBr_2(CO)_3(NCMe)_2]$ with an equimolar amount of 2,5,8-trithia[9]-*F*-benzenophane (ttob) gave the seven-coordinate dicarbonyl complex $[MoBr_2(CO)_2\{ttob\text{-}S,S',S''\}]$(**18**) in high yield. Complex (**18**) was light brown in colour and was characterised by elemental analysis C, H, and S (**Table 3.3**), infra red (**Table 3.4**) and ^1H NMR spectroscopy (**Table 3.5**). The complex was soluble in dichloromethane and dmso but was totally insoluble in diethyl ether. As expected, the complex was highly air-sensitive in both solution and in the solid state and hence was handled accordingly. Conductivity measurements in acetone showed the complex to

be a non-electrolyte (**Equation 2.1**). The infra red spectrum of complex (**18**) was recorded as a KBr disk (**Table 3.4**). The complex showed two carbonyl stretches suggesting a dicarbonyl complex similar to that of previously described complex (**16**). A possible structure for complex (**18**) is shown in **Figure 3.7**.

Similar reactions of $[WBr_2(CO)_3(NCMe)_2]$ with an equimolar amount of 2,5,8-trithia[9]-*σ*-benzenophane (ttob) were attempted but resulted in a mixture of unstable products. Attempts to separate the products were unsuccessful due to decomposition occurring during recrystallisation.

Figure 3.7 Proposed structure of the complex $[MoBr_2(CO)_2\{ttob\text{-}S,S',S''\}]$

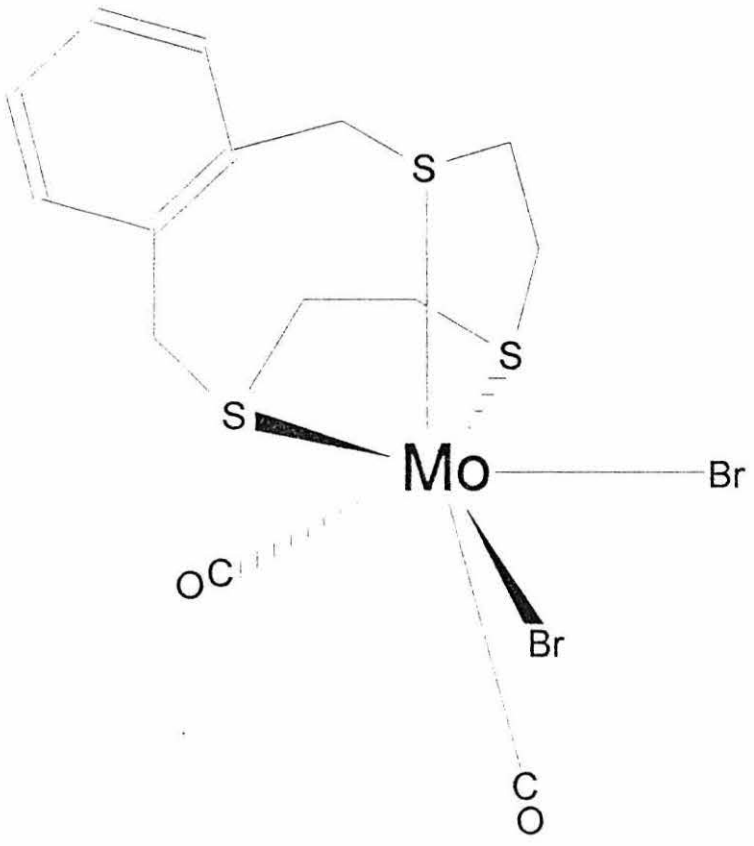

Table 3.1 Analytical data for thioether and diphosphine disulphide ligands

Ligand	Yield %	Elemental Analysis C	H	S
$PhS(CH_2)_2SPh$	37	68.0 (68.3)	6.1 (5.8)	26.0 (26.0)
$4\text{-}FC_6H_4S(CH_2)_2SC_6H_4F\text{-}4$	40	58.8 (59.6)	4.2 (4.3)	21.9 (22.7)
$Ph_2P(S)CH_2P(S)Ph_2$	60	66.8 (67.0)	4.7 (4.9)	14.5 (14.3)
ttob	72	55.9 (56.2)	6.4 (6.1)	37.9 (38.0)

Calculated values shown in parentheses.

Table 3.2 ^1H NMR data for thioether and diphosphine disulphide ligands

Ligand	δ (ppm)
$PhS(CH_2)_2SPh$[a]	7.24 (m, 10H, Ph), 3.0 (s, 4H, CH_2)
$4\text{-}FC_6H_4S(CH_2)_2SC_6H_4F\text{-}4$[a]	7.3 (m, 4H, Ph), 6.8 (m, 4H, Ph), 2.9 (s, 4H,CH_2)
$Ph_2P(S)CH_2P(S)Ph_2$[b]	7.92 (m, 8H, Ph-*ortho*), 7.46 (m, 12H, Ph-*meta/para*), 3.9 (t,2H,CH_2)
$MeS(CH_2)_2S(CH_2)_2SMe$[a]	2.76 (m, 8H, CH_2CH_2), 1.3 (s, CH_3)
ttob[b]	7.3 (m, 4H, Ph), 3.8 (s, 4H, Ph-CH_2-S), 2.8 (m, 8H, S-CH_2-CH_2-S)

s = singlet, d = doublet, t = triplet, m = multiplet

All spectra carried out at 298K and referenced to $SiMe_4$

[a] spectra recorded in CD_2Cl_2, [b] spectra recorded in $(CD_3)_2CO$

Table 3.3 Physical and analytical data for thioether and phosphine disulphide complexes of molybdenum and tungsten*

Compound	Colour	yield %	%C	%H	%S
(8) $[WBr_2(CO)_3\{PhS(CH_2)_2SPh\text{-}S,S'\}]$	orange	45	30.1 (30.3)	2.7 (2.1)	10.3 (9.5)
(9) $[MoBr_2(CO)_3\{PhS(CH_2)_2SPh\text{-}S,S'\}]$	brown	40	34.6 (34.8)	2.9 (2.4)	10.5 (10.9)
(10)$[WBr_2(CO)_3\{F\text{-}C_6H_4S(CH_2)_2SC_6H_4\text{-}F\text{-}S,S'\}]$	orange	44	28.0 (28.8)	1.9 (1.7)	9.2 (9.0)
(11) $[MoBr_2(CO)_3\{F\text{-}C_6H_4S(CH_2)_2SC_6H_4\text{-}F\}]$	brown	46	32.7 (32.8)	1.8 (1.9)	10.0 (10.3)
(12)$[WBr(CO)_3\{PhS(CH_2)_2SPh\text{-}S\}\{PhS(CH_2)_2SPh\text{-}S,S'\}]Br$	brown	41	40.1 (40.5)	3.6 (3.1)	12.4 (13.9)
(13)$[WBr(CO)_3\{F\text{-}C_6H_4S(CH_2)_2SC_6H_4\text{-}F\text{-}S\}\{F\text{-}C_6H_4S(CH_2)_2SC_6H_4\text{-}F\text{-}S,S'\}]Br$	brown	47	37.5 (37.5)	2.0 (2.4)	12.4 (12.9)
(14) $[WBr_2(CO)_3\{Ph_2P(S)CH_2(S)PPh_2\text{-}S,S'\}]$	green	60	38.3 (38.4)	2.6 (2.5)	7.8 (7.3)
(15)$[WBr(CO)_3\{Ph_2P(S)(CH_2)_2(S)PPh_2\text{-}S\}\{Ph_2P(S)(CH_2)_2(S)PPh_2\text{-}S,S'\}]Br$	green	45	48.2 (48.8)	3.5 (3.6)	8.0 (9.5)
(16)$[MoBr_2(CO)_2\{MeS(CH_2)_2S(CH_2)_2SMe\text{-}S,S',S''\}]$	red brown	55	18.9 (19.5)	2.4 (2.9)	19.1 (19.5)
(17)$[WBr_2(CO)_3\{MeS(CH_2)_2S(CH_2)_2SMe\text{-}S,S'\}]$	green	54	16.8 (16.5)	1.9 (2.4)	16.2 (16.5)
(18)$[MoBr_2(CO)_2\{ttob\text{-}S,S',S''\}]$	brown	60	30.1 (29.6)	2.7 (2.8)	16.0 (16.9)

Calculated values in parentheses.

Table 3.4 Infra red carbonyl stretching data* for complexes (**8**) to (**18**)

Compound	ν (CO) cm^{-1}
(**8**)	2035(s), 1965(s), 1908(s)
(**9**)	2042(s), 1959(s), 1901(s)
(**10**)	2025(s), 1965(s), 1908(sh)
(**11**)	2022(s), 1968(s), 1915(sh)
(**12**)	2043(s), 1960(s), 1896(s)
(**13**)	2047(s), 1965(s), 1905(s)
(**14**)	2034(s), 1960(s), 1892(s)
(**15**)	2037(s), 1961(s), 1893(s)
(**16**)	1962(s), 1862(s)
(**17**)	2036(s), 1950(s), 1905(s)
(**18**)	1951(s), 1871(s)

* All data recorded as KBr pellets.

s = strong, sh = shoulder.

Table 3.5 ^{1}H NMR data* for complexes (**8**) to (**18**)

Complex	δ (ppm)
(**8**)	7.5 (m, 10H, Ph); 3.55 (s, 4H, CH_2)
(**9**)	7.4 (m, 10H, Ph); 3.5 (s, 4H, CH_2)
(**10**)	7.35 (m, 4H, C_6H_4); 7.1 (m, 4H, C_6H_4); 3.1 (s, 4H,CH_2)
(**11**)	7.4 (m, 4H, C_6H_4); 7.2 (m, 4H, C_6H_4); 3.1 (s, 4H,CH_2)
(**12**)	7.3 (m, 4H, Ph, coord.); 7.1 (m, 5H, Ph, uncoord.); 3.2 (s, 8H, CH_2)
(**13**)	7.4 (m, 8H, C_6H_4); 7.2 (m, 8H, C_6H_4); 3.1 (s, 8H,CH_2)
(**14**)	8.0 (m, 8H, Ph-*ortho*); 7.5 (m, 12H, Ph-*meta/para*); 4.6 (t, 4H, CH_2)
(**15**)	7.9 (m, 16H, Ph-*ortho*); 7.4 (m, 24H, Ph-*meta/para*); 4.6 (t, 4H, CH_2)
(**16**)	3.1 (m, 8H, CH_2); 2.3 (s, 6H, CH_3)
(**17**)	3.8 (m, 4H,CH_2SCH_2, coord.); 3.7 (m, 2H, CH_2CH_3, coord.); 2.9 (s, 3H, SCH_3, coord.); 2.5 (m, 2H, CH_2SCH_3, unccord.); 2.2 (s, 3H, SCH_3, uncoord.)
(**18**)	7.5 (m, 4H, Ph); 4.2 (m, 4H, $PhCH_2S$); 2.8 (m, 8H, SCH_2CH_2S);

□

* Spectra recorded in dimethyl sulfoxide at 25^{o}C and referenced to $SiMe_4$. s = singlet, m = multiplet, t = triplet.

CHAPTER 4 :
REACTIONS OF THE BIS(ALKYNE)COMPLEXES $[MX_2(CO)(NCMe)(\eta^2\text{-}RC_2R)_2]$ (X = I,Br; R = Me OR Ph) WITH NEUTRAL SULPHUR DONOR LIGANDS.

CHAPTER 4: REACTIONS OF THE BIS(ALKYNE) COMPLEXES $[MX_2(CO)(NCMe)(\eta^2\text{-}RC_2R)_2]$ (X = I, Br; R = Me OR Ph) WITH NEUTRAL SULPHUR DONOR LIGANDS.

4.1 INTRODUCTION

Alkyne complexes of molybdenum(II) and tungsten(II) have been comprehensively reviewed by Templeton[109]. Templeton's review described the literature of alkyne complexes up to 1987. In a later review Baker[52] describes the alkyne halocarbonyl complexes of molybdenum(II) and tungsten(II) from 1987 to 1995. The purpose of this introduction is to describe the reactions of some halocarbonyl alkyne complexes of molybdenum(II) and tungsten(II) with a range of neutral sulphur donor ligands.

4.1.1 Haloalkyne complexes of molybdenum(II) and tungsten(II)

Some of the earliest alkyne complexes of molybdenum(II) and tungsten(II) were prepared by Otsuka and co-workers[110] in 1969. These consisted of the molybdenum and tungsten mono(alkyne) complexes $[Mo(\eta^2\text{-}PhC_2Ph)Cp_2]$ and $[W(\eta^2\text{-}CF_3C_2CF_3)Cp_2]$. Mono(alkyne) complexes of molybdenum(II) have also been prepared *via* the reaction of the dithiocarbamate complex $[Mo(CO)_2(PPh_3)(S_2CNEt_2)_2]$ with a free alkyne to give complexes of the type $[Mo(CO)(\eta^2\text{-}RC_2R')(S_2CNEt_2)_2]$[111].

Haloalkyne complexes of molybdenum(II) and tungsten(II) can be prepared *via* the reactions of many different complexes with free alkynes. For example, the reaction of the seven-coordinate molybdenum(II) complexes $[MoBr_2(CO)_3L_2]$ (L = PEt_3, PPh_3, py) with alkyne, RC_2R', has been shown to

result in the formation of the dihaloalkyne complexes $[MoBr_2(CO)L_2(\eta^2\text{-}RC_2R')]$[112]. Similarly the tungsten(II) complexes $[WI_2(CO)_2L(\eta^2\text{-}RC_2R')]$ ($L = PPh_3$, $OPMe_3$) have been prepared[113] *via* the reaction of $[WI_2(CO)_4L]$ with RC_2R'. A large number of cyclopentadienyl alkyne complexes of molybdenum(II) and tungsten(II) have also been prepared. For example, the reaction of the complexes $[MoX(CO)_3Cp]$ ($X = Cl$, Br, I, SCF_3, SC_6F_5) with RC_2R ($R = CF_3$, Me, Ph) results in the formation of mono(alkyne) complexes of the type $[MoX(CO)(\eta^2\text{-}RC_2R)Cp]$[114,115]. Bis(alkyne) complexes of the type $[MCl(\eta^2\text{-}RC_2R')_2Cp]$ ($M = Mo$, W; $R = R' = CF_3$, Me, Ph; $R = Me$, $R' = Ph$) may also be made *via* the reaction of the cyclopentadienyl complexes $[MCl(CO)_3Cp]$ with two equivalents of the appropriate alkyne, RC_2R'[116]. Similarly, the reaction of $[MCl(CO)(\eta^2\text{-}PhC_2Ph)Cp]$ ($M = Mo$, W) with $CF_3C_2CF_3$ yields the mixed alkyne complexes $[MCl(\eta^2\text{-}CF_3C_2CF_3)(\eta^2\text{-}PhC_2Ph)Cp]$[117].

Since 1988, a large number of alkyne complexes have been prepared *via* the reactions of $[MX_2(CO)_3(NCMe)_2]$ ($M = Mo$, W) with a range of alkynes. For example, the reaction of $[MI_2(CO)_3(NCMe)_2]$ ($M = Mo$, W) with one equivalent of RC_2R' ($R = R' = Me$, Ph, CH_2Cl; $R = Ph$, $R' = Me$, CH_2OH; $R = Me$, $R' = PhS$, *p*-tolS) initially gives the complexes $[MI_2(CO)(NCMe)_2(\eta^2\text{-}RC_2R')]$ which quickly dimerise to give the iodo-bridged complexes $[\{M(\mu\text{-}I)I(CO)(NCMe)(\eta^2\text{-}RC_2R')\}_2]$[118]. However, the reaction of $[MI_2(CO)_3(NCMe)_2]$ ($M = Mo$, W) with an excess of RC_2R' ($R = R' = Ph$; $R = Me$, $R' = Ph$; for $M = W$ only, $R = R' = Me$, CH_2Cl, p-tol; $R = Ph$, R' CH_2OH) gives the monomeric bis(alkyne) complexes $[MI_2(CO)(NCMe)(\eta^2\text{-}RC_2R')_2]$ and the dimeric molybdenum complex $[\{Mo(\mu\text{-}I)I(CO)(\eta^2\text{-}MeC_2Me)_2\}_2]$[119]. The tungsten complexes $[WI_2(CO)(NCMe)(\eta^2\text{-}RC_2R)_2]$ ($R = Me$, Ph) have been crystallographically characterised, and the structure of $[WI_2(CO)(NCMe)(\eta^2\text{-}MeC_2Me)_2]$ is shown in **Figure 4.1**.

Similar treatment of the dibromo-tungsten complex $[WBr_2(CO)_3(NCMe)_2]$ with two equivalents of RC_2R (R = Me, Ph, CH_2Cl) gives the monomeric bis(alkyne) complexes $[WBr_2(CO)(NCMe)(\eta^2\text{-}RC_2R)_2]$ (R = Me, Ph, CH_2Cl)[120]. The mixed halide complex $[WBrI(CO)_3(NCMe)_2]$ has also been shown to react with one equivalent of RC_2R (R = Me, Ph, CH_2Cl) to give the dimeric complexes $[\{W(\mu\text{-}I)Br(CO)(NCMe)(\eta^2\text{-}RC_2R')\}_2]$.

Figure 4.1 X-ray crystal structure of the complex $[WI_2(CO)(NCMe)(\eta^2\text{-}MeC_2Me)_2]$[120]

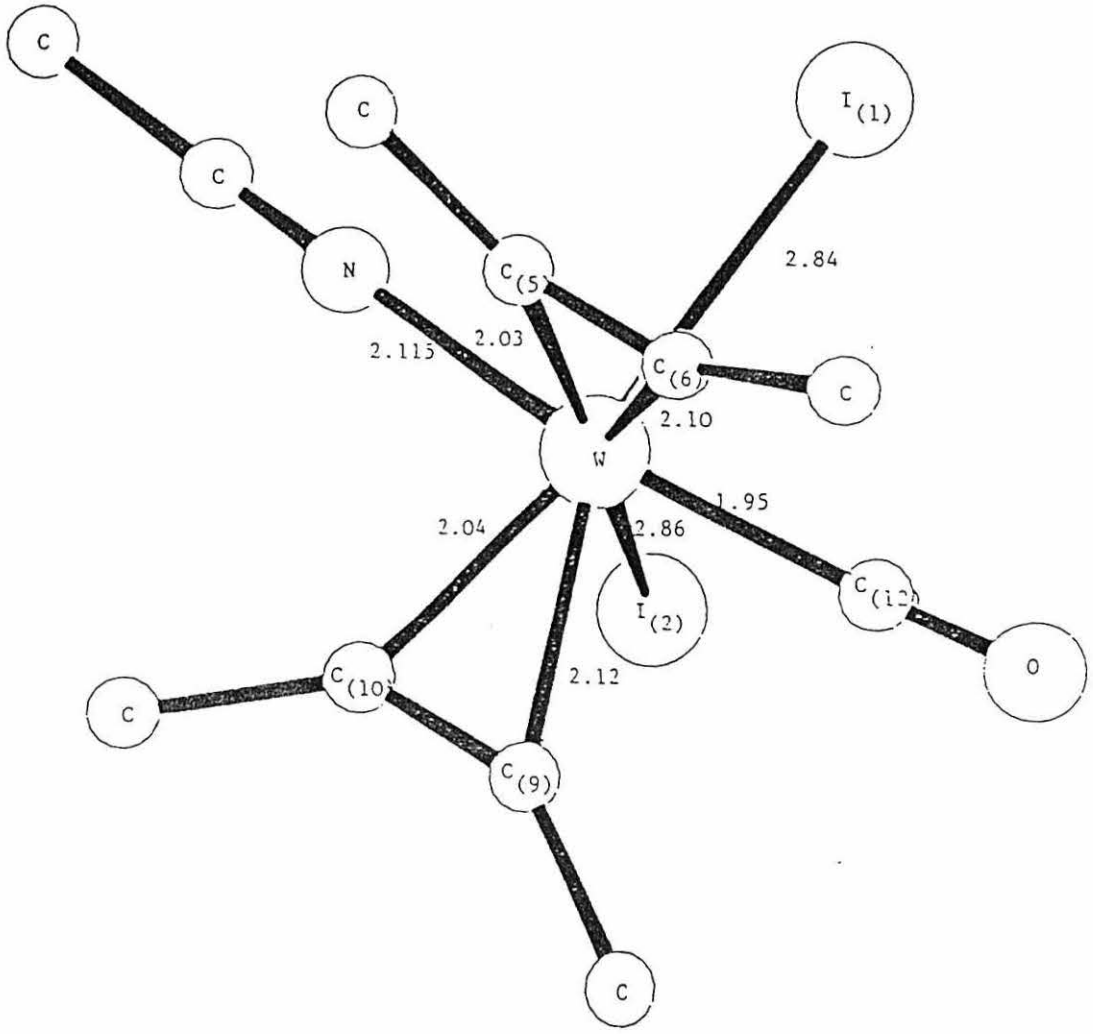

As with previous homohalogeno complexes, the mixed halide complex $[WBrI(CO)_3(NCMe)_2]$ reacts with two equivalents of alkyne to give the bis(alkyne) complexes $[WBrI(CO)(NCMe)(\eta^2\text{-}RC_2R)_2]$ (R = Me, Ph, CH_2Cl)[121]. The very novel molybdenum complexes $[MoCl(GeCl_3)(CO)(NCMe)(PPh_3)(\eta^2\text{-}RC_2R)]$ (R = Me, Ph) containing six-different monodentate ligands has also been synthesised by treatment of $[MoCl(GeCl_3)(CO)_2(NCMe)_2(PPh_3)]$ with one equivalent of RC_2R (R = Me, Ph)[122,123].

Other haloalkyne complexes have also been described, by other workers, since 1987. For example, in 1987 Davidson *et al*[124] described the synthesis of the dibromo bis(alkyne) complex $[WBr_2(CO)(\eta^2\text{-}CF_3C_2CF_3)_2]$ *via* the reaction of the bromo-bridged dimer $[\{W(\mu\text{-}Br)Br(CO)_4\}_2]$ with $CF_3C_2CF_3$. More recently, Brisdon and co-workers have described the preparation of the complexes $[MX_2(CO)L_2(\eta^2\text{-}RC_2R)]$ (M = Mo, X = Br, R = Me, L = PEt_2Ph, $PEtPh_2$, PMe_2Ph, $PMePh_2$; M = Mo, X = Cl, I; L = $PMePh_2$; M = Mo or W, X = Br, R = Ph, L = $PMePh_2$; M = W, R = Me, X = Br, L = $PMePh_2$) *via* the reaction of $[MX_2(CO)_2(NCMe)L_2]$ with the corresponding alkyne[125]. Another very interesting reaction reported by Mayr and Bastos[126] describes the reaction of $[W(\equiv CPh)Cl(CO)(CNBu^t)(PMe_3)_2]$ with three equivalents of HCl to yield two products. The major product is the complex $[WCl_3(CO)(PMe_3)(\eta^2\text{-}PhCNBu^t)]$ whilst the minor product is the very novel amino alkyne complex $[WCl_2(CO)(PMe_3)_2(\eta^2\text{-}PhCNHBu^t)]$.

4.1.2 Reactions of $[WI_2(CO)(NCMe)(\eta^2\text{-}RC_2R)_2]$ (R = Ph, Me) with phosphorus donor ligands

Many reactions of the bis(alkyne) complexes $[WI_2(CO)(NCMe)(\eta^2\text{-}RC_2R)_2]$ (R = Ph, Me) with donor ligands, have been reported[127-135]. The reactions discussed in this section are those with phosphorus and sulphur donor

ligands only. The complexes $[WI_2(CO)(NCMe)(\eta^2\text{-}RC_2R)_2]$ (R = Ph, Me) react with the diphosphine ligands $Ph_2P(CH_2)_nPPh_2$ (n = 1-6) to give the phosphine substituted mono(alkyne) complexes $[WI_2(CO)\{Ph_2P(CH_2)_nPPh_2\}(\eta^2\text{-}RC_2R)]$. The complex $[WI_2(CO)(\eta^2\text{-}Ph_2P(CH_2)PPh_2)(\eta^2\text{-}MeC_2Me)]$ has been crystallographically characterised and is shown in **Figure 4.2**. Similarly, the reactions of $[WI_2(CO)(NCMe)(\eta^2\text{-}RC_2R)_2]$ with two equivalents of phosphines, L (L = PMe_3, PEt_3, PBu^n_3, PMe_2Ph, $PMePh_2$, PEt_2Ph, $PEtPh_2$) gives the complexes $[WI_2(CO)L_2(\eta^2\text{-}RC_2R)]$[136]. It has also been reported that treatment of $[WI_2(CO)(NCMe)(\eta^2\text{-}MeC_2Me)_2]$ with one equivalent of triphos {triphos = $PhP(CH_2CH_2PPh_2)_2$} results in the formation of the complex $[WI_2(CO)(\eta^2\text{-triphos})(\eta^2\text{-}MeC_2Me)]$ which can be used as a ligand which is able to bind to other metal centres *via* the unbound phosphorus atom of the triphos ligand[137].

Figure 4.2 X- ray crystal structure of $[WI_2(CO)\{\eta^2\text{-}Ph_2P(CH_2)PPh_2\}(\eta^2\text{-}MeC_2Me)]$

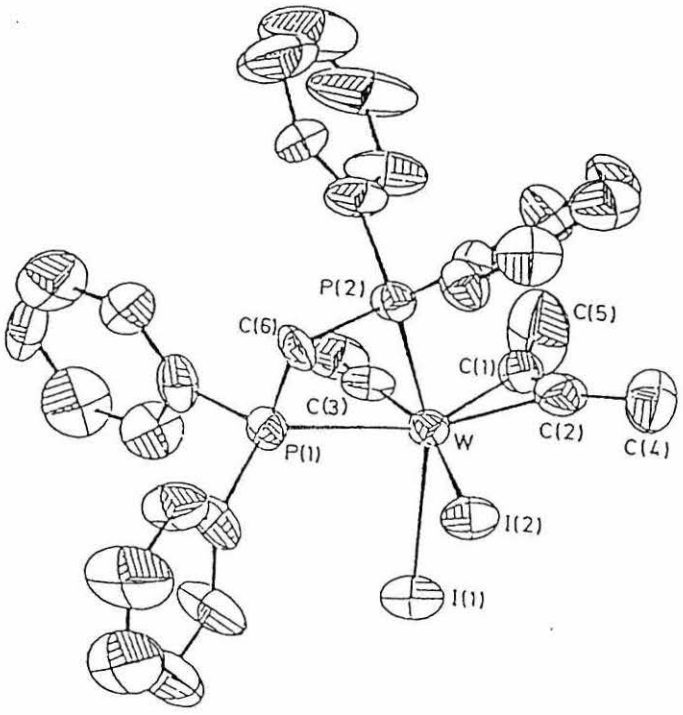

4.1.3 Reactions of $[WI_2(CO)(NCMe)(\eta^2\text{-}RC_2R)_2]$ (R = Ph, Me) with sulphur donor ligands

The complexes $[WI_2(CO)(NCMe)(\eta^2\text{-}RC_2R)_2]$ (R = Ph, Me) have been shown to react with 1 equivalent of $SPPh_3$ to give the complexes $[WI_2(CO)(SPPh_3)(\eta^2\text{-}RC_2R)_2]$. However, reactions with 2 and 3 equivalents of $SPPh_3$ gave the cationic complexes $[WI(CO)(SPPh_3)_2(\eta^2\text{-}RC_2R)_2]I$ and $[W(CO)(SPPh_3)_3(\eta^2\text{-}RC_2R)_2]2I$ respectively[138]. The complex $[WI_2(CO)(NCMe)(\eta^2\text{-}MeC_2Me)_2]$ also reacts with anionic sulphur donor ligands such as $K[SC_5H_4N]$ (SC_5H_4N = pyridine-2-thionate) affording the complex $[WI(CO)(SC_5H_4N\text{-}N,S)(\eta^2\text{-}MeC_2Me)_2]$ with the thionate bound to the tungsten centre via the nitrogen and sulphur atoms of the pyridine-2-thionate ligand[139]. A similar reaction also occurs with pyrimidine-2-thionate affording the complex $[WI(CO)(SC_4H_3N\text{-}N,S)(\eta^2\text{-}MeC_2Me)_2]$[140]. Similar reactions of $[WI_2(CO)(NCMe)(\eta^2\text{-}RC_2R)_2]$ with a range of dithiacarbamates have been reported[141] giving complexes of the type $[WI(CO)(S_2CNC_4H_8\text{-}S,S')(\eta^2\text{-}MeC_2Me)_2]$ which has been crystallographically characterised and is shown in **Figure 4.3** below.

Figure 4.3 X-ray crystal structure of $[WI(CO)(S_2CNC_4H_8\text{-}S,S')(\eta^2\text{-}MeC_2Me)_2]$[139]

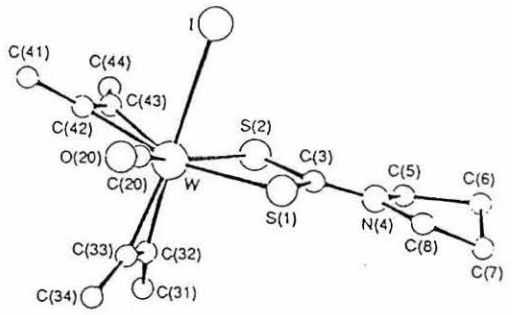

4.1.4 Bonding in transition-metal alkyne complexes

There have been many theories proposed to explain the nature of alkene and alkyne bonding to transition-metal centres[142-144]. The brief description of alkyne-metal bonding in this section is based upon adaptations proposed by Templeton[109] and also Nelson and Janasser[145]. Alkynes are unique in their ability to act as both good single faced π-acceptors and single faced π-donors allowing synergic bonding to the metal centre. The most important bonding interaction is between the σ orbital of the transition-metal and the π orbital of the alkyne ligand {**Figure 4.4**(a)} this is complemented by back donation from the filled d_{xz} orbital of the metal to the unoccupied π* orbital of the alkyne {**Figure 4.4**(b)}.

Figure 4.4 Orbital interactions involved in alkyne transition-metal bonding

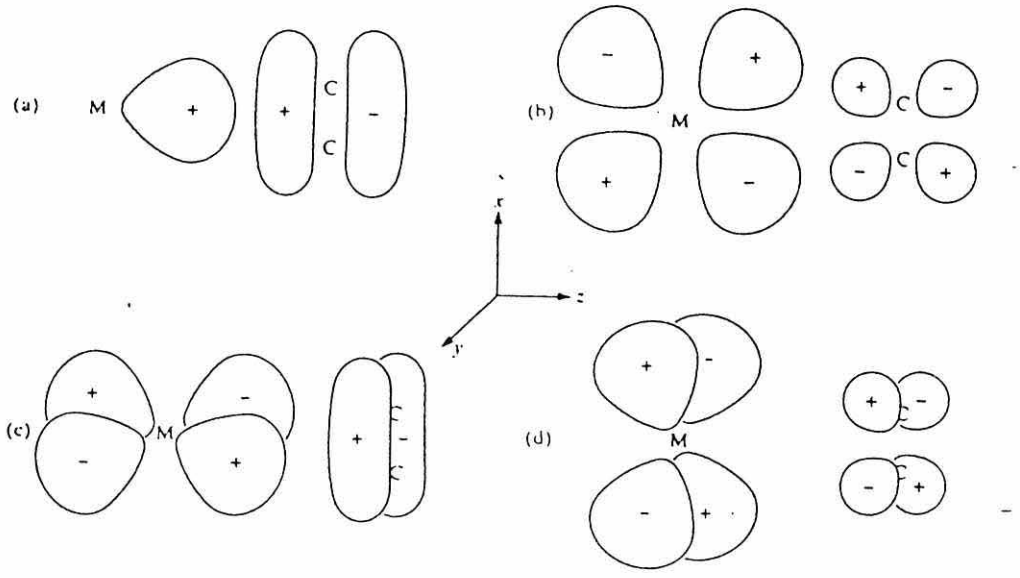

This description of the bonding so far adequately describes two electron donor alkynes. In order to explain further electron donation it it is necessary to consider the pair of π' and π'^* orbitals orthogonal to the ones already considered. There is an important interaction between the metal d_{yz} orbital of the metal and the π' orbital of the alkyne this is combined with the less significant orbital overlap and back donation between the metal d_{xy} orbital and the π'^* orbital of the alkyne. These further orbital interactions {**Figure 4.4**(c),(d)} help explain three- and four-electron alkyne complexes of the transition-metals.

4.2 RESULTS AND DISCUSSION

The starting bis(alkyne) complexes $[WX_2(CO)(NCMe)(\eta^2\text{-}RC_2R)_2]$ (X = Br, I; R = Ph, Me) were prepared by literature methodology. The trithioether $MeS(CH_2)_2S(CH_2)_2SMe$ (TTN) was prepared by a modified literature method[106] while the cyclic trithioether 2,5,8-trithia-*o*-benzenophane (ttob) was prepared as described[108] in chapter 3.

4.2.1 Reactions of the complexes $[WI_2(CO)(NCMe)(\eta^2\text{-}RC_2R)_2]$ (R = Ph, Me) with the trithioether ligand $MeS(CH_2)_2S(CH_2)_2SMe$ (TTN)

The reaction of the orange complex $[WI_2(CO)(NCMe)(\eta^2\text{-}PhC_2Ph)_2]$ with an equimolar amount of $MeS(CH_2)_2S(CH_2)_2SMe$ with stirring in CH_2Cl_2 at room temperature for 72 hours gave the complex $[WI_2(CO)\{MeS(CH_2)_2S(CH_2)_2SMe\text{-}S,S'\}(\eta^2\text{-}PhC_2Ph)]$ (**19**) in high yield. Further reflux of complex (**19**) in CH_2Cl_2 for 6 hours gave the charged complex $[WI(CO)\{MeS(CH_2)_2S(CH_2)_2SMe\text{-}S,S',S''\}(\eta^2\text{-}PhC_2Ph)]I\ Et_2O$(**20**) again in high yield. Both complexes are green in colour, and are soluble in both

dichloromethane and acetonitrile but are only sparingly soluble in diethyl ether. The complexes (**19**) and (**20**) can be distinguished by both their conductivities and by spectroscopic means. Both complexes were characterised by elemental analysis, infra red and ^{1}H NMR spectroscopy (**Tables 4.1-4.3**). Conductivity measurements in acetonitrile showed complex (**19**) to be a non-electrolyte while complex (**20**) was a 1:1 electrolyte (Λ_m = 49 and 138 S cm^2 mol^{-1} respectively).

The infra red spectrum of complex (**19**) in CH_2Cl_2 shows a single carbonyl stretching band at 1968 cm^{-1} suggesting the presence of one isomer in solution (**Figure 4.5**). The relatively low stretching frequency also suggests the loss of one diphenylacetylene ligand during the reaction. The loss of diphenylacetylene results in more electron density at the transition-metal centre and hence increased back bonding to the carbonyl ligand. Similarly, complex (**20**) shows one carbonyl band at 1974 cm^{-1} in the IR spectrum obtained in CH_2Cl_2. Both complexes also exhibit weak alkyne (C=C) stretching bands at around 1650 cm^{-1}, as expected considerably lower than that of the free alkyne.

Complex (**19**) has been structurally characterised by X-ray crystallography[146] (**Figure 4.6**). Single crystals suitable for X-ray analysis were grown from a cooled solution of CH_2Cl_2/Et_2O (-15°C, 85:15 ratio). The crystals were monoclinic with unit cell dimensions of a = 8.458(2)Å, b = 13.494(12) Å, c = 22.03(3) Å, and β = 99.48(8)°. The complex is of a distorted octahedral nature with *cis*-iodo ligands, the diphenylacetylene ligand and an end coordinated sulphur atom of the thioether forming the equatorial plane. The axial positions of the structure are occupied by the central coordinated sulphur of the thioether and the carbon monoxide ligand. As is seen in other d^4 electronic systems the alkyne is positioned parallel to the tungsten-carbon monoxide axis. This configuration optimises both the π-acceptor and σ-donor

properties of the alkyne[119]. Further details of bond lengths and angles for complex (**19**) can be found in **Table A1.8** in **Appendix 1**.

The ^{1}H NMR spectrum of complex (**19**) is consistent with the molecular structure shown in **Figure 4.6** showing a singlet at δ = 2.2 ppm which can be assigned to the methyl group attached to the uncoordinated sulphur atom of the TTN ligand. Another resonance at δ = 2.35 ppm may be assigned to the methylene protons again attached to the uncoordinated sulphur atom of the ligand. However, the ^{1}H NMR of complex (**20**) in $CDCl_3$ shows a more simple spectrum with resonances at δ = 3.1 ppm and δ = 2.2 ppm which can be respectively assigned to the methylene and methyl protons of the tridentately-coordinated TTN ligand.

Figure 4.5 Infra red spectra in the carbonyl regions for complex (**19**) and $[WI_2(CO)(NCMe)(\eta^2\text{-}PhC_2Ph)_2]$

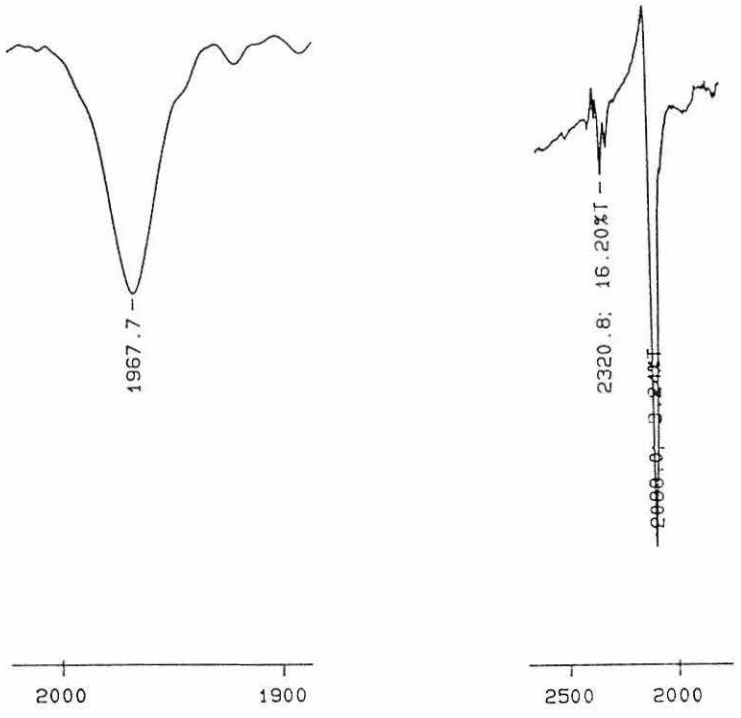

Figure 4.6 X-ray crystal structure of $[WI_2(CO)\{TTN\text{-}S,S'\}(\eta^2\text{-}PhC_2Ph)]$[146]

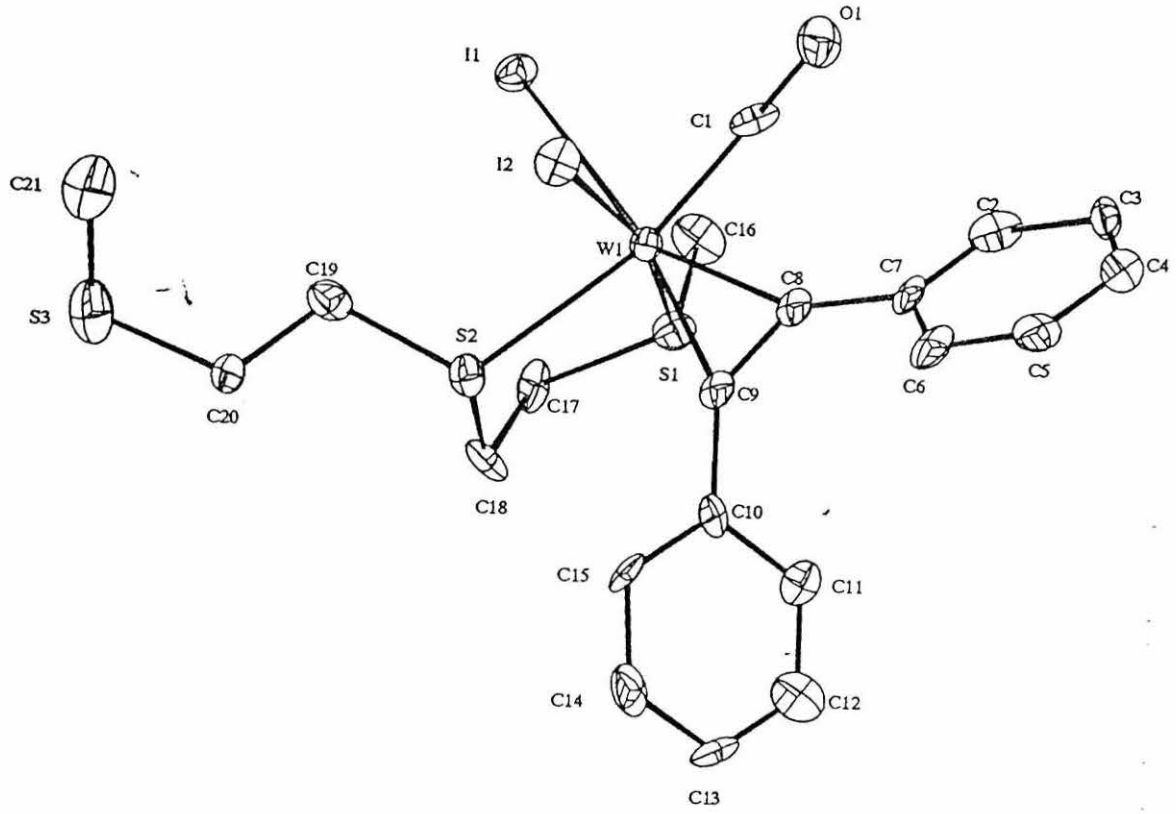

Similarly, the reaction of the yellow starting complex $[WI_2(CO)(NCMe)(\eta^2\text{-}MeC_2Me)_2]$ with an equimolar amount of $MeS(CH_2)_2S(CH_2)_2SMe$ with stirring in CH_2Cl_2 at room temperature for 72 hours gave the complex $[WI(CO)\{MeS(CH_2)_2S(CH_2)_2SMe\text{-}S,S',S''\}(\eta^2\text{-}MeC_2Me)]I\ Et_2O$ (**21**) in high yield. Conductivity measurements showed complex (**21**) to be a 1:1 electrolyte in acetonitrile (Λm = 142 S cm^2 mol^{-1}). Unlike the previously described reaction of $[WI_2(CO)(NCMe)(\eta^2\text{-}PhC_2Ph)_2]$ with TTN, no analogous 2-butyne complex similar to complex (**19**) was isolated even after shorter reaction times. Complex (**21**) was characterised by elemental analysis, infra red and ^1H nmr spectroscopy (**Tables 4.1-4.3**).

The infra red spectrum of complex (**21**) in CH_2Cl_2 shows a single stretching band at 1954 cm^{-1}, which is lower than the analogous diphenylacetylene complex (**20**). The lower carbonyl stretching frequency of complex (**21**) is due to 2-butyne being a weaker π-acceptor than diphenylacetylene hence resulting in more electron density at the tungsten centre available for back bonding to the carbonyl ligand. The ^1H NMR spectrum of complex (**21**) in $CDCl_3$ shows resonances at δ = 2.4 ppm and δ = 3.1 ppm which are again due to the methylene and methyl protons of the tri-coordinated TTN ligand as in the analogous diphenylacetylene complex (**20**). In both cases the signals are shifted downfield in comparison to the free ligand. From the spectroscopic data combined with the X-ray crystal structure of complex (**19**) it is possible to suggest similar stuctures may be adopted by complexes (**20**) and (**21**).

4.2.2 Reactions of the complexes $[WI_2(CO)(NCMe)(\eta^2\text{-}RC_2R)_2]$ (R = Ph, Me) with the trithioether ligand 2,5,8-trithia-*o*-benzenophane (ttob)

The reaction of the orange complex $[WI_2(CO)(NCMe)(\eta^2\text{-}PhC_2Ph)_2]$ with an equimolar amount of ttob with stirring in CH_2Cl_2 at room temperature for 72 hours gave the complex $[WI(CO)\{ttob\text{-}S,S',S''\}(\eta^2\text{-}PhC_2Ph)]I$ (**22**) in high yield. Complex (**22**) is green in colour, soluble in both dichloromethane and acetonitrile, but only sparingly soluble in diethyl ether. Complex (**22**) was characterised by elemental analysis, infra red and ^1H NMR spectroscopy (**Tables 4.1-4.3**). Conductivity measurements in acetonitrile showed complex (**22**) to be a 1:1 electrolyte (Λm = 141 S cm^2 mol^{-1} respectively).

The infra red spectrum of complex (**22**) in CH_2Cl_2 shows a single carbonyl stretching band at 1972 cm^{-1} suggesting the presence of one isomer in solution. The relatively low stretching frequency, as seen previously, again suggests the loss of one diphenylacetylene ligand during the reaction. The loss of diphenylacetylene results in more electron density at the tungsten centre and hence increased back bonding to the carbonyl ligand. The ^1H NMR spectrum of complex (**22**) shows a multiplet at δ = 2.5 ppm which can be assigned to the eight methylene protons bridging the three coordinated sulphur atoms of the ttob ligand. A further pair of doublets at δ = 4.4 ppm and δ = 3.8 ppm may be assigned to the benzylic protons of the ttob ligand.

Further recrystallisation of complex (**22**) from CH_2Cl_2/Et_2O gave more of the green powder $[WI(CO)\{ttob\text{-}S,S',S''\}(\eta^2\text{-}PhC_2Ph)]I$ and also three very well formed dark green crystals. One of these crystals was characterised by X-ray crystallography (**Figure 4.8**) and shown to be the very novel charged complex $[WI\{ttob\text{-}S,S',S''\}(\eta^2\text{-}PhC_2Ph)_2]I_3$ (**23**).

Unfortunately, insufficient material was isolated for further spectroscopic studies and the complex was never isolated again in further reactions. Several attempts at a rational synthesis of complex (**23**) were unsuccessful for example the addition of a catalytic amount of iodine to the reaction mixture. The structure of the cationic complex [WI{ttob-*S,S',S''*}(η^2-$PhC_2Ph)_2$]I_3 can be described as a distorted octahedron with both diphenylacetylene ligands occupying one site each. Tungsten-alkyne distances are very similar, 2.04(2) and 2.09(2) Å respectively. The tungsten atom is bound to all three sulphur atoms of the ttob ligand, with tungsten-sulphur distances of 2.493(5), 2.589(4) and 2.606(5) Å respectively. The shorter W-S distance is to the unique sulphur atom of the ttob ligand. The ttob ligand occupies the site *trans*-to the single iodide. Further details of bond lengths and angles for complex (**23**) can be found in **Table A1.9** in **Appendix 1**.

Similarly, the reaction of the yellow starting complex [WI_2(CO)(NCMe)(η^2-$MeC_2Me)_2$] with an equimolar amount of ttob with stirring in CH_2Cl_2 at room temperature for 72 hours gave a green coloured oil. Recrystallisation from CH_2Cl_2 gave the green complex [WI(CO){ttob-*S,S',S''*}(η^2-MeC_2Me)]I (**24**) in high yield. Conductivity measurements showed complex (**24**) to be a 1:1 electrolyte in acetonitrile (Λ_m = 145 S cm^2 mol^{-1}). The infra red spectrum of complex (**24**) in CH_2Cl_2 shows a single carbonyl stretching band at 1970 cm^{-1} and an alkyne stretch at 1579 cm^{-1}, as expected considerably lower than that of the free alkyne. The ^1H NMR spectrum for complex (**24**) in $CDCl_3$ shows a multiplet at δ = 2.4 ppm which can be assigned to the eight methylene protons bridging the three coordinated sulphur atoms of the ttob ligand. A further two doublets are observed at δ = 4.2 ppm and δ = 3.5 ppm which can be

assigned to the benzylic protons of the ttob ligand while the methyl protons of the remaining alkyne ligand are observed as a singlet at $\delta = 3.6$ ppm.

Figure 4.7 X-ray structure of the complex $[WI\{ttob\text{-}S,S',S''\}(\eta^2\text{-}PhC_2Ph)_2]I_3$

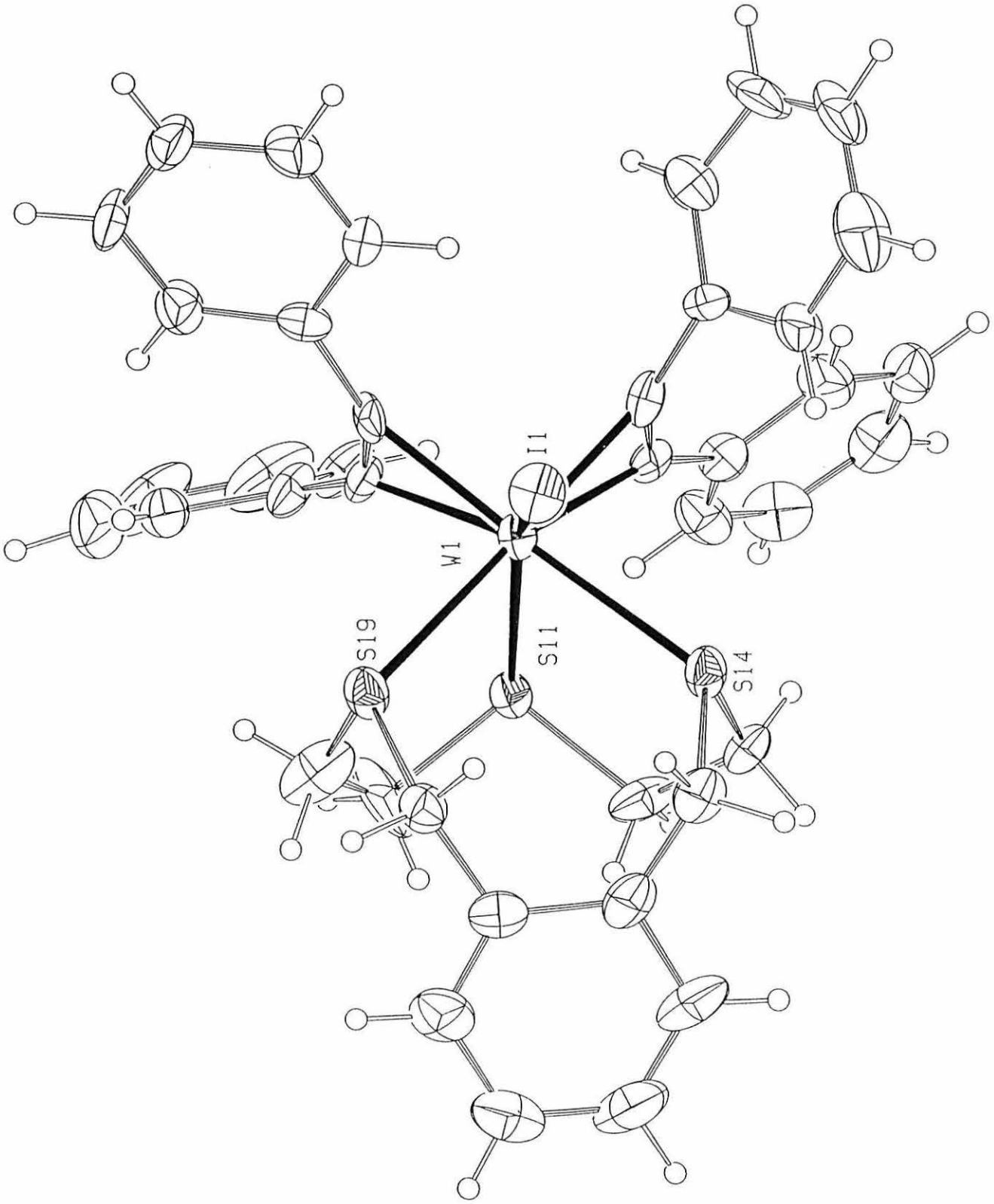

4.2.3 Reactions of the di-bromo complexes [$WBr_2(CO)(NCMe)(\eta^2\text{-}RC_2R)_2$](R= Ph, Me) with $MeS(CH_2)_2S(CH_2)_2SMe$ (TTN) and the cyclic trithioether ttob.

The complex [$WBr_2(CO)(NCMe)(\eta^2\text{-}PhC_2Ph)_2$] was synthesised *via* the reaction of [$WBr_2(CO)_3(NCMe)_2$] with four equivalents of diphenylacetylene in CH_2Cl_2. However, crystals of suitable quality for X-ray analysis were prepared by recrystallisation from CH_2Cl_2/Et_2O at room temperature after 24 hours. The structure has been solved by X-ray crystallography and is shown in **Figure 4.9.** The structure of [$WBr_2(CO)(NCMe)(\eta^2\text{-}PhC_2Ph)_2$] is isomorphous to that of the analogous diiodo complex previosly described[118]. The structure is best described as the metal being octahedral, with the alkyne ligands each occupying one coordination site. The bromides (W-Br 2.679(3) and 2.722(3) Å) are mutually *cis*-to one another and both are *trans*-to an alkyne ligand. The carbonyl (W-C 2.09(2) Å) is *trans*-to the acetonitrile group (W-N 2.20(2) Å) which completes the octahedron. Further details of bond lengths and angles for the complex [$WBr_2(CO)(NCMe)(\eta^2\text{-}PhC_2Ph)_2$] can be found in **Table A1.10** in **Appendix 1**.

The reaction of the yellow complex [$WBr_2(CO)(NCMe)(\eta^2\text{-}PhC_2Ph)_2$] with an equimolar amount of TTN, with stirring in CH_2Cl_2 at room temperature for 24 hours, gave the complex [$WBr(CO)\{TTN\text{-}S,S',S''\}(\eta^2\text{-}PhC_2Ph)$]Br Et_2O (**25**) in high yield. Similarly, the reaction of complex [$WBr_2(CO)(NCMe)(\eta^2\text{-}PhC_2Ph)_2$] with an equimolar amount of ttob with stirring in CH_2Cl_2 at room temperature for 24 hours gave the complex [$WBr(CO)\{ttob\text{-}S,S',S''\}(\eta^2\text{-}PhC_2Ph)$]Br (**26**) also in good yield. Both complexes (**25**) and (**26**) are green in colour and are soluble in dichloromethane and acetonitrile but only sparingly soluble in diethyl ether. Both complexes are very oxygen sensitive both in solution and to a lesser extent in the solid-state. Both complexes (**25**) and (**26**)

were characterised by elemental analysis, infra red and ^{1}H NMR spectroscopy (**Tables 4.1-4.3**). Conductivity measurements in acetonitrile showed both complexes (**25**) and (**26**) to be 1:1 electrolytes (Λ_m = 156 and 160 S cm^2 mol^{-1} respectively).

The infra red spectrum of both complexes (**25**) and (**26**) in CH_2Cl_2 each show a single carbonyl stretching band at 1967 cm^{-1} and 1966 cm^{-1} respectively suggesting the presence of one isomer in solution. The relatively low stretching frequencies again suggests the loss of one diphenylacetylene ligand during the reaction. The loss of diphenylacetylene once again results in more electron density at the tungsten centre and hence increased back bonding to the carbonyl ligand.

The ^{1}H NMR spectrum of complex (**25**) in $CDCl_3$ shows resonances at δ = 2.9 ppm and δ = 2.1 ppm which can be respectively assigned to the methylene and methyl protons of the tri-coordinated TTN ligand. Complex (**26**) shows a doublet at δ = 3.9 ppm and a multiplet at δ = 2.6 ppm. The doublet can be assigned to the benzylic protons of the ttob ligand while the multiplet is due to the remaining methylene protons of the trithioether. Unfortunately, the samples decompose very quickly so some free thioether and other decomposition products are generally observed in the proton spectrum of both complexes. Reactions were also attempted with the complex $[WBr_2(CO)(NCMe)(\eta^2\text{-}MeC_2Me)_2]$ and the ligands TTN and ttob, however, no stable products were isolated.

Figure 4.8 X-ray crystal structure of $[WBr_2(CO)(NCMe)(\eta^2\text{-}PhC_2Ph)_2]$

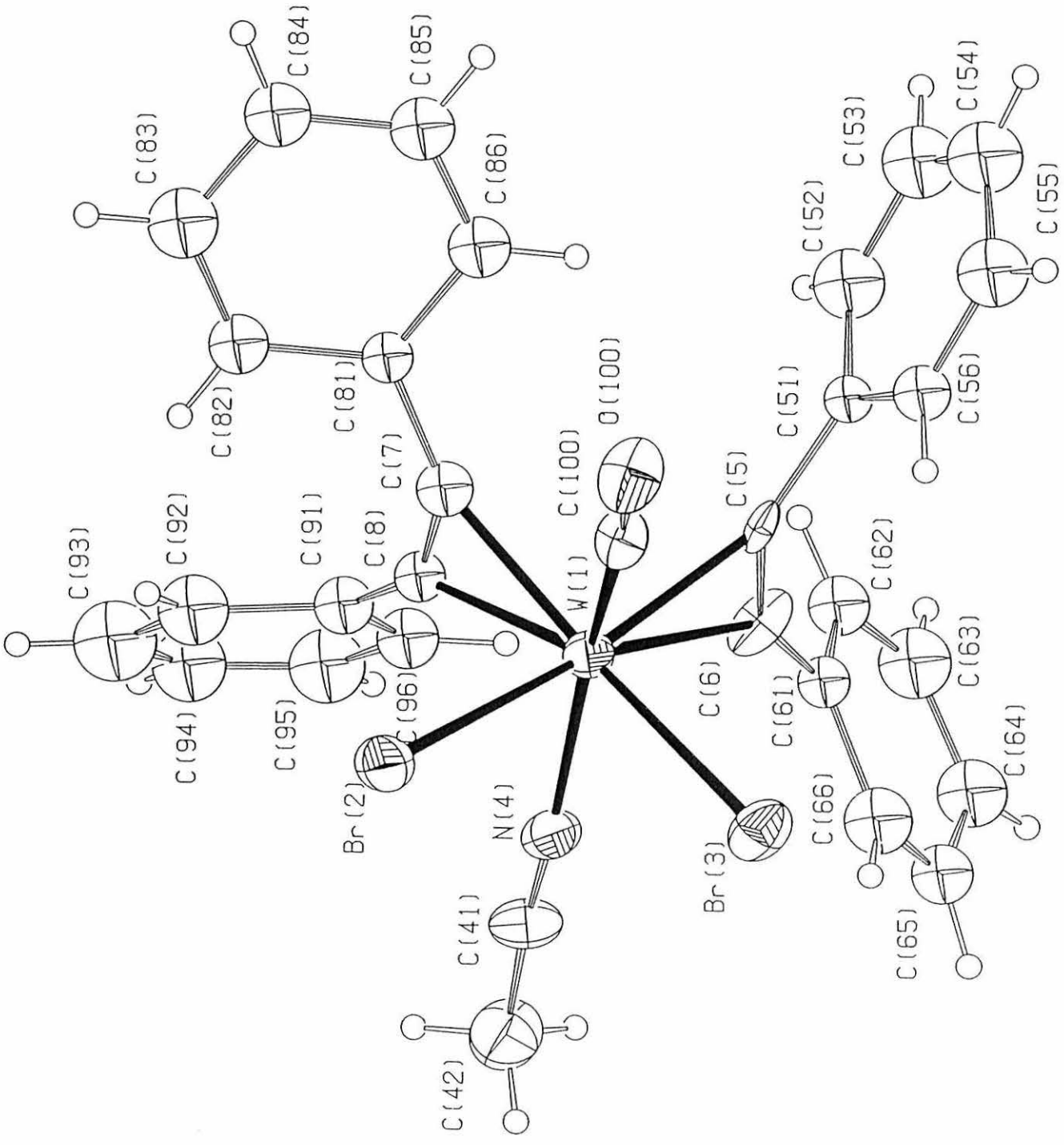

4.2.4 Reaction of the complex [$WI_2(CO)\{MeS(CH_2)_2S(CH_2)_2SMe$-*S,S'*}($\eta^2$-$PhC_2Ph$)] (19) with [$FeI(CO)_2Cp$]

The reaction of the green tungsten-alkyne thioether complex [$WI_2(CO)\{MeS(CH_2)_2S(CH_2)_2SMe$-*S,S'*}($\eta^2$-$PhC_2Ph$)] (**19**) with an equimolar quantity of [$FeI(CO)_2Cp$] in CH_2Cl_2 for four hours at room temperature gave the novel bimetallic complex [$Cp(OC)_2Fe\{S(Me)(CH_2)_2S(CH_2)_2(Me)S$-*S,S',S''*}$WI_2(CO)(\eta^2$-$PhC_2Ph)$]I (**27**) which was fully characterised by characterised by elemental analysis, infra red and ^{1}H NMR spectroscopy (**Tables 4.1-4.3**). The complex is black in colour and is relatively soluble in chlorinated solvents such as dichloromethane and chloroform. The infra red spectrum of complex (**27**) in CH_2Cl_2 shows three strong carbonyl stretching bands at 1960, 1998 and 2045 cm^{-1} and a weak alkyne (C=C) stretch at 1667 cm^{-1}. The presence of only three carbonyl stretching bands suggests the presence of only one isomer in solution. The carbonyl band at 1960 cm^{-1} is probably due to the carbonyl attatched to the tungsten while the two higher frequency bands are due to the carbonyls attatched to the iron centre.

The ^{1}H NMR spectrum of complex (**27**) in $CDCl_3$ shows a singlet at δ = 5.1 ppm, which can be assigned to the five cyclopentadienyl protons attatched to the iron centre. A broad multiplet at δ = 3.4 ppm may be assigned to the two most central methylene groups of the TTN ligand while the broad multiplets at δ = 3.2 ppm and δ = 3.2 ppm may be assigned repectively to the methylene and methyl protons adjacent to the sulphur atom bound to the tungsten metal centre. The remaining broad multiplet at δ = 2.8 ppm can be assigned to the remaining five protons of the thioether ligand.

4.2.5 Reactions of the complexes $[MoI_2(CO)(NCMe)(\eta^2\text{-}RC_2R)_2]$ (R = Ph, Me) with the trithioether ligand $MeS(CH_2)_2S(CH_2)_2SMe$ (TTN)

The reaction of the red/brown complex $[MoI_2(CO)(NCMe)(\eta^2\text{-}PhC_2Ph)_2]$ with an equimolar amount of $MeS(CH_2)_2S(CH_2)_2SMe$ with stirring in CH_2Cl_2 at room temperature for 12 hours gave the complex $[MoI(CO)\{MeS(CH_2)_2S(CH_2)_2SMe\text{-}S,S',S''\}(\eta^2\text{-}PhC_2Ph)]I$ (**28**) in high yield. Similarly, the reaction of the 2-butyne complex $[MoI_2(CO)(NCMe)(\eta^2\text{-}MeC_2Me)_2]$ with an equimolar amount of $MeS(CH_2)_2S(CH_2)_2SMe$ in CH_2Cl_2 at room temperature for twelve hours gave the complex $[MoI(CO)\{MeS(CH_2)_2S(CH_2)_2SMe\text{-}S,S',S''\}(\eta^2\text{-}MeC_2Me)]I$ Et_2O (**29**) once again in high yield. Both complexes are green in colour, and are soluble in both dichloromethane and acetonitrile, but are only sparingly soluble in diethyl ether. The complexes (**28**) and (**29**) are both more air-sensitive in solution, and in the solid-state than their diiodo-tungsten analogues and may only be stored for short periods of time under an atmosphere of dry dinitrogen. Conductivity measurements of both complexes in acetonitrile showed them to both be 1:1 electrolytes (Λ_m = 149 and 152 S cm^2 mol^{-1} respectively). Both complexes were fully characterised by elemental analysis, infra red and ^1H NMR spectroscopy (**Tables 4.1-4.3**).

The infra red spectra of both complexes (**28**) and (**29**) in CH_2Cl_2 show single strong carbonyl stretching bands at 1984 and 1971 cm^{-1} respectively. This, as was previously observed with the diiodo-tungsten analogues, is a relatively low stretching frequency in comparison to the appropriate (bis)alkyne starting complexes with carbonyl stretches at 2074 and 2059 cm^{-1} respectively. The reason for this dramatic shift in carbonyl stretching frequency upon coordination to the thioether ligand is, as before, due to the loss of a diphenylacetylene ligand during the reaction.

The ^{1}H NMR spectrum of complex (**28**) in $CDCl_3$ shows a broad multiplet at δ = 2.9 ppm which can be assigned to the methylene protons of the tridentately bound thioether. Another multiplet at δ = 2.2 ppm may be assigned to the methyl groups of the TTN ligand. The remaining broad multiplet further downfield at δ = 7.6 ppm can be assigned to the remaining ten protons of the diphenylacetylene. The ^{1}H nmr spectrum of the 2-butyne complex (**29**) is very similar in nature to that of complex (**28**) with two multiplets at δ = 2.8 ppm and δ = 2.2 ppm again due to the methylene and methyl protons of the TTN ligand, however, there is also a singlet at δ = 3.2 ppm from the methyl protons of the alkyne.

4.2.6 Reactions of the complexes [$MoI_2(CO)(NCMe)(\eta^2$-$RC_2R)_2$] (R = Ph, Me) with the cyclic trithioether 2,5,8-trithia-*o*-benzenophane (ttob)

The reaction of the complex [$MoI_2(CO)(NCMe)(\eta^2$-$PhC_2Ph)_2$] with an equimolar amount of ttob with stirring in CH_2Cl_2 at room temperature for 20 hours gave the complex [MoI(CO){ttob-*S*,*S*',*S*''}(η^2- PhC_2Ph)]I (**30**) in high yield. Similarly the reaction of the 2-butyne complex [$MoI_2(CO)(NCMe)(\eta^2$-$MeC_2Me)_2$] with an equimolar amount of ttob in CH_2Cl_2 at room temperature for 24 hours gave the analogous complex [MoI(CO){ttob-*S*,*S*',*S*''}(η^2-MeC_2Me)]I (**31**) again in good yield. Both complexes are green in colour and are both soluble in dichloromethane and acetonitrile, but are only sparingly soluble in diethyl ether. The complexes (**30**) and (**31**) are again both more air-sensitive in solution and in the solid-state than their diiodo-tungsten analogues but can be stored for short periods of time under an atmosphere of dry dinitrogen in a refrigerator. Conductivity measurements of both complexes in acetonitrile showed them to both be 1:1 electrolytes (Λ_m = 140 and 142 S cm^2

mol^{-1} respectively). Both complexes were fully characterised by elemental analysis, infra red and ^1H NMR spectroscopy (**Tables 4.1-4.3**).

The infra red spectra of both complexes (**30**) and (**31**) in CH_2Cl_2 show a single strong carbonyl stretching bands at 1992 and 1983 cm^{-1} respectively, again a relatively low stretching frequency in comparison to the appropriate bis(alkyne) starting complexes. The ^1H NMR spectrum of complex (**30**) in $CDCl_3$ shows two doublets of J = 11 Hz at δ = 5.1 ppm and δ= 4.6 ppm which can be assigned to benzylic protons of the tridentately bound ttob ligand. The signal is split into a doublet due to coupling with the adjacent aromatic proton of the ring. Also observed is a multiplet at δ = 3.4 ppm due to the methylene protons of the linkages $S(CH_2)_2S$. The remaining broad multiplet further downfield at δ = 7.6 ppm can be assigned to the remaining protons of the diphenylacetylene and the aromatic protons of the ttob ligand. The ^1H NMR spectrum of the 2-butyne complex (**31**) in $CDCl_3$ has two doublets at δ = 5.1 ppm and δ = 4.8 ppm with coupling constants J = 12 Hz which can be assigned to the benzylic protons of the ttob ligand. A multiplet can also be observed at δ = 2.9 ppm which is due to the remaining methylene protons of the ttob ligand. The alkyne methyl protons are observed as a singlet at δ = 3.2 ppm from the methyl protons of the alkyne.

4.2.7 Reactions of the complexes $[MoI_2(CO)(NCMe)(\eta^2\text{-}RC_2R)_2]$ (R = Ph, Me) with the cyclic trithioether, 1,4,7-trithiacyclononane, [9]aneS$_3$

The reaction of the complex $[MoI_2(CO)(NCMe)(\eta^2\text{-}PhC_2Ph)_2]$ with an equimolar amount of [9]aneS$_3$ with stirring in CH_2Cl_2 at room temperature for 20 hours gave the complex $[MoI(CO)\{[9]aneS_3\text{-}S,S',S''\}(\eta^2\text{-}PhC_2Ph)]I$ (**32**) in high yield. The complex is green in colour, soluble in chlorinated solvents and acetonitrile and is relatively air-sensitive in both solution and the solid-state.

Complex (**32**) has been fully characterised by elemental analysis, infra red, ^{1}H NMR and ^{13}C NMR spectroscopy (**Tables 4.1-4.3**).

The infra red spectrum of complex (**32**) in CH_2Cl_2 shows a single carbonyl stretching band at 1980 cm^{-1} suggesting the presence of one isomer in solution. The relatively low stretching frequency also suggests the loss of one diphenylacetylene ligand during the reaction.

Complex (**32**) has been structurally characterised by X-ray crystallography (**Figure 4.10**). Single crystals suitable for X-ray analysis were grown from a cooled solution of CH_2Cl_2/Et_2O (75 : 25, -15°C). The structure shows the molybdenum atom is bonded to the trithioether, together with an iodide, a carbonyl and a diphenylacetylene ligand. The geometry is best described as octahedral with the alkyne occupying one coordination site. The three Mo-S distances vary significantly with the shortest, *trans*-to the iodine, at 2.449(5) Å and the longest, *trans*-to the diphenylacetylene, at 2.607(6) Å. The bond lengths to the iodide and carbonyl ligands are 2.758(3) and 1.97(2) Å respectively. All four monodentate ligands are *trans*-to the [9]aneS$_3$ ligand, as was observed previously in the similar tungsten tricarbonyl complex [WI(CO)$_3$([9]aneS$_3$)]I . Further details of bond lengths and angles for complex (**32**) can be found in **Table A1.11** in **Appendix 1**.

The ^{1}H NMR spectrum of complex (**32**) in $CDCl_3$ is consistent with the molecular structure shown in **Figure 4.10** showing a broad multiplet centred around δ = 4.0 ppm which can be assigned to the CH_2 groups linking the coordinated sulphur atoms. This is very different to the spectrum of the unbound ligand which shows just one resonance in $CDCl_3$ at δ = 2.1 ppm. The phenyl protons of the alkyne ligand are observed at δ = 7.6 ppm as a multiplet.

The $^{13}C\{^{1}H\}$ NMR spectrum of complex (**32**) in $CDCl_3$ shows six singlets for the [9]aneS$_3$ ligand at δ = 35.3, 37.0, 37.4, 38.4, 39,0 and 44.4 ppm

respectively. This suggests the possibility of two isomers in solution. The aromatic carbon resonances of the diphenylacetylene ligand are observed as eight singlets at δ = 127.0, 128.1, 129.3, 129.8, 131.0, 132.1, 135.1 and 137.1ppm. This again suggests the presence of two isomers in solution with four signals due to each isomer. The alkyne-contact resonances are observed as singlets at 225.8 ppm and 226.9 ppm respectively. The relatively low field nature of the alkyne-contact carbons suggests the alkyne to be a 4-electron donor[147] to the molybdenum centre. Finally, the carbonyl carbon is observed as two signals at slightly lower field at 212.5ppm and 214.0 ppm respectively.

A similar reaction of the 2-butyne complex $[MoI_2(CO)(NCMe)(\eta^2\text{-}MeC_2Me)_2]$ with an equimolar quantity of [9]aneS$_3$ in CH_2Cl_2 at room temperature for twenty hours gave the analogous 2-butyne complex $[MoI(CO)\{[9]aneS_3\text{-}S,S',S''\}(\eta^2\text{-}MeC_2Me)]\ I$ (**33**). Again the complex is green in colour and shows similar spectral properties to complex (**32**).

The infa red spectrum of complex (**33**) shows one carbonyl sretching band at 1970cm^{-1} again suggesting the loss of one alkyne ligand during the reaction. The ^{1}H NMR spectrum of complex (**33**) shows a broad multiplet at δ = 3.9ppm which can be assigned to the CH_2 protons of the [9]aneS$_3$ ligands. The ligand is not seen as a singlet, as is the free ligand, due to the assymetry of the complex upon coordination of the ligand. The alkyne methyl protons are observed as a singlet at δ = 3.2ppm. Conductivity measurements show both complexes (**32**) and (**33**) to be 1:1 electrolytes in acetonitrile (Λ_m = 154 and 152 S cm^2 mol^{-1} respectively).

Figure 4.9 X-ray crystal structure of [Mol(CO){[9]aneS$_3$-*S*,*S*′,*S*″}(η^2-PhC$_2$Ph)]I (**32**)

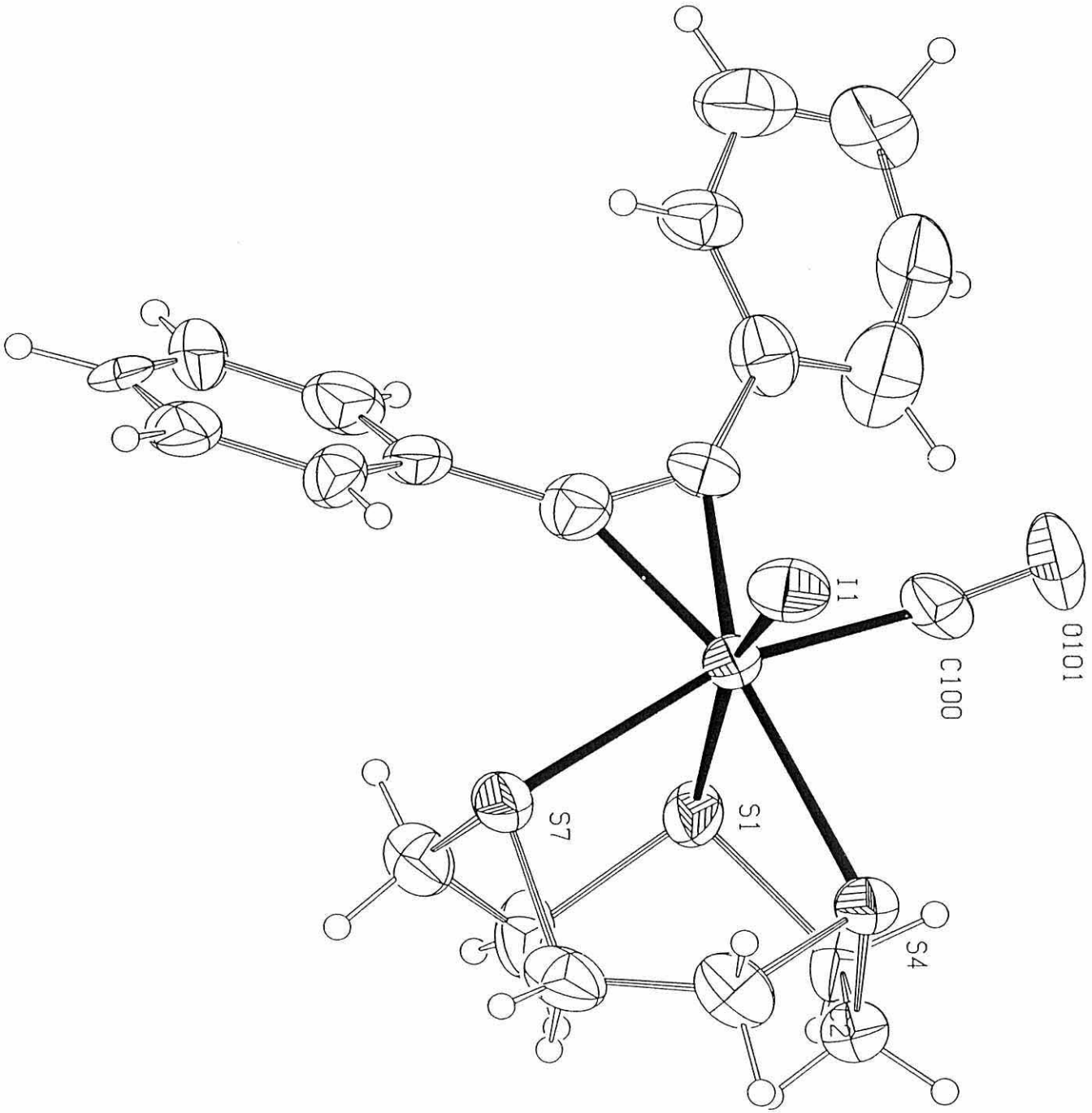

The ^{13}C NMR spectrum of complex (**33**) shows two low field alkyne contact resonances at δ = 225.7 and δ = 226.2 ppm again suggesting the coordinated alkyne donates 4-electrons to the molybdenum centre. As is seen for complex (**32**), six singlets are observed between δ = 34.9 ppm and 44.7 ppm for complex (**33**) again suggesting the presence of two isomers in solution. The methyl protons of the 2-butyne ligand are seen as a multiplet at δ = 22.3 ppm while the carbonyl resonances are observed at δ = 215.3ppm and δ = 214.5ppm. The similarity of spectroscopic data for complexes (**32**) and (**33**) allows the structure shown in **Figure 4.11** to be proposed as a possible structure for complex (**33**).

Figure 4.11 Possible structure for [MoI(CO){[9]aneS$_3$-*S*,*S*',*S*''}(η^2-MeC$_2$Me)]I

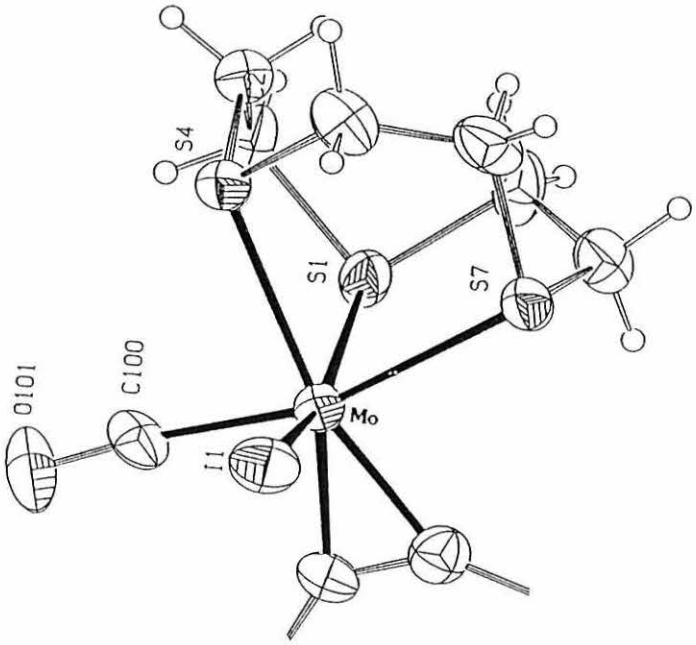

4.2.8 Synthesis of the alkyne complex $[MoI_2(CO)\{Ph_2P(S)CH_2P(S)Ph_2\}(PhC_2Ph)]$.

The starting molybdenum bis(alkyne) complex $[MoI_2(CO)(NCMe)(\eta^2\text{-}PhC_2Ph)_2]$ reacts with the phosphine disulphide ligand $Ph_2P(S)CH_2P(S)Ph_2$, $dppmS_2$, in CH_2Cl_2 over ten hours to give the mono(alkyne) disulphide complex $[MoI_2(CO)\{Ph_2P(S)CH_2P(S)Ph_2\text{-}S,S'\}(\eta^2\text{-}PhC_2Ph)]$(**34**) in good yield. The complex is golden in colour and is a non-electrolyte in acetonitrile solution. The complex (**34**) is fairly air-stable in the solid state, but far less stable in solution. The complex was characterised by elemental analysis, infra red and ^1H NMR spectroscopy (see **Tables 4.1-4.3**). The infra red spectrum shows a single carbonyl stretch at 1973 cm^{-1} and a strong P=S stretch at 560 cm^{-1}. This is in comparison to the P=S stretch of the free $dppmS_2$ ligand which is observed at 626 cm^{-1}. The decrease in υ(P=S) indicates coordination of the ligand to the metal.

The ^1H NMR spectrum of (**34**) shows a triplet at δ = 4.2 ppm in $CDCl_3$ compared to that of the free ligand which shows a triplet at δ = 3.9 ppm. The slight downfield shift again indicates coordination of the ligand. The phenyl resonances of the ligand were slightly down field of the phenyl protons of the alkyne but were all part of the same broad multiplet between δ = 7.3 and 8.0 ppm.

Similar reactions were attempted with both tungsten and molybdenum complexes $[MI_2(CO)(NCMe)(\eta^2\text{-}RC_2R)_2]$ (M = W, Mo; R= Ph, Me) under varying conditions with $dppmS_2$ and other dithioethers $RS(CH_2)_nSR$ (n = 2, 3) but no stable complexes were observed or isolated with starting materials re-obtained in most cases.

4.2.9 Conclusions.

The synthesis of numerous mono(alkyne) thioether complexes has been carried out and several structurally characterised. Further reactivity of the new complexes may be possible and requires further investigation. For example, the complex $[WI_2(CO)\{MeS(CH_2)_2S(CH_2)_2SMe\text{-}S,S'\}(\eta^2\text{-}PhC_2Ph)]$ has been shown to react with the iron complex $[FeI(CO)_2Cp]$ to give the novel bimetallic complex $[Cp(OC)_2Fe\{S(Me)(CH_2)_2S(CH_2)_2(Me)S\text{-}S,S',S''\}WI_2(CO)(\eta^2\text{-}PhC_2Ph)]$, other similar reactions to form bimetallic complexes could be attempted.

Table 4.1 Physical and analytical data[a] for complexes (**19**)-(**34**)

Complex	Colour	Yield %	%C	%H	%S
(**19**) $[WI_2(CO)(TTN\text{-}S,S')(\eta^2\text{-}PhC_2Ph)]$	Green	67	29.9 (30.5)	2.7 (2.9)	11.1 (11.6)
(**20**) $[WI(CO)(TTN\text{-}S,S',S'')(\eta^2\text{-}PhC_2Ph)]I\ Et_2O$	Green	64	30.1 (30.5)	2.5 (2.9)	11.3 (11.6)
(**21**) $[WI(CO)(TTN\text{-}S,S',S'')(\eta^2\text{-}MeC_2Me)]I\ Et_2O$	Green	53	23.6 (23.8)	3.1 (3.7)	12.0 (12.7)
(**22**) $[WI(CO)(ttob\text{-}S,S',S'')(\eta^2\text{-}PhC_2Ph)]I$	Lime Green	55	36.4 (36.0)	2.7 (2.9)	11.5 (10.7)
(**23**) $[WI(ttob\text{-}S,S',S'')(\eta^2\text{-}PhC_2Ph)_2]I_3$	Dark Green	< 2	---	---	---
(**24**) $[WI(CO)(ttob\text{-}S,S',S'')(\eta^2\text{-}MeC_2Me)]I$	Lime Green	40	26.3 (26.3)	2.4 (2.9)	12.9 (12.4)
(**25**)$[WBr(CO)(TTN\text{-}S,S',S'')(\eta^2\text{-}PhC_2Ph)]Br\ Et_2O$	Green	44	38.2 (38.1)	4.0 (4.1)	11.6 (12.2)
(**26**)$[WBr(CO)(ttob\text{-}S,S',S'')(\eta^2\text{-}PhC_2Ph)]Br$	Green	47	39.8 (40.2)	3.1 (3.3)	11.8 (11.9)
(**27**)$[Cp(OC)_2Fe\{TTN\text{-}S,S',S''\}\text{-}WI_2(CO)(\eta^2\text{-}PhC_2Ph)]I$	Black	30	29.6 (29.8)	2.8 (2.6)	9.1 (8.5)
(**28**) $[MoI(CO)(TTN\text{-}S,S',S'')(\eta^2\text{-}PhC_2Ph)]I$	Green	38	36.9 (37.8)	4.4 (4.1)	11.5 (12.1)
(**29**) $[MoI(CO)(TTN\text{-}S,S',S'')(\eta^2\text{-}MeC_2Me)]I\ Et_2O$	Green	49	27.4 (26.9)	3.9 (4.2)	13.8 (14.4)
(**30**) $[MoI(CO)(ttob\text{-}S,S',S'')(\eta^2\text{-}PhC_2Ph)]I$	Green	60	41.4 (39.9)	3.0 (3.2)	11.7 (11.8)
(**31**) $[MoI(CO)(ttob\text{-}S,S',S'')(\eta^2\text{-}MeC_2Me)]I$	Green	42	29.0 (29.7)	3.1 (3.2)	14.0 (14.0)
(**32**) $[MoI(CO)\{[9]aneS_3\text{-}S,S',S''\}(\eta^2\text{-}PhC_2Ph)]I$	Green	48	34.0 (34.3)	3.4 (3.0)	13.8 (13.1)
(**33**) $[MoI(CO)\{[9]aneS_3\text{-}S,S',S''\}(\eta^2\text{-}MeC_2Me)]I$	Green	70	21.0 (21.6)	3.2 (3.0)	15.9 (15.7)
(**34**) $[MoI_2(CO)\{Ph_2P(S)CH_2P(S)Ph_2\text{-}S,S'\}(\eta^2\text{-}PhC_2Ph)$	Gold	56	47.3 (47.8)	3.1 (3.2)	6.4 (6.4)

[a]Calculated values in parentheses

Table 4.2 Infra red carbonyl stretch data[a] for complexes (**19**)-(**34**)

Complex	ν (CO) cm^{-1}*
(**19**)	1968
(**20**)	1974
(**21**)	1954
(**22**)	1972
(**24**)	1970
(**25**)	1967
(**26**)	1966
(**27**)	1960,1998,2045
(**28**)	1984
(**29**)	1971
(**30**)	1992
(**31**)	1983
(**32**)	1980
(**33**)	1970
(**34**)	1985

[b]All spectra were recorded as thin films in CH_2Cl_2 between NaCl plates.

Table 4.3 ^{1}H nmr data[c] for complexes (**19**)-(**34**). All spectra run in $CDCl_3$ at 25°C and referenced to tetramethylsilane.

Complex	^{1}H δ (ppm) J (Hz)
(**19**)	7.3-7.5 (bm, 10H, Ph); 3.2 [bm, 4H, CH_2SCH_2(coord.)]; 3.1 [s,3H,CH_3(coord.)]; 2.6 [m, 2H,CH_2SCH_3(coord)] 2.35 [m, 2H,CH_2SCH_3(uncoord.)]; 2.2 [s,3H,CH_3(uncoord.)]
(**20**)	7.3-7.5 (bm, 10H, Ph); 3.1 [bm, 8H, CH_2S(coord.)]; 3.5 (t, 6H, $C\underline{H}_3CH_2$); 2.2 [m, 6H,CH_3S(coord.)];1.2 (q, CH_2O)
(**21**)	3.4pp [S,6H, MeC_2] 3.4 [bm, 8H, CH_2S(coord.)]; 3.5 (q, 4H, CH_2O); 2.4 [m, 6H, CH_3S(coord.)]; 1.2 (t, 6H, CH_3CH_2)
(**22**)	7.3-7.7ppm (bm,14H, Ph) 4.4, 3.8 (2d, 4H, CH_2S); 2.5 (m, 8H, SCH_2CH_2S)
(**24**)	7.5-7.3(brm,4H, C_6H_4); 3.6 (S, 6H, MeC_2) 4.2, 3.5 (2d, 4H, $PhCH_2S$); 2.4 (m,8H, SCH_2CH_2S)
(**25**)	7.3-7.5ppm (bm, 10H, Ph); 2.9 (bm, 8H, CH_2S); 3.5 (q, 4H, CH_2O); 2.1 (s, 6H, CH_3S);1.2 (t,6H, CH_3CH_2)
(**26**)	7.3-7.7ppm (bm, 14H, Ph); 4.1, 3.9 (2d, 4H, $PhCH_2S$); 2.6 (m, 8H, SCH_2CH_2S)
(**27**)	7.3-7.5 (bm, 10H, Ph); 5.1 (S, 5H, Cp); 3.4 (bm, 4H, CH_2SCH_2); 3.2 (bm, 2H, CH_2CH_3); 3.1 (bm, 3H, SCH_3); 2.8 (bm, 5H, CH_2SCH_3)
(**28**)	7.3-7.5 (bm, 10H, Ph); 3.5 (q, 4H, CH_2O); 2.9 (bm, 8H, CH_2S); 2.2 (m, 6H, CH_3S);1.2 (t,6H, CH_3CH_2)
(**29**)	3.5 (t, 6H, $C\underline{H}_3CH_2$); 3.2 (S, 6H, C_2Me); 2.8 (bm, 8H, CH_2S); 2.2 (m, 6H, CH_3S));1.2 (q, CH_2O)
(**30**)	7.3-7.5 (bm, 10H, Ph); 4.6, 4.1 (2d,4H, $PhCH_2S$, J_{H-H} = 11) 3.4 (m, 8H, SCH_2CH_2S)
(**31**)	7.3-7.5 (bm, 4H, , C_6H_4); 4.8, 4.4 (2d, 4H, $PhCH_2S$, J =12) 3.2 (S, 6H, C_2Me); 2.9 (m, 12H, SCH_2CH_2S)
(**32**)	7.3-7.5 (bm, 10H, Ph); 4.0 (bm, 8H, SCH_2CH_2S)
(**33**)	4.0 (bm, 8H, SCH_2CH_2S) 3.2 (S, 6H, C_2Me)
(**34**)	7.3-8.0 (bm, 3OH, Ph); 4.2 (t, 2H, CH_2)

[c] s = singlet, d = doublet, m = multiplet, bm = broad multiplet.

CHAPTER 5 :

REACTIONS OF THE CUBANE TYPE CLUSTER, $Fe_4CP_4S_6$ WITH THE COMPLEXES $[MI_2(CO)_3(NCMe)_2]$, $[MI_2(CO)_3(dppe)]$, $[MI_2(CO)_3(dppr)]$ AND $[MI_2(CO)_3(NCMe)(\eta^2\text{-}RC_2R)_2]$ (M = Mo, W; R = Ph, Me)

CHAPTER 5: REACTIONS OF THE CUBANE TYPE CLUSTER, $Fe_4Cp_4S_6$ WITH $[MI_2(CO)_3(NCMe)_2]$, $[MI_2(CO)_3(dppe)]$, $[MI_2(CO)_3(dpppr)]$ AND $[MI_2(CO)(NCMe)(\eta^2\text{-}RC_2R)_2]$ (M = Mo, W; R = Ph, Me).

5.1 INTRODUCTION

5.1.1 Iron-sulphur Clusters

In the past two decades many different iron-sulphur clusters have been reported from both naturally occurring and synthetic origins. Of the structurally characterised clusters there are ten main types[148-198] as shown in **Figure 5.1**. Cluster types **1**, **3** and **4** are known to occur in proteins. It can be seen that the different clusters may exist in a wide range of oxidation states depending on the ligands attatched to the iron atoms. Often the different types of clusters may be grouped into quite complex reaction schemes as is shown in **Scheme 5.1** below.

Scheme 5.1 Reaction scheme of Fe_2S_2, Fe_3S_4 and Fe_6S_9 clusters (R = Ph)

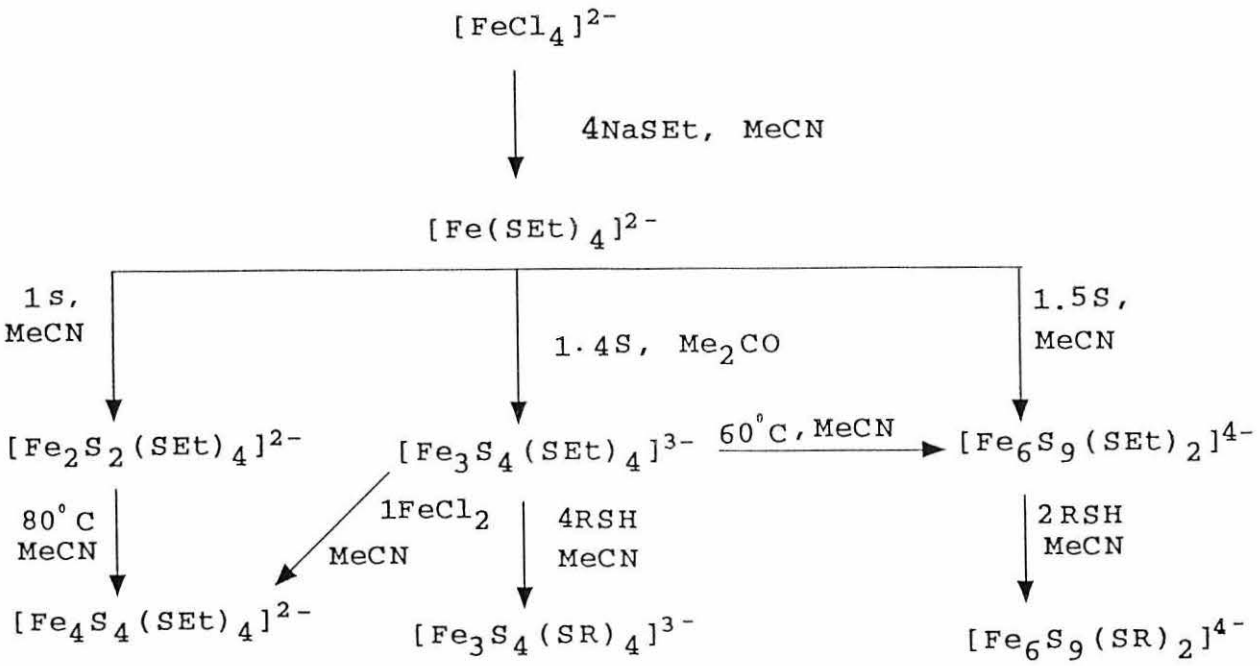

Figure 5.1 Diagrams showing the main types of Fe-S clusters

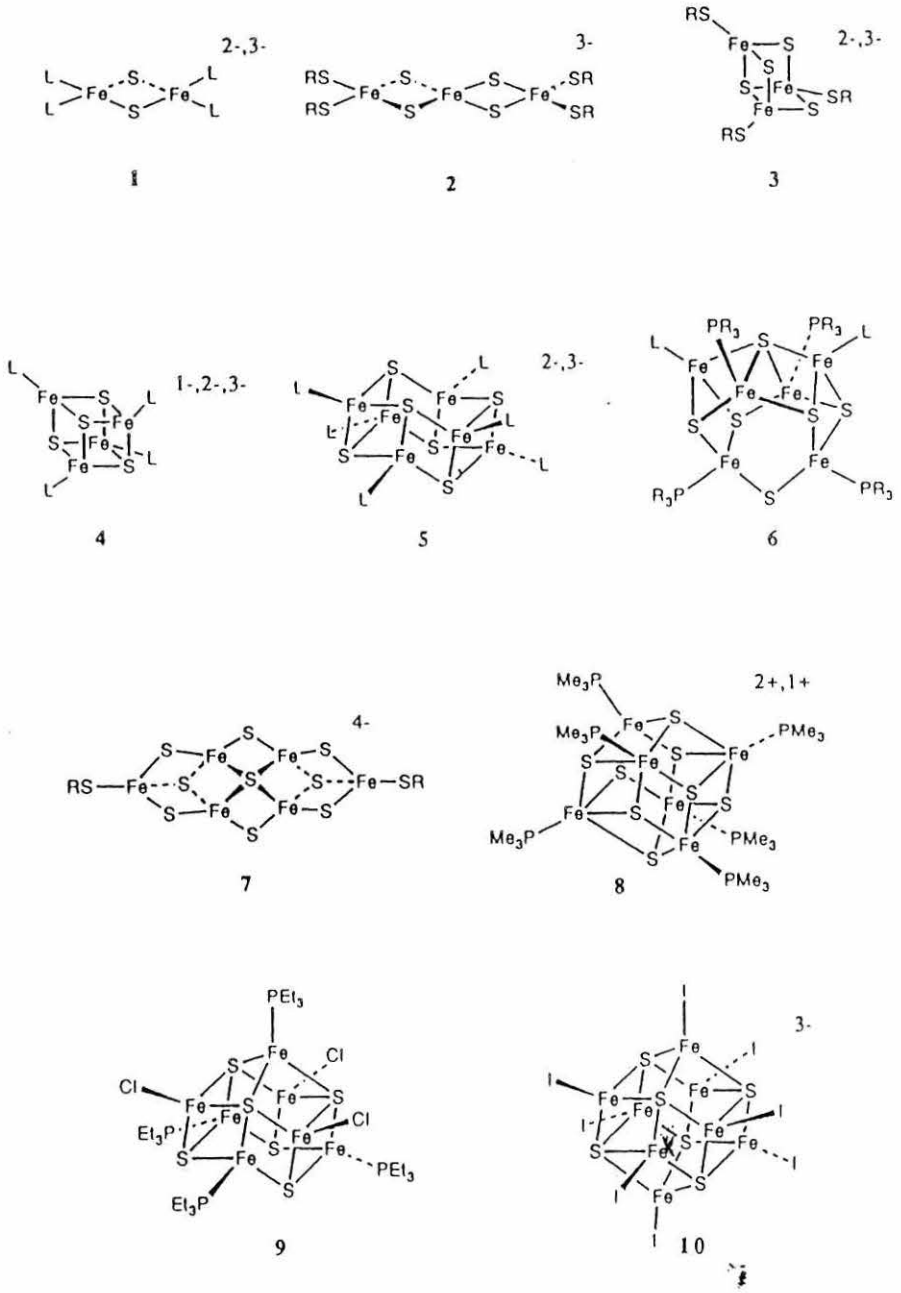

5.1.2 Heterometallic MFe_3S_4 cubane-like clusters

Heterometallic type clusters play a very important role as models for biological active sites such as molybdenum nitrogenase. Of these heterometallic type clusters the ones containing a $MoFe_3S_4$ core unit are some of the most important and widely characterised. The first clusters containing the $MoFe_3S_4$ core (**Figure 5.2**) were prepared by Holm *et al*[199] in 1978 and consisted of two $MoFe_3S_4$ groups bridged by a sulphur atom.

Figure 5.2 Diagram showing simple $MoFe_3S_4$ core

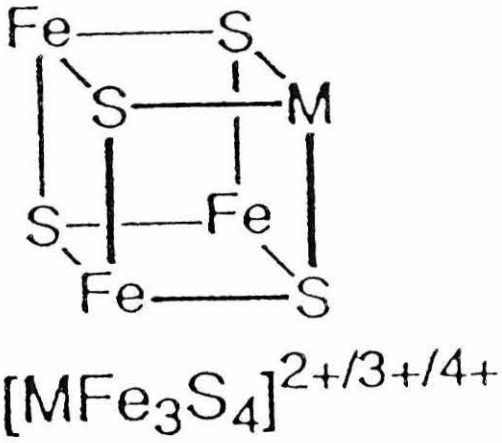

In 1986, Holm *et al*[200] synthesised a whole range of molybdenum cubane clusters as shown in **Figure 5.1**. These clusters include $[MoFe_3S_4(S\text{-}p\text{-}C_6H_4Cl)_4(al_2cat)]^{3-}$, $[MoFe_3S_4(SEt)_4(dmpe)]^-$, $[MoFe_3S_4Cl_3(al_2cat)(THF)]^{2-}$ and $[MoFe_3S_4Cl_4(dmpe)]^-$ (al_2cat = 3,6-diallylcatecholate). Similarly, in 1991 Coucouvanis and co-workers[201] reported the reaction of *fac*-$[Mo(CO)_3(NCMe)_3]$ with the linear cluster $[Et_4N]_3[Fe_3S_4(EtS)_4]$[202,203] to give the cubane-type cluster $[Et_4N]_3[Fe_3S_4(EtS)_3Mo(CO)_3]$. During the reaction the cluster changes configuration

from a linear compound to a cubane type structure with one corner of the cube occupied by the molybdenum atom as shown in **Figure 5.3**.

Figure 5.3 Reaction of $[Et_4N]_3[Fe_3S_4(EtS)_4]$ with *fac*-$[Mo(CO)_3(NCMe)_3]$ to give cubane-type cluster $[Et_4N]_3[Fe_3S_4(EtS)_3Mo(CO)_3]$

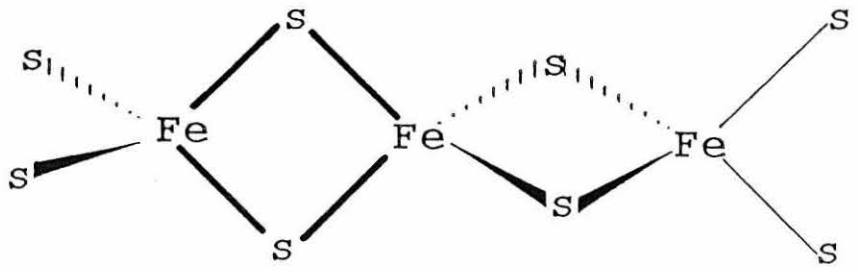

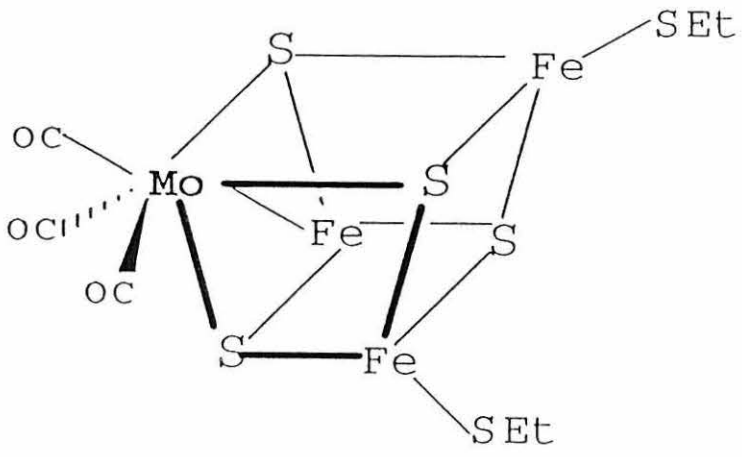

5.1.3 Reaction of the "basket" type cluster $[Fe_4Cp_4S_6]$ with *fac*-$[Mo(CO)_3(NCMe)_3]$

Jordanov and co-workers[204] have shown the reactivity of the cluster $[Fe_4Cp_4S_6]$[205] with the low-valent molybdenum complexes $[Mo(CO)_4(\eta^4\text{-nor})]$ (nor = norbornadiene) and $[MoBr(CO)_2(NCMe)_2(\pi\text{-allyl})]$ to give the complexes $[Mo(CO)_4(Fe_4S_6Cp_4)]$ and $[MoBr(CO)_2(NCMe)(Fe_4S_6Cp_4)]$ respectively (**Figure 5.4**). In both cases the complexes contain a Fe_4S_4 unit, however, the molybdenum atom is not part of the cube, but is bound *via* the two "handle" sulphur atoms of the "basket". Physical studies of the two complexes suggested the integrity of the cluster remained unchanged and the molybdenum atoms were indeed bound via the S-S group of the cluster as opposed to the μ_3 sulphurs of the cage.

Figure 5.4 Structures of the complexes $[Mo(CO)_4(Fe_4S_6Cp_4)]$ and $[MoBr(CO)_2(NCMe)(Fe_4S_6Cp_4)]$

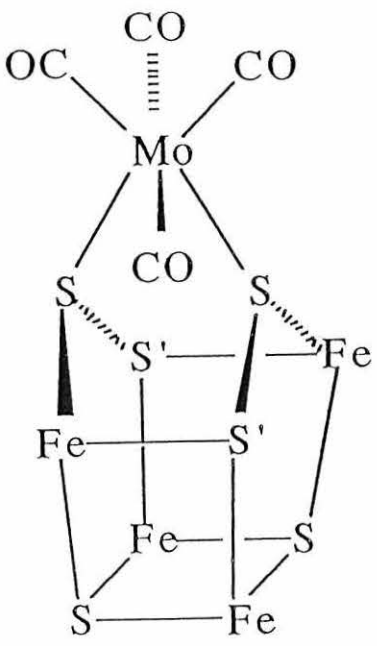

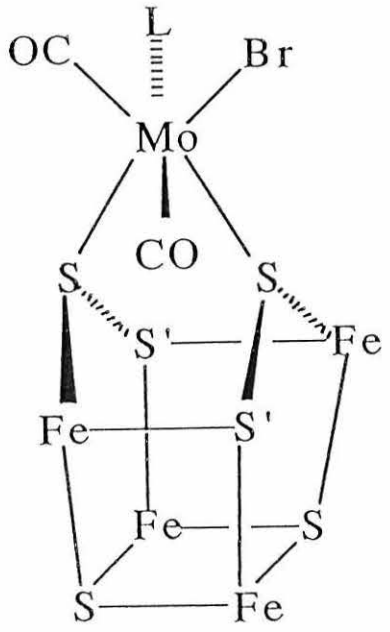

5.1.4 Mössbauer Spectroscopy

Mössbauer or nuclear gamma resonance spectroscopy (NGR) is one of the many analytical techniques used to study iron-sulphur clusters. As the alternative name suggests the technique involves the study of a suitable nucleus using gamma radiation. Some of the nuclei which can be studied using Mössbauer are listed in **Table 5.1** below. However, the most extensively studied isotope is ^{57}Fe which is found in 2.2% natural abundance (^{56}Fe, the most abundant isotope, is Mössbauer silent).

Table 5.1 Most common isotopes for Mössbauer spectroscopy

Isotope	Natural Abundance (%)	Spin (gd)	States (ex)	Eγ (KeV)	Source Isotope	Half life
^{57}Fe	2.2	1/2	3/2	14.4	^{57}Co	270d
^{119}Sn	0.63	1/2	3/2	23.8	^{119m}Sn	240d
^{121}Sb	2.1	5/2	7/2	37.2	^{121m}Sb	77y
^{127}I	100	5/2	7/2	57.6	^{127m}Te	105d
^{129}I	0.6	7/2	5/2	27.7	^{129m}Te	33d
^{99}Ru	12.8	3/2	5/2	89.4	^{99}Rh	16d
^{19}Ir	61.5	1/2	3/2	73.0	^{193m}Os	30h
^{197}Au	100	3/2	1/2	77.3	^{197m}Pt	18h

5.1.4.1 The Mössbauer experiment

In 1957, Mössbauer discovered that a nucleus held within a solid lattice can absorb and emit gamma rays without recoil. It is essential that the nuclear recoil energy is less than the difference between the two nuclear energy levels in order for the Mössbauer effect to be observed. Mössbauer spectroscopy is therefore limited to certain nuclei with suitable energies of nuclear gamma rays, normally those with low-lying excited states. Of the many Mössbauer active nuclei, ^{57}Fe has the most favourable properties and hence is the most common Mössbauer nuclei. The ^{57}Fe Mössbauer experiment invoves the use of a ^{57}Co source which decays to an excited state of ^{57}Fe which further decays to the ground state hence emitting a 14.4 keV gamma ray which is used as the source radiation (**Figure 5.5**)

Figure 5.5 Decay of ^{57}Co to give 14.4 keV gamma ray

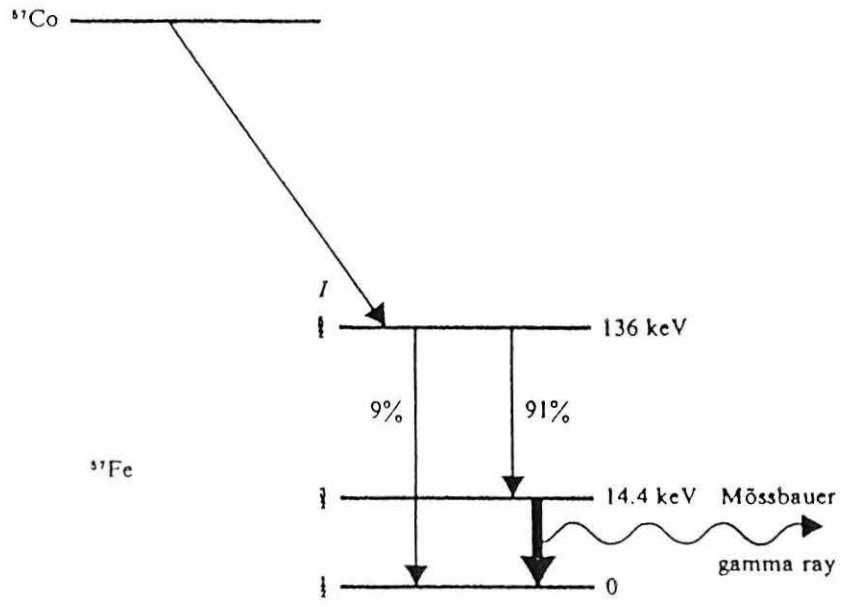

The source radiation is then passed through the iron-containing absorber (sample), where it is partially absorbed and then to a suitable detector. In order to scan a

spectrum the source is mounted on a vibrator and the spectrum scanned *via* the Doppler effect. Hence, Mössbauer spectroscopy uses the unusual energy units of mm s^{-1}. The spectrum is normally accumulated over a period of many hours or days until a satisfactory signal to noise ratio is obtained. A schematic of a typical Mössbauer spectrometer is shown in **Figure 5.6**.

The energy levels within an iron nucleus are altered by the relative enviroment of that nucleus. Mössbauer spectroscopy allows the probing of a sample for the different nuclear enviroments within that sample. A typical Mössbauer spectrum as shown in **Figure 5.7** is characterised by the number, shape, position and relative intensity of the absorption bands.

Figure 5.6 Schematic showing simplified Mössbauer spectrometer.

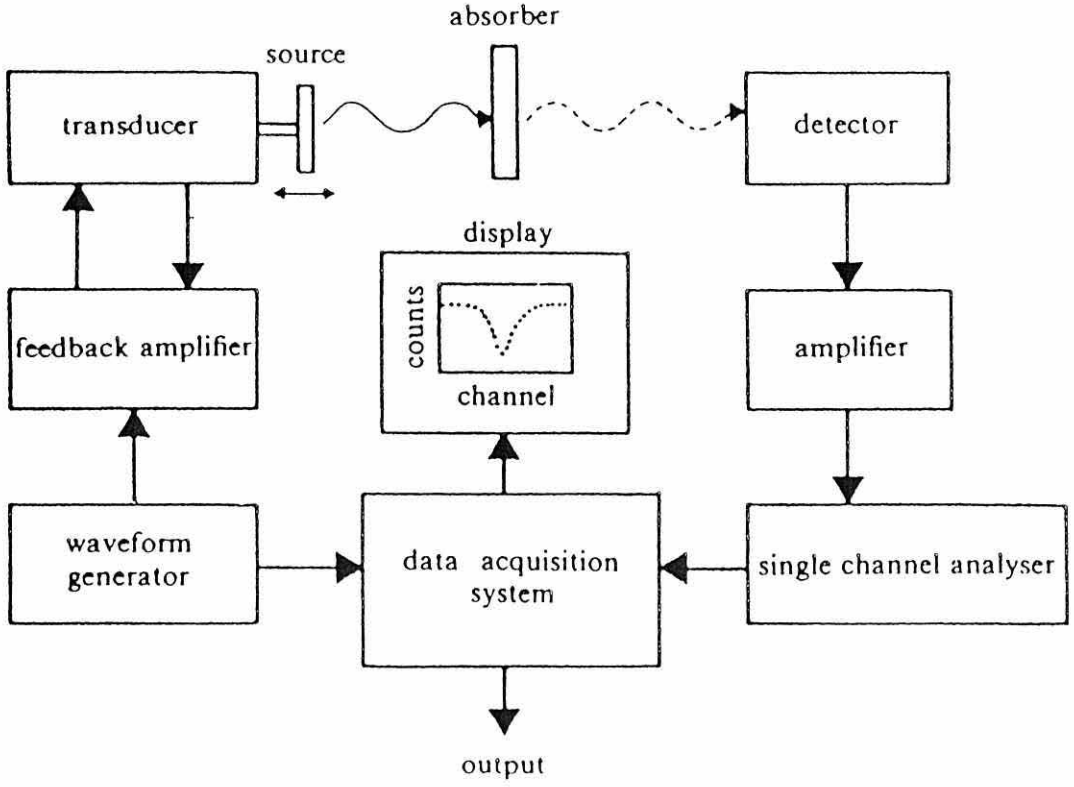

Figure 5.7 Typical Mössbauer doublet showing important parameters

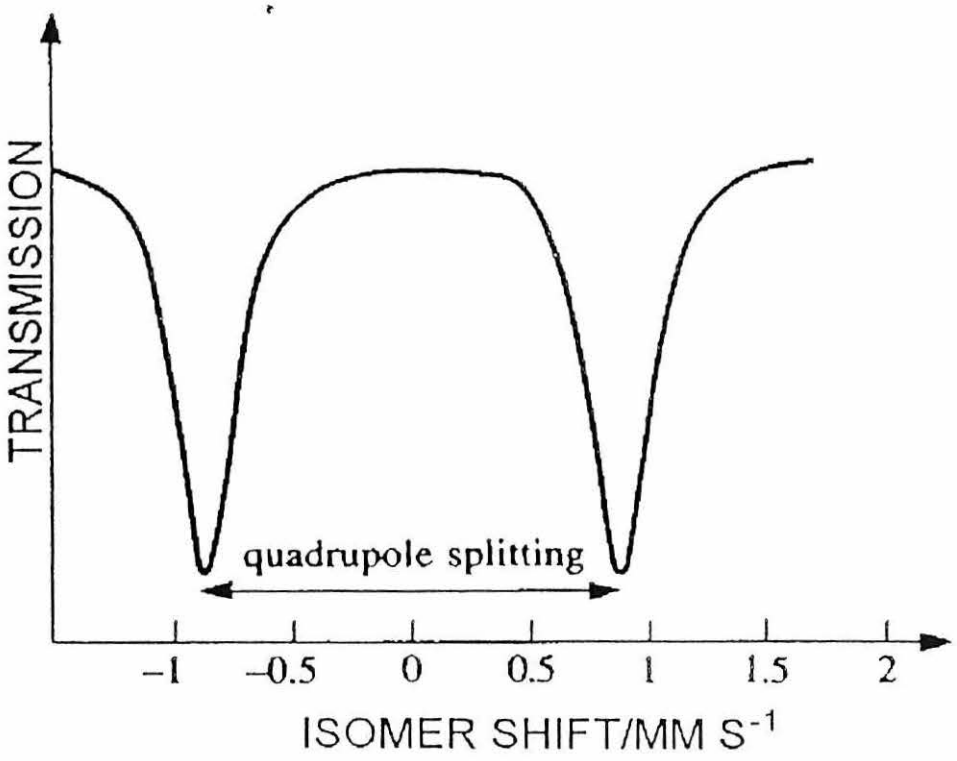

5.1.4.2 The Mössbauer spectrum and parameters

A Mössbauer spectrum contains two major parameters which are "fitted" to the raw absorption data using a computer program. These parameters are the **isomer shift,** δ and the **quadrupole splitting,** Δ.

The isomer shift is the position of the centre of the spectrum on the energy (velocity) scale compared to that of a standard eg. iron foil. The isomer shift is a result of the monopole interaction between the nucleus and the electronic charge surrounding the nucleus (**Figure 5.8**).

The quadrupole splitting is due to the nuclear angular momentum, I, of the nucleus resulting in a non-spherical charge distribution around the nucleus and hence a quadrupole moment. In the case of ^{57}Fe the excited state $I = 3/2$, is split into two sub levels by an electric field gradient to give $m_I = +/- 1/2$ and $m_I = +/- 3/2$. This leads to the splitting of one line into two lines within the Mössbauer

spectrum (**Figure 5.8**). Quadrupole splitting gives information about the symmetry of the bonding environment surrounding the nucleus.

Figure 5.8 Diagram showing a) isomer shift δand b) quadrupole splitting, Δ

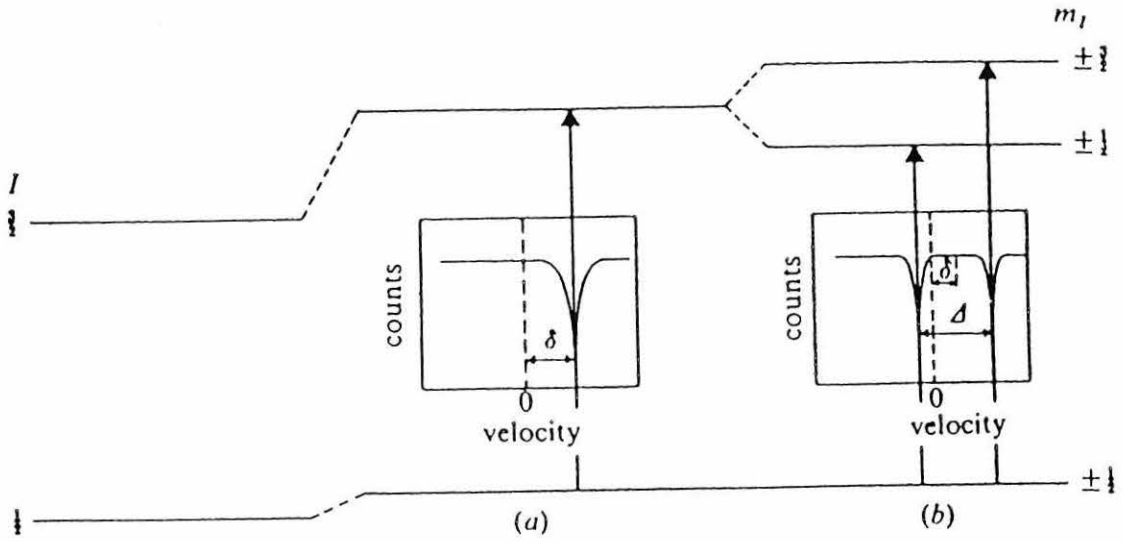

5.2 Results and Discussion

The following sections describe the reactions of the cubane-type cluster $[Fe_4Cp_4S_6]$ with the seven-coordinate starting complexes $[MI_2(CO)_3(NCMe)_2]$ (M = Mo,W) and the reactions of the resulting complexes with a number of thiolates. It can be seen that the cluster $[Fe_4Cp_4S_6]$ (**Figure 5.9**) can be described as a "basket" type cluster with the two top sulphur atoms forming the "handles". It is possible the cluster may coordinate *via* these two "handle" sulphur atoms to the metal centres of

the complexes $[MI_2(CO)_3(NCMe)_2]$ (M = Mo,W). Some preliminary studies of the work described in this chapter were originally carried out by K. Mitchell[206] but all complexes have been prepared and fully characterised during this thesis. The iron-sulphur cluster was prepared *via* the literature method[205].

5.2.1 Reaction of the complex $[WI_2(CO)_3(NCMe)_2]$ with the cubane-type cluster $[Fe_4Cp_4S_6]$

The reaction of the tungsten complex $[WI_2(CO)_3(NCMe)_2]$ reacts with one equivalent of the cluster $[Fe_4Cp_4S_6]$ at room temperature in CH_2Cl_2 to give the new tungsten complex $[WI_2(CO)_3(Fe_4Cp_4S_6\text{-}S,S')]$ (**35**) in relatively good yield. The complex (**35**) is a black crystalline solid which is sparingly soluble in CH_2Cl_2, but relatively insoluble in most other common solvents. The complex is oxygen sensitive in both solution and the solid-state and is best handled and stored in a nitrogen bag or glove box for all but very short periods of time. The complex was characterised by elemental analysis C, H, N, S (**Table 5.1**), infra red, ^{1}H NMR and Mössbauer spectroscopy (**Tables 5.2- 5.4**).

The infra red spectrum of complex (**35**) was recorded as a KBr pellet and shows three distinct strong carbonyl stretches at 1873, 1934 and 2010 cm^{-1} respectively suggesting the retention of three carbonyl ligands during the reaction. The higher frequency stretch at 2010 cm^{-1} may be attributed to the capping carbonyl position suggesting a capped octahedral geometry for the complex. The solution infra red in CH_2Cl_2 also shows three carbonyl stretches suggesting the presence of one isomer in solution.

A weak stretching band is also observed at 450 cm^{-1} which can be attributed to the μ_3-sulphur atoms of the iron-sulphur cluster which are attached to the tungsten centre. This can be compared to the μ_2-sulphur stretch observed for the free cluster at 439cm^{-1}, which is no longer seen upon coordination of the cluster to the tungsten centre.

Figure 5.9 Diagram showing structure of the cluster $[Fe_4Cp_4S_6]$

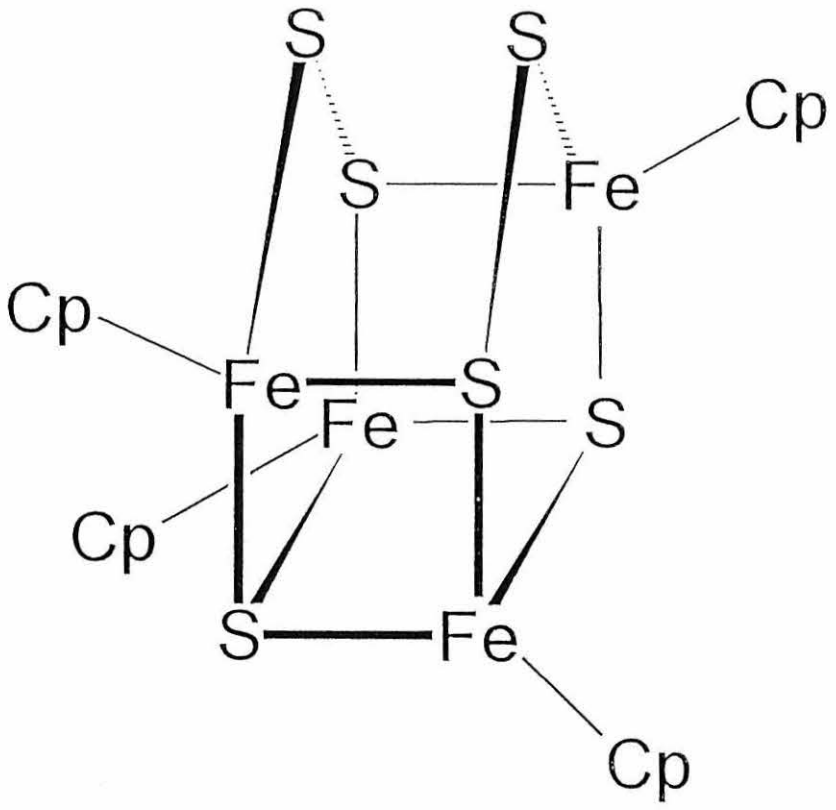

The ^1H NMR spectrum of free $[Fe_4Cp_4S_6]$ in $CDCl_3$ shows two signals of equal intensity at δ = 4.5 and 5.0 ppm respectively. However, upon coordination of the resulting iron-sulphur cluster complex is very insoluble and little is seen in the ^1H NMR spectrum.

The Mössbauer spectrum of complex (**35**) shows an overlapping set of doublets suggesting two iron environments within the cluster-complex. The doublet with the largest quadrupole split may be attributed to the iron atoms at the top of the

cluster closest to the tungsten metal centre. While the doublet with the smaller quadrupole split can be assigned to the other two iron atoms at the base of the cluster.

5.2.2 Reaction of the complex $[MoI_2(CO)_3(NCMe)_2]$ with the cubane-type cluster $[Fe_4Cp_4S_6]$

A similar, but much faster reaction of the molybdenum complex $[MoI_2(CO)_3(NCMe)_2]$ with one equivalent of the cluster $[Fe_4Cp_4S_6]$ at room temperature in CH_2Cl_2 gives the new seven-coordinate complex $[MoI_2(CO)_3(Fe_4Cp_4S_6\text{-}S,S')]$ (**36**) in relatively good yield. The complex (**36**) is a black crystalline solid which is sparingly soluble in CH_2Cl_2, but relatively insoluble in most other common organic solvents. The molybdenum complex is more air-sensitive than the tungsten analogue in both solution and the solid-state and again is best handled and stored in a nitrogen bag or glove box. The complex was characterised by elemental analysis C, H, N, S (**Table 5.1**), infra red , ^1H NMR and Mössbauer spectroscopy (**Tables 5.2- 5.4**).

The infra red spectrum of complex (**36**) was recorded as a KBr pellet and shows three distinct strong carbonyl stretching bands at 1886, 1945 and 2014 cm^{-1} respectively again suggesting the retention of three carbonyl ligands as seen with the analogous tungsten complex, suggesting that complexes (**35**) and (**36**) have a similar solid-state structure.

The high frequency carbonyl band at 2014 cm^{-1} is again indicative of a carbonyl ligand in the capping position. The solution infra red spectrum in CH_2Cl_2 also shows three carbonyl stretches suggesting the presence of one isomer in solution. A weak stretching band is also observed at 450 cm^{-1} which can be attributed to the μ_3-sulphur atoms of the iron-sulphur cluster which are attached to the molybdenum centre. As before no μ_2-sulphur stretch is observed suggesting coordination to molybdenum *via* the two sulphur atoms at the top of the cluster.

The ^{1}H NMR spectrum of complex (**36**) again shows no cyclopentadienyl signals, probably due to the increased insolubility of the complex upon coordination of the iron cluster. The Mössbauer spectrum shows an overlapping set of doublets suggesting two iron environments within the cluster-complex. The doublet with the largest quadrupole splitting may again be attributed to the iron atoms at the top of the cluster closest to the tungsten metal centre. While the doublet with the smaller quadrupole splitting can be assigned to the other two iron atoms at the base of the cluster.

The combined spectroscopic evidence for complexes (**35**) and (**36**) suggests they are similar in composition and structure. The following capped octahedral geometry shown in **Figure 5.11** is suggested as the likely structure for complexes (**35**) and (**36**) in the solid-state. Unfortunately no crystals of suitable quality for X-ray analysis were prepared despite exhaustive attempts over a two year period.

5.2.3 Reaction of the complex $[WI_2(CO)_3(Fe_4Cp_4S_6\text{-}S,S')]$ (35) with the sodium thiolates NaSAr (Ar = Ph or $C_6H_2Me_3$-2,4,6{tmt})

The tungsten complex $[WI_2(CO)_3(Fe_4Cp_4S_6\text{-}S,S')]$ (**35**) reacts with one equivalent of NaSAr (Ar = Ph or $C_6H_2Me_3$-2,4,6) at room temperature in CH_2Cl_2 to give the new seven-coordinate complexes $[WI(SPh)(CO)_3(Fe_4Cp_4S_6\text{-}S,S')]$ (**37**) and $[WI(tmt)(CO)_3(Fe_4(C_5H_5)_4S_6\text{-}S,S')]$ (**38**) in relatively good yield. Both complexes (**37**) and (**38**) are black crystalline solids which are more soluble in CH_2Cl_2 than their diiodo cluster precursors. Both complexes are oxygen sensitive in both solution and the solid-state and are best handled and stored in an inert atmosphere. The complexes (**37**) and (**38**) were characterised by elemental analysis C, H, N, S (**Table 5.1**), infra red, ^{1}H NMR and Mössbauer spectroscopy (**Tables 5.2- 5.4**).

The infra red spectra of both complexes were recorded as KBr pellets and in both cases show three distinct strong carbonyl stretches suggesting the retention of three carbonyl ligands during the reaction. Weak stretches are also observed at

448 cm^{-1} and 451 cm^{-1} for both complexes which can be attributed to the μ_3-sulphur atoms of the iron-sulphur cluster which are attached to the tungsten.

The ^1H NMR spectrum of complex (**37**) in $CDCl_3$ shows two multiplets are also observed at 7.2 and 7.5 ppm corresponding to the two *ortho* and the three *meta* and *para* protons respectively of the thiolate. The ^1H NMR spectrum of complex (**38**) in $CDCl_3$ also shows two shifted multiplets at δ = 2.2 ppm and 2.3 ppm corresponding respectively to the six protons of the *ortho*-methyl groups and the three protons of the *para*-methyl group of the ligand are observed. A multiplet is also observed at δ = 6.9 ppm corresponding to the *meta*-phenyl protons of the tmt ligand.

Figure 5.11 Proposed structure of complexes $[MI_2(CO)_3(Fe_4Cp_4S_6\text{-}S,S')]$

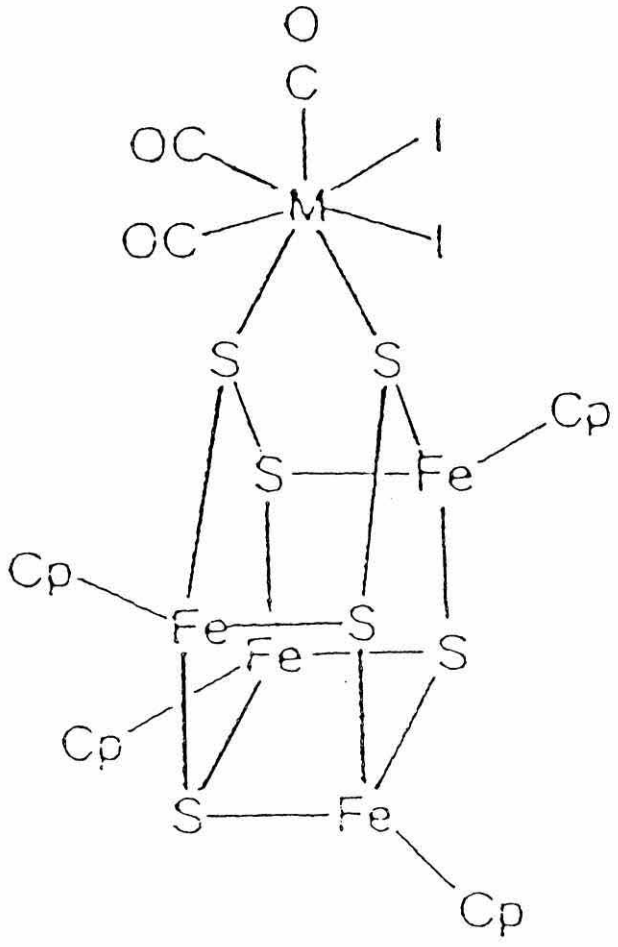

The Mössbauer spectra of both complexes (**37**) and (**38**) show an overlapping set of doublets suggesting two iron environments within the cluster-complex. Both complexes exhibit similar isomer and quadrupole shifts for both doublets. In both cases the doublet with the largest quadrupole split is likely to be due to the iron atoms at the top of the cluster closest to the tungsten metal centre. While the doublet with the smaller quadrupole split can be assigned to the other two iron atoms at the base of the cluster.

Similar reactions of the tungsten complex $[WI_2(CO)_3(Fe_4Cp_4S_6\text{-}S,S')]$ (**35**) with two equivalents of NaSAr (Ar = Ph or $C_6H_2Me_3$-2,4,6) at room temperature in CH_2Cl_2 gave the new seven-coordinate complexes $[W(SPh)_2(CO)_3(Fe_4(C_5H_5)_4S_6$ -S,S')] (**39**) and $[W(tmt)_2(CO)_3(Fe_4Cp_4S_6$ -*S,S'*)] (**40**) in relatively good yield. Both complexes (**39**) and (**40**) are black crystalline solids which are sparingly soluble in CH_2Cl_2 again more than their diiodo-cluster precursors.

The infra red spectra of both complexes (**39**) and (**40**) were recorded as KBr pellets and in both cases show three distinct strong carbonyl stretches suggesting the retention of three carbonyl ligands during the reaction. Similarly to complexes (**37**) and (**38**), weak stretching bands are also observed which can be attributed to the ###$_3$-sulphur atoms for both complexes at around 450 cm^{-1} suggesting coordination to tungsten *via* the two sulphur atoms at the top of the cluster.

The ^1H NMR spectra of both complexes (**39**) and (**40**) in $CDCl_3$ are very similar to those of complexes (**37**) and (**38**) again showing no Cp signals probably due to the insolubility of the complexes. The Mössbauer spectra of both complexes (**39**) and (**40**) show an overlapping set of doublets with similar δ and Δ values to those of complexes (**37**) and (**38**) again suggesting two iron environments within the cluster-complex.

5.2.4 Reaction of the complex $[MoI_2(CO)_3(Fe_4Cp_4S_6\text{-}S,S')]$ (36) with the sodium thiolates NaSAr (Ar = Ph or $C_6H_2Me_3$-2,4,6{tmt})

The molybdenum complex $[MoI_2(CO)_3(Fe_4Cp_4S_6\text{-}S,S')]$ (**36**) reacts with one equivalent of NaSAr (Ar = Ph or $C_6H_2Me_3$-2,4,6) at room temperature in CH_2Cl_2 to give the new seven-coordinate complexes $[MoI(SPh)(CO)_3(Fe_4Cp_4S_6\text{-}S,S')]$ (**41**) and $[MoI(tmt)(CO)_3(Fe_4Cp_4S_6\text{-}S,S')]$ (**42**) fairly good yield. Both complexes (**41**) and (**42**) are black crystalline solids which are sparingly soluble in CH_2Cl_2 more so than their diiodo-cluster precursors. Both complexes are oxygen-sensitive in both solution and the solid-state and are best handled and stored in an inert atmosphere. The complexes (**41**) and (**42**) were characterised by elemental analysis C, H, N, S (**Table 5.1**), infra red, ^1H NMR and Mössbauer spectroscopy (**Tables 5.2- 5.4**).

The infra red spectra of both complexes (**41**) and (**42**) were recorded as KBr pellets and in both cases show three distinct strong carbonyl stretches suggesting the retention of three carbonyl ligands during the reaction. Weak stretching bands are also observed at around 450 cm^{-1} for both complexes which can be attributed to the μ_3-sulphur atoms of the iron-sulphur cluster which are attached to the molybdenum.

The ^1H NMR spectrum of complex (**41**) in $CDCl_3$ shows two shifted multiplets at δ = 7.2 and 7.5 ppm corresponding to the two *ortho* and the three *meta* and *para* protons respectively of the thiolate. The ^1H NMR spectrum of complex (**42**) in $CDCl_3$ shows two shifted multiplets at δ = 2.2 ppm and 2.3 ppm corresponding respectively to the six protons of the *ortho*-methyl groups and the three protons of the *para*-methyl group of the ligand are observed. A multiplet is also observed at δ = 6.9 ppm corresponding to the *meta*-phenyl protons of the tmt ligand.

The Mössbauer spectra of both complexes (**41**) and (**42**) show an overlapping set of doublets suggesting two iron environments within the cluster-complex. Both complexes exhibit similar isomer and quadrupole shifts for both

doublets. In both cases the doublet with the largest quadrupole split is likely to be due to the iron atoms at the top of the cluster closest to the molybdenum metal centre. While the doublet with the smaller quadrupole split can be assigned to the other two iron atoms at the base of the cluster.

Similar reactions of the molybdenum complex $[MoI_2(CO)_3(Fe_4Cp_4S_6\text{-}S,S')]$ (**36**) with two equivalents of NaSAr (Ar = Ph or $C_6H_2Me_3$-2,4,6) at room temperature in CH_2Cl_2 gave the new seven-coordinate complexes $[Mo(SPh)_2(CO)_3(Fe_4Cp_4S_6\text{-}S,S')]$ (**43**) and $[Mo(Stmt)_2(CO)_3(Fe_4Cp_4S_6\text{-}S,S')]$ (**44**) in relatively good yield. Both complexes (**43**) and (**44**) are black crystalline solids which are sparingly soluble in CH_2Cl_2 again more so than their diiodo-cluster precursors.

The infra red spectra of both complexes (**43**) and (**44**) were recorded as KBr pellets and in both cases show three distinct strong carbonyl stretching bands suggesting the retention of three carbonyl ligands during the reaction. Similarly to the molybdenum complexes (**41**) and (**42**), weak stretches are also observed which can be attributed to the μ_3-sulphur atoms for both complexes at around 450 cm^{-1} suggesting coordination to molybdenum *via* the two sulphur atoms at the top of the cluster.

The ^1H NMR spectra of both complexes (**43**) and (**44**) in $CDCl_3$ are very similar to those of complexes (**41**) and (**42**) showing no Cp signals. The Mössbauer spectra of both complexes (**43**) and (**44**) show an overlapping set of doublets with similar i.s and q.s values to those of complexes (**41**) and (**42**) again suggesting two iron environments within the cluster-complex. The Mössbauer spectrum of the complex (**38**) is shown below in **Figure 5.12**. and a schematic of the reactions of both thiolates with complexes (**35**) and (**36**) shown in **Figure 5.13**.

Figure 5.12 Mössbauer spectrum of the complex (**42**)

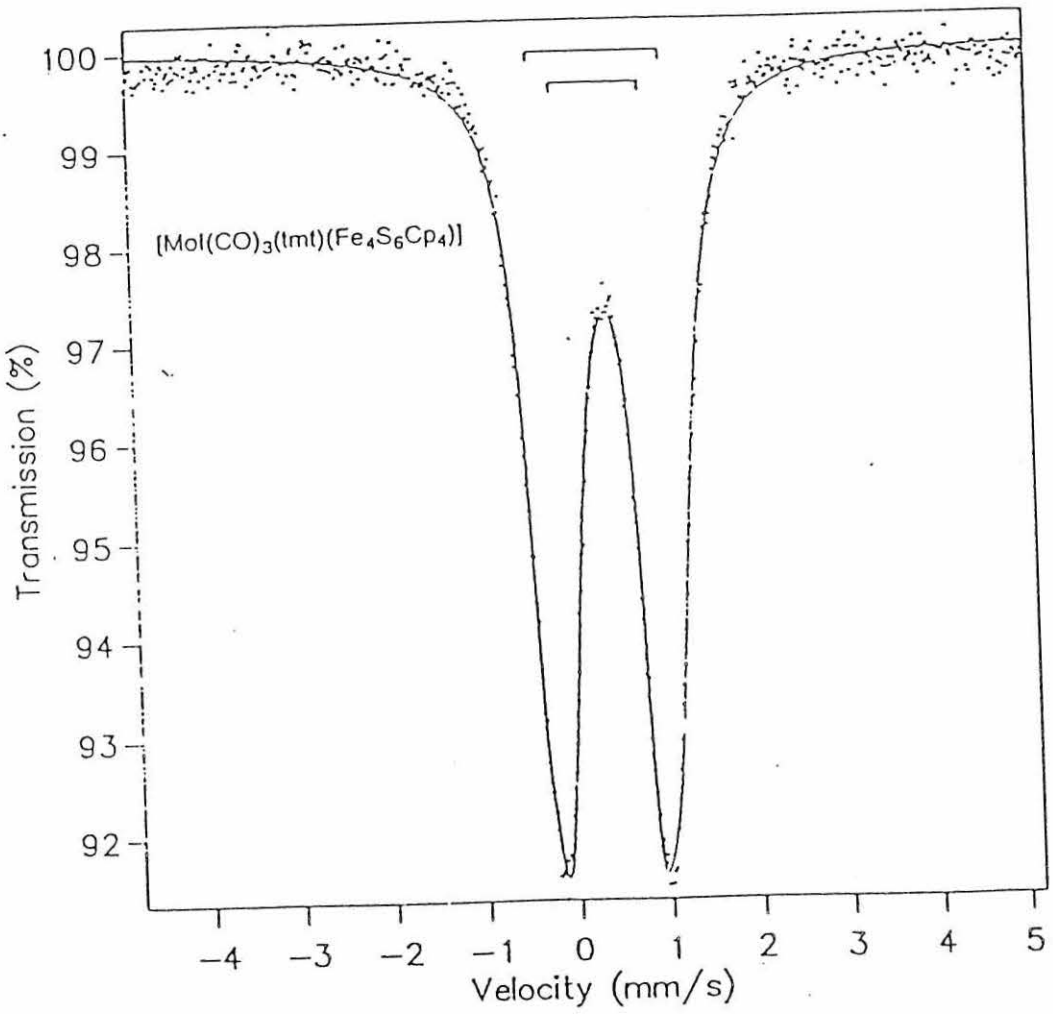

Figure 5.13 Schematic of the reactions of -SPh and tmt with complexes (**35**) and (**36**)

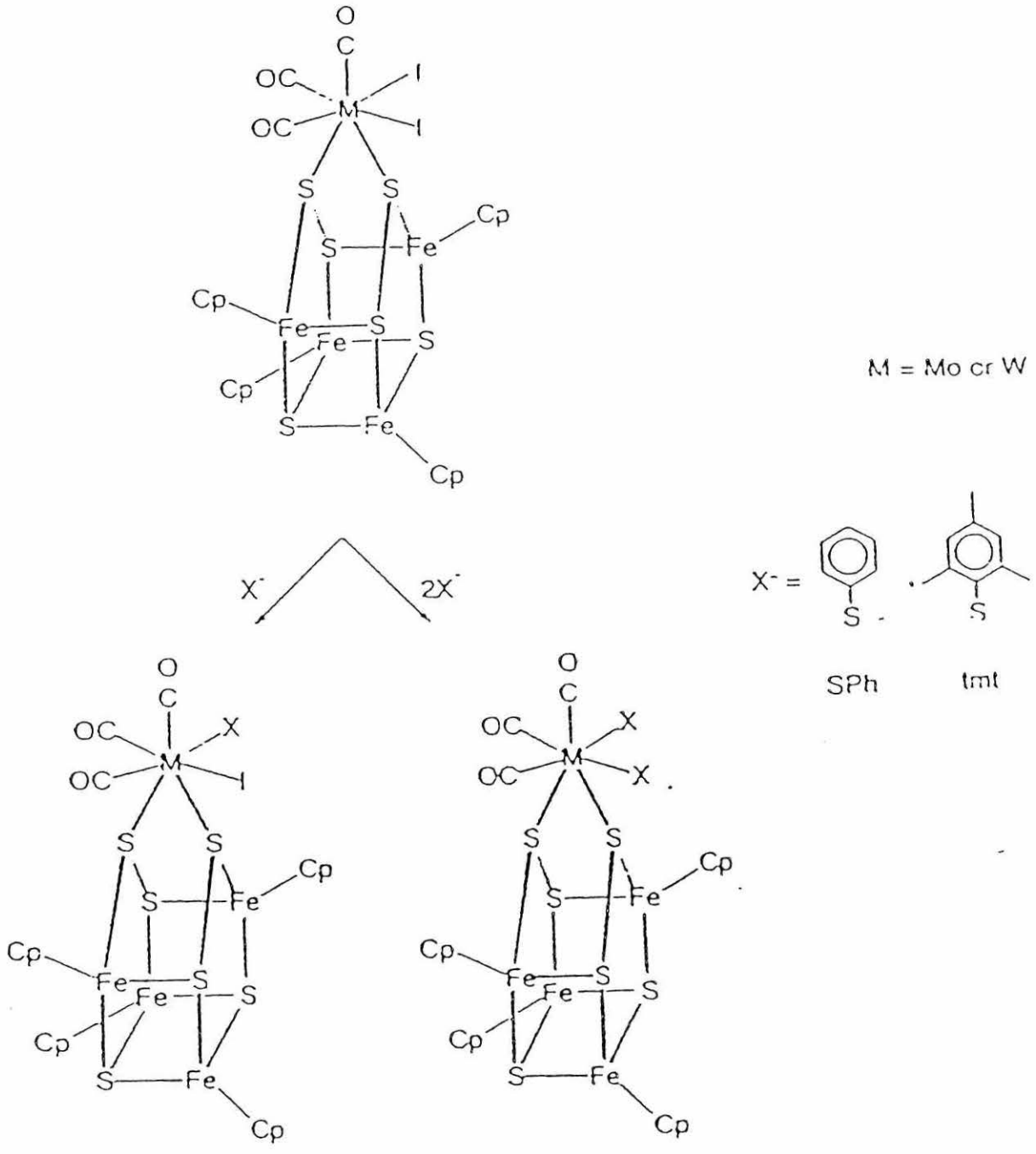

5.2.5 Reactions of the complex $[WI_2(CO)_3(NCMe)_2]$ with one equivalent of dppe or dpppr followed by an *in situ* reaction of the cluster $[Fe_4Cp_4S_6]$

The reaction of the tungsten starting complex $[WI_2(CO)_3(NCMe)_2]$ with one equivalent of dppe at room temperature in CH_2Cl_2 gave the complex $[WI_2(CO)_3(dppe\text{-}P,P')]$ which was reacted, in situ, with one equivalent of $[Fe_4Cp_4S_6]$ to give the 2:1 charged complex $[W(CO)_3(dppe\text{-}P,P')(Fe_4Cp_4S_6\text{-}S,S')]2I$ (**45**). Similarly the reaction of $[WI_2(CO)_3(NCMe)_2]$ with one equivalent of dpppr followed by one equivalent of $[Fe_4Cp_4S_6]$ gave the analogous 2:1 charged complex $[W(CO)_3(dpppr\text{-}P,P')(Fe_4Cp_4S_6\text{-}S,S')]2I$ (**46**).The complexes were black crystalline solids which were sparingly soluble in CH_2Cl_2 but more soluble in acetonitrile. The complexes (**45**) and (**46**) were characterised by elemental analysis C, H, N, S (**Table 5.1**), infra red and ^1H NMR spectroscopy (**Tables 5.2- 5.3**). Conductivity measurements of both complexes in NCMe showed them to be 2:1 electrolytes (Λ_m= 175 and 179 S cm^2 mol^{-1} respectively).

The infra red spectra of both complexes (**45**) and (**46**) were recorded in CH_2Cl_2 and display the expected three strong carbonyl stretches at (2034, 1963 and 1909 cm^{-1}) and (2039, 1969 and 1919 cm^{-1}) respectively (**Figure 5.14**). As with previous complexes upon coordination to the cluster, the stretch at 439 cm^{-1} disappears upon coordination suggesting the tungsten is attached *via* the two top sulphur atoms of the cluster.

The ^1H NMR spectrum of complex (**45**) again has no signals which may be assigned to Cp protons. However, the phenyl protons of the dppe are observed as a broad multiplet at δ = 7.6 ppm slightly shifted from those of the free ligand. Similarly the CH_2 protons of the dppe ligand are observed as multiplet at δ = 2.7 ppm. A very similar ^1H NMR spectrum is observed for complex (**46**) with a multiplet at δ = 7.6 ppm due to the phenyl protons of the diphosphine accompanied by two further multiplets at δ = 2.9 ppm and δ = 2.1 ppm which may be assigned to the CH_2 protons of the dpppr ligand.

Figure 5.14 Infra red carbonyl regions of complexes (**45**) and (**46**) recorded in CH_2Cl_2

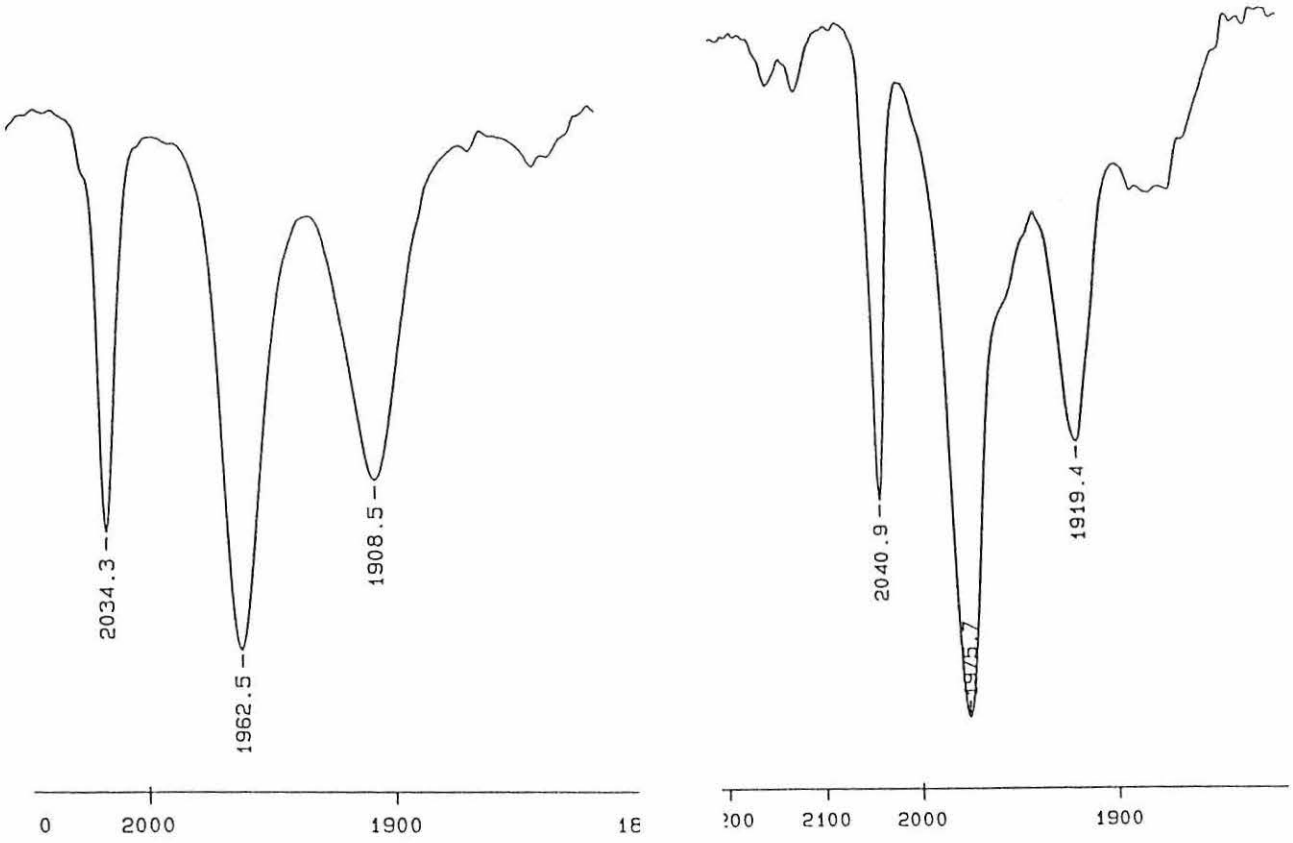

5.2.6 Reaction of the complex $[MoI_2(CO)_3(NCMe)_2]$ with one equivalent of dppe or dpppr followed by an in situ reaction of the cluster $[Fe_4Cp_4S_6]$

The reaction of the molybdenum starting complex $[MoI_2(CO)_3(NCMe)_2]$ with one equivalent of dppe at room temperature in CH_2Cl_2 gave the complex $[MoI_2(CO)_3(dppe\text{-}P,P')]$ which was reacted, in situ, with one equivalent of $[Fe_4Cp_4S_6]$ to give the 2:1 charged complex $[Mo(CO)_3(dppe\text{-}P,P')(Fe_4Cp_4S_6\text{-}S,S')]2I$ (**47**). Similarly the reaction of $[MoI_2(CO)_3(NCMe)_2]$ with one equivalent of dpppr followed by one equivalent of $[Fe_4Cp_4S_6]$ gave the analogous 2:1 charged complex $[Mo(CO)_3(dpppr\text{-}P,P')(Fe_4Cp_4S_6\text{-}S,S')]2I$ (**48**).The complexes were black crystalline solids which were sparingly soluble in CH_2Cl_2 but more soluble in acetonitrile. The complexes (**47**) and (**48**) were characterised by elemental analysis C, H, N, S (**Table 5.1**), infra red and ^1H NMR spectroscopy (**Tables 5.2- 5.3**). Conductivity measurements of both complexes in NCMe showed them to be 2:1 electrolytes (Λm= 177 and 181 S cm^2 mol^{-1} respectively).

The infra red spectra of both complexes (**47**) and (**48**) were recorded in CH_2Cl_2 and display the expected three strong carbonyl stretches at (2041, 1976 and 1919 cm^{-1}) and (2042, 1964 and 1908 cm^{-1}) respectively. As previously seen upon coordination to the cluster, the stretch at 439 cm^{-1} disappears upon coordination suggesting the tungsten is attached *via* the two top sulphur atoms of the cluster.

The ^1H NMR spectrum of complex (**47**) again shows no visible Cp protons. The phenyl protons of the dppe are observed as a broad multiplet at δ = 7.5 ppm slightly shifted from those of the free ligand (δ = 7.8 ppm) and the CH_2 protons of the dppe ligand are observed as multiplet at δ = 2.75 ppm. A very similar ^1H NMR spectrum is observed for complex (**48**) with no Cp resonances. However, seen as a multiplet at δ = 7.5 ppm are the phenyl protons of the diphosphine accompanied by two further multiplets at δ = 2.9 ppm and δ = 2.1 ppm which may be assigned to the CH_2 protons of the dpppr ligand.

5.2.7 Reactions of the alkyne complexes $[WI_2(CO)(NCMe)(\eta^2\text{-}RC_2R)_2]$ with $[Fe_4Cp_4S_6]$ (R = Me, Ph)

The reaction of the tungsten bis(alkyne) complexes $[WI_2(CO)(NCMe)(\eta^2\text{-}MeC_2Me)_2]$ and $[WI_2(CO)(NCMe)(\eta^2\text{-}PhC_2Ph)_2]$ with one equivalent of the cluster $[Fe_4Cp_4S_6]$ at room temperature in CH_2Cl_2 gave the new alkyne-cluster complexes $[WI(CO)(Fe_4Cp_4S_6\text{-}S,S')(\eta^2\text{-}MeC_2Me)_2]I$ (**49**) and $[WI(CO)(Fe_4Cp_4S_6\text{-}S,S')(\eta^2\text{-}PhC_2Ph)_2]I$ (**50**) in relatively high yields. Both complexes (**49**) and (**50**) are black micro-crystalline solids which are soluble in CH_2Cl_2 and NCMe, but relatively insoluble in diethyl ether and hexane. Both complexes are fairly oxygen-sensitive in both solution and the solid-state and are best handled in a nitrogen atmosphere even for short periods of time. The complexes (**49**) and (**50**) were characterised by elemental analysis C, H, N, S (**Table 5.1**), infra red and ^1H NMR spectroscopy (**Tables 5.2 and 5.3**).

The infra red spectra of complexes (**49**) and (**50**) were recorded as a KBr pellets and both exhibit strong carbonyl resonances at 2040 and 2070 cm^{-1} respectively. The relatively high frequency of the carbonyl stretches, similar to those of the starting materials, suggests the retention of both alkyne ligands during the reaction. For both complexes a weak stretch is also observed at 455 cm^{-1} which can be attributed to the μ_3-sulphur atoms of the iron-sulphur cluster which are attached to the tungsten centre. This can be compared to the μ_2-sulphur stretch observed for the free cluster at 439cm^{-1} which is no longer seen upon coordination of the cluster to the tungsten centre. Conductivity measurements of both complexes in acetonitrile showed both to be 1:1 electrolytes (139 and 142 S cm^2 mol^{-1} respectively).

The ^1H NMR spectra of both complexes (**49**) and (**50**) in $CDCl_3$, as with the previously described complexes, show no Cp protons of the cluster. In the case of complex (**49**) there is a resonance at δ = 3.0 ppm which may be assigned to the methyl protons of the alkyne and in complex (**50**) the phenyl protons of the

alkyne are observed as a multiplet at δ = 7.5 ppm. All integrals are in agreement with the proposed formulation of complexes (**49**) and (**50**).

It is interesting to note that the reaction of $[WI_2(CO)(NCMe)(\eta^2\text{-}MeC_2Me)_2]$ with an equimolar amount of 2,2'-bipy in the presence of $Na[BPh_4]$ gives the crystallographically characterised complex $[WI(CO)(2,2'\text{-bipy})(\eta^2\text{-}MeC_2Me)_2][BPh_4]$[206]. The molecule adopts a distorted octahedral geometry with the 2-butyne ligands *cis* and parallel to one another. The carbonyl group is trans to the iodide with the remaining two coordination sites occupied by the nitrogen atoms of the bipyridyl ligand. The complexes (**49**) and (**50**) have very similar spectral properties, in particular the high carbonyl stretching band, to the complex $[WI(CO)(2,2'\text{-bipy})(\eta^2\text{-}MeC_2Me)_2][BPh_4]$ it is possible therefore to suggest similar structures for complexes (**49**) and (**50**).

5.3 CONCLUSIONS

In conclusion we have carried out the reaction of the seven-coordinate complexes $[MI_2(CO)_3(NCMe)_2]$ $[MI_2(CO)_3(dppe)]$, $[MI_2(CO)_3(dpppr)]$ and $[MI_2(CO)(NCMe)(\eta^2\text{-}RC_2R)_2]$ (M = Mo, W; R = Ph, Me) with the cluster $[Fe_4Cp_4S_6]$. The complexes obtained all contain an intact $[Fe_4Cp_4S_6]$ cluster which is bound to the W or Mo metal via the two "handle" sulphurs of the so-called "basket". These complexes provide very simple models for the active site of the metalloenzyme nitrogenase.

Table 5.1 Physical and analytical data[a] for complexes (**35**) - (**50**)

Complex	Colour	Yield %	%C	%H	%S
(**35**) $[WI_2(CO)_3(Fe_4Cp_4S_6\text{-}S,S')]$	Black	65	22.60 (23.06)	1.68 (1.67)	16.00 (16.06)
(**36**) $[MoI_2(CO)_3(Fe_4Cp_4S_6\text{-}S,S')]$	Black	60	23.88 (24.14)	1.81 (1.88)	16.86 (17.33)
(**37**) $[WI(SPh)(CO)_3(Fe_4Cp_4S_6\text{-}S,S')]$	Black	48	29.65 (29.50)	2.42 (2.14)	18.27 (19.02)
(**38**) $[WI(tmt)(CO)_3(Fe_4Cp_4S_6\text{-}S,S')]$	Black	51	31.31 (31.45)	2.65 (2.56)	16.80 (18.36)
(**39**) $[W(SPh)_2(CO)_3(Fe_4Cp_4S_6\text{-}S,S')]$	Black	61	35.95 (36.17)	3.06 (2.60)	23.01 (22.07)
(**40**) $[W(tmt)_2(CO)_3(Fe_4Cp_4S_6\text{-}S,S')]$	Black	58	40.56 (39.51)	3.84 (3.40)	17.62 (20.58)
(**41**) $[MoI(SPh)(CO)_3(Fe_4Cp_4S_6\text{-}S,S')]$	Black	56	31.19 (31.89)	1.85 (2.31)	21.11 (20.55)
(**42**) $[MoI(tmt)(CO)_3(Fe_4Cp_4S_6\text{-}S,S')]$	Black	45	33.78 (33.89)	2.59 (2.75)	18.71 (19.79)
(**43**) $[Mo(SPh)_2(CO)_3(Fe_4Cp_4S_6\text{-}S,S')]$	Black	53	39.13 (39.13)	2.69 (2.81)	25.87 (23.67)
(**44**) $[Mo(tmt)_2(CO)_3(Fe_4Cp_4S_6\text{-}S,S')]$	Black	50	42.47 (42.50)	3.83 (3.65)	22.24 (22.12)
(**45**) $[W(CO)_3(dppe\text{-}P,P')(Fe_4Cp_4S_6\text{-}S,S')]2I$	Black	65	36.10 (36.97)	2.85 (2.79)	11.62 (12.08)
(**46**) $[W(CO)_3(dpppr\text{-}P,P')(Fe_4Cp_4S_6\text{-}S,S')]2I$	Black	67	36.86 (37.29)	2.74 (2.86)	10.80 (11.92)
(**47**) $[Mo(CO)_3(dppe\text{-}P,P')(Fe_4Cp_4S_6\text{-}S,S')]2I$	Black	56	39.13 (39.13)	2.98 (2.95)	12.56 (12.79)
(**48**) $[Mo(CO)_3(dpppr\text{-}P,P')(Fe_4Cp_4S_6\text{-}S,S')]2I$	Black	78	39.32 (39.45)	2.53 (3.02)	13.27 (12.61)
(**48**) $[Mo(CO)_3(dpppr\text{-}P,P')(Fe_4Cp_4S_6\text{-}S,S')]2I$	Black	78	39.32 (39.45)	2.53 (3.02)	13.27 (12.61)
(**49**) $[WI(CO)(Fe_4Cp_4S_6\text{-}S,S')(\eta^2\text{-}MeC_2Me)_2]I$	Black	50	38.76 (39.21)	2.05 (2.74)	12.07 (13.08)
(**50**) $[WI(CO)(Fe_4Cp_4S_6\text{-}S,S')(\eta^2\text{-}PhC_2Ph)_2]I$	Black	67	26.97 (27.87)	2.40 (2.58)	14.29 (15.39)

Table 5.2 Infra red data[b] for complexes (**35**) to (**50**)

Compound	ν C=O cm^{-1}	ν μ3-S cm^{-1}	ν C=C cm^{-1}
(**35**)	1873(s), 1934(s), 2010(s)	448(w)	-----
(**36**)	1886(s), 1945(s), 2014(s)	447(w)	-----
(**37**)	1919(s), 1988(s), 2056(s)	448(w)	-----
(**38**)	1880(s), 1936(s), 2000(s)	451(w)	-----
(**39**)	1830(s), 1850(s), 1981(s)	450(w)	-----
(**40**)	1833(s), 1849(s), 1985(s)	452(w)	-----
(**41**)	1821(s), 1858(s), 1988(s)	450(w)	-----
(**42**)	1829(s), 1858(s), 1989(s)	449(w)	-----
(**43**)	1832(s), 1869(s), 1995(s)	448(w)	-----
(**44**)	1830(s), 1861(s), 1992(s)	450(w)	-----
(**45**)	2034(s), 1963(s),1909(s)	449(w)	-----
(**46**)	2039(s), 1969(s), 1919(s)	447(w)	-----
(**47**)	2041(s), 1976(s), 1919(s)	448(w)	-----
(**48**)	2042(s), 1964(s), 1908(s)	448(w)	-----
(**49**)	2040(s)	455(w)	1650(w)
(**50**)	2070(s)	455(w)	1635(w)

[b]All data recorded as KBr Pellets; s = strong, w =weak.

Table 5.3 Mössbauer data[d] for selected complexes at 77K and zero magnetic field.

Compound	δ (mms^{-1}) Isomer Shift	Δ (mms^{-1}) Quadrupole Split
(36)	0.40 0.42	1.34 0.98
(37)	0.41 0.41	1.39 0.98
(38)	0.41 0.41	1.34 0.98
(39)	0.41 0.41	1.39 0.98
(40)	0.40 0.42	1.38 1.05
(41)	0.41 0.41	1.37 1.03
(42)	0.41 0.41	1.43 0.97
(43)	0.40 0.41	1.44 0.97
(44)	0.40 0.40	1.35 0.98
(45)	0.40 0.41	1.35 0.96

[d]Mossbauer samples were prepared as mulls with Boron nitride

CHAPTER 6:
Experimental for chapters two to five.

CHAPTER SIX: EXPERIMENTAL FOR CHAPTERS TWO TO FIVE.

6.1 INTRODUCTION

All the reactions described were carried out under an atmosphere of dry dinitrogen using standard Schlenk line techniques, with the exception of some ligand syntheses. Dichloromethane was dried by refluxing over phosphorus pentoxide, while diethyl ether and thf were dried over sodium wire. The starting materials $[MI_2(CO)_3(NCMe)_2]$ and $[MI_2(CO)(NCMe)(RC_2R)_2]$ (M = Mo, W; R = Me, Ph) were prepared according to literature methods[50,118]. All other chemicals were obtained commercially, unless otherwise stated, and used without further purification.

Proton NMR spectra were recorded on a Bruker AC/250 (University of Wales, Bangor) or a Jeol GSX 270 (NFL, Norwich) spectrometer and referenced to tetramethylsilane. ^{13}C NMR were carried out on a Jeol GSX 270 spectrometer at the NFL, Norwich, with the help of Dr. Shirley Fairhurst. Inra red spectra were recorded on a Perkin-Elmer 1600 series FTIR spectrophotometer.

Elemental analyses (C,H,N and S) were determined on a Carlo Erba Elemental Analyser MOD 1108 (using helium as a carrier gas) at the University of Wales, Bangor. Conductivities were measured using a Portland Electronics conductivity bridge.

Crystal data was obtained with MoKα radiation using the MAResearch Image Plate System. Data analyses were carried out using the XDS program[207]. The structures were solved using direct methods with the Shelx86 program[208] and the structure refined using Shelx1[209]. All calculations were carried out on a Silicon Graphics Workstation at the University of Reading.

Mössbauer spectroscopy was carried out by Dr. David Evans at the NFL, Norwich. Solid samples were examined at 77K using an ES-Technology MS105 spectrometer with a 925MBq ^{57}Co source in in a rhodium matrix. Samples were referenced to a 25 micron iron foil at 298K.

6.2 EXPERIMENTAL FOR CHAPTER TWO

6.2.1 Preparation of ligands NaSPh and $Na_2[S(CH_2)_nS]$ (n = 2 or 3)

The ligand $Na_2[S(CH_2)_2S]$ was prepared as follows: To 1,2-ethanedithiol (1.78 cm^3, 21.23 mmol) stirring in THF (200 cm^3) under a stream of dry nitrogen was added sodium metal (0.98 g, 42.46 mmol). The mixture was stirred for 72 hrs. The solvent was removed *in vacuo* to give the white crystalline solid $Na_2[S(CH_2)_2S]$ (yield = 2.6 g, 18.80 mmol) which was used without further purification.

A similar reaction using 1, 3-propanedithiol (1.86 cm^3, 18.48 mmol) gave the white crystalline solid $Na_2[S(CH_2)_3S]$ (2.6 g, 16.80 mmol) and again the product was used without further purification.

The ligand NaSPh was prepared as follows: Sodium metal (3.0 g, 130 mmol) was dissolved in dry methanol (150 cm^3) and to the continuously stirring solution under a stream of dry nitrogen was added thiphenol (14.3g, 130 mmol). The solution was stirred for 2 hours. The solvent was removed *in vacuo* to give the white crystalline solid NaSPh (yield = 15,84 g, 120 mmol) which was used without further purification.

6.2.2 Preparation of $[WI_2(CO)_3(PEt_3)_2]$ (1)

To a stirred suspension of $[WI_2(CO)_3(NCMe)_2]$ (0.27 g, 0.44 mmol) in dry, degassed Et_2O (50cm^3) under a stream of dry nitrogen was added 1.0M triethylphosphine in THF (0.88 cm^3, 0.88 mmol). The resulting yellow solution was stirred for 5 mins, filtered and the solvent remove *in vacuo* to give a yellow solid. The yellow solid was recrystallised from CH_2Cl_2 and hexane at 0 °C to give yellow-orange crystals of $[WI_2(CO)_3(PEt_3)_2]$ (1) (yield = 0.27 g, 78 %).

6.2.3 Preparation of $[W\{S(CH_2)_2S\}(CO)_2(PEt_3)_2]$ (2)

To a stirred suspension of $[WI_2(CO)_3(NCMe)_2]$ (0.27 g, 0.44 mmol) in dry, degassed Et_2O ($50cm^3$) under a stream of dry nitrogen was added 1.0M triethyl phosphine in THF (0.88 cm^3, 0.88 mmol). The resulting yellow solution was stirred for 5 minutes and filtered. $Na_2[S(CH_2)_2S]$ (0.06 g, 0.44 mmol) was added *in situ* and the solution stirred for eighteen hrs to give a wine-red solution which was filtered twice over cellite. The solvent was removed *in vacuo* to give a dark red oil, which was recrystallised from Et_2O at 0 °C affording dark red crystals of $[W\{S(CH_2)_2S\}(CO)_2(PEt_3)_2]$ (**2**) (yield = 0.21 g, 85 %), which were suitable for X-ray crystallography.

6.2.4 Preparation of $[W\{S(CH_2)_3S\}(CO)_2(PEt_3)_2]$ (3)

To a stirred suspension of $[WI_2(CO)_3(NCMe)_2]$ (0.22 g, 0.37 mmol) in dry, degassed Et_2O ($50cm^3$) under a stream of dry nitrogen was added 1.0M triethylphosphine in THF (0.74 cm^3, 0.74 mmol). The resulting yellow solution was stirred for 5 minutes and filtered. $Na_2[S(CH_2)_3S]$ (0.06 g, 0.37 mmol) was added *in situ* and the solution stirred for eighteen hrs to give a wine-red solution which was filtered twice over cellite. The solvent was reduced to a minimum and cooled to 0 °C affording dark red crystals of $[W(S(CH_2)_3S)(CO)_2(PEt_3)_2]$ (**3**) (yield = 0.17 g, 80 %), which were suitable for X-ray crystallography.

A similar method using two eqivalents NaSPh (0.13 g, 0.98 mmol) afforded green crystals of $[W(SPh)_2(CO)_2(PEt_3)_2]$ (**4**) (yield = 0.20 g, 60 %), which were suitable for X-ray crystallography.

6.2.5 Preparation of $[Mo\{S(CH_2)_2S\}(CO)_2(PEt_3)_2]$ (5)

To a stirred suspension of $[MoI_2(CO)_3(NCMe)_2]$ (0.25 g, 0.48 mmol) in dry, degassed Et_2O ($50cm^3$) under a stream of dry nitrogen was added 1.0M triethylphosphine

in THF (0.95 cm^3, 0.95 mmol). The resulting solution was stirred for thirty seconds and filtered. $Na_2[S(CH_2)_2S]$ (0.07 g, 0.48 mmol) was added *in situ* and the solution stirred for two hrs to give a wine-red solution which was filtered twice over cellite. The solvent was reduced to a minimum and cooled to 0 °C affording dark red crystals of $[Mo\{S(CH_2)_2S\}(CO)_2(PEt_3)_2]$ (**5**) (yield = 0.21 g, 91 %), which were suitable for X-ray crystallography.

6.2.6 Preparation of $[WI(acac)(CO)_2(PEt_3)_2]$ (6)

To acetylacetone (0.18 cm^3, 1.76 mmol) in dry Et_2O (5 cm^3) was added NaH (0.04 g, 1.76 mmol) and the mixture stirred for five mins. The solvent was removed *in vacuo* and the resulting sodium salt resolvated in CH_2Cl_2 (10 cm^3) and EtOH (10 cm^3). To a stirred suspension of $[WI_2(CO)_3(NCMe)_2]$ (1.07 g, 1.77 mmol) in dry, degassed Et_2O (50cm^3) under a stream of dry nitrogen was added 1.0M triethylphosphine in THF (3.53 cm^3, 3.53 mmol). The resulting yellow solution was stirred for 5 mins and filtered. To the filtered solution was added the previously prepared solution of Na[acac] and the mixture stirred for a further eighteen hrs: after which the solvents were removed *in vacuo*. The product was resolvated in Et_2O (20 cm^3) and CH_2Cl_2 (10 cm^3) and filtered twice to remove any NaI. The solvent was reduced to a minimum and cooled to 0 °C affording red-orange crystals of $[WI(acac)(CO)_2(PEt_3)_2]$ (**6**) (yield = 0.918 g, 85 %), which were suitable for X-ray crystallography.

A similar method using $[MoI_2(CO)_3(NCMe)_2]$ (0.27 g, 0.52 mmol) afforded red-orange crystals of $[MoI(\text{-}acac)(CO)_2(PEt_3)_2]$ (**7**) (yield = 0.27 g, 73 %) which were suitable for X-ray crystallography.

6.3 EXPERIMENTAL FOR CHAPTER THREE

6.3.1 Preparation of the ligands $RS(CH_2)_2SR$ (R = Ph and 4-FC_6H_4)

The ligand $PhS(CH_2)_2SPh$ (s-Diphenylthiolethane) was synthesised as described below: Thiophenol (12.58 cm^3, 123 mmol)in methylated-spirits (100 cm^3) was heated above a steam bath for 1 hour with potassium hydroxide (6.9 g, 123 mmol) (dissolved in a minimum of water) and 1,2-dibromoethane (5.18 cm^3, 60 mmol). The solvent was removed on a rotary evaporator to give acream solid on cooling. This was recrystallised from hot methylated-spirits (825 cm^3) to give crystals of $PhS(CH_2)_2SPh$ (yield = 7.4 g, 24%) on cooling. The crystals obtained had a melting point of 68 - 70°C. A similar procedure using 4-fluorothiophenol (5.60 cm^3) gave 4-$FC_6H_4S(CH_2)_2SC_6H_4F$-4 (yield = 4.3 g, 29%).

6.3.2 Preparation of $[WBr_2(CO)_3\{PhS(CH_2)_2SPh\}]$ (8)

To a stirred solution of $[WBr_2(CO)_3(NCMe)_2]$ (0.21 g, 0.412 mmol) in CH_2Cl_2 (15 cm^3) under a stream of dry nitrogen was added $PhS(CH_2)_2SPh$ (0.11 g, 0.451 mmol). The resulting solution was stirred for 2 hrs before filtering over a fine frit and the solvent was removed *in vacuo* to produce a orange brown powder. The powder was dissolved in a minimum of CH_2Cl_2 and cooled to -15°C to give orange crystals of $[WBr_2(CO)_3\{PhS(CH_2)_2SPh\}]$ (**8**) (0.12 g, 0.185 mmol, 45%) one of which was suitable for X-ray crystallography.

A similar reaction of $[MoBr_2(CO)_3(NCMe)_2]$ (0.19 g, 0.452 mmol) with $PhS(CH_2)_2SPh$ (0.12 g, 0.458 mmol) followed by recrystallisation from CH_2Cl_2 gave the brown complex $[MoBr_2(CO)_3\{PhS(CH_2)_2SPh\}]$ (**9**) (0.11 g, 0.181 mmol, 40%).

6.3.3 Preperation of $[WBr_2(CO)_3\{4\text{-}FC_6H_4S(CH_2)_2SC_6H_4F\text{-}4\}]$ (10)

To a stirred solution of $[WBr_2(CO)_3(NCMe)_2]$ (0.25 g, 0.490 mmol) in CH_2Cl_2 (20 cm^3) under a stream of dry nitrogen was added $4\text{-}FC_6H_4S(CH_2)_2SC_6H_4F\text{-}4$ (0.15 g, 0.513 mmol). The resulting solution was stirred for 23 hrs before filtering over a fine frit and the solvent was removed *in vacuo* to produce a orange brown powder. The powder was dissolved in a minimum of CH_2Cl_2 and cooled to -15°C to give the orange complex $[WBr_2(CO)_3\{4\text{-}FC_6H_4S(CH_2)_2SC_6H_4F\text{-}4\}]$ (**10**) (0.15 g, 0.216 mmol, 44%).

A similar reaction of $[MoBr_2(CO)_3(NCMe)_2]$ (0.19 g, 0.452 mmol) with $4\text{-}FC_6H_4S(CH_2)_2SC_6H_4F\text{-}4$ (0.13 g, 0.453 mmol) in CH_2Cl_2 for 4 hrs followed by recrystallisation from CH_2Cl_2 gave the brown complex $[MoBr_2(CO)_3\{4\text{-}FC_6H_4S(CH_2)_2SC_6H_4F\text{-}4\}]$ (**11**) (0.13 g, 0.208 mmol, 46%).

6.3.4 Preparation of $[WBr(CO)_3\{PhS(CH_2)_2SPh\text{-}S\}\{PhS(CH_2)_2SPh\text{-}S,S'\}]Br$ (12)

To a stirred solution of $[WBr_2(CO)_3(NCMe)_2]$ (0.21 g, 0.412 mmol) in CH_2Cl_2 (15 cm^3) under a stream of dry nitrogen was added $PhS(CH_2)_2SPh$ (0.21 g, 0.828 mmol). The resulting solution was stirred for 17 hrs before filtering over a fine frit and the solvent was removed *in vacuo* to produce a orange brown powder. The powder was dissolved in a minimum of CH_2Cl_2 and cooled to -15°C to give the brown complex $[WBr(CO)_3\{PhS(CH_2)_2SPh\text{-}S\}\{PhS(CH_2)_2SPh\text{-}S,S'\}]Br$ (**12**) (0.15 g, 0.166 mmol, 41%).

A similar reaction of $[WBr_2(CO)_3(NCMe)_2]$ (0.19 g, 0.373 mmol) with $4\text{-}FC_6H_4S(CH_2)_2SC_6H_4F\text{-}4$ (0.21 g, 0.747 mmol) followed by recrystallisation from CH_2Cl_2 gave the brown complex $[WBr(CO)_3\{4\text{-}FC_6H_4S(CH_2)_2SC_6H_4F\text{-}4\text{-}S\}\{4\text{-}FC_6H_4S(CH_2)_2SC_6H_4F\text{-}4\text{-}S,S'\}]Br$ (**13**) (0.17 g, 0.175 mmol, 47%).

6.3.5 Preparation of $[WBr_2(CO)_3\{Ph_2P(S)CH_2(S)PPh_2\}]$ (14)

To a stirred solution of $[WBr_2(CO)_3(NCMe)_2]$ (0.07 g, 0.137 mmol) in CH_2Cl_2 (15 cm^3) under a stream of dry nitrogen was added $Ph_2P(S)CH_2(S)PPh_2$ (0.07 g, 0.145 mmol). The resulting solution was stirred for 4 hrs before filtering over a fine frit and the solvent was removed *in vacuo* to produce a green sticky oil. The oil was washed with hexane and then dissolved in a minimum of CH_2Cl_2 and cooled to -15°C to give the green complex $[WBr_2(CO)_3\{Ph_2P(S)CH_2(S)PPh_2\}]$ (**14**) (0.08 g, 0.086 mmol, 60%).

A similar reaction of $[WBr_2(CO)_3(NCMe)_2]$ (0.07 g, 0.137 mmol) with $Ph_2P(S)CH_2(S)PPh_2$ (0.14 g, 0.290 mmol) in CH_2Cl_2 (15 cm^3) for 12 hrs followed by washing with hexane and recrystallisation from CH_2Cl_2 gave the green complex $[WBr(CO)_3\{Ph_2P(S)CH_2(S)PPh_2\text{-}S\}\{Ph_2P(S)CH_2(S)PPh_2\text{-}S,S'\}]Br$ (**15**) (0.08 g, 0.062 mmol, 45%).

6.3.6 Preparation of $[MoBr_2(CO)_2\{MeS(CH_2)_2S(CH_2)_2SMe\text{-}S,S',S''\}]$ (16)

To a stirred solution of $[MoBr_2(CO)_3(NCMe)_2]$ (0.30 g, 0.722 mmol) in CH_2Cl_2 (15 cm^3) under a stream of dry nitrogen was added $MeS(CH_2)_2S(CH_2)_2SMe$ (TTN) (0.13 g, 0.730 mmol). The resulting solution was stirred for 5 hrs before filtering over cellite and the solvent was removed *in vacuo* to produce a red oily solid. The oil was washed with hexane and then dissolved in a minimum of CH_2Cl_2 and cooled to -15°C to give the red-brown complex $[MoBr_2(CO)_2\{MeS(CH_2)_2S(CH_2)_2SMe\text{-}S,S',S''\}]$ (**16**) (0.20 g, 0.397 mmol, 55%).

A similar reaction of $[WBr_2(CO)_3(NCMe)_2]$ (0.29 g, 0.569 mmol) with $MeS(CH_2)_2S(CH_2)_2SMe$ (TTN) (0.11 g, 0.575 mmol) in CH_2Cl_2 (15 cm^3) for 12 hrs followed by washing with hexane and recrystallisation from CH_2Cl_2 gave the green complex $[WBr_2(CO)_3\{MeS(CH_2)_2S(CH_2)_2SMe\text{-}S,S'\}]$ (**17**) (0.19 g, 0.307 mmol, 54%).

6.3.7 Preperation of [$MoBr_2(CO)_2${ttob-*S,S',S''*}] (18)

To a stirred solution of [$MoBr_2(CO)_3(NCMe)_2$] (0.41 g, 0.986 mmol) in CH_2Cl_2 (15 cm^3) under a stream of dry nitrogen was added ttob (0.26 g, 1.000 mmol). The resulting solution was stirred for 4 hrs before filtering over cellite and the solvent was removed *in vacuo* to produce a brown solid. The solid was washed with hexane and then dissolved in a minimum of CH_2Cl_2 and cooled to -15°C to give the brown complex [$MoBr_2(CO)_2${ttob-*S,S',S''*}] (**18**) (0.34 g, 0.592 mmol, 60%).

6.4 EXPERIMENTAL FOR CHAPTER FOUR

6.4.1 Preparation of [$WI_2(CO){MeS(CH_2)_2S(CH_2)_2SMe$-*S,S'*}($\eta^2$- PhC_2Ph)] (19), [WI(CO){$MeS(CH_2)_2S(CH_2)_2SMe$-*S,S',S''*}(η^2-PhC_2Ph)]I (20) and [WI(CO){$MeS(CH_2)_2S(CH_2)_2SMe$-*S,S'*}(η^2-MeC_2Me)]I Et_2O(21)

To a stirred solution of [$WI_2(CO)(NCMe)(\eta^2$-$PhC_2Ph)_2$] (0.28 g, 0.32 mmol) in dry degassed CH_2Cl_2 (45cm^3) was added $MeS(CH_2)_2S(CH_2)_2SMe$ (0.06 g, 0.33 mmol) and the solution stirred for 72 hrs. The resulting solution was filtered over cellite and the solvent removed *in vacuo* to give the green complex [$WI_2(CO){MeS(CH_2)_2S(CH_2)_2SMe$-*S,S'*}($\eta^2$-$PhC_2Ph$)] (**19**) (yield = 0.18 g, 67%). Recrystallisation of complex (**19**) from CH_2Cl_2/Et_2O at 0 °C gave green crystals of suitable quality for X-ray crystallography.

A similar reaction of [$WI_2(CO)(NCMe)(\eta^2$-$PhC_2Ph)_2$] (0.28 g, 0.32 mmol) with $MeS(CH_2)_2S(CH_2)_2SMe$ (0.06 g, 0.33 mmol), followed by a further reflux of the solution in CH_2Cl_2 (45 cm^3) for 6 hrs gave the charged complex [WI(CO){$MeS(CH_2)_2S(CH_2)_2SMe$-*S,S',S''*}(η^2-PhC_2Ph)]I (**20**). Further recrystallisation

of complex (**20**) from CH_2Cl_2/Et_2O at 0 °C gave the green crystalline solid [WI(CO){$MeS(CH_2)_2S(CH_2)_2SMe$-*S,S',S''*}(η^2- PhC_2Ph)]I (**20**) (yield = 0.17g, 64%).

Similarly, to a stirred solution of [$WI_2(CO)(NCMe)(\eta^2$- $MeC_2Me)_2$] (0.25 g, 0.41 mmol) in dry degassed CH_2Cl_2 (45 cm^3) was added $MeS(CH_2)_2S(CH_2)_2SMe$ (0.08 g, 0.41 mmol) and the solution stirred for 72 hrs. The resulting solution was filtered over cellite and the solvent removed *in vacuo* to give the green complex [WI(CO){$MeS(CH_2)_2S(CH_2)_2SMe$-*S,S',S''*}(η^2-MeC_2Me)]I (**21**) (yield = 0.17 g, 58%).

6.4.2 Preparation of [WI(CO){ttob -*S,S',S''*}(η^2-PhC_2Ph)]I (22), [WI{ttob*S,S',S''*}(η^2-$PhC_2Ph)_2$]I_3 (23) and [WI(CO){ttob-*S,S',S''*}(η^2-MeC_2Me)]I (24)

To the complex [$WI_2(CO)(NCMe)(\eta^2$-$PhC_2Ph)_2$] (0.30 g, 0.35 mmol) was added ttob (0.09 g,0.35 mmol) with stirring in CH_2Cl_2 (50 cm^3) at room temperature for 72 hrs. The resulting green solution was filtered over cellite and the solvent removed *in vacuo* to give the green crystalline complex [WI(CO){ttob -*S,S',S''*} (η^2-PhC_2Ph)]I (**22**) (yield = 0.17 g, 58%). Further recrystallisation of complex (**22**) from CH_2Cl_2/Et_20 for two weeks gave more of the green complex (**22**) and also three very well formed dark green crystals. These crystals were characterised by X-ray crystallography and shown to be the novel charged complex [WI{ttob-*S,S',S''*}(η^2-$PhC_2Ph)_2$]I_3 (**23**) (Yield = <1%). Several further attempts at a rational synthesis of complex (**23**) were unsucessful. Similarly the reaction of [$WI_2(CO)(NCMe)(\eta^2$-$MeC_2Me)_2$] (0.30 g, 0.49 mmol) with ttob (0.13 g, 0.49mmol) with stirring in CH_2Cl_2 (50 cm^3) at room temperature for 72 hrs gave a green sticky oil. Further recrystallisation from CH_2Cl_2/Et_2O at 0 °C gave the lime-green complex [WI(CO){ttob-*S,S',S''*}(η^2-MeC_2Me)]I (**24**) (yield = 0.15 g, 40%)

6.4.3 Preparation of [WBr(CO){TTN-*S,S',S''*}(η^2-PhC_2Ph)]Br Et_2O (25) and[WBr(CO){ttob-*S,S',S''*}(η^2-PhC_2Ph)]Br (26)

The complex [$WBr_2(CO)(NCMe)(\eta^2$-$PhC_2Ph)_2$] was synthesised *via* the reaction of [$WBr_2(CO)_3(NCMe)_2$] with four equivalents of diphenylacetylene as described in the literature. Recrystallisation from CH_2Cl_2/Et_2O (ratio = 90:10) gave yellow crystals of suitable quality for X-ray analysis. To a stirred solution of [$WBr_2(CO)(NCMe)(\eta^2$-$PhC_2Ph)_2$] (0.51 g, 0.66 mmol) in CH_2Cl_2 (50 cm^3) was added $MeS(CH_2)_2S(CH_2)_2SMe$ (0.12 g, 0.66 mmol). The resulting solution was stirred for 24 hrs filtered and the solvent removed to give the green complex [WBr(CO){$MeS(CH_2)_2S(CH_2)_2SMe$-*S,S',S''*}(η^2-PhC_2Ph)]Br Et_2O (**25**) (yield= 0.21 g, 44%). Similarly, the reaction of [$WBr_2(CO)(NCMe)(\eta^2$-$PhC_2Ph)_2$] (0.42g, 0.55 mmol) with ttob (0.14 g, 0.55 mmol) stirring in CH_2Cl_2 (50 cm^3) at room temperature for 24 hrs, followed by filtration and evacuation of solvent, gives the green complex [WBr(CO){ttob-*S,S',S''*}(η^2-PhC_2Ph)]Br (**26**) (yield = 0.21 g, 47%).

6.4.4 Preparation of [$Cp(OC)_2Fe${$S(Me)(CH_2)_2S(CH_2)_2(Me)S$-*S,S',S''*}$WI_2(CO)$ (η^2-PhC_2Ph)]I (27)

To a stirred solution in CH_2Cl_2 (50 cm^3) of [$WI_2(CO)${$MeS(CH_2)_2S(CH_2)_2SMe$-*S,S'*}(η^2-PhC_2Ph)] (**19**) (0.54 g, 0.63 mmol) was added [$FeI(CO)_2Cp$] (0.20 g, 0.63 mmol). The resulting solution was stirred for four hrs at room temperature and the solvent removed *in vacuo*. The resulting black solidwas recrystallised from CH_2Cl_2 (15cm^3) to give the bimetallic complex [$Cp(OC)_2Fe${$S(Me)(CH_2)_2S(CH_2)_2(Me)S$-*S,S',S''*}$WI_2(CO)$ (η^2-PhC_2Ph)]I (**27**) (yield = 0.22 g, 30%).

6.4.5 Preparation of [MoI(CO){MeS(CH$_2$)$_2$S(CH$_2$)$_2$SMe-*S,S',S''*}(η^2-PhC$_2$Ph)]I Et$_2$O (28) and [MoI(CO){MeS(CH$_2$)$_2$S(CH$_2$)$_2$SMe-*S,S',S''*}(η^2MeC$_2$Me)]I Et$_2$O (29)

To a stirring solution in CH_2Cl_2 (50 cm^3) of [MoI$_2$(CO)(NCMe)(η^2-PhC$_2$Ph)$_2$] (0.46 g, 0.59 mmol) was added MeS(CH$_2$)$_2$S(CH$_2$)$_2$SMe (0.11 g, 0.59 mmol). The solution was stirred at room temperature for 12 hrs and the solvent removed *in vacuo* to give the complex [MoI(CO){MeS(CH$_2$)$_2$S(CH$_2$)$_2$SMe-*S,S',S''*}(η^2-PhC$_2$Ph)]I (**28**) (yield = 0.18 g, 38%).

Similarly, MeS(CH$_2$)$_2$S(CH$_2$)$_2$SMe (0.21 g, 1.16 mmol) was added to a stirring solution of [MoI$_2$(CO)(NCMe)(η^2-MeC$_2$Me)$_2$] (0.61 g, 1.16 mmol) in CH_2Cl_2 (50 cm^3) at room temperature for 12 hrs. Removal of the solvent *in vacuo* gave the complex [MoI(CO){MeS(CH$_2$)$_2$S(CH$_2$)$_2$SMe-*S,S',S''*}(η^2-MeC$_2$Me)]I Et$_2$O (**29**) (yield = 0.39 g, 49%). Both complexes (**28**) and (**29**) were recrystallised from CH_2Cl_2 / Et$_2$O solutions before final drying *in vacuo* and analysis.

6.4.6 Preparation of [MoI(CO){ttob -*S,S',S''*}(η^2- PhC$_2$Ph)]I (30) and [MoI(CO){ttob-S,S',S''}(η^2-MeC$_2$Me)]I (31)

To a stirred solution of [MoI$_2$(CO)(NCMe)(η^2-PhC$_2$Ph)$_2$] (0.43 g, 0.55 mmol) in CH_2Cl_2 (50 cm^3) at room temperature was added ttob (0.14 g, 0.55 mmol). The resulting solution was stirred for 20 hrs before filtration over cellite and removal of the solvent *in vacuo* gave the green complex [MoI(CO){ttob-*S,S',S''*}(η^2- PhC$_2$Ph)]I (**30**) (0.27 g, 60%). Similarly addition of ttob (0.17 g, 0.65 mmol) to a stirred solution of [MoI$_2$(CO)(NCMe)(η^2-MeC$_2$Me)$_2$] (0.34g, 0.65 mmol) in CH_2Cl_2 (50cm^3) at room temperature for 24 hrs gave the green complex [MoI(CO){ttob-S,S',S"}(η^2-MeC$_2$Me)]I (**31**) (0.19 g, 42%). Both complexes (**30**) and (**31**) were recrystallised from CH_2Cl_2 solutions before final drying *in vacuo* and analysis.

solvent *in vacuo* gave the green complex [MoI(CO){[9]aneS$_3$-*S,S',S''*}(η^2- PhC$_2$Ph)]I (**32**) (0.18 g, 48%). Recrystallisation of complex (**32**) from CH_2Cl_2/Et_2O at 0 ^oC gave green crystals of suitable quality for X-ray crystallography.

Similarly, addition of [9]aneS$_3$ (0.10 g, 0.57 mmol) to a stirred solution of [MoI$_2$(CO)(NCMe)(η^2-MeC$_2$Me)$_2$] (0.30 g, 0.57 mmol) in CH_2Cl_2 (50 cm^3) at room temperature for 24 hrs gave the green complex [MoI(CO){[9]aneS$_3$-*S,S',S''*}(η^2-MeC$_2$Me)]I (**33**) (0.24 g, 70%). Further purification of complex (33) was carried out *via* recrystallisation from a minimum of CH_2Cl_2 at 0 ^oC.

6.4.8 Preparation of [MoI$_2$(CO){Ph$_2$P(S)CH$_2$P(S)Ph$_2$-*S,S'*}(η^2- PhC$_2$Ph)] (34)

To a stirred solution of [MoI$_2$(CO)(NCMe)(η^2-PhC$_2$Ph)$_2$] (0.40 g, 0.52 mmol) in CH_2Cl_2 (50 cm^3) at room temperature was added Ph$_2$P(S)CH$_2$P(S)Ph$_2$, dppmS$_2$ (0.23 g, 0.52 mmol). The resulting solution was stirred for ten hrs, filtered over cellite and the solvent removed *in vacuo* to give [MoI$_2$(CO){Ph$_2$P(S)CH$_2$P(S)Ph$_2$-*S,S'*}(η^2-PhC$_2$Ph)] (**34**) (0.29 g, 56%). Further purification of complex (**34**) was carried out *via* recrystallisation from a minimum of CH_2Cl_2 at 0 ^oC.

6.5 Experimental for Chapter Five

6.5.1 Preparation of [WI$_2$(CO)$_3$(Fe$_4$Cp$_4$S$_6$-*S,S'*)] (35) and [MoI$_2$(CO)$_3$(Fe$_4$Cp$_4$S$_6$-*S,S'*)] (36)

To a stirred solution of [WI$_2$(CO)$_3$(NCMe)$_2$] (0.30 g, 0.50 mmol) in dry degassed CH_2Cl_2 (45cm^3) was added [Fe$_4$Cp$_4$S$_6$] (0.34 g, 0.50 mmol) and the solution stirred for 2 hrs. The resulting solution was reduced to half the original volume and filtered over a fine frit. The resulting black solid was recrystallised from a minimum of CH_2Cl_2 and dried *in vacuo* for several hours to give [WI$_2$(CO)$_3$(Fe$_4$Cp$_4$S$_6$-*S,S'*)] (**35**) (0.39 g, 65%).

Similarly, to $[MoI_2(CO)_3(NCMe)_2]$ (0.30 g, 0.58 mmol) in dry degassed CH_2Cl_2 ($45cm^3$) was added $[Fe_4Cp_4S_6]$ (0.39 g, 0.58 mmol) and the solution stirred for 30 secs. The resulting solution was reduced to half the original volume and filtered over a fine frit. The resulting black solid was recrystallised from a minimum of CH_2Cl_2 and dried *in vacuo* for several hours to give $[MoI_2(CO)_3(Fe_4Cp_4S_6\text{-}S,S')]$ (**36**) (0.39 g, 60%).

6.5.2 Preparation of $[WI(SPh)(CO)_3(Fe_4Cp_4S_6\text{-}S,S')]$ (37) and $[W(SPh)_2(CO)_3(Fe_4Cp_4S_6\text{-}S,S')]$ (39)

To a stirred solution of $[WI_2(CO)_3(Fe_4Cp_4S_6\text{-}S,S')]$ (**35**) (0.20 g, 0.17 mmol) in dry degassed CH_2Cl_2 ($45cm^3$) was added [NaSPh] (0.022 g, 0.17 mmol) and the solution stirred for 2 hrs. The resulting solution was filtered over a fine frit and the solvent removed *in vacuo*. The resulting black solid was recrystallised from a minimum of CH_2Cl_2 at 0 °Cand dried *in vacuo* for several hours to give $[WI(SPh)(CO)_3(Fe_4Cp_4S_6\text{-}S,S')]$ (**37**) (0.09 g, 48%).

A similar reaction of $[WI_2(CO)_3(Fe_4Cp_4S_6\text{-}S,S')]$ (**35**) (0.20 g, 0.17 mmol) with [NaSPh] (0.044 g, 0.34 mmol) over three hrs gave the complex $[W(SPh)_2(CO)_3(Fe_4Cp_4S_6\text{-}S,S')]$ (**39**) (0.12 g, 61%).

6.5.3 Preparation of $[WI(tmt)(CO)_3(Fe_4Cp_4S_6\text{-}S,S')]$ (38) and $[W(tmt)_2(CO)_3(Fe_4Cp_4S_6\text{-}S,S')]$ (40)

To a stirred solution of $[WI_2(CO)_3(Fe_4Cp_4S_6\text{-}S,S')]$ (**35**) (0.21 g, 0.18 mmol) in dry degassed CH_2Cl_2 ($45cm^3$) was added [Natmt] (0.031 g, 0.18 mmol) and the solution stirred for 2 hrs. The resulting solution was filtered over a fine frit and the solvent removed *in vacuo*. The resulting black solid was recrystallised from a minimum of CH_2Cl_2 at 0 °Cand dried *in vacuo* for several hours to give $[WI(tmt)(CO)_3(Fe_4Cp_4S_6\text{-}S,S')]$ (**37**) (0.11 g, 51%).

A similar reaction of $[WI_2(CO)_3(Fe_4Cp_4S_6\text{-}S,S')]$ (**35**) (0.20 g, 0.17 mmol) with [Natmt] (0.059 g, 0.34 mmol) over three hrs gave the complex $[W(tmt)_2(CO)_3(Fe_4Cp_4S_6\text{-}S,S')]$ (**40**) (0.12 g, 58%). The same reaction methods also gave the analogous molybdenum-cluster complexes $[MoI(SPh)(CO)_3(Fe_4Cp_4S_6\text{-}S,S')]$ (**41**) (51%), $[MoI(tmt)(CO)_3(Fe_4Cp_4S_6\text{-}S,S')]$ (**42**) (45%), $[Mo(SPh)_2(CO)_3(Fe_4Cp_4S_6\text{-}S,S')]$ (**43**) (53%) and $[Mo(tmt)_2(CO)_3(Fe_4Cp_4S_6\text{-}S,S')]$ (**44**) (50%) .

6.5.4 Preparation of $[W(CO)_3(dppe\text{-}P,P')(Fe_4Cp_4S_6\text{-}S,S')]$ 2I (45) and $[W(CO)_3(dpppr\text{-}P,P')(Fe_4Cp_4S_6\text{-}S,S')]$ 2I (46)

To stirred solutions of $[WI_2(CO)_3(NCMe)_2]$ (0.30 g, 0.50 mmol) in dry degassed CH_2Cl_2 ($45cm^3$) were added either dppe (0.20 g, 0.50 mmol) or dpppr (0.21 g, 0.50mmol) and the solutions stirred for five mins. To these was then added $[Fe_4Cp_4S_6]$ (0.34 g, 0.50 mmol) and the solutions stirred for a further 2 hrs. The resulting solutions were filtered over cellite and the solvent removed *in vacuo*. The resulting black solids were recrystallised from a minimum of CH_2Cl_2/Et_2O and dried *in vacuo* for several hours to give $[W(CO)_3(dppe\text{-}P,P')(Fe_4Cp_4S_6\text{-}S,S')]2I$ (**45**) (0.52 g, 65%) and $[W(CO)_3(dppe\text{-}P,P')(Fe_4Cp_4S_6\text{-}S,S')]2I$ (**46**) (0.54 g, 67%) respectively.

Similarly, to a stirred solution of $[MoI_2(CO)_3(NCMe)_2]$ (0.30 g, 0.58 mmol) in dry degassed CH_2Cl_2 ($45cm^3$) was added dppe (0.23 g, 0.58 mmol) or dpppr (0.21 g, 0.58 mmol) and the solutions stirred for five mins. To these was then added $[Fe_4Cp_4S_6]$ (0.39 g, 0.58 mmol) and the solutions stirred for a further 1 hr. The resulting solutions were filtered over a cellite and the solvent removed *in vacuo*. The resulting black solids were recrystallised from a minimum of CH_2Cl_2/Et_2O and dried *in vacuo* for several hours to give $[Mo(CO)_3(dppe\text{-}P,P')(Fe_4Cp_4S_6\text{-}S,S')]2I$ (**47**) (0.49 g, 56%) and $[Mo(CO)_3(dppe\text{-}P,P')(Fe_4Cp_4S_6\text{-}S,S')]2I$ (**48**) (0.69 g, 78%) respectively.

6.5.5 Preparation of [WI(CO)($Fe_4Cp_4S_6$-*S,S'*)(η^2-MeC_2Me)] (49) and [WI(CO)($Fe_4Cp_4S_6$-*S,S'*)(η^2-PhC_2Ph)] (50)

To a stirred solution of [WI_2(CO)(NCMe)(η^2-MeC_2Me)]I (0.30 g, 0.35 mmol) in dry degassed CH_2Cl_2 (45cm^3) was added [$Fe_4Cp_4S_6$] (0.24 g, 0.35 mmol) and the solution stirred for 20 hrs. The resulting solution was filtered over cellite and the solvent removed *in vacuo*. The resulting black solid was recrystallised from a minimum of CH_2Cl_2/Et_2O and dried *in vacuo* for several hours to give [WI(CO)($Fe_4Cp_4S_6$-*S,S'*)(η^2-MeC_2Me)] (**49**) (0.22 g, 50%)

Similarly, To a stirred solution of [WI_2(CO)(NCMe)(η^2-PhC_2Ph)] (0.30 g, 0.49 mmol) in dry degassed CH_2Cl_2 (45cm^3) was added [$Fe_4Cp_4S_6$] (0.32 g, 0.49 mmol) and the solution stirred for 24 hrs. The resulting solution was filtered over cellite and the solvent removed *in vacuo*. The resulting black solid was recrystallised from a minimum of CH_2Cl_2/Et_2O and dried *in vacuo* for several hours to give [WI(CO)($Fe_4Cp_4S_6$-*S,S'*)(η^2-PhC_2Ph)]I (**50**) (0.48 g, 67%)

CHAPTER 7:
Conclusions and Scope for Further Work.

Chapter three describes the synthesis and characterisation of eleven new molybdenum and tungsten di-bromo thioether and disulphide complexes. One of these complexes $[WBr_2(CO)_3\{PhS(CH_2)_2SPh\}]$ (**8**) was crystallographically characterised and its structure is very similar to the previously described structure of the analogous di-iodo complex[57]. The complex is a distorted capped octahedron with a carbonyl ligand in the unique capping position. The molybdenum di-carbonyl complex $[MoBr_2(CO)_2(ttob\text{-}S,S',S'')]$ (**18**) was also synthesised and provides a molybdenum atom attached to three sulphur atoms as is seen in the active site of the enzyme nitrogenase. No analogous tungsten complex is observed probably due to the greater W-C bond strength of the carbonyl ligands in comparison with those of molybdenum.

Chapter four describes the reactions of the bis(alkyne) complexes $[MX_2(CO)(NCMe)(\eta^2\text{-}RC_2R)_2]$ (M = Mo,W; X = I,Br; R = Me, Ph) with neutral sulphur donor ligands. Sixteen complexes are described, three of which, complexes (**19**), (**23**) and (**32**) have been structurally characterised by X-ray crystallography. The complex $[WI_2(CO)\{MeS(CH_2)_2S(CH_2)_2SMe\text{-}S,S'\}(\eta^2\text{-}PhC_2Ph)]$ (**19**) contains an acyclic trithioether ligand bound in a bidentate fashion. The structure of complex (**19**) is best described as a distorted octahedron[146]. Complex (**19**) has been shown to react with $[FeI(CO)_2Cp]$ *via* the free sulphur atom of the trithioether ligand to give the bimetallic complex (**27**). The complex $[MoI(CO)\{[9]aneS_3\text{-}S,S',S''\}(\eta^2\text{-}PhC_2Ph)]I$ (**32**) contains a cyclic trithioether bound in a tridentate fashion by all three sulphur atoms. The structure of complex (**32**), as with (**19**) is best described as a distorted octahedron. The presence of a molybdenum atom bound to three sulphur atoms is a good simple model for the active site of the enzyme nitrogenase. The cationic complex $[WI\{ttob\text{-}S,S',S''\}(\eta^2\text{-}PhC_2Ph)_2]I_3$ (**23**) was isolated, once, in very small amounts and was structurally characterised as a distorted octahedron. The complex (**23**) is a very good model for nitrogenase, even with tungsten as the metal. However the complex was never isolated again in many repeated reactions and no attempted rational syntheses of complex (**23**) were successful.

Chapter five describes the seven-coordinate cluster complexes $[MI_2(CO)_3(Fe_4Cp_4S_6\text{-}S,S')]$ (**35**) and (**36**) (M = Mo, W), $[MI(SAr)(CO)_3(Fe_4Cp_4S_6\text{-}S,S')]$ (**37**), (**38**), (**41**) and (**42**); $[M(SAr)_2(CO)_3(Fe_4Cp_4S_6\text{-}S,S')]$ (**39**), (**40**), (**43**) and (**44**) (Ar = Ph and $C_6H_2Me_3$-2,4,6); $[M(CO)_3(dppe\text{-}P,P')(Fe_4Cp_4S_6\text{-}S,S')]2I$ (**45**) and (**47**); $[M(CO)_3(dpppr\text{-}P,P')(Fe_4Cp_4S_6\text{-}S,S')]2I$ (**46**) and (**48**); and the bis(alkyne)-cluster complexes $[MI(CO)(Fe_4Cp_4S_6\text{-}S,S')(\eta^2\text{-}RC_2R)_2]I$ (**49**) and (**50**) (R = Me, Ph). In total sixteen complexes were synthesised and characterised, however no suitable crystals were grown for X-ray crystallography. The complexes (**37**), (**38**), (**41**) and (**42**) all provide good simple models of the active site of nitrogenase in particular the molybdenum complexes (**41**) and (**42**). The inclusion of an iron-sulphur cluster in the complexes makes them more realistic as simple models of the enzymes active site. The spectroscopic data, detailed in **chapter five** suggests a seven-coordinate structure with an intact cluster for complexes (**35**) to (**44**). It is most likely, the cluster is bound bidentately to the metal atom *via* the two top so called "handle" sulphur atoms. Similarly, with the bis(alkyne) complexes (**49**) and (**50**) the cluster is most likely bound to the tungsten atoms in the same fashion. Complexes (**49**) and (**50**) are again good simple models for the active site of nitrogenase, in many ways more realistic than the complexes previously described, as they include the alkyne ligand which would be the substrate, undergoing reduction, in the enzyme itself.

7.2 SCOPE FOR FURTHER WORK

The main objective of this work has been achieved, in the synthesis and characterisation of fifty new molybdenum(II) and tungsten(II) complexes, containing several different types of sulphur donor ligand. There are many possibilities for further reactions involving any of the complexes described within this thesis. The aim of further reactions would be to synthesise and characterise new complexes, of molybdenum or tungsten, which more closely mimic the active site of the enzyme nitrogenase.

The complex [MoI(CO){[9]aneS$_3$-*S,S',S''*}(η^2-PhC$_2$Ph)]I (**32**), described in **Chapter four**, has a molybdenum atom bound to three sulphur atoms. It may be possible to metathesise the iodide for an oxygen or nitrogen donor ligand. The presence of the strongly bound carbonyl ligand may inhibit the ability of the complex to react further and hence more closely model the active site. The complex [WI{ttob-*S,S',S''*}(η^2-PhC$_2$Ph)$_2$]I$_3$ (**23**) does not contain a carbonyl ligand and it is important that further efforts to devise a rational synthesis are made. Also more reactions of the complex [WI$_2$(CO){MeS(CH$_2$)$_2$S(CH$_2$)$_2$SMe-*S,S'*}(η^2-PhC$_2$Ph)] (**19**) should be carried out due to it's ability to bind to other metal centres, including iron, and give bimetallic complexes. It may also be possible to synthesise a similar complex with molybdenum as the central atom.

The complexes described in **Chapter five** probably are the closest to the environment within the active site of nitrogenase. It is important to continue the investigation of the reaction of iron-sulphur clusters with complexes of molybdenum and, for comparison, tungsten. It would be interesting to investigate the reactions of iron suphur clusters which are able to bind to transition-metal centres *via* three sulphur atoms as is seen in the active site of the enzyme. The complexes [MoI(SAr)(CO)$_3$(Fe$_4$Cp$_4$S$_6$-*S,S'*)] (**41**) and (**42**) may further react with anionic oxygen or nitrogen donor ligands in order to give molybdenum-sulphur-oxygen or molybdenum-sulphur-nitrogen complexes containing the "basket" cluster. **Chapter two** has shown acetylacetonato ligands to readily to both molybdenum(II) and tungsten(II). It may be possible to introduce the acetylacetonato ligands to the complexes [MI$_2$(CO)$_3$(Fe$_4$Cp$_4$S$_6$-*S,S'*)] (**35**) and (**36**) (M = Mo, W), to give complexes which have two sulphurs and two oxygens attached to the metal centre.

It would also be interesting to carry out cyclic voltammetry investigations of the complexes prepared along with further characterisation such as FAB or plasma mass spectrometry. Further NMR data, at low temperatures, may also give more

information about the numerous structurally characterised complexes described in **Chapters two to five**.

Lastly, it is hoped that the information detailed in this work will further advance the studies into and the understanding of the enzyme nitrogenase.

References.

References

1. F. A. Cotton and G. Wilkinson, *Advanced Inorganic Chemistry*, 5th Ed., p.804, Wiley Interscience.
2. M. P. Coughlan, *Molybdenum-Containing Enzymes*. Oxford; Pergamon, 1980.
3. T. G. Spiro, *Molybdenum Enzymes*. New York: Wiley Interscience, 1985.
4. V. Rajagopalan, in *Biochemistry of the Elements* (E. Frieden, ed.) Plenum Press, New York, NY, 1981, p.149.
5. . R. H. Crabtree, *The Organometallic Chemistry of the Transition Metals*, Wiley Interscience.
6. *Inorganic Chemistry (S343), Block 7, Nitrogen Fixation*. The Open University Press, p.5.
7. B. K. Burgess, *Chem. Rev.*, 1990, **90**, 1377.
8. R. H. Holm, S. Ciurli and J. A. Weigel, *Prog. Inorg. Chem.*, 1990, **38**, 1.
9. W. H. Orme-Johnson, *Ann. Rev. Biophys. Chem.*, 1985, **14**, 419.
10. R. R. Eady, in *Nitrogen Fixation, Vol.4, Molecular Biology* (W. J. Broughton and A. Puhler, eds.), Clarendon Press, Oxford, 1986, p.1.
11. B. E. Smith, and R. R. Eady, *Eur. J. Biochem.*, 1992, **205**, 1.
12. T. Bolin, A. E. Ronco, L. E. Mortenson, T. V. Morgan, M. Williamson and N. H. Xuong, in *Nitrogen Fixation: Objectives and Achievments* (P. M. Gresshoff, L. E. Roth, G. Stacey and W. E. Newton, eds.) Chapman and Hall, London, 1990, p.117.
13. J. Kim and D. C. Rees, *Science*, 1992, **257**, 1677.
14. M. K. Chan, J. Kim and D. C. Rees, *Science*, 1993, **260**, 792.
15. R. R. Eady and G. J. Leigh, *J. Chem. Soc., Dalton Trans.*, 1994, 2739.

16. M. W. W. Adams, *Biochem. Biophys. Acta*, 1990, **1020**, 115.

17. M. M. Georgiadis, H. Komiya, P. Chakrabati, D. Woo, J. J. Kornuc and D. C. Rees, *Science*, 1992, **257**, 1653.

18. J. Meyer, J. Gaillard and J. M. Moulis, *Biochemistry*, 1988, **27**, 6150.

19. J. B. Howard, R. Davis, B. Moldenhauer, V. L. Cash and D. Dean, *J. Biol. Chem.*, 1989, **264**, 11270.

20. R. N. F. Thorneley and D. J. Lowe, *Biochem. J.*, 1983, **215**, 393.

21. D. J. Lowe and R. N. F. Thorneley, *Biochem. J.*, 1984, **224**, 895.

22. R. N. F. Thorneley, *Nitrogen Fixation: Objectives and Achievments* (P. M. Gresshoff, L. E. Roth, G. Stacey and W. E. Newton, eds.) Chapman and Hall, London, 1990, p.103.

23. R. N. F. Thorneley and D. J. Lowe, *Molybdenum Enzymes* (T. G. Spiro ed.) Wiley and Sons, New York, 1985, p.221.

24. H. L. Nigam, R. S. Nyholm and M. H. B. Stoddard, *J. Chem. Soc.*, 1960, 1806.

25. M. W. Anker, R. Colton and I. B. Tomkins, *Pure Appl. Chem.*, 1968, 18, 23.

26. R. Colton, *Coord. Chem, Rev.*, 1971, **6**, 269

27. R. Colton and I. B. Tomkins, *Aust. J. Chem.*, 1966, **19**, 1143.

28. R. Colton and I. B. Tomkins, *Aust. J. Chem.*, 1966, **19**, 1519.

29. M. W. Anker, R. Colton and I. B. Tomkins, *Aust. J. Chem.*, 1967, **20**, 9.

30. F. A. Cotton, L. R. Flavello and J. H. Meadows, *Inorg. Chem.*, 1985, **24**, 514.

31. R. Colton and C. J. Commons, *Aust. J. Chem.*, 1973, **26**, 1493.

32. R. Colton and I. B. Tomkins, *Aust. J. Chem.*, 1967, **20**, 13.

33. R. Colton, G. R. Scollary and I. B. Tomkins, *Aust. J. Chem.*, 1968, **21**, 15.

34. M. W. Anker, R. Colton and I. B. Tomkins, *Aust. J. Chem.*, 1968, **21**, 1143.

35. R. Colton and C. J. Rix, *Aust. J. Chem.*, 1968, **21**, 1115.

36. M. W. Anker, R. Colton and I. B. Tomkins, *Aust. J. Chem.*, 1968, **21**, 1159.

37. R. Colton and G. R. Scollary, *Aust. J. Chem.*, 1968, **21**, 1427.

38. R. Colton and G. R. Scollary, *Aust. J. Chem.*, 1968, **21**, 1435.

39. J. A. Bowden and R. Colton, *Aust. J. Chem.*, 1968, **21**, 2657.

40. M. W. Anker, R. Colton C. J. Rix and I. B. Tomkins, *Aust. J. Chem.*, 1969, **22**, 1341.

41. R. Colton and C. J. Rix, *Aust. J. Chem.*, 1969, **22**, 2535.

42. R. Colton and C. J. Rix, *Aust. J. Chem.*, 1970, **23**, 441.

43. M. W. Anker and R. Colton, *Aust. J. Chem.*, 1971, **24**, 2223.

44. J. A. Bowden and R. Colton, *Aust. J. Chem.*, 1972, **25**, 17.

45. J. A. Bowden, R. Colton and C. J. Commons, *Aust. J. Chem.*, 1972, **25**, 1993.

46. R. Colton and P. Panagiotidou, *Aust. J. Chem.*, 1987, **40**, 13.

47. M. G. B. Drew, *Prog. Inorg. Chem.*, 1977, **23**, 67.

48. M. Mélink and P. Sharrock, *Coord. Chem. Rev.*, 1985, **65**, 49.

49. D. P. Tate, W. R. Knipple and J. M. Augl, *Inorg. Chem.*, 1962, **1**, 433.

50. P. K. Baker, S. G. Fraser and E. M. Keys, *J. Organomet. Chem.*, 1986, **309**, 319.

51. M. G. B. Drew, P. K. Baker, E. M. Armstrong and S. G. Fraser, *Polyhedron*, 1988, 7, 245.

52. P. K. Baker, Adv. Organomet. Chem., 1996, **40**, 45.

53. P. K. Baker and D. ap. Kendrick, *J. Coord. Chem.*, 1988, **17**, 355.

54. P. K. Baker and D. ap. Kendrick, *Inorg. Chim. Acta*, 1990, **174**, 119.

55. P. K. Baker and D. ap. Kendrick, *J. Organomet. Chem.*, 1991, **411**, 215.

56. P. K. Baker and S. G. Fraser, *Polyhedron*, 1987, **6**, 2081.

57. P. K. Baker, S. D. Harris, M. C. Durrant, D. L. Hughes and R. L. Richards, *J. Chem. Soc., Dalton Trans.*, 1994, 1401.

58. A. Davison and D. L. Reger, *Inorg. Chem.*, 1971, **10**, 1967.

59. P. K. Baker, S. D. Harris, M. C. Durrant, D. L. Hughes and R. L. Richards, *Polyhedron*, 1996, **15**, 3595.

60. P. K. Baker, S. J. Coles, S. D. Harris, M. C. Durrant, D. L. Hughes and R. L. Richards, *J. Chem. Soc., Dalton Trans.*, 1996, 4003.

61. M. C. Durrant, D. L. Hughes, R. L. Richards, P. K. Baker and S. D. Harris, *J. Chem. Soc., Dalton Trans.*, 1992, 3399.

62. P. K. Baker, M. C. Durrant, B. Goerdt, S. D. Harris, D. L. Hughes and R. L. Richards, *J. Organomet. Chem.*, 1994, **469**, C22.

63. P. K. Baker, M. C. Durrant, S. D. Harris, D. L. Hughes and R. L. Richards, *J. Chem. Soc., Dalton Trans.*, 1997, 509.

64. P. K. Baker and S. G. Fraser, *Transition-Met. Chem.*, 1986, **11**, 273.

65. P. K. Baker, S. G. Fraser and D. ap. Kendrick, *J. Chem. Soc., Dalton Trans.*, 1991, 131.

66. P. K. Baker and S. G. Fraser, *Synth. React. Inorg.Met-Org. Chem.*, 1987, **17**, 371.

67. P. K. Baker and K. R. Flower, *J. Coord. Chem.*, 1987, **15**, 333.

68. E. W. Abel, M. A. Bennett and G. Wilkinson, *J. Chem. Soc.*, 1959, 2323.

69. A. J. Deeming, K. I. Hardcastle and M. Nafees Meah, *J. Chem. Soc., Dalton Trans.*, 1988, 227.

70. A. J. Deeming, M. Nafees Meah, N. P. Randle and K. I. Hardcastle *J. Chem. Soc., Dalton Trans.*, 1989, 2211.

71. N. Zhang, S. R. Wilson and P. A. Shapely, *Organometallics*, 1988, **7**, 1126.

72. A. Casineiras, W. Hiller, J. Strahle, J. Bravo, J. S. Casas, M. Gayoso and J. Sordo, *J. Chem. Soc., Dalton Trans.*, 1986, 1945.

73. A. J. Deeming, M. Karim and N. I. Powell, *J. Chem. Soc., Dalton Trans.*, 1990, 2321.

74. P. K. Baker, M. E. Harman, S. Hughes, M. B. Hursthouse and K. M. A. Malik, *J. Organomet. Chem.*, 1995, **498**, 257.

75. Y. J. -J. Chen, R. O. Yelton and I. B. Tomkins, *Inorg. Chim. Acta*, 1977, **22**, 249.

76. J. L. Templeton and B. C. Ward, *J. Am. Chem. Soc.*, 1980, **102**, 6568.

77. J. L. Templeton and B. C. Ward, *Organometallics*, 1982, **1**, 1007.

78. J. A. Brooomhead and C. J. Young, *Aust. J. Chem.*, 1982, **35**, 277.

79. P. K. Baker and S. G. Fraser, *Trans. Met. Chem. (Weinheihm)*, 1986, **11**, 273.

80. B. Zhaung, L. Huang, L. He, Y. Yang and J. Lu, *Inorg. Chim. Acta*, 1988, **145**, 225.

81. J. L. Dilworth, "*Sulfur- Its significance in the chemistry of the geo-, bio- and cosmosphere and technology*", 1984.

82. L. Carlton, J. L. Davidson, G. Vasapollo, G. Douglas and K. M. Muir, *J. Chem. Soc., Dalton Trans.*, 1993, 3341.

83. V. Riera, F. J. Arnaiz and G. G. Herbosa, *J. Organomet. Chem.*, 1986, **315**, 51.

84. D. C. Brower, P. B. Winston, T. L. Tonker and J. L. Templeton., *Inorg. Chem.*, 1986, **25**, 2883.

85. W. H. Batschelet, R. D. Archer and D. R. Whitcomb, *Inorg. Chem.*, 1979, **18**, 48.

86. R. O. Day, W. H. Batschelet and R. D. Archer, *Inorg. Chem.*, 1980, **19**, 2113.

87. P. K. Baker and D. ap Kendrick, *Polyhedron,* 1991, **10**, 433.

88. P. K. Baker, A. I. Clark, M. M. Meehan, E. E. Parker, A. E. Underhill, M. G. B. Drew, M. C. Durrant and R. L. Richards, Transition-met. Chem., In press, 1997.

89. T. E. Burrow, D. L. Hughes, A. J. Lough, M. J. Maguire, R. H. Morris and R. L. Richards, *J. Chem. Soc., Dalton Trans.*, 1995, 1315.

90. P. Kubacek and R. Hoffmann, *J. Am. Chem. Soc.*, 1981, **103**, 4320.

91. E. W. Abel, K. G. Orrell, G. D. King, G. M. Pring and V. Sik, *Polyhedron*, 1983, **2**, 1117.

92. E. W. Abel, K. G. Orrell and S. K. Bhargava, *Prog. Inorg. Chem.,* 1984, **32**, 1.

93. G. R. Dobson and J. E. Cortes, *Inorg. Chem.*, 1989, **28**, 539.

94. H. H. Awad, C. B. Dobson, G. R. Dobson, J. G. Leipoldt, H. E. Wood, R. van Eldik and K. Schneider, *Inorg. Chem.*, 1989, **28**, 1654.

95. E. W. Abel, D. E. Badgen, K. G. Orrell, I. Moss and V. Sik, *J. Organomet. Chem.,* 1989, **362**, 105.

96. E. W. Abel, K. G. Orrell, I. Moss and V. Sik, *J. Organomet. Chem.,* 1987, **326**, 187.

97. P. S. Braterman, V. A. Wilson and K. K. Joshi, *J. Chem. Soc.*, (**A**), 1971, 191.

98. S. R. Cooper, *Acc. Chem. Res.*, 1988, **21**, 141.

99. M. Schröder, *Pure Appl. Chem.*, 1988, **60**, 517.

100. M. T. Ashby and D. L. Lichtenberger, *Inorg. Chem.*, 1985, **24**, 636.

101. H. J. Kim, Y. Do, H. W. Lee, J. H. Jeong and Y. S. Sohn, *Bull. Korean Chem. Soc.*, 1991, **12**, 257.

102. R. S. Glass, G. S. Wilson and W. N. Setzer, *J. Am. Chem. Soc.*, 1980, **102**, 5068.

103. B. de Groot and S. Loeb, *Inorg. Chem.*, 1990, **29**, 4084.

104. P. K. Baker, M. B. Hursthouse, A. I. Karulov, A. J. Lavery, K. M. A. Malik, D. J. Muldoon and A. Shawcross, *J. Chem. Soc., Dalton Trans.*, 1994, 3493.

105. E. V. Bell and G. M. Bennett, *J. Chem. Soc.,* 1928, 3190.

106. S. D. Harris, PhD. Thesis, 1995, 185.

107. M. T. Ashby, J. H. Enemark, D. L. Lichtenberger and R. B. Ortega, *Inorg. Chem.*, 1986, **25**, 3154.

108. J. Butler and R. M. Kellog, *J. Org. Chem.*, 1981, **46**, 4481.

109. S. L. Templeton, *Adv. Organamet. Chem.*, 1991, **32**, 227.

110. S. Otsuka, A. Nakamura and H. Minamida, *J. Chem. Soc., Chem. Commun.*, **1969**, 1148.

111. J. L. Templeton, R. S. Herrick and J. R. Morrow, *Organometallics*, 1984, **3**, 535.

112. P. B. Winston, S. J. N.Burgamayer, T. L. Tonker and J. L. Templeton, *Organometallics*, 1986, **5**, 107.

113. P. Umland and H. Vahrenkamp, *Chem.Ber.*, 1982, **115**, 3580.

114. J. L. Davidson and D. W. A.Sharp, *J.Chem.Soc., Dalton Trans.*,1975, 2531.

115. P. S. Braterman, J. L. Davidson and D. W. A.Sharp, *J. Chem. Soc., Dalton Trans.*, 1976, 241.

116. J. L. Davidson, M. Green, D. W. A. Sharp, F. G. A. Stone and A. J. Welch, *J. Chem. Soc., Chem. Commun.*, 1974, 706.

117. J. L. Davidson, M. Green, F. G. A. Stone and A. J. Welch, *J. Chem. Soc., Dalton Trans.*, 1976, 738.

118. E. M. Armstrong, P. K. Baker, and S. G. Fraser, *J. Chem. Res.*, 1988,(s),52, *J. Chem. Res.*, 1988,(m), 410.

119. E. M. Armstrong, P. K. Baker and M. G. B. Drew, *Organometallics*, 1988, **7**, 319.

120. P. K. Baker, D. J. Muldoon, A. J. Lavery and A. Shawcross, *Polyhedron*, 1994, **13**, 2915.

121. P. K. Baker, A. Bury and K. R. FLower, *Polyhedron*, 1989, **8**, 2587.

122. P. K. Baker and D. ap Kendrick, *Polyhedron*, 1991, **10**, 2519.

123. P. K. Baker and D. ap Kendrick, *J. Chem. Soc., Dalton Trans.*, 1993, 1039.

124. J. L. Davidson, G. Vaspollo, J. C. Millar and K. W. Muir, *J.Chem.Soc., Dalton Trans.*, 1987, 2165.

125. B. J. Brisdon, A. G. W. Hodson, M.F.Mahon, K.C.Molloy and R. A. Walton, *Inorg.Chem.*, 1990, **29**, 2701.

126. A. Mayr and C. M. Bastos, *J.Chem.Soc.*, 1990, **112**, 7797.

127. E. M. Armstrong, P. K. Baker, and M. G. B.Drew, *J.Organomet.Chem.*, 1987, **336**, 377.

128. E. M. Armstrong, P. K. Baker, T. Callow, K. R. Flower, P. D. Jackson and L. M. Severs, *J.Organomet.Chem.*, 1992, **434**, 321.

129. E. M. Armstrong and P. K. Baker, *Inorg.Chim.Acta*, 1988, **141**, 17.

130. P. K. Baker, M. G. B. Drew, S. Edge and S. D. Ridyard, *J. Organomet. Chem.*, 1991, **409**, 207.

131. P. K. Baker, G . A.Cartwright, P. D. Jackson, K. R. Flower,N. Galeatti and L. M. Severs, *Polyhedron*, 1992, **11**, 1043.

132. P. K. Baker and S. D. Ridyard, *Synth. Read .Inorg. Met.-Org. Chem.*, 1995, **24**, 345.

133. P. K.Baker, E. M. Armstrong and M. G. B.Drew, *Inorg.Chem.*, 1988, **27**, 2287.

134. P. K. Baker and E. M. Armstrong, *Polyhedron*, 1988, **7**, 63.

135. E. M. Armstrong and P. K. Baker, *Synth. Read. Inorg. Met.-Org. Chem.*, 1988, **18**, 1.

136. E. M. Armstrong, P. K. Baker, M. E. Harman and M. B. Hursthouse, *J. Chem. Soc., Dalton Trans.*, 1989, 295.

137. P. K. Baker, S. J.Coles, M. B. Hursthouse, M. M. Meehan and S. D. Ridyard, *J. Organomet. Chem.*, 1995, **503**, C8.

138. P. K. Baker and S. D. Ridyard, *Polyhedron*, 1993, **12**, 915.

139. P. K. Baker, P. D . Jackson and M. G. B. Drew, *J. Chem. Soc., Dalton Trans.*, 1994, 37.

140. P. K. Baker, P. D. Jackson, M. E. Harman and M. B. Hursthouse, *J. Organomet. Chem.*, 1994, **468**, 171.

141. E. M. Armstrong, P. K. Baker, K. R. Flower and M. G. B. Drew, *J. Chem. Soc., Dalton Trans.*, 1990, 2535.

142. A. D. Gelman, *Compt. Rend. Acad. Sci.*, USSR., 1934, **24**, 549.

143. M. J. S.Dewar, *Bull. Soc. Chem. France*, 1951, **18**, C79.

144. J. Chatt and L. H. Duncanson, *J. Chem. Soc.*, 1953, 2939.

145. J. H. Nelson and H. B. Janasser, *Coord. Chem. Rev.*, 1979, **6**, 67.

146. P. K. Baker, A. I. Clark, S. J. Coles, M. B. Hursthouse and R. L. Richards, *J. Organomet. Chem.*, 1996, **518**, 235-237.

147. J. L. Templeton and B. C. Ward, *J. Am. Chem. Soc.*, 1980, **102**, 3288.

148. J. M. Berg and R. H. Holm , in *Iron- Sulfur Proteins* , 1982 , Vol. 4 , T. G. Spiro , Ed. , Wiley- Interscience , New York , **1.**

149. J. J. Mayerle, S. E. Denmark, B. V. Depampailis, J. A. Ibers and R. H. Holm, *J. Am. Chem. Soc.*, 1975, **97**, 1032.

150. M. A. Bobrik, K. O. Hodgson and R. H. Holm, *Inorg. Chem.*, 1977, **16,** 1851.

151. W. Saak and S. Phol, *Z. Naturforsch.*, 1985, **40b**, 1105.

152. A. Salifoglou, A. Simopoulos, A. Kostikas, W. R. Dunham, M. G. Kanatzidis and D. Coucouvanis, *Inorg. Chem.,* 1988, **27**, 3394.

153. T. Tsukihara, K. Fukuyama, M. Nakamura, Y. Katsube, N. Tanaku, M. Kakudo, K. Wada, T. Hase and H. Matsubara *J. Biochem. (Tokyo)*, 1981. **90**, 1763.

154. T. Tuskihara, K. Fukyuama, and Y. Katsube, in *Iron- Sulpher Protein Research;* 1986. H. Matsubara, Y. Katsube and K. Wada, Eds., Japan Scientific Societies Press, Tokyo. pp. 59- 68.

155. J. L. Sussman, J. H. Brown, and M. Shoman, in *Iron- Sulpher Protein Research;* 1986. H Matsubara, Y. Katsube and K. Wada, Eds., Japan Scientific Societies Press, Tokyo. pp. 69- 82.

156. K. S. Hagen, A. D. Watson and R. H. Holm , *J. Am. Chem. Soc.,* 1983, **105**, 3905.

157. G. H. Stout, S. Turley, L. Sieker and L. H. Jensen , *Proc. Natl. Acad. Sci.,* 1988, **85**, 1020.

158. C. R. Kissinger, E. T. Adman, L. C. Sieker and L. H. Jenson, *J. Am. Chem. Soc.*, 1988, **110**, 8721.

159. C. D. Stout, *J. Biol. Chem.*, 1988, **263**, 9256.

160. C. D. Stout, *J. Mol. Biol.*, 1989, **205**, 545.

161. C. R. Kissinger, E.T. Adman, L. C. Sieker, L. H. Jensen and J. Legall, *FEBS Lett.*, 1989, **244**, 447.

162. B. À. Averill, T. Herskovitz, R. H. Holm and J. A. Ibers, *J. Am. Chem. Soc.*, 1973, **95**, 3523.

163. L. Que. Jr., J. A. Ibers and R. H. Holm, *J. Am. Chem. Soc.*, 1974, **96**, 4168.

164. M. A. Bobrik, E. J. Laskowski, R. W. Johnson, W. O. Gillum, J. M. Berg, K. O. Hodgson and R. H. Holm, *Inorg. Chem.*, 1978, **17**, 1402.

165. P. K. Mascharak, K. S. Hagen, J. T. Spence and R. H. Holm, *Ignorg. Chim. Acta* , 1983, **80**, 157.

166. G. Christou, C. D. Garner, M. G. B. Drew and R. Cammack , *J. Chem. Soc. Dalton Trans.*, 1981, 1550.

167. W.E. Cleland, D. A. Holtman, M. Sabat, J. A . Ibers, G. C. Defotis and B. A. Averill, *J. Am. Chem. Soc.*, 1983, **105,** 6021.

168. R. E. Johnson, G. C. Papaefthymiou, R. B. Frankel and R. H. Holm, *J. Am. Chem. Soc.*, 1983, **105,** 7280.

169. M. G. Kanatzidis, N. C. Baenziger, D. Coucouvanis, A. Simopoulos and A. Kostikas, *J. Am. Chem. Soc.*, 1984, **106**, 4500.

170. M. G. Kanatzidis, D. Coucouvanis, A. Simopoulos, A. Kostikas and V. Papaefthymiou, *J. Am. Chem. Soc.*, 1985, **107**, 4925.

171. A. Muller, N. Schladerbeck and H. Bögge, *Chimia*, 1985, **39**, 24.

172. T. J. Ollerenshae, C. D. Garner, B. Odell and W. Clegg , *J. Am. Chem. Soc. Dalton Trans.*, 1985, 2161.

173. N. Ueyama, T. Sugawara, M. Fuji, A. Nakamura and N. Yasuoka, *Chem. Lett.*, 1985, 175.

174. W. Cen, and H. Liu , *Jiegou Huaxue (J. Struct. Chem.)*, 1986, **5**, 203.

175. J. Gloux, P. Gloux, H. Hendriks and G. Ruis, *J. Am . Chem. Soc.*, 1987. **109**, 3220.

176. A. Muller, N. Schladerbeck and H. Bögge, *J. Chem. Soc. Chem. Commun.*, 1987, 35.

177. S. Pohl and W. Saak, *Z. Naturforsch.*, 1988, **43b**, 457.

178. S. Rutchik, S. Kim and M. A. Walters, *Inorg. Chem.*, 1988, **27**, 1513.

179. D. T. P. Stack and R. H. Holm, *J. Am. Chem. Soc.*, 2546, **110**, 2484.

180. T. O' Sullivan and M. M. Millar, *J. Am .Chem. Soc.*, 1985, **107**, 4096.

181. E. J. Laskowski, R. B. Frankel, W. O. Gillum, G. C. Papaefthymiou, J. Renaud, J. A. Ibers and R. H. Holm, *J. Am. Chem. Soc.*, 1985, **100,** 5322.

182. J. M. Berg, K. O. Hodgson and R. H. Holm, *J. Am. Chem. Soc.*, 1979, **101**, 4586.

183. W. D. Stephan, G. C. Papaefthymiou, R. B. Frankel and R H. Holm, *Inorg Chem.*, 1983, **22**, 1550.

184. K. S. Hagen, A. D. Watson and R. H. Holm, *Inorg. Chem.*, 1984, **23**, 2984.

185. M. J. Carney, G. C. Papaefthymiou, M. A. Whitener, K. Spartalian, R. B. Frankel and R. H. Holm, *Inorg. Chem.*, 1988, **27**, 346.

186. M. J. Carney, G. C. Papaefthymiou, K. Spartalian, R. B. Frankel and R. H. Holm, *J. Am. Chem. Soc.*, 1988, **110,** 6048.

187. M. J. Carney, G. C. Papaefthymiou, R. B. Frankel and R. H. Holm, *Inorg. Chem.*, 1989. **28,** 1479.

188. C. W. Carter, Jr. , J. Kraut, S. T. Freer, R. A. Halden, L C. Sieker, E. Adman and L. H. Jenson, *Proc. Natl. Acad. Sci. USA.*, 1972, **69**, 3526.

189. C. W. Carter, Jr., J Kraut, S. T. Freer and R. A. Alden, *J. Biol. Chem.*, 1974, **249**, 6339.

190, E. T. Adman, L. C. Sieker and L. H. Jenson, *J. Biol. Chem.* 1973, **248**, 3987.

191. K. Fukuyama, Y. Nagahara, T. Tsukihara, Y. Katsube, T. Hase and H. Matsubarâ, *J. Mol. Biol.*, 1988, **199**, 183.

192. C. D. Stout, in *Iron- Sulpher Proteins*, 1982. T. G. Spiro, Ed., Wiley-Interscience, New York. **3**.

193. M. G. Kanatzidis, W. R. Hagen, W. R. Dunham, R. K. Lester and D. Coucouvanis, *J. Am. Chem. Soc.*, 1985, **107,** 953.

194. M. G. Kanatzidis, A. Salifoglou and D. Coucouvanis, *Inorg. Chem.*, 1986, **25**, 2460.

195. W. Saak, G. Henkel and S. Pohl, *Agnew Chem. Int. Ed. Engl.*, 1984, **23,** 150.

196. B. S. Snyder, M. S. Reynolds, I. Noda and R. H. Holm, *Inorg. Chem.*, 1988, **27,** 1398.

197. B. S. Snyder and R. H. Holm, *Inorg. Chem.,* 1988, **27**, 2339.

198. M. S. Reynolds and R. H. Holm, *Inorg. Chem.*, 1988, **27,** 4494.

199. T. E. Wolff, J. M. Berg, C. Warrick, K. O. Hodgson, R. H. Holm and R. B. Frankel, *J. Am. Chem. Soc.*, 1978, **100**, 4630.

200. M.J. Carney, J. A. Kovacs, Y. -P. Zhang, G. C. Papaefthymiou, K. Spartalian, R. B. Frankel and R. H. Holm, *Inorg. Chem.*, 1987, **26**, 719.

201. D. Coucouvanis, S. A. Al-Ahmad, A. Salifoglou, V. Papaefthymiou, A. Kostikas and A. Simopoulos, *J. Am. Chem. Soc.*, 1992, **114**, 2472.

202. J. -J. Girerd, G.C. Papaefthymiou, A. D. Watson, E. Gamp, K. S. Hagen, N. Edelstein, R.D. Frankel and R. H. Holm, *J. Am. Chem. Soc.*, 1984, **106**, 5941.

203. S. Ciurli and R. H. Holm, *Inorg. Chem.*, 1989, **28**, 1685.

204. J. Jordanov, H. M. J. Hendriks, N. Dupré, A. Viari, P. Vigny and G. Diakun, *Inorg. Chem.*, 1988, **27**, 2997.

205. K. A. Mitchell, *MSc. Dissertation University of Wales, Bangor*, 1993.

206. G. J. Kubas and P. Vergami, *Inorg. Chem.*, 1981, **20**, 2667.

207. W. Kabsch, *J. Appl. Cryst.*, 1988, **21**, 916.

208. Shelx86, G. M. Sheldrick, *Acta Cryst.*, 1990, **A46**, 467.

209. Shelx1, G. M. Sheldrick, program for crystal structure refinement., University of Göttingen.

APPENDIX 1.

TABLES
A1.1 to A1.4

Table 1. Crystal data and structure refinement for 1, 2, 3 and 4.

	(1)	(2)	(3)	(4)
Empirical formula	C26 H40 S2 P2 O2 W	C16 H34 Mo O2 P2 S2	C16 H34 O2 P2 S2 W	C16 H36 O2 P2 S2 W
Formula weight	694.5	480.4	568.34	570.36
Temperature (K)	293(2)	293(2)	293(2)	293(2)
Wavelength (Å)	0.71073	0.71073	0.71073	0.71073
Crystal system	monoclinic	tetragonal	tetragonal	tetragonal
Space group	$P2_1/a$	$P4_2$	$P4_2$	$P4_2$
Unit cell dimensions a/Å	10.402(9)	14.514(9)	14.343(9)	14.318(9)
b/Å	16.263(14)	14.514(9)	14.343(9)	14.318(9)
c/Å	10.029(8)	11.006(11)	10.900(11)	11.206(9)
β/°	112.69(1)	(90)	(90)	(90)
Volume	1565(2)	2319(3)	2242(3)	2297(3)
Z	2	4	4	4
Density (calculated) Mgm^{-3}	1.474	1.376	1.683	1.649
Absorption coefficient (mm^{-1})	3.945	0.889	5.486	5.355
F(000)	696	1000	1128	1136
Crystal size (mm)	0.25 * 0.25 * 0.30	0.35 * 0.15 * 0.20	0.35 * 0.25 * 0.25	0.20 * 0.25 * 0.25
() range for data collection	2.70 to 24.90	2.32 to 25.07	2.01 to 24.85	2.71 to 24.73

Index ranges		0<=h<=12, -19<=k<=19, -11<=l<=10	-14<=h<=14 -14<=k<=14 0<=l<=11	0<=h<=16 -16<=k<=16 -12<=l<=12	-16<=h<=16 -16<=k<=16 0<=l<=13
Reflections collected		4117	6423	6291	4499
Independent reflections (R(int)		2260(0.0655)	1868(0.0452)	3651(0.0572)	1944(0.0862)
Data / restraints / parameters		2260 / 0 / 155	1868 / 0 / 215	3651 / 0 / 215	1925 / 0 / 209
Goodness-of-fit on F^2		1.257	1.168	1.092	1.061
Weighting Scheme (a,b)*		0.0825, 42.247	0.0735, 1.7536	0.0304, 26.116	0.
Final R indices [I>2σ(I)]	R1	0.0915	0.0458	0.0497	0.0482
	wR2	0.2548	0.1114	0.1082	0.1170
R indices (all data)	R1	0.1008	0.0615	0.0621	0.0546
	wR2	0.2593	0.1221	0.1136	0.1331
Extinction coefficient		0.042(5)	0.016(2)	0.000(1)	0.0142(11)
Largest diff. peak and hole eÅ^{-3}		1.937, -1.227	0.677, -1.613	0.968, -0.835	1.170, -2.073

* Weighting scheme $w = 1/(\sigma^2(F_o^2) + (aP)^2 + bP)$, where $P = (F_o^2 + 2F_c^2)/3$

Table 2

Dimensions in the Metal Coordination Spheres of 1,2,3 and 4

(distances, A, angles, degrees)

Bond lengths [A] and angles [deg] for 1.

W(1)-C(61)	2.04(3)
W(1)-S(1)	2.402(5)
W(1)-P(3)	2.563(6)
C(61)-W(1)-S(1)	84.8(6)
C(61)-W(1)-P(3)	89.8(5)
S(1)-W(1)-P(3)	87.5(2)

Bond lengths [A] and angles [deg] for 2,3,4

	2 (M=Mo)	3 (M=W)	4 (M=W)
M(1)-C(3)	1.966(10)	1.922(13)	1.94(2)
M(1)-C(1)	1.973(10)	1.957(14)	1.99(2)
M(1)-S(5)	2.426(3)	2.389(4)	2.404(4)
M(1)-S(9)	2.430(3)	2.386(4)	2.409(4)
M(1)-P(21)	2.516(3)	2.485(4)	2.452(5)
M(1)-P(11)	2.517(3)	2.500(4)	2.497(5)
C(3)-M(1)-C(1)	105.7(4)	105.6(6)	105.3(7)
C(3)-M(1)-S(5)	94.0(3)	94.0(5)	90.0(5)
C(1)-M(1)-S(5)	146.2(3)	146.2(4)	147.2(4)
C(3)-M(1)-S(9)	147.2(3)	147.6(5)	149.3(5)
C(1)-M(1)-S(9)	93.3(3)	93.4(5)	89.5(4)
S(5)-M(1)-S(9)	83.76(9)	83.40(12)	91.50(13)
C(3)-M(1)-P(21)	79.2(3)	79.7(5)	80.0(5)
C(1)-M(1)-P(21)	77.0(3)	76.8(4)	74.3(4)
S(5)-M(1)-P(21)	134.63(11)	134.8(2)	137.8(2)
S(9)-M(1)-P(21)	79.33(9)	79.53(14)	78.32(14)
C(3)-M(1)-P(11)	76.6(3)	75.8(5)	75.5(5)
C(1)-M(1)-P(11)	78.9(3)	78.9(4)	78.5(4)
S(5)-M(1)-P(11)	79.30(9)	79.64(14)	77.7(2)
S(9)-M(1)-P(11)	134.31(11)	134.6(2)	134.7(2)
P(21)-M(1)-P(11)	139.52(8)	139.04(11)	136.74(11)

TABLES
A1.5 AND A1.6

Table 1. Crystal data and structure refinement for 1 and 2

Compound		$Mo(CO)_2(acac)(PEt_3)_2I$	$W(CO)_2(acac)(PEt_3)_2I$
Empirical formula		C19 H37 I Mo O4 P2	C19 H37 I W O4 P2
Formula weight		614.27	702.18
Temperature (K)		293(2)	293(2)
Wavelength (Å)		0.71073	0.71073
Crystal system		monoclinic	monoclinic
Space group		$P2_1/a$	$P2_1/n$
Unit cell dimensions	a(Å)	12.707(13)	16.749(14)
	b(Å)	15.691(14)	10.499(11)
	c(Å)	13.623(14)	16.793(14)
	β(deg)	103.46(1)	117.07(1)
Volume ($Å^3$)		2642	2630
Z		4	4
Density (calculated) Mg/m^3		1.545	1.774
Absorption coefficient mm^{-1}		1.805	5.708
F(000)		1232	1360
Crystal size mm		0.32 * 0.25 * 0.25	0.25 * 0.25 * 0.35
θ range for data collection(deg)		2.36 to 25.10	2.33 to 25.20
Index ranges		0<=h<=15, -18<=k<=18, -16<=l<=15	-20<=h<=19 0<=k<=11 -17<=l<=18

Reflections collected		8250	6263
Independent reflections [R(int)]		4587 [0.0635]	3768 [0.1019]
Weighting Scheme (a,b)*		0.165, 0.000	0.247, 0.000
Data / restraints / parameters		4582 / 0 / 253	3768/ 0 / 253
Goodness-of-fit on F^2		1.023	0.978
Final R indices [I>2σ(I)]	R1	0.0736	0.0935
	wR2	0.1862	0.2576
R indices (all data)	R1	0.0977	0.1822
	wR2	0.2064	0.3131
Extinction coefficient		0.027(2)	0.002(1)
Largest diff. peak and hole e.A^{-3}		3.173	2.959
		-1.976	-3.179

* Weighting scheme $w = 1/(\sigma^2(F_o^2) + (aP)^2 + bP)$, where $P = (F_o^2 + 2F_c^2)/3$

Table 3. Bond lengths [A] and angles [deg] for 1 and 2

	(1), M= Mo	(2), M = W
M(1)-C(100)	1.950(11)	1.94(3)
M(1)-C(200)	1.994(10)	1.96(3)
M(1)-O(21)	2.158(6)	2.14(2)
M(1)-O(25)	2.161(6)	2.15(2)
M(1)-P(1)	2.541(2)	2.524(7)
M(1)-P(2)	2.543(3)	2.564(7)
M(1)-I(2)	3.005(1)	3.029(3)
C(100)-M(1)-C(200)	102.8(4)	100.4(10)
C(100)-M(1)-O(21)	93.8(3)	101.3(7)
C(200)-M(1)-O(21)	139.2(3)	134.4(8)
C(100)-M(1)-O(25)	100.2(3)	101.0(8)
C(200)-M(1)-O(25)	131.2(4)	131.9(9)
O(21)-M(1)-O(25)	80.3(2)	81.7(6)
C(100)-M(1)-P(1)	79.9(3)	75.6(6)
C(200)-M(1)-P(1)	71.0(3)	72.4(7)
O(21)-M(1)-P(1)	149.4(2)	152.2(5)
O(25)-M(1)-P(1)	71.5(2)	72.0(5)
C(100)-M(1)-P(2)	80.7(3)	78.1(6)
C(200)-M(1)-P(2)	71.6(3)	73.9(7)
O(21)-M(1)-P(2)	74.8(2)	72.2(4)
O(25)-M(1)-P(2)	155.1(2)	153.0(5)
P(1)-M(1)-P(2)	132.43(8)	132.0(2)
C(100)-M(1)-I(2)	176.8(3)	177.1(5)
C(200)-M(1)-I(2)	78.5(3)	77.7(8)
O(21)-M(1)-I(2)	83.4(2)	81.5(5)
O(25)-M(1)-I(2)	80.9(2)	78.9(6)
P(1)-M(1)-I(2)	103.24(6)	101.7(2)
P(2)-M(1)-I(2)	97.02(6)	103.3(2)

TABLES
A1.7

Table 1. Crystal data and structure refinement for 1.

Empirical formula	C17 H14 Br2 O3 S2 W
Formula weight	674.07
Temperature	293(2) K
Wavelength	0.71073 A
Crystal system	monoclinic
Space group	P21/c
Unit cell dimensions	a = 12.438(12)A b = 13.162(12)A β = 106.11(1) deg. c = 12.728(12)A
Volume	2002(3) A^3
Z	4
Density (calculated)	2.237 Mg/m^3
Absorption coefficient	9.984 mm^-1
F(000)	1264
Crystal size	0.25 * 0.25 * 0.30 mm
Theta range for data collection	2.30 to 23.61 deg.
Index ranges	0<=h<=13, -14<=k<=14, -14<=l<=13
Reflections collected	3661
Independent reflections	2503 [R(int) = 0.0831]
Weighting Scheme (a,b)*	0.059, 52.08
Data / restraints / parameters	2503 / 0 / 212
Goodness-of-fit on F^2	1.079
Final R indices [I>2sigma(I)]	R1 = 0.0819, wR2 = 0.1941
R indices (all data)	R1 = 0.1124, wR2 = 0.2063
Largest diff. peak and hole	0.792 and -1.071 e.A^-3

* Weighting scheme $w = 1/(\sigma^2(F_o^2) + (aP)^2 + bP)$, where $P = (F_o^2 + 2F_c^2)/3$

Table 2. Atomic coordinates (x 10^4) and equivalent isotropic displacement parameters (A^2 x 10^3) for 1. U(eq) is defined as one third of the trace of the orthogonalized Uij tensor.

	x	y	z	U(eq)
W(1)	1931(1)	1334(1)	2716(1)	77(1)
Br(1)	-181(2)	1354(2)	1486(2)	86(1)
Br(2)	1220(2)	2145(2)	4285(2)	94(1)
C(1)	1475(26)	-1344(22)	2537(22)	103(9)
C(2)	1070(26)	-987(22)	1357(26)	107(9)
S(1)	1287(5)	-329(6)	3415(5)	84(2)
C(11)	2084(21)	-764(19)	4760(20)	82(7)
C(12)	1402(22)	-778(18)	5515(22)	84(7)
C(13)	2050(32)	-1137(28)	6519(30)	131(12)
C(14)	3098(27)	-1483(22)	6834(26)	101(9)
C(15)	3584(29)	-1472(30)	5991(31)	148(16)
C(16)	3139(20)	-1101(20)	4948(18)	79(7)
S(2)	1908(6)	115(5)	1146(6)	85(2)
C(21)	3220(18)	-479(17)	1179(17)	64(5)
C(22)	3433(23)	-690(17)	202(21)	82(7)
C(23)	4439(29)	-1098(24)	200(30)	118(10)
C(24)	5281(30)	-1209(29)	1097(26)	132(13)
C(25)	5234(23)	-942(19)	2159(26)	96(8)
C(26)	4007(20)	-528(20)	2062(21)	85(7)
C(100)	3201(31)	1729(29)	2178(29)	126(11)
O(100)	3904(15)	1981(15)	1813(15)	102(6)
C(200)	1704(20)	2829(21)	2388(21)	79(7)
O(200)	1543(20)	3644(15)	2105(19)	125(7)
C(300)	3193(17)	1233(16)	3842(17)	61(5)
O(300)	3981(15)	1176(14)	4743(15)	102(6)

Table 3. Bond lengths [A] and angles [deg] for 1.

W(1)-C(300)	1.81(2)
W(1)-C(100)	1.96(4)
W(1)-C(200)	2.01(3)
W(1)-S(2)	2.557(7)
W(1)-S(1)	2.573(7)
W(1)-Br(2)	2.626(3)
W(1)-Br(1)	2.659(4)
C(300)-W(1)-C(100)	71.9(12)
C(300)-W(1)-C(200)	106.0(10)
C(100)-W(1)-C(200)	75.4(13)
C(300)-W(1)-S(2)	113.0(7)
C(100)-W(1)-S(2)	74.2(11)
C(200)-W(1)-S(2)	118.7(7)
C(300)-W(1)-S(1)	87.0(7)
C(100)-W(1)-S(1)	134.8(11)
C(200)-W(1)-S(1)	149.7(7)
S(2)-W(1)-S(1)	78.4(2)
C(300)-W(1)-Br(2)	80.1(6)
C(100)-W(1)-Br(2)	129.2(11)
C(200)-W(1)-Br(2)	72.7(7)
S(2)-W(1)-Br(2)	156.5(2)
S(1)-W(1)-Br(2)	83.1(2)
C(300)-W(1)-Br(1)	164.4(6)
C(100)-W(1)-Br(1)	123.6(10)
C(200)-W(1)-Br(1)	79.0(7)
S(2)-W(1)-Br(1)	75.6(2)
S(1)-W(1)-Br(1)	82.0(2)
Br(2)-W(1)-Br(1)	87.58(11)
C(1)-C(2)	1.52(4)
C(1)-S(1)	1.80(3)
C(2)-S(2)	1.85(3)
S(1)-C(11)	1.82(2)
C(11)-C(16)	1.34(3)
C(11)-C(12)	1.45(3)
C(12)-C(13)	1.39(4)
C(13)-C(14)	1.33(4)
C(14)-C(15)	1.37(4)
C(15)-C(16)	1.38(4)
S(2)-C(21)	1.80(2)
C(21)-C(26)	1.27(3)
C(21)-C(22)	1.37(3)
C(22)-C(23)	1.36(4)
C(23)-C(24)	1.33(4)
C(24)-C(25)	1.41(4)
C(25)-C(26)	1.59(3)
C(100)-O(100)	1.15(4)
C(200)-O(200)	1.13(3)
C(300)-O(300)	1.29(2)
C(2)-C(1)-S(1)	109(2)
C(1)-C(2)-S(2)	110(2)
C(1)-S(1)-C(11)	102.8(12)
C(1)-S(1)-W(1)	108.1(9)
C(11)-S(1)-W(1)	117.0(9)
C(16)-C(11)-C(12)	127(2)
C(16)-C(11)-S(1)	121(2)
C(12)-C(11)-S(1)	111(2)
C(13)-C(12)-C(11)	108(3)

C(14)-C(13)-C(12)	131(4)
C(13)-C(14)-C(15)	112(3)
C(14)-C(15)-C(16)	128(3)
C(11)-C(16)-C(15)	114(2)
C(21)-S(2)-C(2)	101.6(13)
C(21)-S(2)-W(1)	116.2(8)
C(2)-S(2)-W(1)	105.3(10)
C(26)-C(21)-C(22)	120(2)
C(26)-C(21)-S(2)	121(2)
C(22)-C(21)-S(2)	118(2)
C(23)-C(22)-C(21)	119(3)
C(24)-C(23)-C(22)	123(3)
C(23)-C(24)-C(25)	124(3)
C(24)-C(25)-C(26)	108(3)
C(21)-C(26)-C(25)	125(2)
O(100)-C(100)-W(1)	176(3)
O(200)-C(200)-W(1)	174(2)
O(300)-C(300)-W(1)	171(2)

Table 4. Anisotropic displacement parameters (A^2 x 10^3) for 1.
The anisotropic displacement factor exponent takes the form:
-2 pi^2 [h^2 a*^2 U11 + ... + 2 h k a* b* U12]

	U11	U22	U33	U23	U13	U12
W(1)	78(1)	77(1)	79(1)	-1(1)	24(1)	-2(1)
Br(1)	82(2)	99(2)	77(2)	2(1)	22(1)	0(1)
Br(2)	99(2)	98(2)	86(2)	-14(2)	26(1)	11(2)
C(1)	113(22)	102(22)	88(19)	-11(17)	18(16)	-29(17)
C(2)	123(23)	91(20)	127(25)	6(19)	65(20)	-17(17)
S(1)	78(4)	93(5)	76(4)	9(4)	15(3)	-7(3)
C(11)	83(17)	82(18)	79(16)	3(14)	18(13)	30(13)
C(12)	92(17)	65(16)	98(18)	37(14)	32(15)	8(13)
C(13)	121(30)	147(33)	121(28)	-16(25)	25(23)	-10(24)
C(14)	105(23)	98(23)	93(20)	-5(17)	14(18)	-16(17)
C(15)	102(24)	200(42)	139(30)	89(30)	27(22)	-15(23)
C(16)	82(16)	115(21)	50(12)	-3(13)	33(11)	-5(14)
S(2)	101(5)	66(4)	97(5)	-1(4)	43(4)	-15(3)
C(21)	75(14)	65(14)	54(12)	1(11)	19(11)	7(11)
C(22)	113(20)	60(15)	87(17)	-25(13)	49(15)	6(13)
C(23)	135(29)	98(24)	128(27)	22(21)	48(24)	21(20)
C(24)	120(26)	182(37)	85(21)	3(23)	15(19)	50(25)
C(25)	101(19)	66(16)	130(25)	-20(17)	48(18)	5(14)
C(26)	85(17)	89(18)	79(17)	7(14)	18(14)	1(13)
O(100)	88(12)	116(15)	103(13)	-12(12)	27(11)	-9(11)
O(200)	170(21)	75(13)	136(18)	0(12)	54(15)	32(13)
O(300)	97(13)	96(14)	109(14)	-19(11)	23(11)	15(10)

Table 5. Hydrogen coordinates (x 10^4) and isotropic displacement parameters (A^2 x 10^3) for 1.

	x	y	z	U(eq)
H(1A)	2259(26)	-1531(22)	2712(22)	123
H(1B)	1051(26)	-1936(22)	2642(22)	123
H(2A)	287(26)	-797(22)	1186(26)	129
H(2B)	1141(26)	-1535(22)	871(26)	129
H(12)	656(22)	-581(18)	5356(22)	100
H(13)	1688(32)	-1136(28)	7068(30)	158
H(14)	3455(27)	-1703(22)	7538(26)	121
H(15)	4299(29)	-1748(30)	6140(31)	178
H(16)	3532(20)	-1085(20)	4424(18)	95
H(22)	2896(23)	-556(17)	-454(21)	99
H(23)	4541(29)	-1309(24)	-464(30)	142
H(24)	5947(30)	-1480(29)	1023(26)	158
H(25)	5815(23)	-997(19)	2799(26)	115
H(26)	3855(20)	-306(20)	2700(21)	102

TABLES
A1.8 TO A1.11

[$WI_2CO(S_3C_6)(PhC_2Ph)$]

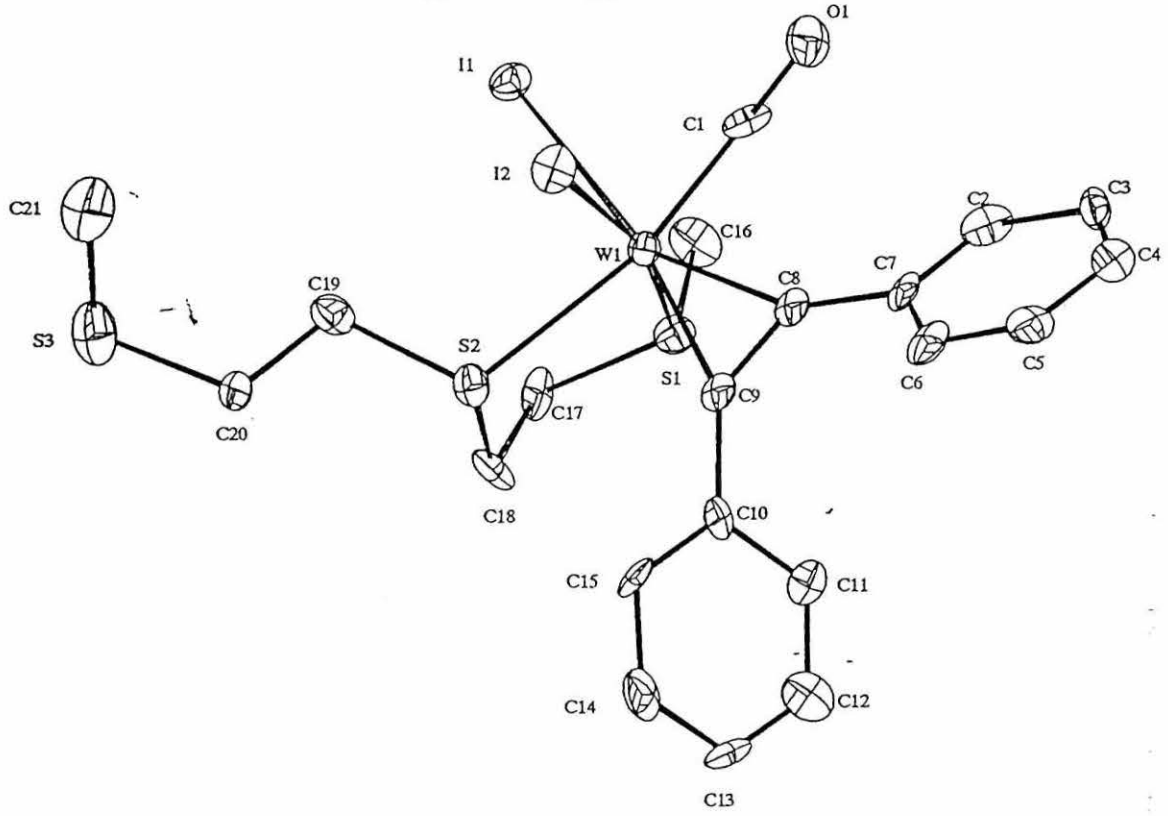

Identification code	94SRC207	Absorption coefficient	7.412 mm^{-1}
Empirical formula	$WI_2CO(S_3C_6)(PhC_2Ph)$	F(000)	1544
Formula weight	826.23	Crystal size	0.2 x 0.1 x 0.1 mm
Temperature	120(2) K	Theta range for data collection	2.41 to 22.76 deg.
Crystal system	Monoclinic	Index ranges	-6<=h<=8 -10<=k<=14 -23<=l<=22
Space group	$P2_1/c$		
Unit cell dimensions		Reflections collected	6633
a =	8.458(2) Å	Independent reflections	2830
b =	13.494(12) Å	R(int) =	0.0670
c =	22.03(3) Å	Absorption correction factors	0.875 / 1.094
α =	90.0 °	Data / parameters	2828 / 249
β =	99.48(8) °	Goodness-of-fit on F^2	0.790
γ =	90.0 °	Final R indices [I>2sigma(I)]	R_1=0.0349 wR_2=0.0684
Volume	2480(4) $Å^3$	R indices (all data)	R_1=0.0602 wR_2=0.0743
Z	4	Largest diff. peak and hole	1.208 and -0.742 $e.Å^{-3}$
Density (calculated)	2.213 Mg/m^3		

Ï

Table 1. Crystal data and structure refinement for 4, 10 and 16 .

		(4)	(10)	(16)
Empirical formula		C21 H24 O S3 W I2	C29 H22 Cl2 I2 Mo O3.5 S3	C40.166 H36.33 Cl0.33 I4 S3 W
Formula weight		826.23	842.75	1318.47
Temperature(K)		120(2)	293(2)	293(2)
Wavelength/Å		0.71069	0.71073	0.71073
Crystal system, space group		monoclinic, $P2_1/c$	monoclinic, C2/c	trigonal, P-3
Unit cell dimensions(Å,°)	a	8.458(2)	32.78(3)	23.80(2)
	b	13.494(12)	11.645(13)	23.80(2)
	c	22.03(3)	21.77(2)	12.999(13)
	β	99.48(8)	125.78(1)	(90)
Volume($Å^3$)		2480(4)	6742(12)	6379(11)
Z,		4,	8	6
Calculated Density (Mgm^{-3})		2.213	1.707	2.059
Absorption coefficient (mm-1)		7.412	2.586	5.815
F(000)		1544	3352	3702
Crystal size(mm)		0.11 * 0.11 *0.21	0.35 * 0.30 * 0.25	0.25*0.25*0.25
θ range for data collection(°)		2.44 to 22.76	2.89 to 25.05	2.32 to 24.95
Index ranges		-6<h<8 -10<k<14 -23<l<22	0<=h<=38, -12<=k<=13, -25<=l<=20	-28<=h<=28 -27<=k<=27 -15<=l<=15
Reflections collected		6633	8011	18293

Table 3. Bond lengths [A] and angles [deg] in the metal coordination sphere for 1.

W(1)-C(100)	2.09(2)
W(1)-C(7)	2.11(2)
W(1)-C(5)	2.117(18)
W(1)-C(8)	2.16(2)
W(1)-C(6)	2.19(2)
W(1)-N(4)	2.20(2)
W(1)-Br(3)	2.679(3)
W(1)-Br(2)	2.722(3)
C(100)-W(1)-C(7)	77.6(9)
C(100)-W(1)-C(5)	76.2(8)
C(7)-W(1)-C(5)	92.1(7)
C(100)-W(1)-C(8)	113.9(8)
C(7)-W(1)-C(8)	36.5(8)
C(5)-W(1)-C(8)	103.9(7)
C(100)-W(1)-C(6)	110.3(9)
C(7)-W(1)-C(6)	107.7(8)
C(5)-W(1)-C(6)	35.3(8)
C(8)-W(1)-C(6)	97.5(8)
C(100)-W(1)-N(4)	159.5(7)
C(7)-W(1)-N(4)	115.4(8)
C(5)-W(1)-N(4)	117.0(7)
C(8)-W(1)-N(4)	79.4(7)
C(6)-W(1)-N(4)	81.7(8)
C(100)-W(1)-Br(3)	81.3(6)
C(7)-W(1)-Br(3)	157.4(7)
C(5)-W(1)-Br(3)	90.6(4)
C(8)-W(1)-Br(3)	160.9(5)
C(6)-W(1)-Br(3)	87.0(5)
N(4)-W(1)-Br(3)	83.0(5)
C(100)-W(1)-Br(2)	80.5(6)
C(7)-W(1)-Br(2)	84.0(6)
C(5)-W(1)-Br(2)	156.7(5)
C(8)-W(1)-Br(2)	86.7(6)
C(6)-W(1)-Br(2)	165.2(6)
N(4)-W(1)-Br(2)	85.1(5)
Br(3)-W(1)-Br(2)	84.67(11)

Table 2. Atomic coordinates (x 10^4) and equivalent isotropic displacement parameters (A^2 x 10^3) for 1.
U(eq) is defined as one third of the trace of the orthogonalized Uij tensor.

	x	y	z	U(eq)
W(1)	6201(1)	1553(1)	1786(1)	40(1)
Br(2)	6276(1)	3191(2)	796(2)	61(1)
Br(3)	6706(1)	143(2)	1361(2)	62(1)
C(100)	5726(7)	880(2)	779(12)	45(5)
O(100)	5456(6)	584(16)	191(10)	70(5)
N(4)	6830(6)	2281(18)	2591(12)	54(5)
C(41)	7146(7)	2720(2)	3037(14)	57(6)
C(42)	7547(9)	3160(3)	3620(2)	90(10)
C(5)	5961(6)	0(16)	2131(10)	32(4)
C(6)	6324(7)	260(2)	2708(11)	53(6)
C(51)	5593(6)	-954(18)	1902(11)	37(4)
C(52)	5329(9)	-980(3)	2300(18)	80(8)
C(53)	4967(10)	-1790(3)	2040(2)	88(9)
C(54)	4882(11)	-2520(3)	1429(19)	88(9)
C(55)	5157(9)	-2550(3)	1067(18)	77(8)
C(56)	5511(7)	-1760(2)	1305(13)	52(5)
C(61)	6635(6)	-47(19)	3431(12)	44(5)
C(62)	6522(8)	-90(2)	4069(15)	60(6)
C(63)	6831(10)	-500(3)	4795(19)	84(8)
C(64)	7247(9)	-820(3)	4935(18)	74(7)
C(65)	7368(8)	-630(2)	4304(15)	59(6)
C(66)	7078(9)	-330(3)	3590(17)	73(7)
C(7)	5652(7)	2600(2)	1662(14)	51(5)
C(8)	5986(6)	3059(19)	2261(12)	42(5)
C(81)	5178(6)	2834(19)	1193(12)	42(5)
C(82)	5037(8)	4050(2)	922(15)	59(6)
C(83)	4597(9)	4290(3)	462(18)	79(8)
C(84)	4301(9)	3300(2)	307(16)	69(7)
C(85)	4440(8)	2120(3)	565(16)	66(7)
C(86)	4868(8)	1870(2)	987(15)	61(6)
C(91)	6139(7)	3920(2)	2905(14)	55(6)
C(92)	6064(9)	5190(3)	2733(19)	81(8)
C(93)	6219(12)	6070(4)	3350(2)	107(11)
C(94)	6433(10)	5630(3)	4070(2)	89(9)
C(95)	6518(11)	4470(3)	4240(2)	91(9)
C(96)	6375(8)	3580(2)	3633(15)	61(6)
C(11A)	7500	5780(9)	2500	180(3)
C(12A)a	7070(6)	6040(17)	2640(10)	230(8)
O(13A)a	6760(3)	6490(8)	1850(5)	160(3)
C(11B)a	7260(7)	7010(17)	1990(10)	290(10)
C(12B)a	7050(6)	6730(18)	2330(13)	220(7)
O(13B)a	6760(3)	6490(8)	1850(5)	160(3)

a 50% occupancy

Table 1. Crystal data and structure refinement for 1.

Identification code	$WBr_2(CO)(NCMe)(C_6H_5CCC_6H_5)_2, C_2H_5OH$
Empirical formula	C33 H29 Br2 N O W
Formula weight	8221.6
Temperature	293(2) K
Wavelength	0.71073Å
Crystal system, space group	monoclinic, C2/c
Unit cell dimensions	a = 33.86(3)Å b = 10.993(13)Å. c = 19.42(2)Å β= 114.54(1) deg
Volume	6577(13)$Å^3$
Z, Calculated density	8, 1.614 Mgm^{-3}
Absorption coefficient	5.97 mm^{-1}
F(000)	3088
Crystal size	0.25 * 0.15 * 0.15 mm
Theta range for data collection	1.97 to 24.63 deg.
Index ranges	0<=h<=39, -12<=k<=12, -22<=l<=18
Reflections collected / unique	6960 / 4469 [R(int) = 0.1032]
Completeness to 2theta = 24.63	80.4%
Weighting Scheme (a,b)*	0.076, 638.25
Data / restraints / parameters	4469 / 0 / 219
Final R indices [I>2σ(I)]	R1 = 0.0934, wR2 = 0.2208
R indices (all data)	R1 = 0.1296, wR2 = 0.2456
Extinction coefficient	0.00068(9)
Largest diff. peak and hole	1.223 and -2.079 e.A^-3

* Weighting scheme $w = 1/(\sigma^2(F_o^2) + (aP)^2 + bP)$, where $P = (F_o^2 + 2F_c^2)/3$

Table 3. Bond lengths [A] and angles [deg] in the metal coordination sphere for 1.

W(1)-C(100)	2.09(2)
W(1)-C(7)	2.11(2)
W(1)-C(5)	2.117(18)
W(1)-C(8)	2.16(2)
W(1)-C(6)	2.19(2)
W(1)-N(4)	2.20(2)
W(1)-Br(3)	2.679(3)
W(1)-Br(2)	2.722(3)
C(100)-W(1)-C(7)	77.6(9)
C(100)-W(1)-C(5)	76.2(8)
C(7)-W(1)-C(5)	92.1(7)
C(100)-W(1)-C(8)	113.9(8)
C(7)-W(1)-C(8)	36.5(8)
C(5)-W(1)-C(8)	103.9(7)
C(100)-W(1)-C(6)	110.3(9)
C(7)-W(1)-C(6)	107.7(8)
C(5)-W(1)-C(6)	35.3(8)
C(8)-W(1)-C(6)	97.5(8)
C(100)-W(1)-N(4)	159.5(7)
C(7)-W(1)-N(4)	115.4(8)
C(5)-W(1)-N(4)	117.0(7)
C(8)-W(1)-N(4)	79.4(7)
C(6)-W(1)-N(4)	81.7(8)
C(100)-W(1)-Br(3)	81.3(6)
C(7)-W(1)-Br(3)	157.4(7)
C(5)-W(1)-Br(3)	90.6(4)
C(8)-W(1)-Br(3)	160.9(5)
C(6)-W(1)-Br(3)	87.0(5)
N(4)-W(1)-Br(3)	83.0(5)
C(100)-W(1)-Br(2)	80.5(6)
C(7)-W(1)-Br(2)	84.0(6)
C(5)-W(1)-Br(2)	156.7(5)
C(8)-W(1)-Br(2)	86.7(6)
C(6)-W(1)-Br(2)	165.2(6)
N(4)-W(1)-Br(2)	85.1(5)
Br(3)-W(1)-Br(2)	84.67(11)